frontiers

RESEARCH TOPICS

RECENT PROGRESS IN MELIOIDOSIS AND GLANDERS

Hosted by
Alfredo G. Torres and Ivo Steinmetz

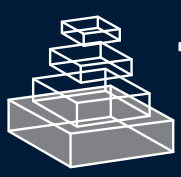

frontiers in MICROBIOLOGY

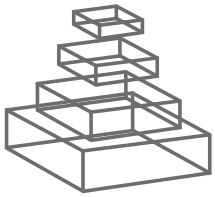

frontiers

Cover image provided by Ibbl sarl, Lausanne CH

ISSN 1664-8714
ISBN 978-2-88919-081-2
DOI 10.3389/978-2-88919-081-2

ABOUT FRONTIERS

Frontiers is more than just an open-access publisher of scholarly articles: it is a pioneering approach to the world of academia, radically improving the way scholarly research is managed. The grand vision of Frontiers is a world where all people have an equal opportunity to seek, share and generate knowledge. Frontiers provides immediate and permanent online open access to all its publications, but this alone is not enough to realize our grand goals.

FRONTIERS JOURNAL SERIES

The Frontiers Journal Series is a multi-tier and interdisciplinary set of open-access, online journals, promising a paradigm shift from the current review, selection and dissemination processes in academic publishing.
All Frontiers journals are driven by researchers for researchers; therefore, they constitute a service to the scholarly community. At the same time, the Frontiers Journal Series operates on a revolutionary invention, the tiered publishing system, initially addressing specific communities of scholars, and gradually climbing up to broader public understanding, thus serving the interests of the lay society, too.

DEDICATION TO QUALITY

Each Frontiers article is a landmark of the highest quality, thanks to genuinely collaborative interactions between authors and review editors, who include some of the world's best academicians. Research must be certified by peers before entering a stream of knowledge that may eventually reach the public - and shape society; therefore, Frontiers only applies the most rigorous and unbiased reviews.
Frontiers revolutionizes research publishing by freely delivering the most outstanding research, evaluated with no bias from both the academic and social point of view.
By applying the most advanced information technologies, Frontiers is catapulting scholarly publishing into a new generation.

WHAT ARE FRONTIERS RESEARCH TOPICS?

Frontiers Research Topics are very popular trademarks of the Frontiers Journals Series: they are collections of at least ten articles, all centered on a particular subject. With their unique mix of varied contributions from Original Research to Review Articles, Frontiers Research Topics unify the most influential researchers, the latest key findings and historical advances in a hot research area!
Find out more on how to host your own Frontiers Research Topic or contribute to one as an author by contacting the Frontiers Editorial Office: researchtopics@frontiersin.org

RECENT PROGRESS IN MELIOIDOSIS AND GLANDERS

Hosted By:
Alfredo G. Torres, University of Texas Medical Branch, USA
Ivo Steinmetz, University of Greifswald, Germany

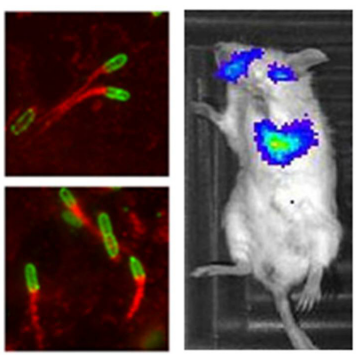

Left: *B. pseudomallei*, image from Bast A, Schmidt IHE, Brauner P, Brix B, Breitbach K and Steinmetz I (2012) Defense mechanisms of hepatocytes against Burkholderia pseudomallei. *Front. Microbio.* 2:277. doi: 10.3389/fmicb.2011.00277. Right: *B. mallei*, image from Massey S, Johnston K, Mott TM, Judy BM, Kvitko BH, Schweizer HP, Estes DM and Torres AG (2011) In vivo bioluminescence imaging of Burkholderia mallei respiratory infection and treatment in the mouse model. *Front. Microbio.* 2:174. doi: 10.3389/fmicb.2011.00174.

Burkholderia pseudomallei and *B. mallei*, causes melioidosis and glanders, respectively, which are two endemic infectious diseases in many parts of the world. The recent reports of glanders outbreaks in horses in Pakistan and Bahrain and the increasing incidence of human melioidosis in Thailand and other tropical regions have resulted in increased research efforts to prevent these diseases. Moreover, both *B. mallei* and *B. pseudomallei* exhibit an intriguing intracellular life cycle including the induction of actin tail formation and cell fusion and thereby have developed as model organisms in infection biology.

This Research Topic summarizes recent progress to understand these pathogens at the molecular level, with emphasis in their virulence traits, host pathogen interactions, population structure and potential targets for therapeutic intervention and vaccine development.

Table of Contents

frontiers in
MICROBIOLOGY

EDITORIAL
published: 19 April 2012
doi: 10.3389/fmicb.2012.00149

Recent progress in melioidosis and glanders

Alfredo G. Torres[1]* and Ivo Steinmetz[2]

[1] *Department of Microbiology and Immunology, University of Texas Medical Branch, Galveston, TX, USA*
[2] *Friedrich Loeffler Institute of Medical Microbiology, University of Greifswald, Greifswald, Germany*
**Correspondence: altorres@utmb.edu*

Burkholderia mallei, the causative agent of glanders, an endemic disease in many parts of the world including the Middle East and Asia, and *B. pseudomallei*, the etiological agent of melioidosis, an environmental saprophyte endemic in Southeast Asia and Northern Australia, are two pathogens with renewed scientific interest. This is due to their potential to cause severe infections by airborne transmission, non-satisfying treatment options, but also due to their fascinating intracellular life cycle and high virulence in rodents, which makes them most promising model pathogens to study basic infection mechanisms.

This Frontiers Research Topic is focused on the recent progress to understand these two pathogens and their diseases at the molecular level, with special emphasis on bacterial virulence mechanisms in host–pathogen interactions, and the development of therapeutic interventions and vaccines to combat those infections.

In the paper by Allwood et al. (2011), the authors reviewed the pathogenesis of melioidosis in the hallmark of *B. pseudomallei*'s ability to enter, survive, and replicate within mammalian host cells. The mechanisms used by the bacteria to circumvent autophagy and other intracellular defense mechanisms, resulting in bacterial intracellular replication and spread to adjacent cells with the subsequent formation of multi-nucleated giant cells is also discussed.

The review by Lazar Adler et al. (2011) provides and up-to-date perspective of the *in silico*, *in vitro*, and *in vivo* studies on the autotransporter proteins of *B. pseudomallei* and *B. mallei*. Special emphasis is given to BimA, the best characterized autotransporter of pathogenic *Burkholderia* and its role as a mediator of actin-based motility; however, the predicted functions of the other autotransporters found in these organisms is also discussed.

Warawa et al. (2011) describe a bioluminescent imaging technique that permits *in vivo* investigation of pulmonary melioidosis in a murine respiratory disease model. This approach helped the investigators to reveal distinct temporal patterns of bacterial colonization of the mice organs and permitted the evaluation of a capsule mutant, which colonized the upper respiratory tract better than the wild type strain.

Since the liver is a commonly affected organ during melioidosis, the study by Bast et al. (2011), aimed to investigate the anti-*B. pseudomallei* activity of hepatocytes. The investigators established an *in vitro* hepatocyte infection model to study host defense mechanisms against *B. pseudomallei*, and observed that the bacteria can invade, escape the vacuole, and replicate within hepatocytes. Further, they determined that IFNγ can restrict growth of the pathogen in these cells.

Another area of active investigation focuses in the fact that *B. pseudomallei* and *B. mallei* can survive hostile conditions, becoming resilient to many antimicrobial agents, including antibiotics.

In the paper by Rholl et al. (2011), the resistance to β-lactams, such as ceftazidime, was investigated. Genetic analysis of *penA* gene, encoding a putative twin arginine translocase (TAT)-secreted β-lactamase, demonstrated that PenA is secreted via the TAT system and that this β-lactamase plays a significant role in *B. pseudomallei*'s resistance to these family of antibiotics.

Massey et al. (2011) also took advantage of the bioluminescent imaging technology to study the progression of a *B. mallei* respiratory infection in the murine model, as well as to establish the efficacy of antibiotic therapy against this pathogen in real-time. This study demonstrated that the *B. mallei* reporter strain maintained similar virulence properties as the wild type strain and allowed visualization of the bacteria in the lungs and through progression to the liver and spleen over the course of infection. Finally, bioluminescence was useful to study efficacy of the antibiotic treatment against murine glanders.

The review by Patel et al. (2011) presents a summary of *B. pseudomallei* vaccine development efforts, including a summary of the immune responses required for protective immunity, the animal models available for preclinical testing of potential candidates, the different experimental vaccine strategies which have being pursued, and the obstacles and opportunities for eventual registration of a licensed vaccine in humans.

In the case of the *B. mallei* vaccine efforts, the manuscript by Whitlock et al. (2011) describes the global evaluation of the genome of *B. mallei* ATCC23344 strain by expression library immunization for gene-encoded protective antigens. The study revealed new putative vaccine candidates, including five candidates that were individually tested and found to confer significant partial protection against a lethal pulmonary infection in a murine model of disease.

Overall, this Special Research Topic, dedicated to study *B. mallei* and *B. pseudomallei* pathogenesis and therapeutic approaches, summarizes the progress that has been made over the past few years in this field, and highlights potential opportunities for future research. It is evident that understanding glanders and melioidosis disease requires more investigators to participate because many areas remained to be understood. With the continue threat that represent the use these pathogens as bioweapons and the limited options for antimicrobial treatment, and no vaccines available, further research in this field is critical.

REFERENCES

Allwood, E. M., Devenish, R. J., Prescott, M., Adler, B., and Boyce, J. D. (2011). Strategies for intracellular survival of *Burkholderia pseudomallei*. *Front. Microbiol.* 2:170. doi: 10.3389/fmicb.2011.00170

Bast, A., Schmidt, I. H., Brauner, P., Brix, B., Breitbach, K., and Steinmetz, I. (2011). Defense mechanisms of hepatocytes against *Burkholderia pseudomallei*. *Front. Microbiol.* 2:277. doi: 10.3389/fmicb.2011.00277

Lazar Adler, N. R., Stevens, J. M., Stevens, M. P., and Galyov, E. E. (2011). Autotransporters and their role in the virulence of *Burkholderia pseudomallei* and *Burkholderia mallei*. *Front. Microbiol.* 2:151. doi: 10.3389/fmicb.2011.00151

Massey, S., Johnston, K., Mott, T. M., Judy, B. M., Kvitko, B. H., Schweizer, H. P., Estes, D. M., and Torres, A. G. (2011). *In vivo* bioluminescence imaging of *Burkholderia mallei* respiratory infection and treatment in the mouse model. *Front. Microbiol.* 2:174. doi: 10.3389/fmicb.2011.00174

Patel, N., Conejero, L., De Reynal, M., Easton, A., Bancroft, G. J., and Titball, R. W. (2011). Development of vaccines against *Burkholderia pseudomallei*. *Front. Microbiol.* 2:198. doi: 10.3389/fmicb.2011.00198

Rholl, D. A., Papp-Wallace, K. M., Tomaras, A. P., Vasil, M. L., Bonomo, R. A., and Schweizer, H. P. (2011). Molecular investigations of PenA-mediated β-lactam resistance in *Burkholderia pseudomallei*. *Front. Microbiol.* 2:139. doi: 10.3389/fmicb.2011.00139

Warawa, J. M., Long, D., Rosenke, R., Gardner, D., and Gherardini, F. C. (2011). Bioluminescent diagnostic imaging to characterize altered respiratory tract colonization by the *Burkholderia pseudomallei* capsule mutant. *Front. Microbiol.* 2:133. doi: 10.3389/fmicb.2011.00133

Whitlock, G. C., Robida, M. D., Judy, B. M., Qazi, O., Brown, K. A., Deeraksa, A., Taylor, K., Massey, S., Loskutov, A., Borovkov, A. Y., Brown, K., Cano, J. A., Torres, A. G., Estes, D. M., and Sykes, K. F. (2011). Protective antigens against glanders identified by expression library immunization. *Front. Microbiol.* 2:227. doi: 10.3389/fmicb.2011.00227

Received: 29 March 2012; accepted: 29 March 2012; published online: 19 April 2012.

Citation: Torres AG and Steinmetz I (2012) Recent progress in melioidosis and glanders. Front. Microbio. ***3****:149. doi: 10.3389/fmicb.2012.00149*

This article was submitted to Frontiers in Cellular and Infection Microbiology – closed section, a specialty of Frontiers in Microbiology.

frontiers in
MICROBIOLOGY

ORIGINAL RESEARCH ARTICLE
published: 16 June 2011
doi: 10.3389/fmicb.2011.00133

Bioluminescent diagnostic imaging to characterize altered respiratory tract colonization by the *Burkholderia pseudomallei* capsule mutant

Jonathan M. Warawa[1,2]*, Dan Long[3], Rebecca Rosenke[3], Don Gardner[3] and Frank C. Gherardini[1]

[1] *Laboratory of Zoonotic Pathogens, Rocky Mountain Laboratories, National Institute of Allergy and Infectious Diseases, National Institute of Health, Hamilton, MT, USA*
[2] *Center for Predictive Medicine, Department of Microbiology and Immunology, University of Louisville, Louisville, KY, USA*
[3] *Rocky Mountain Veterinary Branch, Rocky Mountain Laboratories, National Institute of Allergy and Infectious Diseases, National Institute of Health, Hamilton, MT, USA*

Edited by:
Alfredo G. Torres, University of Texas Medical Branch, USA

Reviewed by:
Miguel A. Valvano, University of Western Ontario, Canada
Ifor Beacham, Griffith University, Australia

****Correspondence:***
Jonathan M. Warawa, Center for Predictive Medicine, Department of Microbiology and Immunology, University of Louisville, 505 South Hancock Street, CTRB 619, Louisville, KY 40202, USA.
e-mail: jonathan.warawa@louisville.edu

Pneumonia is a common manifestation of the potentially fatal disease melioidosis, caused by the select agent bacteria *Burkholderia pseudomallei*. In this study we describe a new model system to investigate pulmonary melioidosis *in vivo* using bioluminescent-engineered bacteria in a murine respiratory disease model. Studies were performed to validate that the stable, light producing *B. pseudomallei* strain JW280 constitutively produced light in biologically relevant host–pathogen interactions. Hairless outbred SKH1 mice were used to enhance the ability to monitor *B. pseudomallei* respiratory disease, and were found to be similarly susceptible to respiratory melioidosis as BALB/c mice. This represents the first demonstration of *in vivo* diagnostic imaging of pulmonary melioidosis permitting the detection of *B. pseudomallei* less than 24 h post-infection. Diagnostic imaging of pulmonary melioidosis revealed distinct temporal patterns of bacterial colonization unique to both BALB/c and SKH1 mice. Validation of these model systems included the use of the previously characterized capsule mutant, which was found to colonize the upper respiratory tract at significantly higher levels than the wild type strain. These model systems allow for high resolution detection of bacterial pulmonary disease which will facilitate studies of therapeutics and basic science evaluation of melioidosis.

Keywords: bioluminescent diagnostic imaging, hairless mouse model, upper respiratory tract infection, pulmonary disease, *Burkholderia pseudomallei*, melioidosis, capsular polysaccharide, intranasal infection

INTRODUCTION

Burkholderia pseudomallei is a Gram-negative bacterial pathogen responsible for the potentially fatal disease melioidosis. *B. pseudomallei* has naturally developed the resistance to numerous classes of antibiotics, and presently there is no licensed vaccine for immunoprotection. Susceptible hosts acquire melioidosis through several possible routes of infection including ingestion, percutaneous inoculation, and inhalation (Currie et al., 2000; Inglis et al., 2000). The potential for respiratory acquisition of fatal melioidosis from a bioweapon has contributed to the identification of *B. pseudomallei* as a category B Select Agent organism (Rotz et al., 2002).

The lung is the most commonly affected organ in human melioidosis (Wiersinga et al., 2006), and radiological imaging approaches have identified the liver and spleen as additional key sites of infection (Muttarak et al., 2008; Lim and Chong, 2010). Mice have been used as an excellent surrogate model which allow for studies of bacterial colonization at all major sites of infection, including the lung, liver, and spleen, approximating numerous aspects of clinical melioidosis (Warawa, 2010). Dissemination and progression of disease in the lung are poorly characterized phenomena in both clinical melioidosis and the mouse model due to the lack of diagnostic tools to monitor disease progression. Bioluminescently engineered *B. pseudomallei* were recently used to study respiratory melioidosis in mice, in which *in vivo* detection of bacteria was limited to the upper respiratory tract (URT) with no bioluminescent detection of pulmonary disease (Owen et al., 2009). In the same study, *ex vivo* bioluminescence was detected additionally in the liver, spleen, and NALT in euthanized animals. A goal of this current study was to establish the ability to detect bacterial colonization of the lung *in vivo*, early in the infectious process, in order to facilitate both therapeutic and basic science investigations of mechanisms of virulence employed by *B. pseudomallei*.

Several virulence determinants have been identified as critical to the virulence of *B. pseudomallei* in animal models including Type 3 Secretion, Type 6 Secretion, LPS, and capsular polysaccharide (CPS I; Deshazer et al., 1998; Reckseidler et al., 2001; Atkins et al., 2002; Stevens et al., 2004; Warawa and Woods, 2005; Burtnick et al., 2011). Of these, all but LPS have been additionally demonstrated to be important for murine respiratory melioidosis (Pilatz et al., 2006; Warawa et al., 2009). We have previously characterized the role of the capsular polysaccharide in respiratory disease and found that a capsule operon mutant is attenuated $10^{1.8}$ fold and

facilitates efficient initial pulmonary colonization, but that capsule is not critically required for dissemination of *B. pseudomallei* to the liver and spleen (Warawa et al., 2009). In developing the ability to perform diagnostic imaging of respiratory melioidosis, we included use of the capsular polysaccharide mutant to attempt to further characterize the role for this virulence determinant in pulmonary disease.

MATERIALS AND METHODS

BACTERIAL STRAINS AND MEDIA

All strains, plasmids, and oligonucleotides are summarized in **Table 1**. Luria broth (LB; Lennox, 1955) or trypticase soy broth (dialyzed and chelated) (TSBDC; Brett et al., 1997) were used to culture *B. pseudomallei* strains at 37°C with shaking. *E. coli* strain TOP10 was used for cloning purposes. Antibiotics were used at the following concentrations: kanamycin (Km: 25 μg/ml), streptomycin (Sm: 100 μg/ml), gentamicin (Gm: 20 μg/ml), and polymyxin B (Pm: 50 μg/ml).

CHROMOSOMAL INTRODUCTION OF *LUX* OPERON

The cloning site of pGSV3-*lux* was modified to allow for directional cloning of DNA fragments upstream of the *luxCDABE* operon. A 850-bp fragment was amplified by PCR from pGSV3-*lux* [pGSV4 ApaI(+)/luxCAatII(−)] and cloned into pCR4. This fragment was excised from pCR4 using *Eco*RI/*Aat*II, and cloned into the same restriction sites of pGSV3-*lux* to yield pGSV4. Subsequently, two PCR fragments from the *B. pseudomallei* genome [5′ara EcoRI(+)/5′ara ApaI(−) and 3′ara NotI(+)/3′ara SpeI(−)] were cloned into pGSV4 as *Eco*RI/*Apa*I (812 bp) and *Not*I/*Spe*I (867 bp) fragments to yield pGSV7. The *tolC* promoter was PCR amplified from *B. pseudomallei* genomic DNA [PtolC(+)/PtolC(−)] and cloned into pGSV7 as an *Nhe*I/*Bam*HI fragment. A 7.6-kb *Eco*RI/*Kpn*I fragment was excised from pGSV7-*PtolC* and cloned into the same sites of pKAS46 to yield pKAS46-*ara*P*tolC-lux*, which was transformed into the *E. coli* strain S17-1. S17-1/ pKAS46-*ara*P*tolC-lux* was conjugated with *B. pseudomallei* strains for the insertion of the P*tolC-lux* construct into the ancestrally deleted arabinose utilization operon in an allelic exchange protocol described elsewhere (Warawa et al., 2009). The DD503::P*tolC-lux* strain was named JW280, and the capsule mutant JW270::P*tolC-lux* strain was named JW280Δ*wcb*. Strains JW280 and JW280Δ*wcb* were identified by their ability to produce light, their resistance to streptomycin, and sensitivity to kanamycin.

INFECTION OF CULTURED CELLS

J774A.1 cells were maintained in DMEM supplemented with 10% heat inactivated fetal bovine serum (Invitrogen) and grown at 37°C with 5% CO_2. For infection studies, J774A.1 cells were seeded at 7.5×10^4 cells per well (100 μl) in a white 96-well plate (Greiner Bio-One) 1 day before infection. *B. pseudomallei* strains were subcultured 1:25 (v/v) from an LB overnight culture into TSBDC and grown at 37°C with shaking for 3 h. The bacterial concentration was estimated from OD_{600} measurements, bacterial suspensions were appropriately diluted into PBS, and a 5-μl aliquot of *B. pseudomallei* suspension was used to inoculate each well of J774A.1 cells. Four replicate plates were infected with *B. pseudomallei* strains JW280 and JW280Δ*wcb* and treated with gentamicin (20 μg/ml final) 1 h after infection. Lux measurements were taken (Victor, Perkin Elmer) from one of the replicate plates at either 3, 5, 7, or 9 h post-infection, then immediately samples were processed for plate enumerations by removing the media, lysing the samples in 0.1% Triton X-100 for 5 min, serially diluting samples in PBS, and enumerating on LB plates.

Table 1 | Bacterial strains, plasmids and oligonucleotides.

Strain	Genotype/description	Source
DD503	*B. pseudomallei* 1026b derivative, Pm^R, Sm^R, AG^S, Tc^S	Moore et al. (1999)
JW270	*B. pseudomallei* Δ*wcb*	Warawa et al. (2009)
JW280	*B. pseudomallei* DD503::P*tolC-lux*	This study
JW280Δ*wcb*	*B. pseudomallei* JW270::P*tolC-lux*	This study
TOP10	Chemically competent *E. coli* cloning strain	Invitrogen
S17-1	*E. coli* strain for conjugation	Simon et al. (1983)
Plasmid		
pKAS46	Suicide vector	Skorupski and Taylor (1996)
pGSV3-*lux*	Promoterless *lux* reporter construct	Moore et al. (2004)
pGSV4	Promoterless *lux* reporter construct, directional MCS	This study
pGSV7	pGSV4 with *B. pseudomallei* arabinose operon fragments	This study
pGSV7-*PtolC*	P*tolC* driven *lux* expression	This study
pKAS46-*ara*P*tolC-lux*	Suicide vector harboring P*tolC-lux*	This study

Oligonucleotide	Sequence (5′ → 3′)
pGSV4 ApaI(+)	GGGCCCACTCGAGGTAAAATGGATGGCAAATATG
luxC AatII(−)	ACTAAAAAAATTTC GCACCTGTCGCTGCGGACGTCAAATCAACAGGAT
5′ara EcoRI(+)	TATCGA GTGGAATTCTCCCGCGCGGCATCGCGAATCGCCTC
5′ara ApaI(−)	GAGGGCCCATCAGGATCCGAGGCTAGCTAGCCCG
3′ara NotI(+)	CGCACGACTTCCATCG GCACGCGGCCGCGGATCGTTCGTCGGTATTTCG
3′ara SpeI(−)	TTTC GCCACTAGTGCGCGCCTTCGATGGGTACCCAGTA
PtolC(+)	CAGCGCGTG GCGATTGCTAGCCGGAATCAGGCTATCATGCACTC
PtolC(−)	AAGTTGG GGTGGATCCAGGATCGTCAAAAACCGATATAAGAC GGGACCG

ANIMAL INFECTIONS – SURVIVAL CHALLENGE

Murine infection studies were conducted at BSL-3 confinement and were approved by the Rocky Mountain Laboratories Biosafety and Animal Care and Use Committees in accordance with National

Institutes of Health guidelines. Intranasal (i.n.) infection of groups of six 8-week-old female BALB/c mice (Charles River Laboratories) was carried out as previously described (Warawa et al., 2009), using *lux*+ *B. pseudomallei* strains JW280 and JW280Δ*wcb*. Animals were euthanized at the onset of terminal disease symptoms, thus 50% infectious dose (ID_{50}) values were calculated as opposed to death endpoint based lethal dose (LD_{50}) values. Statistical analysis of survival data was conducted using GraphPad Prism 5 to evaluate significant differences in survival curves by log-rank (Mantel–Cox) test. StatPlus 2008 was used to perform Probit Analysis to estimate ID_{50} values for JW280 and JW280Δ*wcb* in the SKH1 model.

HISTOLOGICAL ANALYSIS OF INFECTED TISSUE

Tissues were harvested from animals involved in the survival studies. Tissues were fixed in formalin, processed and stained with hematoxylin and eosin (H&E), and the histopathology of lung, liver, and spleen was scored as previously described (Warawa et al., 2009).

TIME COURSE LUX IMAGING

Groups of six BALB/c and SKH1 female 8-week-old mice (Charles River Laboratories) were infected i.n. with 30 μl of PBS bacterial suspension containing either 1×10^4 CFU JW280 or 1×10^6 CFU JW280Δ*wcb*. BALB/c mice were shaved to reduce the amount of fur covering their dorsal thoracic cavities. Mice were anesthetized with 2.5% isoflurane and imaged at ∼12 h intervals, with 5 min exposures from the dorsal perspective using an IVIS Lumina (Caliper Life Sciences). Measurements of lung-specific lux activity were taken by selecting regions of interest (ROI; Living Image 3.0, Caliper Life Sciences) of the dorsally viewed chest cavity and area-normalized backgrounds were subtracted. Animals were euthanized at first presentation of terminal disease symptoms, and lungs were harvested for bacterial enumeration, as described previously (Warawa et al., 2009).

DATA PRESENTATION AND STATISTICAL ANALYSIS

Unless otherwise stated, Graph Pad Prism 5 was used to plot data and conduct statistical analysis by unpaired Student's *t*-test.

RESULTS

GENERATING *LUX*+ *B. PSEUDOMALLEI* STRAINS

We sought to engineer a strain of *B. pseudomallei* which constitutively and stably produced light from the *Photorhabdus luminescens luxCDABE* operon. To ensure stability of the *lux* operon in the absence of antibiotic selection, the operon was introduced into the chromosome by allelic exchange. The insertion site chosen for insertion of the *lux* operon was the site of an ancestrally deleted arabinose utilization operon, known to be present in *B. thailandensis* while only gene fragments are present in the *B. pseudomallei* genome (Moore et al., 2004). Several promoters were evaluated for their ability to constitutively produce light under a variety of growth conditions. One such promoter, P*tolC*, was previously demonstrated to constitutively produce high level photon emission in *Pseudomonas aeruginosa* (Kadurugamuwa et al., 2003). Therefore, the P*tolC-lux* construct was introduced into the genome of wild type *B. pseudomallei* strain DD503 to generate a stable Lux-expressing strain JW280. Similarly, the previously characterized capsular polysaccharide operon mutant, JW270, was engineered to produce light resulting in strain JW280Δ*wcb*.

INTRACELLULAR SURVIVAL OF LUX-EXPRESSING *B. PSEUDOMALLEI*

To investigate whether the light production from JW280 and JW280Δ*wcb* correlates with bacterial numbers, *B. pseudomallei* strains were examined in a cell culture model system. It has been reported that *B. pseudomallei* survive within cultured macrophages, escape from the phagosome in a type III secretion-dependent mechanism, and replicate in the cytoplasm (Stevens et al., 2002). The capsular polysaccharide was previously found to not be critical for intracellular survival of *B. pseudomallei* at early time points (Warawa et al., 2009), however capsule mutants may be required for prolonged survival within macrophages (Wikraiphat et al., 2009).In a gentamicin protection assay, light producing *B. pseudomallei* strains JW280 and JW280Δ*wcb* were found to infect J774A.1 macrophages and proliferate as previously reported (**Figure 1A**). No significant difference in growth was observed between wild type and capsule mutant at 3, 5, or 7 h post-infection. However, at 9 h post-infection the capsule mutant had fewer organisms in infected J774A.1 macrophages than wild type.

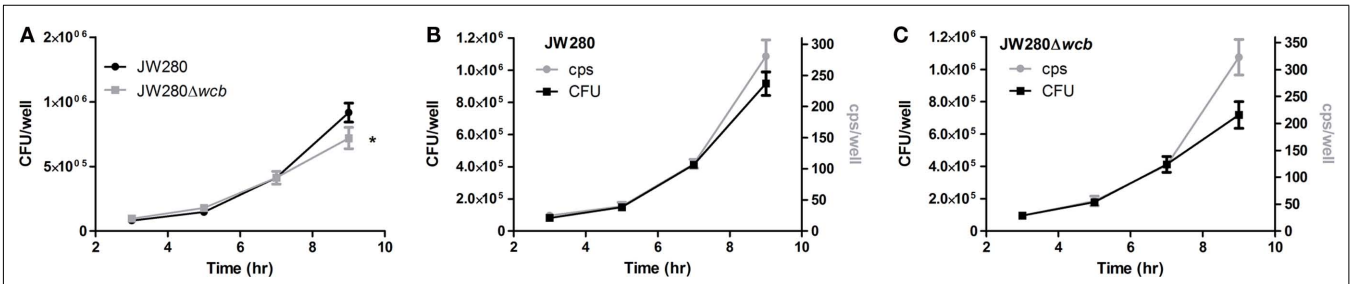

FIGURE 1 | Intracellular survival of *B. pseudomallei* in J774A.1 cell line. *B. pseudomallei* strains JW280 and JW280Δ*wcb* were used to infect 7.5×10^4 J774A.1 murine macrophages in triplicate at an MOI of 0.5. After 1 h, extracellular bacteria were killed with gentamicin. At time points of 3, 5, 7, and 9 h post-inoculation, the light production of triplicate set of samples was measured, then samples were lysed with 0.1% Triton X-100 and enumerated by plate counting. The CFU/well was plotted as a function of time for both JW280 and JW280Δ*wcb* **(A)**. Similarly both CFU/well (left *y*-axis) and cps/well (right *y*-axis) were jointly plotted as a function of time for JW280 **(B)** and JW280Δ*wcb* **(C)**. The mean and standard deviation were plotted for each strain/time point. Asterisks indicate significant difference in bacterial colonization of J774A.1 cells at specific time points ($*p < 0.05$).

This was consistent with previous reports which suggested that the capsule mutant was not as fit as wild type bacteria during late stage infection of macrophages (Wikraiphat et al., 2009). Bioluminescence was measured by plate reader immediately before harvesting samples for bacterial enumeration (counts per second, cps). Changes in both bacterial number and emitted photons were plotted as a function of time for both wild type JW280 (**Figure 1B**) and the capsule mutant (**Figure 1C**). Both JW280 and JW280Δ*wcb* produced light consistent with bacterial number from 3 to 7 h post-infection with an average cps/CFU ratio of 2.79×10^{-4} and 3.02×10^{-4}, respectively. At 9 h post-infection, relative light production increased with JW280 and JW280Δ*wcb* ratios calculated to be 3.07×10^{-4} and 4.49×10^{-4} cps/CFU, respectively. Thus, both JW280 and JW280Δ*wcb* produce light constitutively during host–pathogen interaction studies, with the potential for variations in the cps/CFU ratio based on bacterial fitness during these interactions.

SKH1 MOUSE SUSCEPTIBILITY TO MELIOIDOSIS

We have previously demonstrated that a *B. pseudomallei* capsule mutant is attenuated $10^{1.8}$ fold when introduced by the i.n. route in the BALB/c mouse model (Warawa et al., 2009). Using both wild type and capsule mutant strains of *B. pseudomallei*, we examined whether the SKH1 mouse strain represents a viable model for the study of respiratory melioidosis, and whether Lux-producing strains of *B. pseudomallei* are attenuated. SKH1 mice are an immunocompetent hairless strain that potentially permit enhanced bioluminescent detection due to their lack of fur. A pairwise comparison of *lux*− and *lux*+ versions of both wild type (DD503 and JW280) and capsule mutant (JW270 and JW280Δ*wcb*) strains were not significantly different in their virulence in BALB/c mice (**Figure 2A**, DD503 and JW270 survival curves reproduced as per Warawa et al., 2009). This finding indicates that introduction of the *luxCDABE* operon into the *B. pseudomallei* genome did not significantly impact its virulence in a characterized disease model. The Lux-producing wild type and capsule mutant strains were next used to compare the susceptibility of the SKH1 mouse line to melioidosis relative to the previously characterized BALB/c mouse line. Both SKH1 and BALB/c mice were similarly susceptible to respiratory melioidosis when infected with the wild type strain (**Figure 2B**, left panel). Interestingly, SKH1 mice were more resistant to infection with the capsule mutant than BALB/c mice (**Figure 2B**, right panel), suggesting that greater resolution may be observed in the SKH1 model when evaluating attenuation of bacterial strains or potentially when studying therapeutic interventions. A dose response evaluation of wild type and capsule mutant strains was next conducted in SKH1 mice to facilitate estimation of the 50% ID_{50} values. Probit analysis of the survival curve data (**Figure 2C**) was used to estimate an ID_{50} of 2.47×10^3 CFU (95% CI: 3.5×10^2 to 1.72×10^4 CFU) for JW280 and 5.23×10^5 CFU (95% CI: 2.47×10^5 to 1.11×10^6 CFU) for JW280Δ*wcb*. It is noteworthy that infection with 10^7 CFU of JW280Δ*wcb* produced rapid morbidity suggestive of endotoxicity rather than disease, where the ID_{50} of JW280Δ*wcb* may be higher than estimated. Thus, the capsule mutant is attenuated greater than 200-fold in the SKH1 model.

Infected SKH1 tissues were harvested for evaluation of histopathological damage. As previously reported in the BALB/c model (Warawa et al., 2009), both the wild type and capsule mutant strains produce significant pathology in the lung and liver at the moribund stage of disease (**Figure 3**). Extensive lesions are present throughout the lung associated with inflammatory cell recruitment, fibrin deposition, and cellular necrosis. The liver pathology was characterized by multifocal lesions, and as previously reported, the capsule mutant was found to induce fewer and smaller lesions. Pathology was also detected in the nasal cavity (rhinitis), middle ear (otitis media), and brain (meningitis; data not shown). Blind scoring of the tissue histopathology was conducted to confirm that the capsule mutant indeed produced significantly reduced hepatic damage (**Figure 4**). It was noted, however, that neither the wild type nor capsule mutant strains induced significant pathology in the spleen. This is in contrast to our previous finding of wild type, but not capsule mutant, pathology being detected in the spleen of BALB/c mice. This suggests that *B. pseudomallei* may not colonize the spleen of SKH1 to the same extent as in BALB/c mice, or that the response to *B. pseudomallei* in the spleen of SKH1 is altered from the response in BALB/c mice.

IN VIVO DETECTION OF RESPIRATORY TRACT *B. PSEUDOMALLEI* INFECTION

In order to investigate the potential for *in vivo* diagnostic imaging using bioluminescent *B. pseudomallei*, SKH1 and BALB/c mice were infected i.n. with 10^4 CFU of JW280 or 10^6 CFU of JW280Δ*wcb*, and time course *in vivo* imaging was conducted. Mice were euthanized at the onset of moribund disease and lung, liver, and spleen tissues were collected to enumerate bacterial colonization at key sites of infection. Both the SKH1 and BALB/c mice in the moribund stage of melioidosis were found to be colonized at similar levels by both wild type and capsule mutant strains of *B. pseudomallei*, with the exception that there were significantly fewer JW280 detected in the late stage infected lung of BALB/c mice relative to SKH1 mice with a 2.5-fold difference in average bacterial colonization (**Figure 5**). It was noted that the spleen of SKH1 mice was colonized at a similar level as the spleen of BALB/c mice, suggesting that bacterial colonization does not account for the lack of splenic pathology in SKH1 mice (**Figure 4**). It was also determined that the lung is the most significantly colonized organ in SKH1 infected mice with an average $10^{4.2}$ fold more *B. pseudomallei* in the lung than the liver, and $10^{5.4}$ fold more *B. pseudomallei* in the lung than the spleen. In BALB/c mice, the average colonization ratios are $10^{2.8}$ fold lung to liver and $10^{4.7}$ fold lung to spleen.

Images of bioluminescence detection from *in vivo* diagnostic imaging were collected using an IVIS Lumina system. **Figure 6** presents a representative collection of images demonstrating the potential to track developing pulmonary infection in mice over numerous time points in individual mice, where the last image of each panel represents moribund disease. In both mouse models and using both *B. pseudomallei* strains, *in vivo* detection of pulmonary infection was successfully achieved. Consistent with the bacterial enumeration data, less light emission is detected in the lung of JW280-infected BALB/c mice at moribund disease relative to JW280 infection of SKH1 mice.

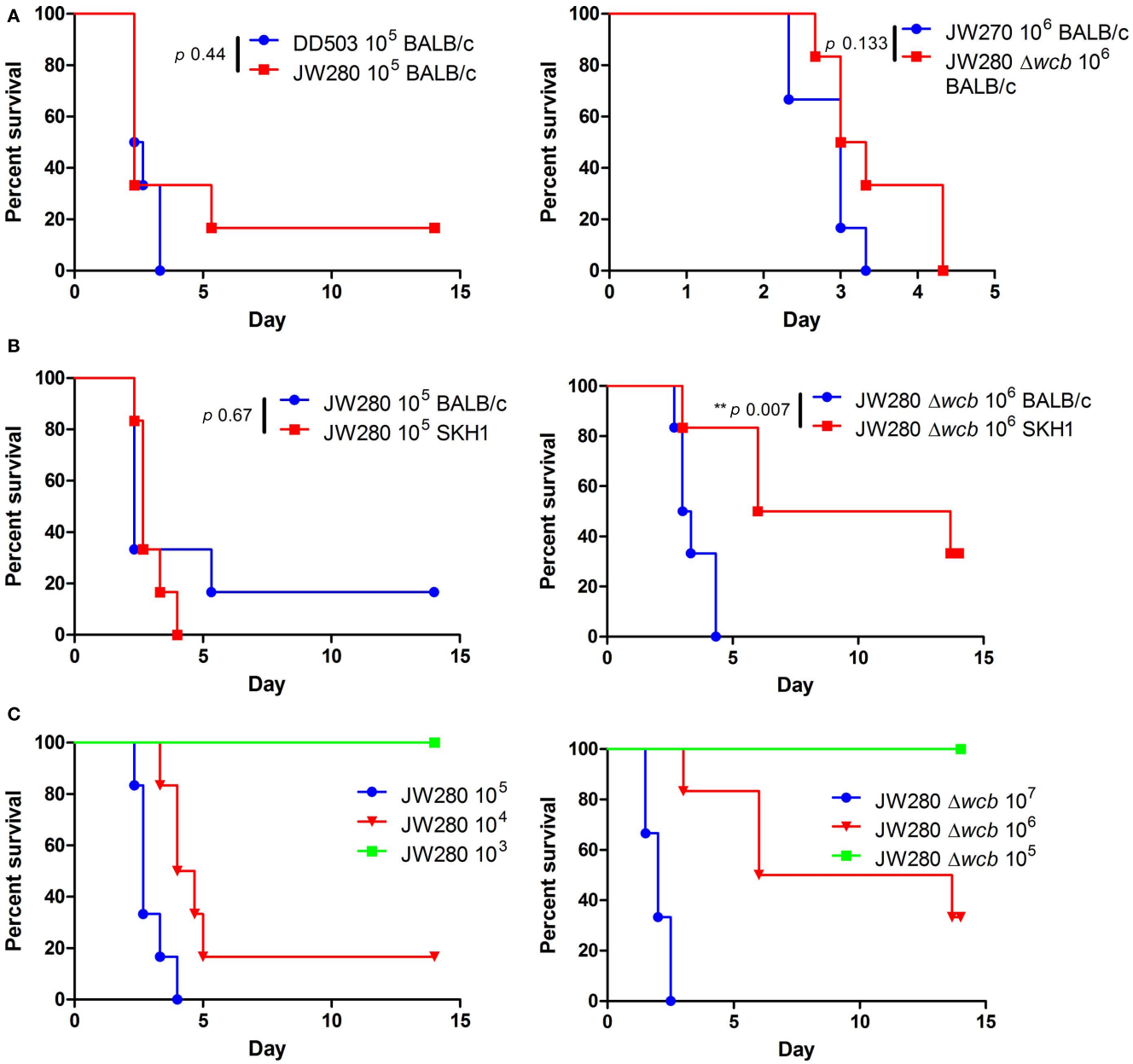

FIGURE 2 | Virulence of Lux-producing *B. pseudomallei* strains. Groups of six mice were infected by the i.n. route with *B. pseudomallei* and monitored for 14 days. **(A)** Groups of BALB/c mice were infected with 10^5 CFU of wild type strains DD503 (*lux*−) or JW280 (*lux*+, left panel) or with 10^6 CFU of capsule mutant strains JW270 (*lux*−) or JW280Δ*wcb* (*lux*+, right panel). **(B)** Groups of SKH1 or BALB/c mice were infected with 10^5 CFU of JW280 (left panel) or 10^6 CFU JW280Δ*wcb* (right panel) to compare the susceptibility of each mouse strain to melioidosis. **(C)** SKH1 mice were infected with 3- to 10-fold serial dilutions of JW280 (10^3–10^5 CFU, left panel) or JW280Δ*wcb* (10^5–10^7 CFU, right panel) to facilitate estimation of the ID_{50} for each strain. Mice were euthanized at the onset of moribund disease. Asterisks indicate significant differences between survival curves using the log-rank (Mantel–Cox) test.

Photon emission was quantified from both the URT and dorsal thoracic cavity in all imaged mice beginning 24 h post-infection. An analysis of the correlation between total emitted light (total flux) from the thoracic cavity and bacterial colonization of the lung was performed. Trend lines were constrained through the *y*-axis at the level of noise estimated from mock-infected animals. It was determined that BALB/c mice have a much higher level of noise ($2.6 \pm 0.7 \times 10^4$ p/s) than SKH1 mice ($3.1 \pm 2.1 \times 10^3$ p/s; $^{**}p = 0.0064$), which was subsequently found to relate to the amount of residual fur present on BALB/c mice (data not shown). In both the BALB/c and SKH1 mouse models, the capsule mutant produced greater light per CFU than the wild type strain in the lung (**Figure 7A**) as previously observed in cell culture assays (**Figure 1**), suggesting that the capsule mutant may be experiencing

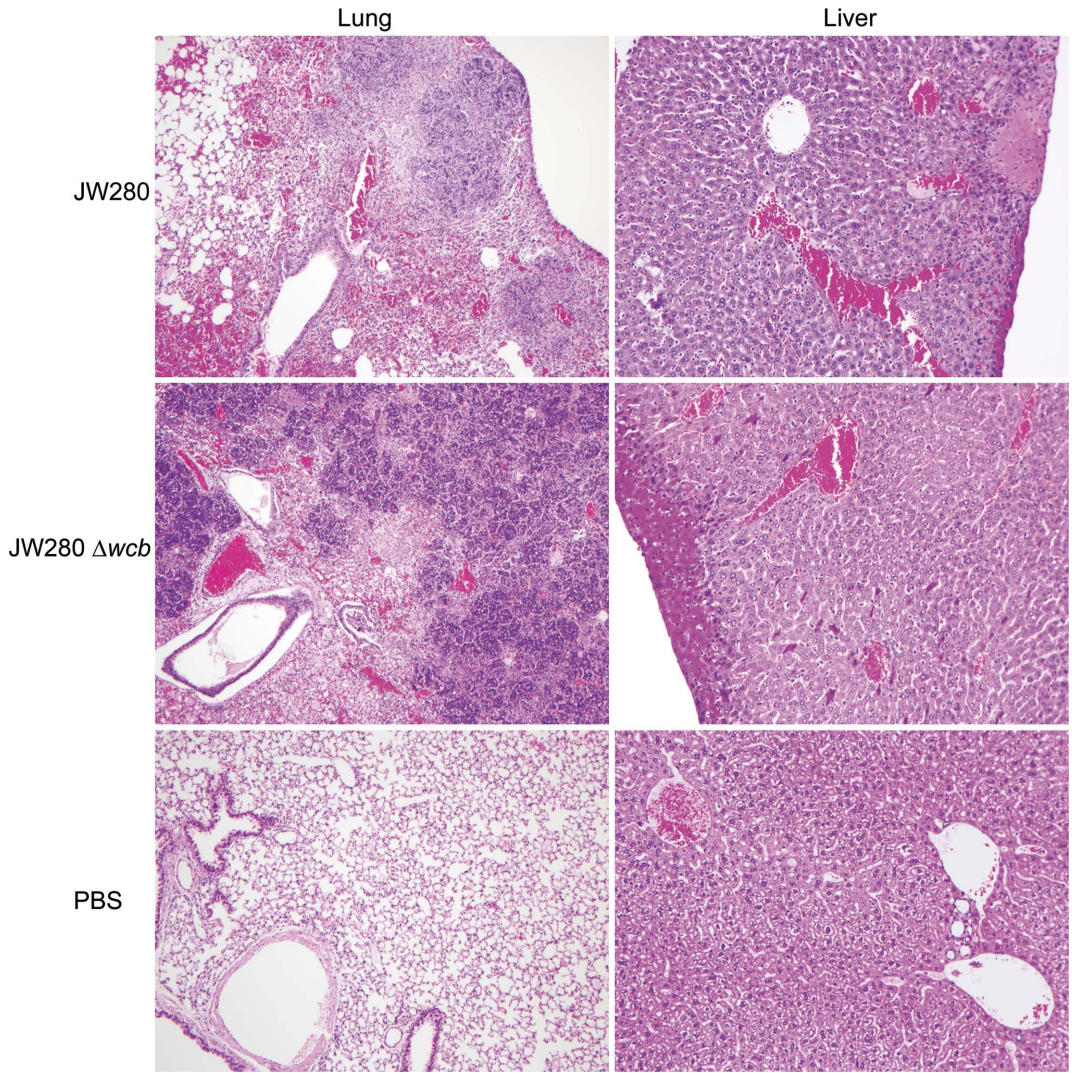

FIGURE 3 | Histological analysis of *B. pseudomallei*-infected tissues. Photomicrographs of representative tissue samples from SKH1 mice infected i.n. with JW280 (10^4 CFU), JW280Δ*wcb* (10^6 CFU), or PBS mock-infected control animals. Samples were formalin-fixed, stained with hematoxylin and eosin (H&E), and imaged by bright field microscopy using either a ×10 (lung) or ×20 (liver) objectives.

a similar environment *in vivo* as that modeled in cultured murine macrophages. Using the calculated equations of the trend lines, it was estimated that the level of detection of wild type and capsule mutant bacteria in the lung of SKH1 mice is 5.7×10^6 and 2.1×10^6 CFU, respectively, at one standard deviation of noise above the average level of noise. Similarly, the BALB/c detection levels were estimated to be 2.6×10^7 and 4.4×10^6 CFU for the wild type and capsule mutant strains, respectively.

The total flux was also plotted as a function of time for wild type and capsule mutant infections of BALB/c (**Figure 7B**) and SKH1 (**Figure 7C**) mice, and the noise level indicated in each plot. The ability to sensitively detect photon emission from BALB/c mice was reduced relative to SKH1 mice, with temporal plots of total flux often overlapping the estimated noise level (**Figure 7B**, horizontal bar). In the BALB/c model, both the wild type and capsule mutants exhibited a biphasic expansion in the lung characterized by an initial increase in pulmonary bacterial burden until approximately 40 h post-infection, followed by a decrease in lung-associated bacteria and subsequent second phase expansion beginning at approximately 60 h post-infection (**Figure 7B**).

In the hairless SKH1 model, the low noise (**Figure 7C**, *x*-axis) allows for sensitive detection of both wild type and capsule mutant bacteria at 24 h post-infection, with the potential for detection at much earlier time points. Unlike the BALB/c model, a biphasic expansion is not observed, and instead both wild type and capsule mutant strains *B. pseudomallei* exhibit an initial lag phase prior to logarithmic expansion in the lung (**Figure 7C**). Of the four wild type-infected SKH1 mice which became morbidly infected, one mouse had two drops in bacterial colonization before the onset of late stage disease, indicating that individual-to-individual alterations in disease kinetics can be detected using this system. The wild type and capsule mutant strains are associated with an

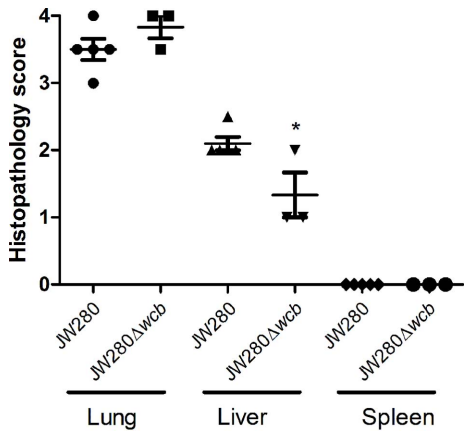

FIGURE 4 | Histopathological scoring of SKH1 infected tissue. Lung, liver, and spleen from SKH1 mice infected i.n. with JW280 (10^4 CFU) or JW280Δ*wcb* (10^6 CFU) were fixed, stained with H&E, and scored in a blind study for varying degrees of pathology. The scoring system was defined as: 0 = within normal limits, 1 = minimal, 2 = mild, 3 = moderate, 4 = severe. Individual data points, the mean, and standard deviation are plotted, and statistically significant variation from JW280-infected tissue scoring is indicated by asterisks (*$p < 0.05$).

initial low rate expansion in the lung until a titer of approximately 3.2×10^4 organisms is achieved, at which point rapid exponential increase is observed. Statistical analysis was conducted on parsed data sets representing early and late stage expansion for both strains, and slopes from logarithmically transformed data were significantly different when comparing early to late stage colonization rates for each strain, but no intra-strain differences were statistically significant (data not shown).

Mice that survived the pneumonia phase of infection (first 5 days) were also evaluated for fluctuations in total flux as a function of time (**Figure 7D**). These mice were characterized as having oscillatory changes in total flux throughout the imaging conducted to day 6. Wild type-infected total flux plots trended downward from 100 h post-infection, which was consistent with the inability to culture organisms from the lung at the termination of the experiment at 14 days post-infection. In contrast, the oscillating total flux of the capsule mutant survivors (**Figure 7D**, right panel) trended upward, and at 14 days post-infection, a bacterial burden of 9.5×10^3 ($\pm 1.52 \times 10^3$) CFU/lung was observed. This data suggests that the capsule mutant potentially establishes a chronic infection in SKH1 mice while survivors of wild type infection effectively clear *B. pseudomallei*.

A striking feature of the bioluminescence overlay images is the observation of significant colonization of the URT as a result of i.n. infection (**Figure 6**), as observed previously (Owen et al., 2009). An evaluation of the ratio of nasal cavity total flux was conducted as a function of the level of thoracic cavity total flux in order to estimate the fold increase in number of *B. pseudomallei* associated preferentially with the nasal cavity. This analysis made use of mice that develop lethal pneumonia and therefore achieve high titers of *B. pseudomallei* in the lung. At all measured time points, the ratio of nasal cavity flux to thoracic cavity flux was included to account for temporal fluctuations. In both the SKH1 and BALB/c models, the capsule mutant had a significantly higher proportion of bacteria associated with the URT with an average of 4.5-fold higher flux in SKH1 mice and 3.1-fold higher flux in BALB/c mice (**Figure 8**). These data indicate that the capsule mutant colonizes the nasal cavity at a significantly higher level than wild type *B. pseudomallei*.

DISCUSSION

This study focused on characterizing and validating a diagnostic imaging model for investigating respiratory melioidosis in mouse models. The approach we selected was use of optical imaging strategies using *B. pseudomallei* strains engineered to constitutively produce bioluminescence. Bioluminescence offers the advantage over fluorescent for detection of weak signals due to the enzymatic amplification of signal, and bioluminescence offers the added benefit of detecting only metabolically active bacteria as the production of light requires energy from the cell. The *luxCDABE* operon from *P. luminescens* allows for light production in the absence of addition of foreign substrates. This is in contrast to the eukaryotic luciferases which require exogenous addition of D-luciferin.

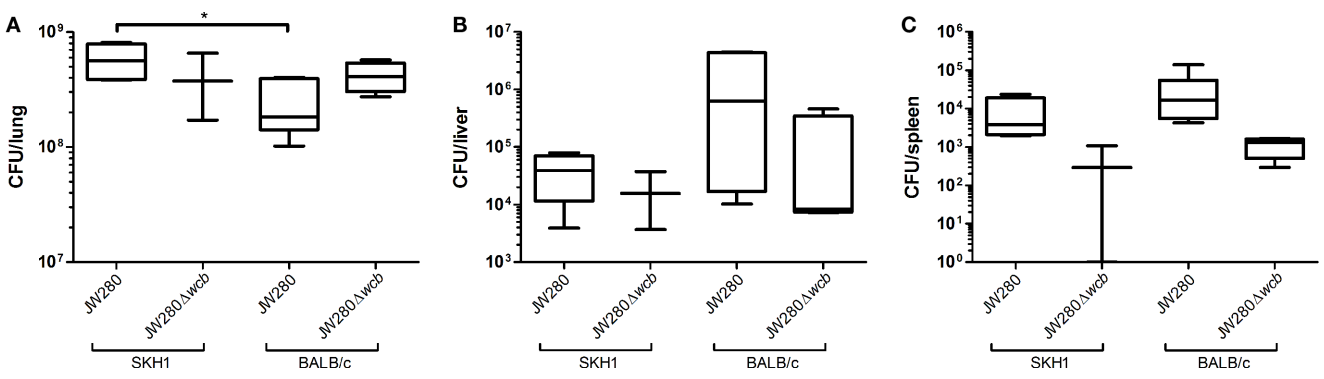

FIGURE 5 | *B. pseudomallei* colonization of key sites of infection. SKH1 and BALB/c mice infected i.n. with JW280 (10^4 CFU) or JW280Δ*wcb* (10^6 CFU) were euthanized at the onset of morbid disease symptoms, organs were harvested, homogenized in PBS and bacteria were enumerated. Data indicates the total number of bacteria detected per organ for lung **(A)**, liver **(B)**, and spleen **(C)**. Significant difference between data sets indicated by asterisk (*$p < 0.05$).

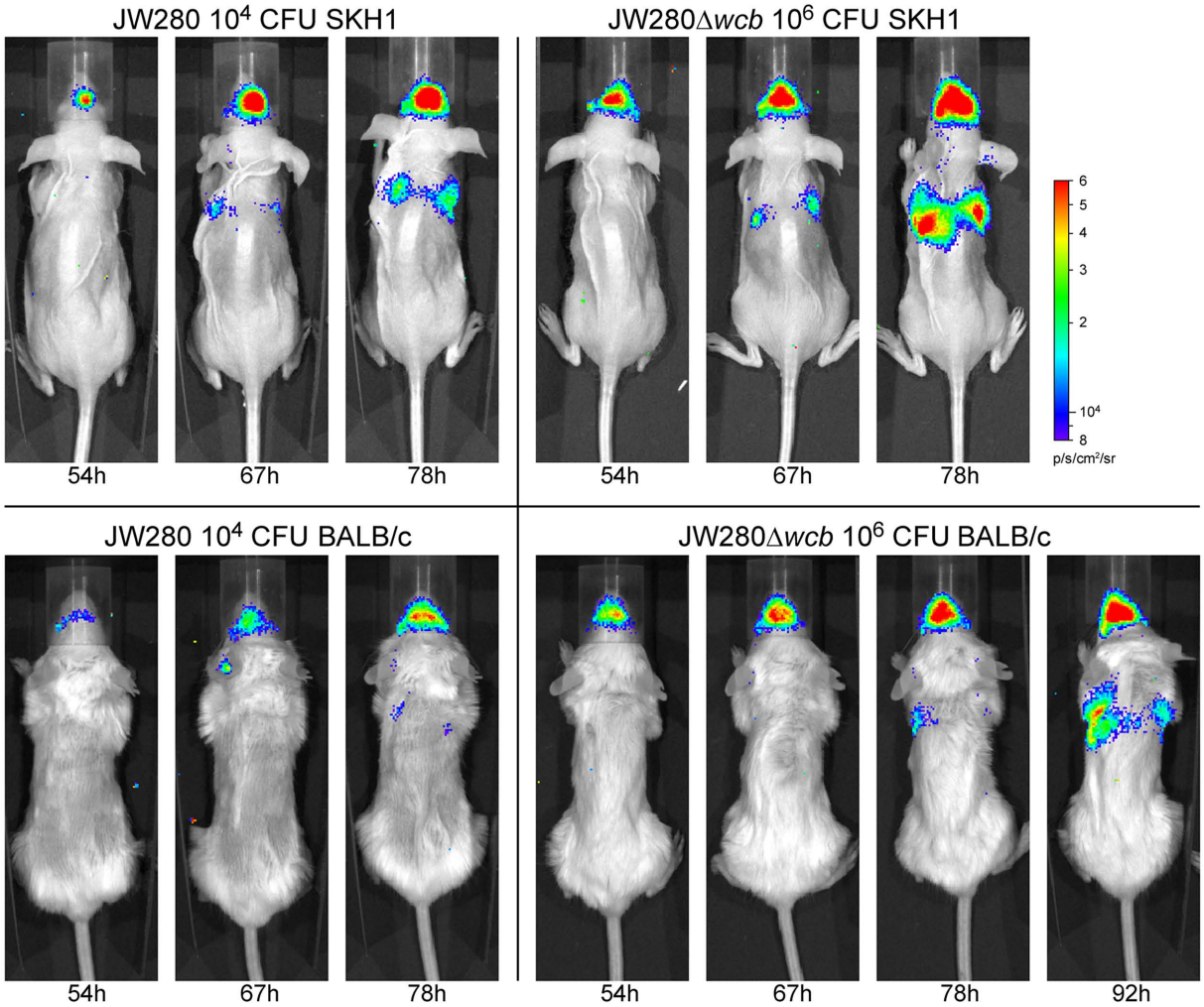

FIGURE 6 | *In vivo* detection of a developing *B. pseudomallei* infection. Overlay images captured with an IVIS Lumina system of representative SKH1 and BALB/c mice infected i.n. with JW280 (10^4 CFU) or JW280Δ*wcb* (10^6 CFU). Infected mice were imaged twice daily and images from late infection (54–92 h) are presented until the time point at which mice were euthanized due to terminal disease. All images were normalized to the same photon saturation scale.

We preferentially selected use of the *lux* operon as *B. pseudomallei* are known to traffic in intracellular environments *in vivo*, and the *lux* operon allows for stable access to endogenous luciferase substrate using the accessory *luxCDE* gene products. The same *luxCDABE* operon was previously introduced by transposon into *B. pseudomallei* strain 08, where i.n. infections of mice resulted *in vivo* detection bacteria only in the URT, with *ex vivo* analysis demonstrating bioluminescence of the liver, spleen, and NALT (Owen et al., 2009). The authors do not comment on the absence of morbid disease when infecting with 3.6×10^5 organisms, however we hypothesize that the small delivery volume (12 μl) may have contributed to a minimal pulmonary infection, and similarly the low bacterial burden reported in the lung (Owen et al., 2009). Thus, *B. pseudomallei* strain 08 may represent a low virulence strain, or may indicate that infections limited to the URT do not lead to morbid disease due to the importance of the lung in *B. pseudomallei* virulence. However, our current model has been shown to facilitate sensitive detection of virulent *B. pseudomallei* in cell culture and mouse disease models, allowing for ratiometric detection of changes in bacterial burdens *in vivo*.

The bioluminescent strain of *B. pseudomallei* engineered in this study, JW280, was found to maintain an excellent correlation between bacterial number and photon production in a biologically relevant macrophage cell culture model. Furthermore, stable, chromosomal introduction of the *lux* operon was not found to significantly attenuate *B. pseudomallei* virulence. Both wild type and capsule mutant *B. pseudomallei* strains maintained a close relationship between measured cps and CFU for the majority of time points investigated in macrophage survival assays. At a late time point, the capsule mutant was found to proliferate less efficiently than wild type in J774A.1 cells, and this reduction in fitness was associated with an increase in relative light production. Interestingly, the relative light production of the capsule mutant in the mouse lung was similarly higher than the wild type strain in

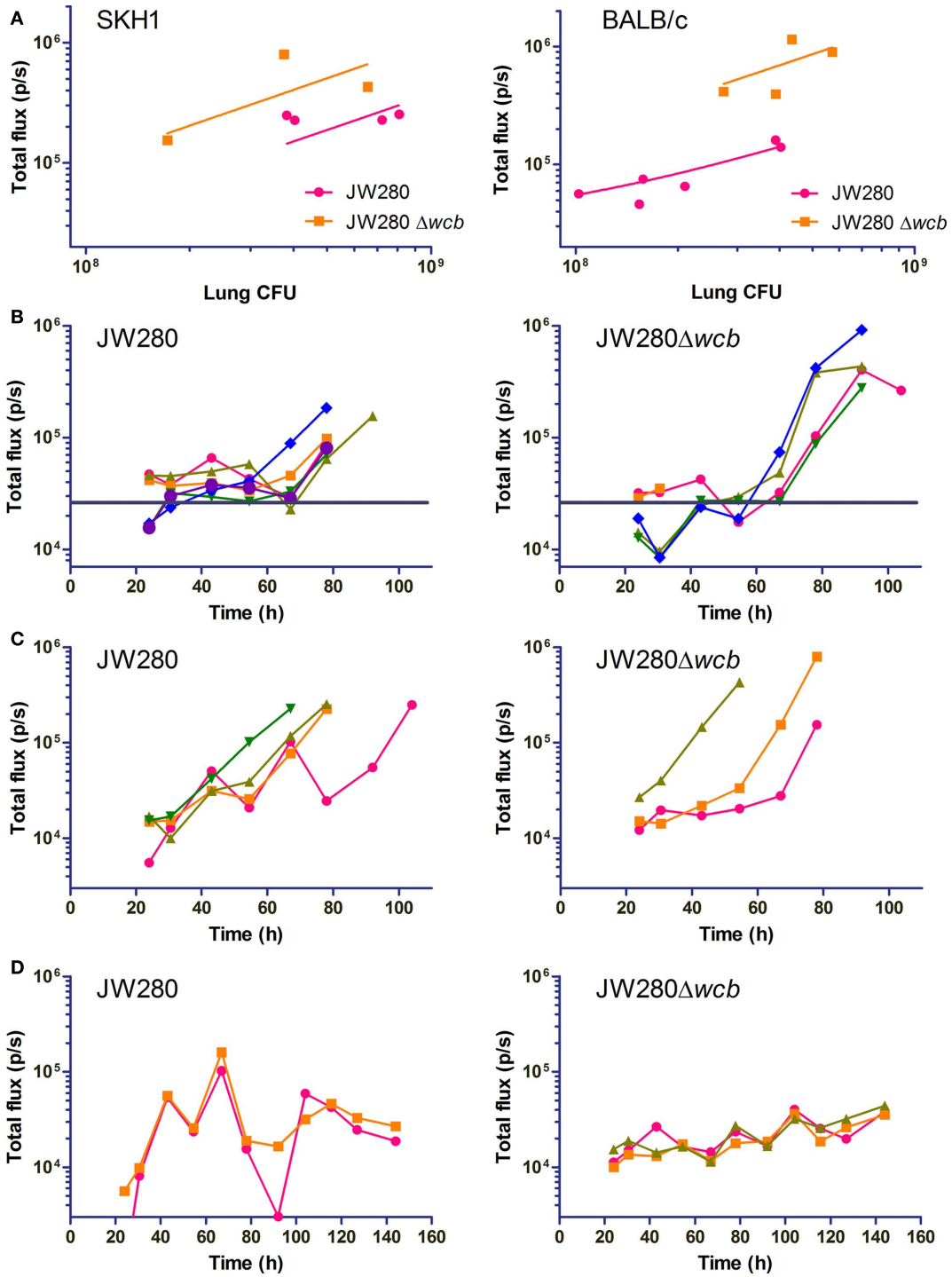

FIGURE 7 | Dynamic assessment of lung colonization by *B. pseudomallei*. SKH1 and BALB/c mice were infected i.n. with JW280 (10^4 CFU), JW280Δ*wcb* (10^6 CFU) or PBS mock-infected, and mice were imaged dorsally with an IVIS Lumina system beginning 24 h post-infection. Living Image 3.0 software was used to enumerate light emission from the lung. PBS mock-infected mice were used to establish baseline noise. At onset of morbid disease, mice were euthanized and bacteria enumerated from the lung. **(A)** Plot of emitted light immediately before euthanization of mice in morbid disease stage as a function of bacterial burden in the lung. The *y*-intercept of the trend line was constrained through the estimated noise determined from mock-infected mice. **(B,C)** Total flux plotted as a function of time for mice which developed morbid disease in BALB/c **(B)** and SKH1 **(C)** mice. The average noise level estimated from mock-infected mice is indicated with a horizontal bar **(B)** or the *x*-axis **(C)**. **(D)** Total flux plotted as a function of time for mice which survived the pneumonia phase of disease in SKH1 mice. The average noise level estimated from mock-infected mice is set at the *x*-axis.

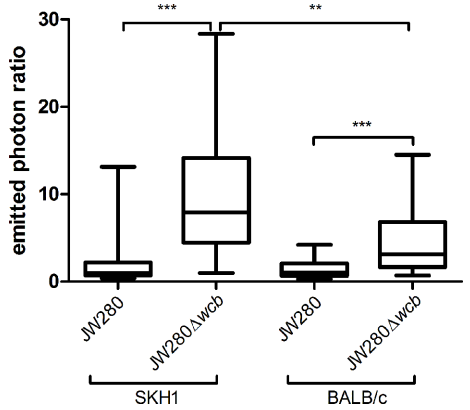

FIGURE 8 | Preferential colonization of the nasal cavity by *B. pseudomallei*. SKH1 and BALB/c mice were infected i.n. with JW280 (10^4 CFU) or JW280Δ*wcb* (10^6 CFU) and mice were imaged dorsally with an IVIS Lumina system beginning 24 h post-infection. The background corrected nasal cavity to thoracic cavity ratio was evaluated at all time points for mice that developed lethal pneumonia. The collective of all experimental ratios were plotted for each group. Significant differences between groups are indicated by asterisks (**$p < 0.01$, ***$p < 0.001$).

both BALB/c and SKH1 mice. Prolonged incubation of a capsule mutant in cultured macrophages was previously reported to be associated with a decrease in capsule mutant viability (Wikraiphat et al., 2009), and the data from this current study suggests that the same mechanism affecting capsule mutant viability in cell culture models may be exerted *in vivo* during pulmonary disease.

This study represents the first characterization of SKH1 mice to investigate melioidosis. SKH1 mice are a hairless mouse model useful for studying a variety of dermatologically important events such as burn models, UV sensitivity, skin aging, and also offer the ability to enhance optical diagnostic imaging for both bioluminescent and fluorescence detection strategies (Benavides et al., 2009). The effect of fur on masking photon emission has been previously estimated to account for up to a 10-fold loss in signal in fluorescence imaging approaches (Nishijo et al., 2009). In this present study, we found that fur also contributes to the noise level which also affects sensitivity of detection, where shaved BALB/c mice have a greater than eight-fold higher noise level than SKH1 mice. Shaving was performed in preference to use of depilatory creams as it has been reported that depilatory creams allow for complete hair regrowth over a 14-day period while shaving results in much slower hair regrowth (Faia et al., 2008).

Unlike nude mice, hairless SKH1 are considered to be an immunocompetent mouse strain which we hypothesized would represent an excellent new model for bioluminescent-based diagnostic imaging of melioidosis. In this study, outbred SKH1 were found to be similarly sensitive to respiratory melioidosis as inbred BALB/c mice. Interestingly, SKH1 mice were found to be more resistant to the virulence of the capsule mutant, such that the capsule mutant attenuation was higher in the SKH1 mouse model than we previously reported in the BALB/c model. Thus, SKH1 mice may allow for higher resolution determination of attenuation when investigating roles of bacterial virulence determinants. We have also demonstrated that SKH1 mice provide a benefit over BALB/c mice in that they: (i) do not have to be shaved, (ii) have no residual fur to mask photon emission or create noise, and (iii) allow for higher levels of lung colonization of wild type *B. pseudomallei*. The most significant caveat we observed in the SKH1 model is the lack of splenic pathology when infected with wild type *B. pseudomallei* even though the bacterial burden in SKH1 mice is similar to that of BALB/c mice. We previously characterized the role of the capsular polysaccharide in stimulating a proinflammatory response in the liver and spleen of BALB/c mice associated with wild type-specific elevations in histopathologic damage in these tissues (Warawa et al., 2009). Splenic pathology is a hallmark of clinical melioidosis (Laopaiboon et al., 2009), and it is therefore a concern that SKH1 mice do not allow for a full study of the host response to melioidosis in the spleen. SKH1 mice possess a retroviral leukemia virus which interrupts the *hr* gene resulting in the autosomal recessive hairless phenotype, and have been reported to possess altered subpopulations of naïve and memory T cells relative to other common mouse strains (Schaffer et al., 2010). While symptoms of leukemia do not exhibit until mice reach adulthood, it is possible that T cell sub-population alterations in 8-week-old SKH1 mice lead to the lack of the host response triggering splenic pathology. Thus, SKH1 mice represent an excellent model for the study of pulmonary disease kinetics during *B. pseudomallei* infection, but caution should be taken if this strain is used to study the host response in disseminated tissues.

Optical imaging strategies for the detection of *B. pseudomallei* in mice appear to be limited to detection of pathogen specifically in the lung. We estimated the level of detection of *B. pseudomallei* in the lung to be $10^{6.3}$–$10^{6.8}$ CFU in SKH1 mice, and $10^{6.6}$–$10^{7.4}$ CFU in BALB/c mice. At terminal disease, *B. pseudomallei* burdens do not exceed 10^5 CFU in the liver or spleen of BALB/c or SKH1 mice with the exception of the livers of BALB/c-infected mice which may exceed 10^6 CFU. It is possible that some punctate visualization of hepatic colonization may be detected during terminal disease, but the ability to monitor disease kinetics in the liver or spleen during murine melioidosis may not be achievable with optical diagnostic imaging. Engineering of new *B. pseudomallei* strains that produce higher levels of light may allow for limited detection in the spleen, but it is likely that the close proximity of the liver to the lung, the significant pigmentation of the liver, and the relatively higher pulmonary colonization rates may mask the hepatic signal. Some strains of *B. pseudomallei* also exhibit altered organ colonization patterns, such as the NCTC 13178 strain which does not colonize the lung at high titer, even when delivered intranasally (Barnes and Ketheesan, 2005). Similarly, the *lux*+ *B. pseudomallei* 08 strain did not colonize the lung at high titer when introduced intranasally (Owen et al., 2009), but it is unclear whether this is due to the low delivery volume or low strain virulence, as discussed above. Therefore not all *B. pseudomallei* strains may be amenable to bioluminescent engineering for the *in vivo* detection of pulmonary disease.

Diagnostic imaging was used in this study to identify unique patterns of bacterial expansion in the lungs of BALB/c and SKH1 mice. BALB/c mice were found to be associated with a biphasic expansion while SKH1 mice were more typically associated with a low initial rate of expansion prior to rapid exponential

expansion. Net bacterial expansion in the lung can be affected by several variables including: (i) variation in bacterial growth rates in different host niches, (ii) host immune-mediated clearance of bacteria, and (iii) reduction of lung colonization due to dissemination to other key sites of infection. Additional studies will be required to characterize the contribution of each of these variables on the biphasic expansion in BALB/c mice and lag expansion in SKH1 mice. Importantly, this study highlights how diagnostic imaging can critically impact our understanding of how melioidosis progresses in the lung in a mouse strain specific manner. Respiratory disease in the mouse model is typically very acute with symptoms of lethal pneumonia presenting within 3–4 days post-infection. The findings of this study suggest that use of arbitrary time designations to identify stages of disease (e.g., 24 h post-infection designation of early disease) may not allow for meaningful study of host–pathogen interaction *in vivo*. Diagnostic imaging is therefore a critically important tool to aid in high resolution definition of host–pathogen interactions in the study of both host and pathogen responses during infection.

A phenotype identified for the capsular polysaccharide *B. pseudomallei* mutant in this study was the elevated colonization of the URT during infection. The high degree of nasal cavity colonization for both the wild type and capsule mutant strains had been an unexpected observation, with the nasal cavity bacterial burden exceeding that of the lung in the majority of instances of diagnostic imaging. This finding suggests that the murine nasal cavity is a primary colonization niche for *B. pseudomallei* delivered by the i.n. route, while we have not found evidence to suggest that clinical melioidosis is associated with similar URT carriage. The reason for a potential difference between human and murine URT carriage may be due to opportunistic colonization in mice due to the high relative surface area, where mice have been reported to have over 100-fold greater relative surface area than the human nasal cavity (Warawa, 2010). Alternatively, normal resident flora specific to the human URT may outcompete *B. pseudomallei* in interspecies competition, a reported phenomenon for other respiratory pathogens (Lysenko et al., 2005). Additional studies are required to characterize the murine-specific tolerance for URT-related melioidosis and the role of capsular polysaccharide in directing elevated URT colonization, which may shed light on our general understanding of *B. pseudomallei* colonization of mucosal surfaces.

In conclusion, we have characterized the first *in vivo* pulmonary diagnostic imaging model of melioidosis using a fully virulent, stable, bioluminescent strain of *B. pseudomallei*. We validated the ability to detect *B. pseudomallei* in the lung of infected mice in both BALB/c and SKH1 mice, with the higher level of sensitivity being achieved in SKH1 mice. Different patterns of bacterial expansion in the lung were observed in the two mouse strains suggesting that altered kinetics of host response and/or dissemination profiles may affect disease in these strains. We also identified the high propensity for URT colonization by *B. pseudomallei* with the intact capsular polysaccharide modulating the level of colonization of the nasal cavity. These findings highlight the importance of using diagnostic imaging to characterize *in vivo* models of melioidosis.

ACKNOWLEDGMENTS

This research was supported by the Intramural Research Program of the NIH, NIAID. We thank Dr. Matthew Lawrenz for his critical evaluation of this manuscript.

REFERENCES

Atkins, T., Prior, R., Mack, K., Russell, P., Nelson, M., Prior, J., Ellis, J., Oyston, P. C., Dougan, G., and Titball, R. W. (2002). Characterisation of an acapsular mutant of *Burkholderia pseudomallei* identified by signature tagged mutagenesis. *J. Med. Microbiol.* 51, 539–547.

Barnes, J. L., and Ketheesan, N. (2005). Route of infection in melioidosis. *Emerging Infect. Dis.* 11, 638–639.

Benavides, F., Oberyszyn, T. M., Vanbuskirk, A. M., Reeve, V. E., and Kusewitt, D. F. (2009). The hairless mouse in skin research. *J. Dermatol. Sci.* 53, 10–18.

Brett, P. J., Deshazer, D., and Woods, D. E. (1997). Characterization of *Burkholderia pseudomallei* and *Burkholderia pseudomallei*-like strains. *Epidemiol. Infect.* 118, 137–148.

Burtnick, M. N., Brett, P. J., Harding, S. V., Ngugi, S. A., Ribot, W. J., Chantratita, N., Scorpio, A., Milne, T. S., Dean, R. E., Fritz, D. L., Peacock, S. J., Prior, J. L., Atkins, T. P., and Deshazer, D. (2011). The cluster 1 type VI secretion system is a major virulence determinant in *Burkholderia pseudomallei*. *Infect. Immun.* 79, 1512–1525.

Currie, B. J., Fisher, D. A., Howard, D. M., Burrow, J. N., Selvanayagam, S., Snelling, P. L., Anstey, N. M., and Mayo, M. J. (2000). The epidemiology of melioidosis in Australia and Papua New Guinea. *Acta Trop.* 74, 121–127.

Deshazer, D., Brett, P. J., and Woods, D. E. (1998). The type II O-antigenic polysaccharide moiety of *Burkholderia pseudomallei* lipopolysaccharide is required for serum resistance and virulence. *Mol. Microbiol.* 30, 1081–1100.

Faia, K., Mandley, E., Dembski, S., Pien, C., Macdougall, J., Hoyt, J., Campbell, M., Lin, G., Lo, P., Read, M., and Mcgovern, K. (2008). "Abstract #2827: depilation induced anagen as a model to study hedgehog pathway antagonist IPI-926 implications for biomarker development," in *Annual Meeting of the American Association of Cancer Research*, San Diego, CA.

Inglis, T. J., Garrow, S. C., Henderson, M., Clair, A., Sampson, J., O'Reilly, L., and Cameron, B. (2000). *Burkholderia pseudomallei* traced to water treatment plant in Australia. *Emerging Infect. Dis.* 6, 56–59.

Kadurugamuwa, J. L., Sin, L., Albert, E., Yu, J., Francis, K., Deboer, M., Rubin, M., Bellinger-Kawahara, C., Parr, T. R. Jr., and Contag, P. R. (2003). Direct continuous method for monitoring biofilm infection in a mouse model. *Infect. Immun.* 71, 882–890.

Laopaiboon, V., Chamadol, N., Butham, H., and Sukeepaisarnjareon, W. (2009). CT findings of liver and splenic abscesses in melioidosis: comparison with those in non-melioidosis. *J. Med. Assoc. Thai.* 92, 1476–1484.

Lennox, E. S. (1955). Transduction of linked genetic characters of the host by bacteriophage P1. *Virology* 1, 190–206.

Lim, K. S., and Chong, V. H. (2010). Radiological manifestations of melioidosis. *Clin. Radiol.* 65, 66–72.

Lysenko, E. S., Ratner, A. J., Nelson, A. L., and Weiser, J. N. (2005). The role of innate immune responses in the outcome of interspecies competition for colonization of mucosal surfaces. *PLoS Pathog.* 1, e1. doi: 10.1371/journal.ppat.0010001

Moore, R. A., Deshazer, D., Reckseidler, S., Weissman, A., and Woods, D. E. (1999). Efflux-mediated aminoglycoside and macrolide resistance in *Burkholderia pseudomallei*. *Antimicrob. Agents Chemother.* 43, 465–470.

Moore, R. A., Reckseidler-Zenteno, S., Kim, H., Nierman, W., Yu, Y., Tuanyok, A., Warawa, J., Deshazer, D., and Woods, D. E. (2004). Contribution of gene loss to the pathogenic evolution of *Burkholderia pseudomallei* and *Burkholderia mallei*. *Infect. Immun.* 72, 4172–4187.

Muttarak, M., Peh, W. C., Euathrongchit, J., Lin, S. E., Tan, A. G., Lerttumnongtum, P., and Sivasomboon, C. (2008). Spectrum of imaging findings in melioidosis. *Br. J. Radiol.* 82, 514–521.

Nishijo, K., Hosoyama, T., Bjornson, C. R., Schaffer, B. S., Prajapati, S. I., Bahadur, A. N., Hansen, M. S., Blandford, M. C., Mccleish, A. T., Rubin, B. P., Epstein, J. A., Rando, T. A., Capecchi, M. R., and Keller, C. (2009). Biomarker system for studying muscle, stem cells, and cancer in vivo. *FASEB J.* 23, 2681–2690.

Owen, S. J., Batzloff, M., Chehrehasa, F., Meedeniya, A., Casart, Y., Logue, C. A., Hirst, R. G., Peak, I. R., Mackay-Sim, A., and Beacham, I. R. (2009). Nasal-associated lymphoid tissue and olfactory epithelium as portals of entry for *Burkholderia pseudomallei* in murine melioidosis. *J. Infect. Dis.* 199, 1761–1770.

Pilatz, S., Breitbach, K., Hein, N., Fehlhaber, B., Schulze, J., Brenneke, B., Eberl, L., and Steinmetz, I. (2006). Identification of *Burkholderia pseudomallei* genes required for the intracellular life cycle and in vivo virulence. *Infect. Immun.* 74, 3576–3586.

Reckseidler, S. L., Deshazer, D., Sokol, P. A., and Woods, D. E. (2001). Detection of bacterial virulence genes by subtractive hybridization: identification of capsular polysaccharide of *Burkholderia pseudomallei* as a major virulence determinant. *Infect. Immun.* 69, 34–44.

Rotz, L. D., Khan, A. S., Lillibridge, S. R., Ostroff, S. M., and Hughes, J. M. (2002). Public health assessment of potential biological terrorism agents. *Emerging Infect. Dis.* 8, 225–230.

Schaffer, B. S., Grayson, M. H., Wortham, J. M., Kubicek, C. B., Mccleish, A. T., Prajapati, S. I., Nelon, L. D., Brady, M. M., Jung, I., Hosoyama, T., Sarro, L. M., Hanes, M. A., Rubin, B. P., Michalek, J. E., Clifford, C. B., Infante, A. J., and Keller, C. (2010). Immune competency of a hairless mouse strain for improved preclinical studies in genetically engineered mice. *Mol. Cancer Ther.* 9, 2354–2364.

Simon, R., Priefer, U., and Pühler, A. (1983). A broad range mobilization system for in vivo genetic engineering: transposon mutagenesis in gram-negative bacteria. *Biotechnology* 1, 784–791.

Skorupski, K., and Taylor, R. K. (1996). Positive selection vectors for allelic exchange. *Gene* 169, 47–52.

Stevens, M. P., Haque, A., Atkins, T., Hill, J., Wood, M. W., Easton, A., Nelson, M., Underwood-Fowler, C., Titball, R. W., Bancroft, G. J., and Galyov, E. E. (2004). Attenuated virulence and protective efficacy of a *Burkholderia pseudomallei* bsa type III secretion mutant in murine models of melioidosis. *Microbiology* 150, 2669–2676.

Stevens, M. P., Wood, M. W., Taylor, L. A., Monaghan, P., Hawes, P., Jones, P. W., Wallis, T. S., and Galyov, E. E. (2002). An Inv/Mxi-Spa-like type III protein secretion system in *Burkholderia pseudomallei* modulates intracellular behaviour of the pathogen. *Mol. Microbiol.* 46, 649–659.

Warawa, J., and Woods, D. E. (2005). Type III secretion system cluster 3 is required for maximal virulence of *Burkholderia pseudomallei* in a hamster infection model. *FEMS Microbiol. Lett.* 242, 101–108.

Warawa, J. M. (2010). Evaluation of surrogate animal models of melioidosis. *Front. Microbio.* 1:141. doi: 10.3389/fmicb.2010.00141

Warawa, J. M., Long, D., Rosenke, R., Gardner, D., and Gherardini, F. C. (2009). Role for the *Burkholderia pseudomallei* capsular polysaccharide encoded by the wcb operon in acute disseminated melioidosis. *Infect. Immun.* 77, 5252–5261.

Wiersinga, W. J., Van Der Poll, T., White, N. J., Day, N. P., and Peacock, S. J. (2006). Melioidosis: insights into the pathogenicity of *Burkholderia pseudomallei. Nat. Rev. Microbiol.* 4, 272–282.

Wikraiphat, C., Charoensap, J., Utaisincharoen, P., Wongratanacheewin, S., Taweechaisupapong, S., Woods, D. E., Bolscher, J. G., and Sirisinha, S. (2009). Comparative in vivo and in vitro analyses of putative virulence factors of *Burkholderia pseudomallei* using lipopolysaccharide, capsule and flagellin mutants. *FEMS Immunol. Med. Microbiol.* 56, 253–259.

Conflict of Interest Statement: The authors declare that the research was conducted in the absence of any commercial or financial relationships that could be construed as a potential conflict of interest.

Received: 01 May 2011; paper pending published: 13 May 2011; accepted: 06 June 2011; published online: 16 June 2011.

*Citation: Warawa JM, Long D, Rosenke R, Gardner D and Gherardini FC (2011) Bioluminescent diagnostic imaging to characterize altered respiratory tract colonization by the Burkholderia pseudomallei capsule mutant. Front. Microbio. **2**:133. doi: 10.3389/fmicb.2011.00133*

This article was submitted to Frontiers in Cellular and Infection Microbiology, a specialty of Frontiers in Microbiology.

frontiers in
MICROBIOLOGY

ORIGINAL RESEARCH ARTICLE
published: 01 July 2011
doi: 10.3389/fmicb.2011.00139

Molecular investigations of PenA-mediated β-lactam resistance in *Burkholderia pseudomallei*

Drew A. Rholl[1,2], Krisztina M. Papp-Wallace[3], Andrew P. Tomaras[4], Michael L. Vasil[4], Robert A. Bonomo[3,5,6,7] and Herbert P. Schweizer[1,2]*

[1] Department of Microbiology, Immunology and Pathology, Colorado State University, Fort Collins, CO, USA
[2] Rocky Mountain Regional Center of Excellence for Biodefense and Emerging Infectious Diseases Research, Colorado State University, Fort Collins, CO, USA
[3] Louis Stokes Cleveland Department of Veterans Affairs Medical Center, Cleveland, OH, USA
[4] Department of Microbiology, University of Colorado School of Medicine, Aurora, CO, USA
[5] Department of Medicine, Case Western Reserve University School of Medicine, Cleveland, OH, USA
[6] Department of Pharmacology, Case Western Reserve University School of Medicine, Cleveland, OH, USA
[7] Department of Molecular Biology and Microbiology, Case Western Reserve University School of Medicine, Cleveland, OH, USA

Edited by:
Alfredo G. Torres, University of Texas Medical Branch, USA

Reviewed by:
David Aucoin, University of Nevada School of Medicine, USA
Narisara Chantratita, Mahidol University, Thailand

***Correspondence:**
Herbert P. Schweizer, Department of Microbiology, Immunology and Pathology, Colorado State University, Infectious Disease Research Center at Foothills Campus, 0922 Campus Delivery, Fort Collins, CO 80523, USA. e-mail: herbert.schweizer@colostate.edu

Burkholderia pseudomallei is the etiological agent of melioidosis. Because of the bacterium's intrinsic resistance and propensity to establish latent infections, melioidosis therapy is complicated and prolonged. Newer generation β-lactams, specifically ceftazidime, are used for acute phase therapy, but resistance to this cephalosporin has been observed. The chromosomally encoded *penA* gene encodes a putative twin arginine translocase (TAT)-secreted β-lactamase, and *penA* mutations have been implicated in ceftazidime resistance in clinical isolates. However, the role of PenA in resistance has not yet been systematically studied in isogenetic *B. pseudomallei* mutant backgrounds. We investigated the effects of *penA* deletion, point mutations, and up-regulation, as well as *tat* operon deletion and PenA TAT-signal sequence mutations. These experiments were made possible by employing a *B. pseudomallei* strain that is excluded from Select Agent regulations. Deletion of *penA* significantly (>4-fold) reduced the susceptibility to six of the nine β-lactams tested and ≥16-fold for ampicillin, amoxicillin, and carbenicillin. Overexpression of *penA* by single-copy, chromosomal expression of the gene under control of the inducible P_{tac} promoter, increased resistance levels for all β-lactams tested 2- to 10-fold. Recreation of the C69Y and P167S PenA amino acid substitutions previously observed in resistant clinical isolates increased resistance to ceftazidime by ≥85- and 5- to 8-fold, respectively. Similarly, a S72F substitution resulted in a 4-fold increase in resistance to amoxicillin and clavulanic acid. Susceptibility assays with PenA TAT-signal sequence and Δ*tatABC* mutants, as well as Western blot analysis, confirmed that PenA is a TAT secreted enzyme and not periplasmic but associated with the spheroplastic cell fraction. Lastly, we determined that two LysR-family regulators encoded by genes adjacent to *penA* do not play a role in transcriptional regulation of *penA* expression.

Keywords: *Burkholderia pseudomallei*, melioidosis, antibiotic resistance, β-lactams, β-lactamase, TAT secretion

INTRODUCTION

Burkholderia pseudomallei, the etiological agent of melioidosis, is a saprophytic Gram negative bacterium endemic to many tropical and subtropical regions of the world although much of the disease and its investigation has historically been confined to Northern Australia and regions of SE Asia, notably NE Thailand, Singapore, and Malaysia (Cheng and Currie, 2005; Wiersinga et al., 2006; Currie et al., 2008). Partially because of its large genome and diverse repertoire of metabolic functions *B. pseudomallei* can survive hostile conditions and is resilient to many antimicrobial agents, including antibiotics (Holden et al., 2004). This makes choosing effective therapeutic strategies difficult. In the past three decades even the most effective treatment could not prevent a mortality rate of 74% (White et al., 1989). Clinical outcomes improved steadily with implementation of new therapies but the real breakthrough was achieved with the introduction of ceftazidime, an extended-spectrum cephalosporin, which halved the mortality rate compared to the traditional multidrug therapy of chloramphenicol, doxycycline, and trimethoprim–sulfamethoxazole (White et al., 1989). Currently recommended melioidosis treatment involves acute phase therapy followed by a lengthy eradication therapy. Initial parenteral therapy involves ceftazidime or a carbapenem for a minimum of 10–14 days and longer (4–8 weeks) for deep-seated infection. This regimen may be supplemented with trimethoprim–sulfamethoxazole given orally for treatment of patients with neurologic, prostatic, bone, or joint melioidosis. Oral eradication therapy is trimethoprim–sulfamethoxazole with or without doxycycline for at least 3–6 months (Peacock et al., 2008).

Because of the pivotal role that β-lactams play in the acute phase treatment of melioidosis emergence of resistance, though still considered rare, is of concern. It is believed that *B. pseudomallei*'s resistance to β-lactams is due to chromosomally encoded β-lactamases (Livermore et al., 1987; Godfrey et al.,

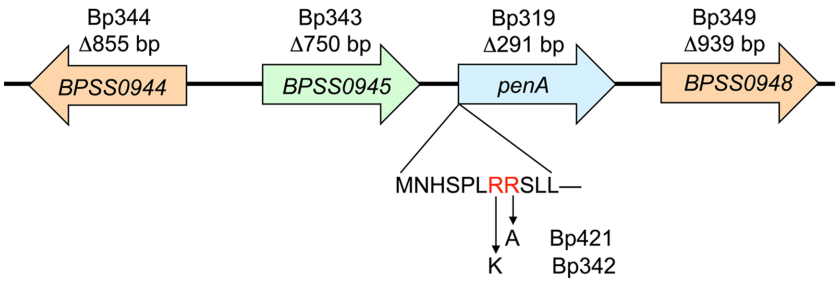

FIGURE 1 | Genomic organization of the *B. pseudomallei penA* region. The genes and gene order are from sequenced strain K96243 (GenBank accession number NC_006351). The *penA* region encodes two LysR-type regulators (BPSS0944 and BPSS0948) and a putative peptidase (BPSS0945). The names of the mutants harboring gene deletion and extents of deleted sequences are shown above each gene. The putative PenA twin arginine translocase (TAT) signal sequence is shown below the *penA* gene with the two conserved arginine residues shown in red letters. Arrows indicate amino acid substitutions, R7K and R8A, in the TAT-signal sequence and the names of the mutants are shown next to the respective amino acids replacing the original arginines.

1991). These include a number of Ambler Class A, B, and D β-lactamases that are encoded by the K96243 and other *B. pseudomallei* genomes (Holden et al., 2004). The *penA* gene (K96243 gene *BPSS0946* found on chromosome II; **Figure 1**) encodes a Class A β-lactamase (Cheung et al., 2002; Tribuddharat et al., 2003). This gene is present and expressed in prototype *B. pseudomallei* strains. PenA confers resistance to numerous β-lactam antibiotics when expressed in *Escherichia coli* (Cheung et al., 2002; Tribuddharat et al., 2003) and several reports described a role of this enzyme in acquired ceftazidime resistance in patients treated with this antibiotic (Godfrey et al., 1991; Tribuddharat et al., 2003; Sam et al., 2009). Mutations identified in clinical strains included a C69Y substitution leading to high-level ceftazidime resistance (Sam et al., 2009), a P167S substitution leading to medium-level ceftazidime resistance (Tribuddharat et al., 2003) and a S72F mutation that led to resistance to clavulanic acid (Tribuddharat et al., 2003). A Class D Oxa-57 β-lactamase has been studied *in vitro* but its role in clinically significant β-lactam resistance remains unclear (Keith et al., 2005).

While *B. pseudomallei* PenA β-lactamase has been studied in some detail, previously published reports suffered until recently from some unavoidable shortcomings. First, many mutations contributing to clinically significant β-lactam resistance were identified in genetically largely intractable clinical isolates. Thus, it remained unclear whether the mutations were solely responsible for causing the observed resistance. Second, because methods for genetic manipulation of *B. pseudomallei* were rather rudimentary until recently, most studies involved expression of putative β-lactamase enzymes in *E. coli*. Third, United States Select Agent and recombinant DNA regulations, as well as dual use concerns, do complicate studies of clinically significant antibiotic resistance mechanisms. To address shortcomings of previous studies, we employed state-of-the-art Select Agent-compliant genetic and biochemical methods and a defined genetic background of a Select Agent excluded *B. pseudomallei* strain, where applicable, to study the contribution of PenA to *B. pseudomallei*'s resistance to clinically significant β-lactam antibiotics. The studies also revealed that PenA is secreted via the twin arginine translocase system and that its expression in prototype strains does not seem to be regulated by local transcriptional regulators.

Table 1 | *Burkholderia pseudomallei* strains used in this study.

Strain	Description	Source
	Strain 1026b-based mutants	
1026b	Clinical isolate, wild-type	DeShazer et al. (1997)
Bp319	1026b Δ*penA*	This study
Bp409	1026b Δ*tatABC*	This study
Bp420	1026b Δ*penA* Δ*tatABC*	This study
Bp343	1026b Δ*BPSS0945*	This study
Bp344	1026b Δ*BPSS0944*	This study
Bp349	1026b Δ*BPSS0948*	This study
Bp342	1026b PenA R7K	This study
Bp421	1026b PenA R8A	This study
	Strain Bp82-based mutants	
Bp82	1026b Δ*purM*	Propst et al. (2010)
Bp82.3	Bp82 PenA C69Y	This study
Bp82.4	Bp82 PenA S72F	This study
Bp82.5	Bp82 PenA P167S	This study
Bp82.11	Bp82 Δ*penA*	This study
Bp82.14	Km^r; Bp82:Tn*7*T-P_{s12}-FKM-*lox-BPSS0944*[a]	This study
Bp82.15	Km^r; Bp82:Tn*7*T-P_{s12}-FKM-*lox-BPSS0945*	This study
Bp82.16	Km^r; Bp82:Tn*7*T-P_{s12}-FKM-*lox-BPSS0948*	This study
Bp82.21	Km^r; Bp82:Tn*7*T-LAC-FKM-*penA*$^{+}$[b]	This study

[a] *Cloned genes are transcribed from the constitutive B. thailandensis ribosomal s12 gene promoter.*

[b] *Cloned penA gene is transcribed from the IPTG-inducible E. coli lactose operon/tryptophan hybrid promoter* P_{tac}.

MATERIALS AND METHODS

BACTERIAL STRAINS AND GROWTH CONDITIONS

Burkholderia pseudomallei strains used in this study are listed in **Table 1**. *E.* coli strains DH5α (Liss, 1987) and MACH1 (Invitrogen, Carlsbad, CA, USA) were used as general cloning strains, and DB3.1 (Invitrogen) for cloning with Gateway Vectors. RHO3 was used as a mobilizer strain for conjugation of plasmids from *E. coli* to *B. pseudomallei* (López et al., 2009). Bacterial strains were grown in Lennox LB (MO BIO Laboratories, Carlsbad, CA, USA) or LB without salt (10 g/L tryptone and 5 g/L yeast extract) at 37°C. Antibiotics were used

at the following concentrations: 100 μg/mL ampicillin (Amp), 35 μg/mL kanamycin (Km), and 15 μg/mL zeocin (Zeo) for *E. coli* and 1,000 μg/mL Km and 2,000 μg/mL Zeo for *B. pseudomallei*. Antibiotics were purchased from Sigma (St. Louis, MO, USA) except Zeo which was from Invitrogen. The Δ*purM* strain Bp82 was grown in media supplemented with 0.6 mM adenine to ensure growth rates comparable to strain 1026b. RHO3 was grown in media containing 400 μg/mL diaminopimelic acid (DAP; LL-, DD-, and meso-isomers; Sigma). Induction of gene expression from P_{tac} was achieved by adding 1 mM isopropyl β-d-1-thiogalactopyranoside (IPTG; Gold Biotechnology, St. Louis, MO, USA) to growth media.

ISOLATION OF MUTANTS CONTAINING CHROMOSOMAL DELETION OR POINT MUTATIONS

All deletion and allelic-exchange procedures were based on pEXKm5 (López et al., 2009; plasmids used in this study are listed in **Table 2**) and were performed using previously described protocols. The desired chromosomal deletions were verified by colony PCR (Choi et al., 2008).

For construction of *penA* deletion mutants, PCR with primers 1687 + 1712 (PCR primers and mutagenic oligonucleotides are listed in **Table 3**) and *Taq* polymerase (New England BioLabs, Ipswich, MA, USA) was used to amplify a 1,308-bp region containing the *BPSS0946* (*penA*) gene from 1026b chromosomal DNA. The gel-purified PCR fragment was cloned into the *Sma*I site of pUCP20 to yield pPS2370. This plasmid was then cleaved with *Nsi*I + *Pml*I, blunt ended with T4 DNA polymerase, followed by re-ligation. This procedure deleted a 291-bp *Nsi*I − *Pml*I fragment from the *penA* gene and resulted in pPS2549. A 1,339-bp *Pvu*II Δ*penA* fragment was excised from this plasmid and ligated into the *Sma*I site of pEXKm5 to create pPS2550. This plasmid was used to create Bp82.11 and Bp319 by transferring the plasmid-borne deletion alleles to either Bp82 or 1026b, respectively, via conjugation from RHO3.

For deletion of *tatABC,* splicing by overlap extension (SOEing) PCR was employed for engineering of deletion constructs. SOEing reactions consisted of separately amplifying two fragments, one using an "internal" primer with overlapping sequence with the internal primer from the other fragment. These bands were gel purified and 50 ng of each product was added to a new PCR reaction where it underwent PCR for five cycles (95˚C for 60 s, 54˚C 30 s, and 72˚C for 60 s). At this point, the two non-overlapping primers were added and the reaction proceeded for another 30 cycles. Using in-house purified *Pfu* polymerase and primer sets 2018 + 2019 (amplifying a 537-bp *tatA* 5′ fragment) and 2020 + 2021 (amplifying a 501-bp *tatC* 3′ fragment), a 1,038-bp SOEing PCR product was generated to delete 1,527 bp from the *tatABC* gene cluster. This PCR product was ligated into pGem-T Easy (Promega; Madison, WI, USA) to create pPS2612. An *Eco*RI fragment was rescued from this plasmid and inserted into pEXKm5 to create pPS2617, which was used to create Bp409 and Bp420 by transferring the plasmid-borne deletions to either 1026b or Bp319 (1026b Δ*penA*), respectively. PCR using primers 2047 + 2048 was used to confirm the deletion.

Other genes located in the *penA* region of the chromosome were deleted using a SOEing PCR strategy and pCR2.1 (Invitrogen) as TA cloning vector. The *BPSS0944* deletion construct was created using primer sets 2014 + 2015 and 2016 + 2017 to generate pPS2609, from which a *Bst*XI fragment was excised and inserted into the *Sma*I site of pEXKm5 to yield pPS2614. The *BPSS0945* deletion construct was generated using primer sets 2010 + 2011 and 2012 + 2013 to create pPS2610, from which an *Eco*RI fragment was excised and inserted into the *Eco*RI site of pEXKm5 to yield pPS2615. The *BPSS0948* deletion construct was created using primer sets 2006 + 2007 and 2008 + 2009 to generate pPS2611, from which an *Eco*RI fragment was excised and inserted into the *Eco*RI site of pEXKm5 to yield pPS2616. The plasmid-borne deletion alleles were transferred to the *B. pseudomallei* 1026b genome which resulted in strains Bp343, Bp344 and Bp349, respectively. Deletions were verified by colony PCR using primer sets 2045 + 2446, 2041 + 2042 and 2043 + 2044, respectively.

Chromosomal *penA* point mutations were engineered using the QuikChange Multi Kit (Stratagene, La Jolla, CA, USA), 5′-phosphorylated mutagenic oligonucleotides, and plasmid DNA templates. Mutagenic oligonucleotide 2075 was used with pPS2674 to create pPS2675 for the PenA C69Y mutation. A 736-bp *Eco*RI fragment from pPS2675 was then ligated into the *Eco*RI site of pEXKm5 to construct pPS2677. Plasmid pPS2712 was created as a platform for other mutations by ligating the *Nru*I–*Hinc*II containing *penA* fragment from pPS2676 into the *Sma*I site of pEXKm5. Employing pPS2712 template DNA, mutagenic oligonucleotides 2136 and 2137 were used separately to create pPS2721 and pPS2722 carrying PenA P167S and PenA S72F substitutions, respectively. Allelic exchange was carried out by conjugal transfer of pPS2677 (C69Y), pPS2721 (P167S), and pPS2722 (S72F) from RHO3 into Bp82. Mutations were verified by PCR amplifying and sequencing the region containing the expected mutation. TAT-signal sequence mutations were generated using a similar strategy. The R7K mutation was engineered using mutagenic oligonucleotide 2022 and pPS2674 to create pPS2613. The 736-bp *Eco*RI fragment from this plasmid was ligated into pEXKm5 to yield pPS2618. The R7K allele contained on this fragment was transferred to the 1026b genome which created Bp342. The mutagenic oligonucleotide 2076 was used with pPS2674 to engineer pPS2676 to create an R8A mutation. The 736-bp *Eco*RI fragment was excised from this plasmid and ligated into pEXKm5 to create pPS2678. The R8A allele contained on this fragment was transferred to the 1026b genome which created Bp421. The presence of the desired point mutations on plasmids and the genome was verified by DNA sequencing.

GENE COMPLEMENTATION AND OVEREXPRESSION USING SINGLE-COPY, CHROMOSOMALLY INTEGRATED MINI-Tn*7* VECTORS

The mini-Tn*7* system was used for introducing site-specific, stable insertions into the *B. pseudomallei* genome for purposes of gene complementation or overexpression (Choi et al., 2008). Tn*7* transposition was achieved by tri-parental mating involving RHO3 harboring the mini-Tn*7* vector, RHO3 containing the helper plasmid pTNS3 and the *B. pseudomallei* recipient strain, as previously described (Choi et al., 2006). Integration events were verified using primers Tn*7*L and either BPGLMS1, BPGLMS2, or BPGLMS3

Table 2 | Plasmids used in this study.

Designation	Description[a]	Source
PLASMIDS FOR *penA* DELETION AND OVEREXPRESSION		
pUCP20	Ap^r; Broad host-range cloning vector	West et al. (1994)
pEXKm5	Km^r; Allelic-exchange plasmid	López et al. (2009)
pTNS3	Ap^r; Tn*7* insertion helper plasmid	Choi et al. (2008)
pUC18T-mini-Tn*7*T-Km-LAC	Ap^r Km^r; Tn*7* cassette vector with P_{tac} and *lacI*^{q} for regulated expression of cloned genes	This study
pPS2370	Ap^r; pUCP20 with a 1,308 bp *penA* fragment (amplified with primers 1687 + 1712) inserted into *Sma*I site	This study
pPS2549	Ap^r; pPS2370 with 291 bp *Nsi*I-*Pml*I fragment deleted from *penA*	This study
pPS2550	Km^r; 1,339 bp *Pvu*II fragment from pPS2549 was inserted into the *Sma*I site of pEXKm5	This study
pPS2605	Ap^r Km^r; pCR2.1 with 1,230 bp *penA* fragment (amplified with primers 2003 + 2005)	This study
pPS2608	Ap^r Km^r; pCR2.1 with the 1,261 bp *penA* fragment from pPS2605 (amplified with primers 2003 + 2004 to modify the 5′ region)	This study
pPS2627	Ap^r Km^r; pUC18T-mini-Tn*7*T-Km-LAC with the 1,266 bp *penA* fragment from pPS2608	This study
PLASMIDS FOR *penA* PUTATIVE REGULATORY GENE DELETION AND OVEREXPRESSION		
pPS2609	Ap^r Km^r; 1,043 bp SOEing PCR product using primer sets 2014 + 2015 and 2016 + 2017 was ligated into pCR2.1	This study
pPS2610	Ap^r Km^r; 1,300 bp SOEing PCR product using primer sets 2010 + 2011 and 2012 + 2013 was ligated into pCR2.1	This study
pPS2611	Ap^r Km^r; 1,239 bp SOEing PCR product using primer sets 2006 + 2007 and 2008 + 2009 was ligated into pCR2.1	This study
pPS2614	Km^r; blunt ended 1,085 bp *Bst*XI fragment from pPS2609 ligated into *Sma*I site of pEXKm5	This study
pPS2615	Km^r; 1,316 bp *Eco*RI fragment from pPS2610 ligated into *Eco*RI site of pEXKm5	This study
pPS2616	Km^r; 1,255 bp *Eco*RI fragment from pPS2611 ligated into *Eco*RI site of pEXKm5	This study
pUC18-mini-Tn7T-Gm-Gateway	Ap^r Gm^r; mini-Tn*7*T-Gm with GATEWAY cassette. GenBank accession number AY737004	Choi et al. (2005)
pPS2735	Ap^r Km^r; pUC18T-mini-Tn*7*T-Km-*FRT* with P_{s12}	This study
pPS2737	Ap^r Km^r; Gateway-ready Tn*7* cassette vector with *s12* promoter toward insert (*Kpn*I-*Afe*I fragment containing 1,824 bp Gateway cassette from pPS1612 ligated into pPS2735 between *Kpn*I-*Stu*I)	This study
pPS2745	Km^r; Nested PCR with primers 2015 + 2016, then 2155 + 2156 for 1,051 bp fragment, cloned into pENTR-SD-D-TOPO	This study
pPS2746	Km^r; Nested PCR with primers 2013 + 2010, then 2157 + 2158 for 1,056 bp fragment, cloned into pENTR-SD-D-TOPO	This study
pPS2747	Km^r; Nested PCR with primers 2009 + 2006, then 2159 + 2160 for 1,456 bp fragment, cloned into pENTR-SD-D-TOPO	This study
pPS2748	Ap^r Km^r; Gateway LR recombination reaction with pPS2737 + pPS2745	This study
pPS2749	Ap^r Km^r; Gateway LR recombination reaction with pPS2737 + pPS2746	This study
pPS2750	Ap^r Km^r; Gateway LR recombination reaction with pPS2737 + pPS2747	This study
PLASMIDS FOR ENGINEERING OF TAT-SIGNAL SEQUENCE MUTATIONS		
pPS2674	Ap^r Km^r; 740 bp of the 5′ region of *penA* gene amplified with primers 2010 + 2011 and cloned into pCR2.1	This study
pPS2613	Ap^r Km^r; Mutagenic primer 2022 substituted AAG for CGC at bases 19-21 of *penA* in pPS2674 to provide a R7K substitution	This study
pPS2618	Km^r; 736 bp *Eco*RI fragment from pPS2676 ligated into *Eco*RI of pEXKm5	This study
pPS2676	Ap^r Km^r; Mutagenic primer 2076 substituted GC for CG at bases 22-23 of *penA* in pPS2674 to provide a R8A substitution	This study
pPS2678	Km^r; 736 bp *Eco*RI fragment from pPS2676 ligated into *Eco*RI of pEXKm5	This study
PLASMIDS FOR ENGINEERING OF *penA* POINT MUTATIONS		
pPS2675	Ap^r Km^r; Mutagenic primer 2075 mutated G to A at base 224 of *penA* to provide a C69Y substitution in pPS2674 sequence	This study
pPS2677	Km^r; 736 bp *Eco*RI fragment from pPS2675 ligated into *Eco*RI of pEXKm5	This study
pPS2712	Km^r; 1,094 bp *Nru*I-*Hinc*II fragment (entire *penA*) from pPS2370 ligated into the *Sma*I site of pEXKm5	This study

(Continued)

Table 2 | Continued

Designation	Description[a]	Source
PLASMIDS FOR ENGINEERING OF *penA* POINT MUTATIONS		
pPS2721	Km^r; Mutagenic primer 2136 mutated C to T at base 517 of *penA* to provide a P167S substitution using pPS2712 (pEXKm5-based)	This study
pPS2722	Km^r; Mutagenic primer 2137 C to T at base 233 of *penA* to provide a S72F mutation using pPS2712 (pEXKm5-based)	This study
PLASMIDS FOR *tatABC* DELETION		
pPS2612	Ap^r; 1,038 bp Soeing PCR product using primer sets 2018 + 2019 and 2020 + 2021 ligated into pGem-T Easy (Promega, Madison, WI, USA)	This study
pPS2617	Km^r; 1,058 bp *Eco*RI fragment from pPS2612 ligated into *Eco*RI of pEXKm5	This study

[a]*Ap, ampicillin; Km, kanamycin; Gm, gentamicin; Ps12, B. thailandensis ribosomal s12 gene promoter.*

(Choi et al., 2008). All Tn*7* mutants retained and used for further experimentation had insertions at the *glmS*2-associated Tn*7* insertion site.

For regulated *penA* expression and overproduction, the gene was PCR amplified from pPS2370 using primers 2003 + 2005 and *Pfu* polymerase and the 1,230-bp PCR product cloned into pCR2.1 (Invitrogen) to yield pPS2605. An optimized ribosome binding site (RBS) was introduced upstream of *penA* to create pPS2608 by PCR amplifying the *penA* region of pPS2605 with primers 2003 + 2004 and cloning the resulting 1,261 bp fragment into pCR2.1. (The amplicon was expected to be 1,295 bp but the 5′ end was truncated by 34 bp which did not affect the integrity of the *penA* gene.) An expression construct where *penA* was transcribed from the inducible P_{tac} was obtained by cloning the 1,300-bp *Eco*RI fragment from pPS2608 into pUC18T-mini-Tn*7*T-Km-LAC to create pPS2627. The mini-Tn*7* expression cassette from pPS2627 was integrated into the genome of Bp82 at the *glmS*2-associated Tn*7* integration site to form Bp82.21.

Constitutive expression of genes was achieved from chromosomally integrated mini-Tn*7* elements where the respective genes were transcribed from the *B. thailandensis s12* promoter (Choi et al., 2008). Nested PCR and *Pfu* polymerase was used to PCR amplify *BPSS0944* (primers 2015 + 2016 and 2155 + 2156), *BPSS0945* (primers 2010 + 2013 and 2157 + 2158), and *BPSS0948* (primers 2006 + 2009 and 2159 + 2160) from strain 1026b genomic DNA. Each PCR began with three cycles using only the outside set (listed first) then the inner set (listed second) was added for 30 more cycles. Inner primers were designed for use with the pENTR/SD/D-TOPO cloning vector (Invitrogen, Carlsbad, CA, USA), which provides a RBS and directionality, and created pPS2745, pPS2746, and pPS2747, respectively. These plasmids then underwent the Gateway LR recombination reaction (Invitrogen) with pPS2737, a mini-Tn*7* vector which enables constitutive expression from the *B. thailandensis s12* promoter (this promoter is directed toward the Gateway recombination cassette). To create pPS2737 the 1,824-bp Gateway-cassette-containing the *Kpn*I-*Afe*I fragment from pUC18-mini-Tn*7*T-Gm-Gateway was ligated into pPS2735 between the *Kpn*I and *Stu*I sites. This Gateway-compatible mini-Tn*7* element was used to create pPS2748, pPS2749, and pPS2750 for constitutive expression of *BPSS0944, BPSS0945,* and *BPSS0948*, respectively. The mini-Tn*7* elements contained on these plasmids were individually inserted at the *glmS*2 site of Bp82 with the help of pTNS3 to create Bp82.14, Bp82.15, and Bp82.16.

MIC DETERMINATIONS

MICs were determined following general procedures recommended by the Clinical and Laboratory Standards Institute (2010). However, since Δ*tatABC* mutants do not grow well in the presence of salts LB without salt was substituted for Mueller–Hinton Broth. MICs for ampicillin, carbenicillin, and BAL30072 (obtained from Basilea Pharmaceutica, Basel, Switzerland) were determined by the two-fold broth microdilution technique. Etest strips were used to determine MICs for amoxicillin, amoxicillin–clavulanic acid, ceftazidime, imipenem, meropenem, and piperacillin according to manufacturer's instructions (AB BioMérieux, Marcy l'Etoile, France). When needed, IPTG was added to media at a final concentration of 1 mM. The MICs were recorded after incubation at 37°C for 18–24 h.

QUANTIFICATION OF *penA* TRANSCRIPT LEVELS

Overnight cultures were subcultured into LB medium, grown to an $OD_{600\,nm}$ of 0.5 and RNA was extracted with the RNeasy Protect Bacteria Mini Kit (Qiagen, Valencia, CA, USA). cDNA was synthesized using the SuperScript III First-Strand Synthesis SuperMix for qRT-PCR (Invitrogen) and quantified using SYBR GreenER qPCR SuperMix for iCycler Instruments (Invitrogen) and the Bio-Rad iQ5 iCycler. The Bp23S-F + Bp23S-R primer set was used for the 23s rRNA housekeeping gene for data normalization and primers 2077 + 2078 were used to quantify the *penA* transcript. Data analyses were performed using the iCycler software. For induction studies with both wild-type and the mutants with constitutive regulatory gene expression or deletion several methods were employed. For salt stress testing, strains were grown in media with 150 mM NaCl or no NaCl according to Pumirat et al. (2009). For testing induction by β-lactams at sub-inhibitory levels, strains were subcultured into LB with 4-fold lower than MIC concentrations of either ceftazidime or carbenicillin until an $OD_{600\,nm}$ of 0.5 was reached. Induction was also tested with fourfold higher than MIC concentrations of ceftazidime, carbenicillin, imipenem, or penicillin G (2,000 μg/mL for penicillin G) by growing in LB to an $OD_{600\,nm}$ of 0.5, then adding β-lactams and shaking for an additional 2 h before RNA extraction, according to Trépanier et al. (1997).

Table 3 | Primers used in this study.

Primer	Sequence[a,b,c,d]	Source
CLONING/DELETION		
1687	5′-**GGATCC**GACGAGAGCTGATACGCTAG	This study
1712	5′-**AAGCTT**ATACCGGCATCGTTTCGCTG	This study
2003	5′- GAATTCGATACCGGCATCGTTTCG	This study
2004	5′-GATATCAGCCGTTGACTTAGTTGGTATTTCCGGAATATCATGCTGGTTCCGAATAA TTTTGTTTAACTTTAAGAAGGAGATATAC	This study
2005	5′-ACTTTAAGAAGGAGATATACATGAATCATTCTCCGTTGCGC	This study
2006	5′-CAATCTCGACGGAGCACG	This study
2007	5′-CTTGAATGCCCTGCAGATCTTGGCCGCTACAGATACGACAC[b]	This study
2008	5′-AAGATCTGCAGGGCATTCAAG	This study
2009	5′-GGTCATCGGGGACGAGTG	This study
2010	5′-CGAATAGCGGATGAGATCG	This study
2011	5′-GTTGTCTCGAGCATGAGCAAGGATTTTCTGACCGCTTACG	This study
2012	5′-TTGCTCATGCTCGAGACAAC	This study
2013	5′-AATGGGCGATACGGTAACAG	This study
2014	5′-ACGAGCTTCCGAAATACACG	This study
2015	5′-ATCGAGACGATTCGTTCAGC	This study
2016	5′-CGAGCATCTCAAAATTCATCC	This study
2017	5′-CGTGTATTTCGGAAGCTCGTTAATGGGCGATACGGTAACAG	This study
2018	5′- ATGAATCACGACCCGAACTG	This study
2019	5′- CTTGCTCTCGTCCTCTTCCTACGATCAGCAACACGATCAG	This study
2020	5′- AGGAAGAGGACGAGAGCAAG	This study
2021	5′- GACGAAGCTGCTGAACGTC	This study
2041	5′-AGATACGGCATCGGATTGAC	This study
2042	5′-GTCGCCGGCTGATTATTTC	This study
2043	5′-GCAACGCTTGTTTCAATACG	This study
2044	5′-GAAAGGCTCGGTCACGTTC	This study
2045	5′-AATTCGTCACACGAACATGC	This study
2046	5′-CGTCATTCCACCTTCCATTG	This study
2047	5′-AGGAGGTCTACCACCTGCAC	This study
2048	5′-TTTTGTTTGCCGCCATTC	This study
2187	5′-CGAGCTTTCGCTGTCCTATC	This study
2188	5′-CGTGATCTTCGTGTCCTTGAGTTGTGTCATTGCGCTTCTC	This study
2189	5′-TCAAGGACACGAAGATCACG	This study
2190	5′-CCGGCAATTGATCGAACTC	This study
2191	5′-CGATCAACGTGATCTTCGTG	This study
MUTAGENIC PRIMERS		
2022	5′Phos/-GAATCATTCTCCGTTG *AAG* CGCTCGCTGCTCGTCGCAGC	This study
2075	5′Phos/-GCTTTCCCGTTCT *A* CAGCACATCCAAGATGATGC	This study
2076	5′Phos/-GAATCATTCTCCGTTGCGC *GC* CTCGCTGCTCGTCGCAGC	This study
2136	5′Phos/-GCGCCGTGTTCAGCTCAG *A* CTCGCGGCGATCGAGC	This study
2137	5′Phos/-AAAGCATCATCTTG *A* ATGTGCTGCAGAACTGG	This study
REAL TIME PCR PRIMERS		
Bp23S-F	5′-GTAGACCCGAAACCAGGTGA	Mima and Schweizer (2010)
Bp23S-R	5′-CACCCCTATCCACAGCTCAT	Mima and Schweizer (2010)
2077	5′-GTTCTGCAGCACATCCAAGA	This study
2078	5′-CGGTGTTGTCGCTGTACTGA	This study
CLONING		
1687	5′-**GGATCC**GACGAGAGCTGATACGCTAG	This study
1712	5′-**AAGCTT**ATACCGGCATCGTTTCGCTG	This study
2010	5′-AGGCTGGCTGTACTTGAACG	This study
2011	5′-CGGGCGATATTCTGATGTC	This study

(Continued)

Table 3 | Continued

Primer	Sequence[a,b,c,d]	Source
TN7 INTEGRATION CONFIRMATION		
Tn*7*L	5′-ATTAGCTTACGACGCTACACCC	Choi et al. (2005)
BPGLMS1	5′-GAGGAGTGGGCGTCGATCAAC	Choi et al. (2008)
BPGLMS2	5′-ACACGACGCAAGAGCGGAATC	Choi et al. (2008)
BPGLMS3	5′-CGGACAGGTTCGCGCCATGC	Choi et al. (2008)

[a] *Bold indicates a newly generated restriction enzyme cleavage site.*

[b] *Underline indicates overlapping sequence for SOEing PCR; a double underline indicates a ribosome binding site.*

[c] *Italics indicates introduced point mutations.*

[d] *Phos, 5′ phosphorylated oligonucleotide.*

PROTEIN TECHNIQUES

Burkholderia pseudomallei cells were fractionated into periplasm and spheroplastic protein fractions (cytosol and membranes) using the PeriPreps™ Periplasting Kit (Epicentre Biotechnologies, Madison, WI, USA) Cells were grown overnight and diluted 1:100 at 37°C in LB medium without NaCl until an optical density of 0.7 (600 nm) was reached. The kit was used according to manufacturer's protocols, including extended incubation times and higher concentrations of lysozyme (25 μg/reaction), as recommended for hardier bacteria.

Escherichia coli Origami 2 *DE3* cells (Novagen, Madison, WI, USA) expressing bla_{penA} minus the first 90 nucleotides (30 amino acids) which encode the N-terminal signal sequence were subcloned in the pET24a(+) vector (Stratagene) and used for protein production and purification. The PenA β-lactamase was extracted from *E. coli* and purified using preparative isoelectric focusing. After verification of purity by SDS PAGE, 3.0 mg of PenA was sent to New England Peptide (Gardner, MA, USA) where the polyclonal anti-PenA antibodies were raised in rabbits. The antibodies were subsequently isolated from serum using a Protein G column (GE Healthcare Life Sciences, Piscataway, NJ, USA) purification according to the manufacturer's instructions.

For Western blots, protein samples were separated on NuPAGE® 4–12% Bis–Tris polyacrylamide gels (Invitrogen) alongside Precision Plus Protein Prestained Dual Color Standards (Bio-Rad, Hercules, CA, USA). A goat anti-Rabbit IgG alkaline phosphatase-conjugated antibody (Sigma) was used as a secondary antibody and SIGMAFAST™ BCIP®/NBT tablets (Sigma) as a detection reagent according to the manufacturer's protocol.

RESULTS

THE ROLE OF OF penA IN β-LACTAM RESISTANCE

To assess whether Bp82 and its parent 1026b could interchangeably be used for PenA characterization experiments, the susceptibilities of these strains to various β-lactams were tested. Observable differences in the susceptibilities of these two strains for any of the beta-lactams and clavulanic acid tested (**Table 4**) were not seen, thereby validating the use of Bp82 in experiments otherwise not feasible under Select Agent regulations. Deletion of the *penA* gene from 1026b (strain Bp319) and Bp82 (strain Bp82.11) caused a significant (≥4-fold) decrease in the susceptibilities for six of nine β-lactams tested, and ≥16-fold for three of them (ampicillin, amoxicillin, and carbenicillin; **Table 4**). Likewise, up-regulation of *penA* by single-copy expression from the IPTG-inducible P_{tac} (Bp82.21) significantly increased the MIC for seven of the eight β-lactams tested with meropenem showing only slight change. (Amoxicillin could not be tested as the resistance level for the wild-type was already beyond detection.) Quantitative real time PCR experiments showed that in the P_{tac}-*penA* strain (Bp82.21) *penA* transcript levels were 36-fold higher when compared to transcript levels observed in the wild-type strain (data not shown). This increase in transcript levels corresponds to the observed increases in resistance to all β-lactams. These experiments demonstrated that although PenA is a clinically significant β-lactam resistance mechanism, it affects some β-lactams more than others. While mutations in *penA* can significantly affect the utility of ceftazidime and amoxicillin + clavulanic acid, the enzyme has a lesser effect on the activity of carbapenems and novel experimental drugs such as BAL30072.

penA MUTATIONS ARE RESPONSIBLE FOR CLINICALLY SIGNIFICANT CEFTAZIDIME AND AMOXICILLIN + CLAVULANIC ACID RESISTANCE

Previous studies identified several *penA* mutations in clinical and laboratory isolates that led to clinically significant ceftazidime or clavulanic acid resistance. Specifically, a C69Y substitution caused high-level ceftazidime resistance (Sam et al., 2009), a P167S substitution medium-level ceftazidime resistance (Tribuddharat et al., 2003), and a S72F mutation resistance to clavulanic acid (Tribuddharat et al., 2003). To assess whether these mutations alone were sufficient to cause the observed resistance phenotypes, they were engineered into the *penA* gene of strain Bp82 resulting in expression of a mutated PenA from the native *penA* promoter. Susceptibility studies revealed that the C69Y (Bp82.3) and P167S (Bp82.5) point mutations caused significant increases in ceftazidime resistance of ≥85- and 5- to 8-fold, respectively (**Table 4**). These changes are clinically significant since the ceftazidime susceptibility, intermediate and resistance breakpoints are defined as MICs of ≤8, 16, and ≥32 μg/mL, respectively. The C69Y mutation sensitized strains to other β-lactams such as amoxicillin, ampicillin, carbenicillin, and imipenem but not amoxicillin + clavulanic acid, piperacillin, meropenem, and BAL30072, whose MICs were already at low levels. The S72F point mutation caused a four-fold increase in resistance to amoxicillin + clavulanic acid in the resulting strain Bp82.4 and did not cause any changes in susceptibility to other β-lactams.

Table 4 | β-lactam susceptibilities of PenA, TAT-signal sequence, and TAT secretion apparatus mutants.

		MIC (μg/mL)								
Strain[a]	**Mutation**	**Amoxicillin**	**Amoxicillin + clavulanic acid**	**Ampicillin**	**Piperacillin**	**Carbenicillin**	**Ceftazidime**	**Imipenem**	**Meropenem**	**BAL30072**
1026b	None	≥256[b]	3	256	8	1024	3	1.5	0.75	0.065
Bp82	None[c]	≥256	3	128	8	1024	3	1.5	0.75	0.031
Bp319	Δ*penA*	6	3	8–16	2	32	2	0.25	0.75	0.016
Bp82.11	Δ*penA*	ND	3	ND	ND	ND	ND	ND	ND	ND
Bp82.21	Tn*7-penA* + IPTG	≥256	16	2048	64	>4096	32	16	1.5	0.25
Bp82.3	PenA C69Y	6	3	4–8	6–8	32–64	≥256	0.19	0.75	0.031
Bp82.4	PenA S72F	≥256	12–16	64–128	8	512	3	1–2	0.75	0.031
Bp82.5	PenA P167S	6	3	4–8	4	32–64	16–24	0.19	0.5–0.75	0.031
Bp409	Δ*tatABC*	4–6	3	4–8	3	16–32	1.5	0.19	0.5	0.016
Bp420	Δ*penA* Δ*tatABC*	4	3	4	2	16	1	0.25	0.05	0.016
Bp342	PenA R7K	≥256	3	128	8	1024	3	2	0.75	0.031
Bp421	PenA R8A	8	3	8	2	32	1	0.25	0.5	0.031

[a] *Bp319, Bp342, Bp409, Bp420, and Bp421 were derived from 1026b; Bp82.11 and Bp82.21 were derived from Bp82.*

[b] *≥256, the detection limit is 256 μg/mL.*

[c] *No penA or tat mutation but strain is a 1026b ΔpurM derivative.*

ND, not done.

PenA IS SECRETED VIA THE TAT SYSTEM

Analysis of the amino-terminal PenA amino acid sequence revealed the presence of a putative TAT-signal sequence indicating that it may be a TAT secreted protein (**Figure 1**). To test this notion, the two signature arginine residues at positions 7 and 8 were changed to a lysine or alanine, respectively. MIC determinations revealed that disruption of the TAT-signal sequence by an R7K mutation (Bp342) did not affect PenA activity. This is in accordance with previous studies which have shown that mutation of the first arginine to a lysine can either have little effect or be completely inhibitory, depending on the rest of the signal sequence (Stanley et al., 2000). However, an R8A substitution (Bp421) completely abrogated PenA activity, consistent with PenA being a TAT secreted enzyme. This notion was further supported by the finding that a *tatABC* deletion mutant (Bp409) exhibited a susceptibility profile similar to those of the R8A substitution (Bp421) and Δ*penA* deletion strains (Bp319 and Bp82.11). As expected then, a Δ*penA* Δ*tatABC* double mutant (Bp420) was most susceptible to PenA substrates.

CELLULAR LOCALIZATION OF PenA

We next attempted to localize the PenA protein in the cell envelope using Western blot analysis and polyclonal α-PenA antibodies. Using this method, PenA could not be localized to the periplasmic fraction but rather only to the spheroplastic fraction which contains both cytosolic and membrane proteins. Multiple attempts at isolation of PenA from the periplasmic fraction employing other fractionation methods such as chloroform (Ames et al., 1984) or magnesium chloride (Imperi et al., 2009) extraction yielded the same results. Western blot analysis of the spheroplastic fraction (**Figure 2**) showed the mature 27 kDa PenA protein is seen only in an extract derived from wild-type 1026b (lane 5). In contrast, the unprocessed 31 kDa PenA protein was observed in extracts from the R8A (lane 1) and Δ*tatABC* (lane 2) mutants Bp421 and Bp409, respectively. A mixture of mature and unprocessed PenA was seen in the R7K mutant Bp342 extract with the majority being the mature protein (lane 3). As expected, no PenA protein was observed in the extract from the Δ*penA* mutant Bp319 (lane 4). This experiment provides biochemical evidence for PenA processing only in 1026b and the R7K mutants, both of which secrete active PenA via the TAT system as judged by β-lactam susceptibility assays. All other strains are susceptible to β-lactams.

LOCAL REGULATORS ARE NOT INVOLVED IN REGULATION OF *penA* GENE EXPRESSION

As shown in **Figure 1**, the *B. pseudomallei penA* region encodes two LysR-type transcriptional regulators and a putative peptidase. Since chromosomal β-lactamase gene expression was shown to be regulated by products of adjacent regulatory genes in several bacteria, including *B. cepacia* (Trépanier et al., 1997), the structural genes encoding for these regulators were either deleted or overexpressed and their effects on PenA transcription and activity assessed by either qRT-PCR or MIC determinations. Carbenicillin was used as a "sentry" β-lactam for assessing PenA activity by MIC experiments because it is one of the best PenA substrates (**Table 4**). MIC determinations showed that neither deletion of putative regulators (Bp343 and Bp349 nor constitutive expression of the regulators (Bp82.14 and Bp82.16) affected PenA activity (data not shown). The same observations were made when ceftazidime was used in susceptibility assays instead of carbenicillin. Likewise, deletion (Bp344 and Bp82.31) or overexpression (Bp82.15) of the putative peptidase gene upstream of *penA* had no effect on PenA activity (data not shown). Lastly, since bacterial β-lactamase gene expression can either be subject to substrate induction or influenced by environmental factors such as salts (Pumirat et al., 2009), MIC determinations were performed in the presence or absence of substrate and salt. However, presence of ceftazidime, carbenicillin, or high salt and the absence salt had no apparent effect on β-lactam susceptibilities. qRT-PCR assays supported the MIC data, with no change in *penA* expression levels observed between controls and strains treated with ceftazidime, carbenicillin, imipenem, penicillin G, or high salt (data not shown).

DISCUSSION

The data presented in this study employing isogenetic mutants in a defined genetic background confirm that PenA is a major β-lactam resistance factor in *B. pseudomallei*. Increased expression of *penA* conferred increased resistance levels to the majority of β-lactams tested. Conversely, *penA* deletion resulted in susceptibility to all β-lactams tested. Furthermore, clinically observed *penA* mutations were responsible for the altered β-lactam substrate spectrum of the enzyme and consequently the new resistance profile. Point mutations near the active site are the most common reason for substrate profile shifting because they accommodate different side chains of various β-lactams by either changing the active site steric properties or locations of the actual active residues (Drawz and Bonomo, 2010). Complete shifts in substrate profiles have been previously documented, such as with a mutant gram negative TEM-1 β-lactamase showing increased ceftazidime hydrolysis but decreased activity against ampicillin (Venkatachalam et al., 1994). The good news is that the *B. pseudomallei* C69Y PenA mutation sensitizes the cell to other β-lactams thus possibly enabling new therapeutic strategies. Additionally, our studies showed that of all β-lactams tested meropenem is the only β-lactam not affected

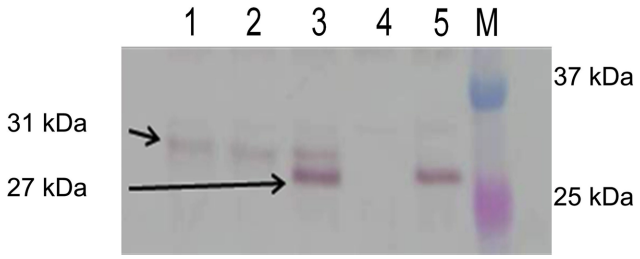

FIGURE 2 | PenA is a TAT secreted protein. Spheroplastic proteins were analyzed by Western blot using anti-PenA polyclonal antibodies. The arrows point to the expected unprocessed (31 kDa) and processed (27 kDa) forms of PenA. Lanes: 1, R8A TAT-signal sequence mutant; 2, Δ*tatABC* mutant; 3, R7K TAT signal sequence mutant; 4, Δ*penA* mutant; 5, wild-type 1026b; M, molecular weight markers (two proteins of the 10- to 250-kDa Precision Plus Protein Dual Color Standards from Bio-Rad, Hercules, CA, USA).

by *penA* mutations and overproduction, and thus the superior β-lactam antibiotic for melioidosis treatment with regard to potential emergence of PenA β-lactamase mutants. Unfortunately, current costs limit use of meropenem in many clinical settings, especially resource poor areas of the world (Cheng et al., 2004).

The mutants created and analyzed in this study did not precisely mimic previously documented mutants. In all cases, our strains had an equal or lower resistance level. This may simply be due to variations in MIC methodologies, which can change the measurements significantly (Wuthiekanun et al., 2005, or *B. pseudomallei* strain variability that may affect resistance patterns (Thibault et al., 2004). Using the S72F clinical mutant as an example, two groups determined the MIC of the parental strain 392a and its mutant, 392f. The first group showed a 16-fold increase in amoxicillin–clavulanic acid resistance (Godfrey et al., 1991) but the other group only showed a two-fold increase (Tribuddharat et al., 2003). These numbers are significantly different from one another. The susceptibilities observed with our isogenetic Bp82 derivatives fell between the two previously reported set of numbers at 4- to 5- fold. Another potential cause for inconsistency was that some of the published experiments cloned the mutant *penA* gene and expressed it in an unrelated bacterium, *E. coli*, from a high-copy number plasmid (Ho et al., 2002; Tribuddharat et al., 2003). Our data showed that increased expression of *penA* from a single-copy, chromosomally inserted expression element with a strong inducible promoter can change the profile from susceptible to resistant. A high-copy number plasmid will obviously lead to higher gene expression and consequently high resistance levels. Additionally, other cellular factors, including outer membrane permeability, can affect the efficacy of resistance mechanisms. For the P167S mutation, Tribuddharat et al. (2003) showed a 16-fold increase in ceftazidime resistance in *B. pseudomallei*, but only a two-fold change in an *E. coli* strain expressing recombinant *penA* genes.

Besides playing a crucial role in the export of virulence factors in many bacteria (De Buck et al., 2008), the TAT system has previously been shown to be required for the export of β-lactamases in *Mycobacterium smegmatis* (McDonough et al., 2005). Through deletion of the *tatABC* operon and mutation of a crucial arginine residue of the putative TAT-signal sequence of *B. pseudomallei* PenA, we showed that PenA is indeed a TAT secreted enzyme. The exact cellular location of PenA β-lactamase could not be pinpointed. Various periplasmic extraction techniques failed to localize the enzyme to the periplasm but rather indicated that it is localized in the spheroplastic compartments of the cell which encompasses the cytosol and the membranes. Since a secreted enzyme is unlikely to be localized in the cytosol this experimental evidence points to the fact that PenA may be a membrane-associated enzyme. This is in agreement with earlier findings by Livermore et al. (1987) who demonstrated that after sonication and centrifugation, the vast majority of β-lactamase activity was present in the membrane fraction. Membrane association of β-lactamases is not common but has been documented. The first account of a membrane-associated β-lactamase in Gram negative bacteria was from work with *Moraxella catarrhalis* (Bootsma et al., 1999). In this case it was hypothesized that the gene was a lipoprotein of Gram positive origin, as membrane association in Gram positive bacteria had been previously observed. This is unlikely the case for PenA because *penA* has 70% GC content, comparable to the overall genome (68%). How *B. pseudomallei* PenA could become membrane associated is unclear since there is no evidence of the enzyme being a lipoprotein.

Further evidence for TAT secretion was obtained by analyzing the PenA processing. Tullman-Ercek et al. (2007) describe the processing of TAT-signal sequences and the cleavage of their amino-termini upon passing through the inner membrane, using MdoD as an example. The authors describe a hydrophobic region before the processing site determined to be an AXA motif. A comparative analysis of the amino-termini of MdoD (MDRRRFKGSMAMAAVCGTSGASLFSQAAFA) and PenA (MNHSPLRRSLLVAAISTPLIGACAOLRGQAKNVAAA) at http://expasy.org/tools/protscale.html using the Kyte and Doolittle hydrophobicity algorithm revealed that the two sequences exhibited a similar hydrophobicity profile and comparable predicted processing sites (underlined AFA in MdoD and AAA in PenA). Using this information, we calculated that the molecular mass of PenA changes from 31 to 27 kDa after processing. Bands corresponding to these sizes were seen observed using Western blot analysis (**Figure 2**).

Some β-lactamase genes require LysR regulatory factors for expression, with or without a β-lactam inducer. Trépanier et al. (1997) showed that the *penA* gene from *B. cepacia* was regulated by a LysR-family regulator encoded by the divergently transcribed *penR* gene when expressed from plasmids in *E. coli*. PenA β-lactamase gene expression was not only regulated by PenR but was also inducible in the presence of imipenem in this system. A gene, *BPSS0948*, homologous to *B. cepacia penR* is found in *B. pseudomallei* downstream of *penA* (**Figure 1**). An additional LysR-family regulator encoding gene, *BPSS0944*, is located upstream of *penA*, but it has less sequence homology to *penR* and is separated from *penA* by a putative peptidase gene. Our analyses involving gene deletions, induction experiments, as well as growing cells under conditions such as salt stress (Pumirat et al., 2009 that may trigger β-lactamase induction showed that neither the LysR-type regulators BPSS0944 and BPSS0948 nor the putative peptidase encoded by *BPSS0945* are involved in regulation of *penA* expression in *B. pseudomallei* strain 1026b, at least not under the experimental conditions employed during these studies. Although many chromosomal β-lactamases are inducible, others are constitutively expressed (Neu and Chin, 1985; Jacoby and Bush, 2005). When multiple β-lactamases are present in a bacterial strain, they can be subject to complex regulation, including co-regulation with penicillin binding protein 2 (Hackbarth and Chambers, 1993; Naas et al., 1995). In this context it is noteworthy that by analysis of clinical strains obtained from patients that failed ceftazidime therapy and studies of recreated 1026b-based mutants we and others recently identified deletion of a *B. pseudomallei* PBP3 homolog as a mechanism causing high-level ceftazidime resistance (Chantratita et al., unpublished observations).

Definition of the molecular basis of resistance mechanisms for clinically significant β-lactams forms the basis for design of diagnostic tools that allow rapid detection of emergence of resistance and thus redirection (clinical settings) or initiation (biodefense) of proper melioidosis therapy or prophylaxis.

ACKNOWLEDGMENTS

This work was supported by grant AI065357 from the National Institutes of Health-National Institute for Allergies and Infectious Diseases to Herbert P. Schweizer and Michael L. Vasil. We thank Lily Trunck for constructing pUC18T-mini-Tn*7*T-Km-LAC. The Veterans Affairs Career Development Program (Krisztina M. Papp-Wallace), the Veterans Affairs Merit Review Program (Robert A. Bonomo), the National Institutes of Health (RO1 AI063517-01 to Robert A. Bonomo), and the Veterans Integrated Service Network 10 Geriatric Research, Education, and Clinical Center (VISN 10 GRECC) also supported this work. BAL30072 was provided by Basilea Pharmaceutica International, Ltd., Basel, Switzerland.

REFERENCES

Ames, G. F., Prody, C., and Kustu, S. (1984). Simple, rapid, and quantitative release of periplasmic proteins by chloroform. *J. Bacteriol.* 160, 1181–1183.

Bootsma, H. J., Aerts, P. C., Posthuma, G., Harmsen, T., Verhoef, J., van Dijk, H., and Mooi, F. R. (1999). *Moraxella* (*Branhamella*) *catarrhalis* BRO β-lactamase: a lipoprotein of Gram-positive origin? *J. Bacteriol.* 181, 5090–5093.

Cheng, A. C., and Currie, B. J. (2005). Melioidosis: epidemiology, pathophysiology, and management. *Clin. Microbiol. Rev.* 18, 383–416.

Cheng, A. C., Fisher, D. A., Anstey, N. M., Stephens, D. P., Jacups, S. P., and Currie, B. J. (2004). Outcomes of patients with melioidosis treated with meropenem. *Antimicrob. Agents Chemother.* 48, 1763–1765.

Cheung, T. K., Ho, P. L., Woo, P. C., Yuen, K. Y., and Chau, P. Y. (2002). Cloning and expression of class A beta-lactamase gene *blaA*(BPS) in *Burkholderia pseudomallei*. *Antimicrob. Agents Chemother.* 46, 1132–1135.

Choi, K.-H., DeShazer, D., and Schweizer, H. P. (2006). mini-Tn*7* insertion in bacteria with multiple *glmS*-linked *att*Tn*7* sites: example *Burkholderia mallei* ATCC 23344. *Nat. Protoc.* 1, 162–169.

Choi, K.-H., Gaynor, J. B., White, K. G., López, C., Bosio, C. M., Karkhoff-Schweizer, R. R., and Schweizer, H. P. (2005). A Tn*7*-based broad-range bacterial cloning and expression system. *Nat. Methods* 2, 443–448.

Choi, K.-H., Mima, T., Casart, Y., Rholl, D., Kumar, A., Beacham, I. R., and Schweizer, H. P. (2008). Genetic tools for select agent compliant manipulation of *Burkholderia pseudomallei*. *Appl. Environ. Microbiol.* 74, 1064–1075.

Clinical and Laboratory Standards Institute. (2010). *Performance Standards for Antimicrobial Susceptibility* testing: *Twentieth Informal Supplement M100-S20*. Wayne, PA.

Currie, B. J., Dance, D. A. B., and Cheng, A. C. (2008). The global distribution of *Burkholderia pseudomallei* and melioidosis: an update. *Trans. R. Soc. Trop. Med. Hyg.* 102, S1–S4.

De Buck, E., Lammertyn, E., and Anné, J. (2008). The importance of the twin-arginine translocation pathway for bacterial virulence. *Trends Microbiol.* 19, 442–453.

DeShazer, D., Brett, P., Carlyon, R., and Woods, D. (1997). Mutagenesis of *Burkholderia pseudomallei* with Tn*5*-OT182: isolation of motility mutants and molecular characterization of the flagellin structural gene. *J. Bacteriol.* 179, 2116–2125.

Drawz, S. M., and Bonomo, R. A. (2010). Three decades of beta-lactamase inhibitors. *Clin. Microbiol. Rev.* 23, 160–201.

Godfrey, A. J., Wong, S., Dance, D. A., Chaowagul, W., and Bryan, L. E. (1991). *Pseudomonas pseudomallei* resistance to beta-lactam antibiotics due to alterations in the chromosomally encoded beta-lactamase. *Antimicrob. Agents Chemother.* 35, 1635–1640.

Hackbarth, C. J., and Chambers, H. F. (1993). *blaI* and *blaR1* regulate beta-lactamase and PBP 2a production in methicillin-resistant *Staphylococcus aureus*. *Antimicrob. Agents Chemother.* 37, 1144–1149.

Ho, P. L., Cheung, T. K., Yam, W. C., and Yuen, K. Y. (2002). Characterization of a laboratory-generated variant of BPS beta-lactamase from *Burkholderia pseudomallei* that hydrolyses ceftazidime. *J. Antimicrob. Chemother.* 50, 723–726.

Holden, M. T. G., Titball, R. W., Peacock, S. J., Cerdeño-Tárraga, A. M., Atkins, T., Crossman, L. C., Pitt, T., Churcher, C., Mungall, K., Bentley, S. D., Sebaihia, M., Thomson, N. R., Bason, N., Beacham, I. R., Brooks, K., Brown, K. A., Brown, N. F., Challis, G. L., Cherevach, I., Chillingworth, T., Cronin, A., Crossett, B., Davis, P., DeShazer, D., Feltwell, T., Fraser, A., Hance, Z., Hauser, H., Holroyd, S., Jagels, K., Keith, K. E., Maddison, M., Moule, S., Price, C., Quail, M. A., Rabbinowitsch, E., Rutherford, K., Sanders, M., Simmonds, M., Songsivilai, S., Stevens, K., Tumapa, S., Vesaratchavest, M., Whitehead, S., Yeats, C., Barrell, B. G., Oyston, P. C. F., and Parkhill, J. (2004). Genomic plasticity of the causative agent of melioidosis, *Burkholderia pseudomallei*. *Proc. Natl. Acad. Sci. U.S.A.* 101, 14240–14245.

Imperi, F., Tiburzi, F., and Visca, P. (2009). Molecular basis of pyoverdine siderophore recycling in *Pseudomonas aeruginosa*. *Proc. Natl. Acad. Sci. U.S.A.* 106, 20440–20445.

Jacoby, G. A., and Bush, K. (2005). "Beta-lactam resistance in the 21st century," in *Frontiers in Antimicrobial Resistance: A Tribute to Stuart B. Levy*, eds D. G. White, M. N. Alekshun, and P. F. McDermot (Washington, DC: ASM Press), 53–65.

Keith, K. E., Oyston, P. C., Crossett, B., Fairweather, N. F., Titball, R. W., Walsh, T. R., and Brown, K. A. (2005). Functional characterization of OXA-57, a class D beta-lactamase from *Burkholderia pseudomallei*. *Antimicrob. Agents Chemother.* 49, 1639–1641.

Liss, L. (1987). New M13 host: DH5αF′ competent cells. *Focus* 9, 13.

Livermore, D. M., Chau, P. Y., Wong, A. I., and Leung, Y. K. (1987). Beta-lactamase of *Pseudomonas pseudomallei* and its contribution to antibiotic resistance. *J. Antimicrob. Chemother.* 20, 313–321.

López, C. M., Rholl, D. A., Trunck, L. A., and Schweizer, H. P. (2009). Versatile dual-technology system for markerless allele replacement in *Burkholderia pseudomallei*. *Appl. Environ. Microbiol.* 75, 6496–6503.

McDonough, J. A., Hacker, K. E., Flores, A. R., Pavelka, M. S. Jr., and Braunstein, M. (2005). The twin-arginine translocation pathway of *Mycobacterium smegmatis* is functional and required for the export of mycobacterial beta-lactamases. *J. Bacteriol.* 187, 7667–7679.

Mima, T., and Schweizer, H. P. (2010). The BpeAB-OprB efflux pump of *Burkholderia pseudomallei* 1026b does not play a role in quorum sensing, virulence factor production, or extrusion of aminoglycosides but is a broad-spectrum drug efflux system. *Antimicrob. Agents Chemother.* 54, 3113–3120.

Naas, T., Livermore, D. M., and Nordmann, P. (1995). Characterization of an LysR family protein, SmeR from *Serratia marcescens* S6, its effect on expression of the carbapenem-hydrolyzing beta-lactamase Sme-1, and comparison of this regulator with other beta-lactamase regulators. *Antimicrob. Agents Chemother.* 39, 629–637.

Neu, H. C., and Chin, N. X. (1985). A perspective on the present contribution of beta-lactamases to bacterial resistance with particular reference to induction of beta-lactamase and its clinical significanceinduction of beta-lactamase and its clinical significance. *Chemioterapia* 4, 63–70.

Peacock, S. J., Schweizer, H. P., Dance, D. A. B., Smith, T. L., Gee, J. E., Wuthiekanun, V., DeShazer, D., Steinmetz, I., Tan, P., and Currie, B. J. (2008). Consensus guidelines on the management of accidental laboratory exposure to *Burkholderia pseudomallei* and *Burkholderia mallei*. *Em. Infect. Dis.* 14, e2.

Propst, K. L., Mima, T., Choi, K.-H, Dow, S. W., and Schweizer, H. P. (2010). A *Burkholderia pseudomallei* Δ*purM* mutant is avirulent in immune competent and immune deficient animals:

candidate strain for exclusion from select agent lists. *Infect. Immun.* 78, 3136–3143.

Pumirat, P., Saetun, P., Sinchaikul, S., Chen, S. T., Korbsrisate, S., and Thongboonkerd, V. (2009). Altered secretome of *Burkholderia pseudomallei* induced by salt stress. *Biochim. Biophys. Acta* 1794, 898–904.

Sam, I. C., See, K. H., and Puthucheary, S. D. (2009). Variations in ceftazidime and amoxicillin-clavulanate susceptibilities within a clonal infection of *Burkholderia pseudomallei*. *J. Clin. Microbiol.* 47, 1556–1558.

Stanley, N. R., Palmer, T., and Berks, B. C. (2000). The twin arginine consensus motif of Tat signal peptides is involved in Sec-independent protein targeting in *Escherichia coli*. *J. Biol. Chem.* 275, 11591–11596.

Thibault, F. M., Hernandez, E., Vidal, D. R., Girardet, M., and Cavallo, J. D. (2004). Antibiotic susceptibility of 65 isolates of *Burkholderia pseudomallei* and *Burkholderia mallei* to 35 antimicrobial agents. *J. Antimicrob. Chemother.* 54, 1134–1138.

Trépanier, S., Prince, A., and Huletzky, A. (1997). Characterization of the *penA* and *penR* genes of *Burkholderia cepacia* 249 which encode the chromosomal class A penicillinase and its LysR-type transcriptional regulator. *Antimicrob. Agents Chemother.* 41, 2399–2405.

Tribuddharat, C., Moore, R. A., Baker, P., and Woods, D. E. (2003). *Burkholderia pseudomallei* class a beta-lactamase mutations that confer selective resistance against ceftazidime or clavulanic acid inhibition. *Antimicrob. Agents Chemother.* 47, 2082–2087.

Tullman-Ercek, D., DeLisa, M. P., Kawarasaki, Y., Iranpour, P., Ribnicky, B., Palmer, T., and Georgiou, G. (2007). Export pathway selectivity of *Escherichia coli* twin arginine translocation signal peptides. *J. Biol. Chem.* 282, 8309–8316.

Venkatachalam, K. V., Huang, W., LaRocco, M., and Palzkill, T. (1994). Characterization of TEM-1 beta-lactamase mutants from positions 238 to 241 with increased catalytic efficiency for ceftazidime. *J. Biol. Chem.* 269, 23444–23450.

West, S. E. H., Schweizer, H. P., Dall, C., Sample, A. K., and Runyen-Janecky, L. J. (1994). Construction of improved *Escherichia-Pseudomonas* shuttle vectors derived from pUC18/19 and the sequence of the region required for their replication in *Pseudomonas aeruginosa*. *Gene* 128, 81–86.

White, N. J., Dance, D. A., Chaowagul, W., Wattanagoon, Y., Wuthiekanun, V., and Pitakwatchara, N. (1989). Halving of mortality of severe melioidosis by ceftazidime. *Lancet* 2, 697–701.

Wiersinga, W. J., van der Poll, T., White, N. J., Day, N. P., and Peacock, S. J. (2006). Melioidosis: insights into the pathogenicity of *Burkholderia pseudomallei*. *Nat. Rev. Microbiol.* 4, 272–282.

Wuthiekanun, V., Cheng, A. C., Chierakul, W., Amornchai, P., Limmathurotsakul, D., Chaowagul, W., Simpson, A. J. H., Short, J. M., Wongsuvan, G., Maharjan, B., White, N. J., and Peacock, S. J. (2005). Trimethoprim/sulfamethoxazole resistance in clinical isolates of *Burkholderia pseudomallei*. *J. Antimicrob. Chemother.* 55, 1029–1031.

Conflict of Interest Statement: The authors declare that the research was conducted in the absence of any commercial or financial relationships that could be construed as a potential conflict of interest.

Received: 05 May 2011; paper pending published: 01 June 2011; accepted: 14 June 2011; published online: 01 July 2011.
Citation: Rholl DA, Papp-Wallace KM, Tomaras AP, Vasil ML, Bonomo RA and Schweizer HP (2011) Molecular investigations of PenA-mediated β-lactam resistance in Burkholderia pseudomallei. Front. Microbio. ***2****:139. doi: 10.3389/fmicb.2011.00139*
This article was submitted to Frontiers in Cellular and Infection Microbiology, a specialty of Frontiers in Microbiology.

frontiers in
MICROBIOLOGY

REVIEW ARTICLE
published: 15 July 2011
doi: 10.3389/fmicb.2011.00151

Autotransporters and their role in the virulence of *Burkholderia pseudomallei* and *Burkholderia mallei*

Natalie R. Lazar Adler[1], Joanne M. Stevens[2], Mark P. Stevens[2] and Edouard E. Galyov[1]*

[1] Department of Infection, Immunity and Inflammation, University of Leicester, Leicester, UK
[2] The Roslin Institute and Royal (Dick) School of Veterinary Studies, University of Edinburgh, Easter Bush, UK

Edited by:
Alfredo G. Torres, University of Texas Medical Branch, USA

Reviewed by:
Peggy Cotter, University of North Carolina, Chapel Hill, USA
Fernando Navarro-Garcia, Center for Research and Advanced Studies, Mexico

***Correspondence:**
Edouard E. Galyov, Department of Infection, Immunity and Inflammation, University of Leicester, Medical Sciences Building, Leicester, LE1 9HN, UK.
e-mail: eg98@leicester.ac.uk

Burkholderia pseudomallei and *Burkholderia mallei* are closely related Gram-negative bacteria responsible for the infectious diseases melioidosis and glanders, respectively. Autotransporters (ATs) comprise a large and diverse family of secreted and outer membrane proteins that includes virulence-associated invasins, adhesins, proteases, and actin-nucleating factors. The *B. pseudomallei* K96243 genome contains 11 predicted ATs, eight of which share homologs in the *B. mallei* ATCC 23344 genome. This review distils key findings from *in silico, in vitro*, and *in vivo* studies on the ATs of *B. pseudomallei* and *B. mallei*. To date, the best characterized of the predicted ATs of *B. pseudomallei* and *B. mallei* is BimA, a predicted trimeric AT mediating actin-based motility which varies in sequence and mode of action between *Burkholderia* species. Of the remaining eight predicted *B. pseudomallei* trimeric autotransporters, five of which are also present in *B. mallei*, two (BoaA and BoaB), have been implicated in bacterial adhesion to epithelial cells. Several predicted *Burkholderia* ATs are recognized by human humoral and cell-mediated immunity, indicating that they are expressed during infection and may be useful for diagnosis and vaccine-mediated protection. Further studies on the mode of secretion and functions of *Burkholderia* ATs will facilitate the rational design of control strategies.

Keywords: ***Burkholderia pseudomallei, Burkholderia mallei,* autotransporter, secreted, protein**

BURKHOLDERIA PSEUDOMALLEI AND *BURKHOLDERIA MALLEI*

Melioidosis, a febrile illness with disease states ranging from acute pneumonia or septicemia to chronic or localized abscess formation, was first documented by Whitmore and Krishnaswami (1912). The causative agent, *Burkholderia pseudomallei*, was subsequently identified as a motile, Gram-negative bacillus, which is principally a saprophyte found in soil and water in subtropical areas. The disease is acquired by inhalation, aspiration, subcutaneously, or occasionally via ingestion. Most cases occur in patients with immunosuppression, especially those with diabetes mellitus. Melioidosis has become an increasingly important disease in endemic areas such as South-East Asia and Northern Australia causing a significant number of deaths despite antibiotic treatment. Furthermore, *B. pseudomallei* is also recognized as a pathogen of numerous animal species (reviewed in Lazar Adler et al., 2009; Galyov et al., 2010).

Burkholderia mallei is closely related to *B. pseudomallei* and is the etiological agent of Glanders, an infectious equine disease that can be transmitted to humans. The disease may be acute or chronic, with the chronic form usually occurring in horses and the acute form occurring in mules and donkeys. Clinical signs include swollen lymphatics, a chronic nasal discharge, and ulcers. Contact with nasal discharge or infected ulcers is a major risk factor for infection. *B. mallei* is adapted to a narrower range of hosts than *B. pseudomallei* and is not considered able to persist for protracted periods in the environment. Horses are the primary carriers of disease and are largely responsible for transmission. Infections in humans frequently involve sepsis, pneumonia and abscess formation and have a high mortality rate. The incubation period ranges from days to weeks, and animals can die within a week of the onset of clinical symptoms (reviewed in Whitlock et al., 2007; Galyov et al., 2010).

THE AUTOTRANSPORTER FAMILY

Autotransporters (ATs) are a large and diverse family of bacterial secreted and outer membrane (OM) proteins that are translocated from the bacterial cytoplasm via the Type V pathway, one of seven recognized secretion pathways in Gram-negative bacteria. ATs play diverse roles, and many such proteins influence pathogenesis and immunity, for example by acting as invasins, adhesins, proteases, or actin-nucleating factors. ATs typically consist of a 20–400-kDa passenger domain that contains the effector functions and a 10–30-kDa β domain facilitating translocation across the OM (Dautin and Bernstein, 2007). ATs can be further divided into classical ATs and trimeric autotransported adhesins (TAAs), referred to as Type Va and Type Vc respectively. TAAs have a coiled-coil motif of unknown function, and are therefore referred to as oligomeric coiled-coil adhesins (Oca). Trimerization of TAAs is essential for their translocation and function as a single β barrel is formed from the three shorter 4-stranded β barrel domains which is superimposable with the classical ATs 12-stranded β barrel. While classical ATs have diverse effector functions, all characterized TAAs, with the notable exception of BimA from *Burkholderia* spp., are adhesins

(Cotter et al., 2005; Dautin and Bernstein, 2007). The threefold symmetry provides the potential for a multivalent interaction to enhance avidity, which could overcome mechanical forces and provide stability against proteases and detergents within extracellular secretions (Cotter et al., 2005).

Despite diversity in sequence, length, and function of the passenger domains, most ATs are variations on a single structural theme: an elongated solenoid (a coil wound into a tightly packed helix) which may contribute to protein folding after transport and/or allow effector domains to traverse LPS and capsule layers. This conserved shape creates a scaffold for various loops and domains without disturbing structural integrity and allows multiple interfaces to mediate interactions (Wells et al., 2007; Nishimura et al., 2010). Classical ATs form a right-handed β helical structure while TAAs have a β roll (two β strands contributing to a single superhelical turn); these structural differences affect curvature and binding specificity (Dautin and Bernstein, 2007). However, the recent full structure for the *Pseudomonas aeruginosa* classical AT EstA demonstrated an exception to the solenoid structure, with a α-β-α globular fold (Van Den Berg, 2010), which may relate to its function as a lipase rather than an adhesin.

ATs must cross both plasma membranes of Gram-negative bacteria. Classical ATs are then predominantly cleaved for secretion into the extracellular milieu whereas TAAs remain integrated in the bacterial OM via their β barrel domain. Firstly, ATs are targeted to the IM by their N-terminal signal sequence, where translocation occurs via the general secretory (Sec) pathway. The N-terminal signal sequence ranges from 20 to 60 aa, with the most elongated signal peptides being associated with large (>1000 aa) passenger domains in TAAs (Dautin and Bernstein, 2007). Such extended signal peptides exhibit reduced interaction with the Sec complex promoting delayed post-translational translocation across the inner membrane which is proposed to allow partial folding for subsequent OM secretion (Peterson et al., 2006; Desvaux et al., 2007). Once in the periplasm, ATs can undergo modifications including glycosylation and lipidation and may also form disulfide bonds. As implied in their name, ATs were originally believed to mediate their own transport across the OM. However, recent research suggests that they are chaperoned by periplasmic proteins, such as SurA and DegP to the Bam (Omp85) complex located within the OM which may assist in translocation (Oomen et al., 2004; Dautin and Bernstein, 2007). Several ATs have been shown to interact directly with the Bam complex (Ieva and Bernstein, 2009; Sauri et al., 2009; Lehr et al., 2010), as well as periplasmic chaperones including SurA and DegP (Ieva and Bernstein, 2009; Ruiz-Perez et al., 2009). Furthermore, depletion of the essential BamA protein significantly affects AT secretion (Jain and Goldberg, 2007). BamA forms a 16-strand β barrel with a pore size of ∼2.5 nm which is significantly larger than the AT β barrel (∼1.2 nm) and would allow for translocation of partially folded ATs. Additionally, BamA oligomerizes *in vitro* and could possibly form oligomer pores capable of translocating folded ATs. These observations have led to two hypotheses: translocation of the unfolded passenger domain through the Bam-stabilized AT β barrel via a hairpin curvature or translocation of the entire AT, possibly partially folded, via the Bam complex (Sauri et al., 2009). Structural analysis indicates that sequential folding of the passenger domain may act as the driving force for translocation of AT (Van Den Berg, 2010), although evidence suggests that partially folded or misfolded ATs are still capable of translocation (Dautin and Bernstein, 2007). Therefore, the translocation of ATs is dependent on periplasmic chaperones and the Bam complex via a mechanism which remains to be elucidated but which appears to be mediated by interaction with the β domain of the ATs. This would account for the observation that the C-terminal domains of TAAs from diverse bacterial species are functionally interchangeable (Ackermann et al., 2008).

AUTOTRANSPORTERS OF *B. PSEUDOMALLEI* AND *B. MALLEI*

The *B. pseudomallei* K96243 genome contains 11 predicted ATs, annotated as such based on sequence similarity to known ATs (**Table 1**). Additionally, 10 of these ATs are conserved across the other three completed *B. pseudomallei* genomes, while BPSL1705 is missing from both the 1106a and 688 strains. The *B. mallei* ATCC 23344 genome has eight homologs of the *B. pseudomallei* ATs (**Table 1**). Six of these are conserved across the three additional *B. mallei* completed genomes, with BMA1027 being present only in *B. mallei* ATCC 23344, while the avirulent *B. mallei* SAVPI strain also lacks BMAA0649. Homologs for seven of the *B. pseudomallei* ATs are also found in avirulent *B. thailandensis* (**Table 1**). However, we caution that conservation of loci in pathogenic *Burkholderia* and *B. thailandensis* does not necessarily imply that the genes play no role in virulence or host cell-interactions, as demonstrated by our analysis of the *bsa* Type III secretion locus shared by such strains (Stevens et al., 2002, 2004). Only two ATs are predicted to be classical ATs: BPSS0962/BMAA1263 (a putative serine protease) and BPSL2237/BMA1647 (a putative lipase/esterase). The remainder are predicted TAAs (Tiyawisutsri et al., 2007). An *in silico* subtractive hybridization of pathogenic versus non-pathogenic *Burkholderia* species to generate a 650 gene virulome, identified six ATs (BPSS0962, BPSL2237, BPSL1631, BPSL2063, BPSS796, BPSS0908; Schell et al., 2008). Furthermore, a "gain of function" genomic library screen identified five ATs as having a possible role in invasion and survival within macrophages (BPSL1705, BPSL2237, BPSS0088, BPSS0796, BPSS1492; Dowling et al., 2010). Neither approach identified a common set of dominant ATs, which may indicate that the ATs have a cumulative importance. However, direct experimental evidence for a role of ATs in virulence or intramacrophage survival, as proposed by Schell et al. (2008) and Dowling et al. (2010), is lacking at the time of writing. Several predicted ATs are recognized by human convalescent sera, in some cases with a specificity adequate for serodiagnosis, and such data indicate that the proteins are expressed *in vivo* (Tiyawisutsri et al., 2007; Felgner et al., 2009; Suwannasaen et al., 2011). To date, the best characterized of the predicted ATs of *B. pseudomallei* and *B. mallei* is a factor influencing intracellular motility, BimA.

BURKHOLDERIA INTRACELLULAR MOTILITY AND THE BIMA PROTEIN

In common with selected species of *Listeria*, *Shigella*, *Rickettsia*, and *Mycobacterium marinum*, *B. pseudomallei* shares the ability to induce polymerization of actin at one pole of the bacterial cell to promote its movement within and between host cells (**Figure 1**). The formation of actin-rich bacteria-containing

Table 1 | Autotransporters of *B. pseudomallei* K96243 and *B. mallei* ATCC 23344. The 11 *B. pseudomallei* ATs and their eight *B. mallei* homologs are listed below alongside relevant functional information.

Bp K96243	Bm ATCC 23344	Size (aa)	Annotation	Biological characteristics
Classical autotransporters				
BPSL2237*	BMA1647	610, 610		
BPSS0962*	BMAA1263	1131, 1129		
Trimeric autotransporter adhesins				
BPSL1631	BMA1027	1124, 1012		Immunogenic (Bm; Tiyawisutsri et al., 2007)
BPSL1705	–	1606	BoaB	Adhesin (Balder et al., 2010)
BPSL2063	BMA0840	1090, 1090		Immunogenic (Bp, Bm; Tiyawisutsri et al., 2007)
BPSS0088*	–	1645		Serodiagnostic (Felgner et al., 2009)
BPSS0796	BMAA0649	1653, 1535	BoaA	Adhesin (Balder et al., 2010), immunogenic (Bp, Bm; Tiyawisutsri et al., 2007)
BPSS0908*	BMAA1324*	1324, 831		Serodiagnostic (Felgner et al., 2009), immunogenic (Bp, Bm; Tiyawisutsri et al., 2007)
BPSS1434*	–	2634	BpaA	Characteristic TAA head crystal structure (Edwards et al., 2010), serodiagnostic (Felgner et al., 2009)
BPSS1439*	BMAA0810*^	1530, 459^		Immunogenic (Bp; Tiyawisutsri et al., 2007)
BPSS1492*	BMAA0749*	516, 373	BimA	Actin-based motility (Stevens et al., 2005b), serodiagnostic (Felgner et al., 2009), immunogenic (Bp; Tiyawisutsri et al., 2007)

**B. thailandensis homolog identified in E264 genome.*

^Putative pseudogene.

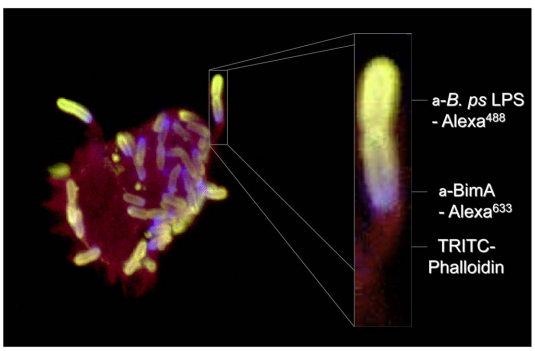

FIGURE 1 | Actin-based motility of *B. pseudomallei* in a J774.2 murine macrophage-like cell 8 h post-infection. *B. pseudomallei* was detected with antibodies to its lipopolysaccharide (green) and BimA was detected with a panel of specific monoclonal antibodies (blue). Polymerized (F-) actin was stained red with fluorophore-labeled phalloidin.

membrane protrusions was first described in *B. pseudomallei*-infected HeLa and J774.1 cells (Kespichayawattana et al., 2000), but is also a feature of *B. mallei* and *B. thailandensis* infection (Stevens et al., 2005a). The bacterial factor(s) required for actin-based motility of *B. pseudomallei* have been sought by screening random mutants for a small plaque phenotype (Pilatz et al., 2006) and by targeted inactivation of candidate factors (Stevens et al., 2005b). One such candidate (BPSS1492, BimA) belongs to the Oca/type Vc family of TAAs with a β barrel sequence and linker region with 48% similarity to the *Y. enterocolitica* YadA C-terminal (pfam domain 03895). This was targeted on the basis that *Shigella* and *Rickettsia* use ATs for actin-based motility (IcsA and Sca2, respectively). The predicted BPSS1492 protein also contained domains associated with actin binding, including proline-rich motifs and Wiskott–Aldrich syndrome protein (WASP) homology-2 (WH2) domains that suggested it may be involved in actin assembly (Stevens et al., 2005b). Actin-based motility of *B. pseudomallei* in J774.2 cells was abolished by inactivation of *bimA* and could be restored by transient expression of the gene *in trans* (Stevens et al., 2005b). BimA is located at the pole of the bacterial cell at which actin polymerization occurs and polar localization is frequently seen in only one daughter cell at division (**Figure 1**), implying that polar targeting of BimA may rely on distinguishing the new and old poles of the cell (Stevens et al., 2005b).

Burkholderia pseudomallei BimA possesses an unusually long signal sequence typical of autotransporters and a passenger domain containing several putative functional domains. Within this effector domain, the two WH2 motifs have each been found to influence actin binding and polymerization *in vitro* (Sitthidet et al., 2011). In addition, *B. pseudomallei* BimA contains between 2 and 7 predicted target sites for host cell casein kinase II (PDASX), with variation across sequenced strains (Sitthidet et al., 2008). The PDASX repeats have since been established to act in an additive manner to enhance actin polymerization *in vitro* (Sitthidet et al., 2011). It remains unclear if such repeats are phosphorylated *in vivo*, or what the functional consequences of post-translational modification of BimA may be. Interestingly a 13 aa repeat region of BimA was found to be required for intercellular spread of *B. pseudomallei* but was dispensable for actin binding and polymerization (Sitthidet et al., 2011). Other bacterial factors involved in actin-based motility have been shown to promote intracellular survival through evasion of cytosolic killing by autophagy and further studies with defined mutants are required to determine if BimA or its domains confer such activity.

BimA orthologs exist in *B. mallei* ATCC23344 (BMAA0749) and *B. thailandensis* E264 (BTH_II0875) and can restore actin-based motility of a *B. pseudomallei bimA* mutant (Stevens et al., 2005a). The BimA passenger domain of the three species differ markedly in primary sequence resulting in differences in the

number of WH2 domains, sequence of proline-rich motifs and the presence of a central and acidic (CA) domain, indicating that they may initiate actin assembly by distinct mechanisms (Stevens et al., 2005a). Many mechanisms of bacterial actin-based motility converge on activation of the cellular Arp (actin-related protein) 2/3 complex. Activation of the Arp2/3 complex requires cellular nucleation-promoting factors (NPFs) such as WASP-family members, and pathogens capable of actin-based motility often mimic the activity of NPFs or recruit and activate them at the bacterial pole (reviewed in Stevens et al., 2006). In recent years however, a number of virulence-associated factors have been identified in bacteria that initiate actin assembly in an Arp2/3-independent manner. For example, the AT Sca2 facilitates actin-based motility of certain *Rickettsia* species in an Arp2/3-independent manner akin to cellular formin proteins (Haglund et al., 2010; Kleba et al., 2010). It is notable that truncated recombinant *B. pseudomallei* BimA purified from *E. coli* polymerizes actin *in vitro* in the absence of any other cellular and bacterial co-factor in an Arp2/3-independent manner (Stevens et al., 2005b; Sitthidet et al., 2010); however, it remains unclear if such intrinsic activity would be adequate to propel the bacteria inside cells. In contrast, the ability of the *B. thailandensis* BimA ortholog to assemble actin *in vitro* is Arp2/3-dependent and requires the Arp2/3-recruiting CA domain (Sitthidet et al., 2010). Little is presently known about the mechanism of action of the *B. mallei* BimA ortholog; however, it is considered unlikely to be Arp2/3-dependent as it lacks an invariant tryptophan residue within an acidic stretch of residues required for Arp2/3 binding and activation (Stevens et al., 2005b). Intra-species conservation of BimA in natural populations of *B. pseudomallei* and *B. thailandensis* is high, with the exception of a geographically restricted subset of *B. pseudomallei* isolates harboring a *B. mallei*-like BimA variant (Sitthidet et al., 2008, 2010). The impact of sequence variation within BimA on pathogenesis and recognition by host immunity remains to be elucidated.

BimA has attracted much interest as a diagnostic tool. Recently, researchers have developed PCR-based methods to discriminate between *Burkholderia* species in a clinical setting (Ulrich et al., 2006a,b; Sitthidet et al., 2011), and protein microarray studies led to inclusion of BimA in a 10-protein multiplex classifier to improve diagnosis of human *B. pseudomallei* infection (Felgner et al., 2009; Suwannasaen et al., 2011). Curiously the *B. mallei* BimA protein was non-immunogenic in a test with serum from *B. mallei*-infected horses (Tiyawisutsri et al., 2007), yet *B. pseudomallei* BimA is one of the most immunogenic proteins recognized by sera from convalescent melioidosis patients (Felgner et al., 2009; Suwannasaen et al., 2011) and also serves as a T cell antigen (Felgner et al., 2009; Suwannasaen et al., 2011). The role of BimA in the pathogenesis and virulence of *B. mallei* and *B. pseudomallei* also appears to differ, with *B. mallei* BimA being dispensable for virulence in a Syrian hamster model of glanders (Schell et al., 2007) whilst *B. pseudomallei* BimA contributes to pathogenesis in murine models of melioidosis and confers protection against homologous challenge (Galyov et al., unpublished data). This may reflect differences in the animal species, dose and route of inoculation. BimA in *B. mallei* is regulated by the VirAG two-component system that is encoded nearby and which also controls expression of a virulence-associated Type VI secretion system (Schell et al., 2007). BimA appears to be poorly expressed *in vitro* and the stimuli for its expression are ill-defined.

CHARACTERIZATION OF OTHER CANDIDATE *B. PSEUDOMALLEI* AND *B. MALLEI AUTOTRANSPORTERS*

In addition to BimA, two predicted TAAs have been the subject of further characterization: BPSS0796/BMAA0649 and BPSL1705, re-annotated as BoaA and BoaB respectively, were expressed in a heterologous *E. coli* host where they were displayed on the bacterial surface and promoted attachment of the recombinant *E. coli* strains to epithelial cell lines (Balder et al., 2010). In common with the role of other TAA family members in adherence, *B. pseudomallei* and/or *B. mallei* mutants with disruptions in *boaA* or *boaB* exhibited reduced adherence to epithelial cells and a double mutant, but neither single mutant, displayed a growth defect in phagocytic cell lines (Balder et al., 2010). Though suggestive of a role in virulence, studies with defined mutant and repaired or complemented strains in animals are required to establish the role of BoaA and BoaB in pathogenesis.

Evidence of expression of selected TAAs has been obtained by screening of expression libraries with convalescent sera. Serum from *B. mallei*-infected horses identified multiple independent clones for four TAAs (BMA0840, BMA1027, BMA0649, and BMAA1324) suggestive of a strong antibody response (Tiyawisutsri et al., 2007). A similar screen with convalescent serum from human melioidosis patients identified five TAAs (BPSL2063, BPSS0908, BPSS0796, BPSS1439, and BPSS1492); however, these were found at a low frequency indicative of a relatively poor immune response (Tiyawisutsri et al., 2007). Further studies are required to determine if this reflects genuine differences in immunogenicity of the predicted proteins, or the distinct hosts, nature of exposure and/or sampling times. Additionally, a protein microarray probed with pooled melioidosis patients sera identified 4 ATs (BPSS0088, BPSS0796, BPSS1434/BpaA, BPSS1492/BimA) as having serodiagnostic potential due to their ability to interact with melioidosis-specific antibodies (Felgner et al., 2009). The ATs identified by these two studies demonstrate minimal overlap although this may reflect the variation in *in vivo* bacterial gene expression or the host immune response. Microarray studies under 82 *in vitro* different conditions demonstrated that the 11 ATs of *B. pseudomallei* are constitutively expressed (Tan, personal comm.), while qRT-PCR analysis of the transcription of two AT genes (*boaA*, *boaB*) demonstrated low expression (Balder et al., 2010).

Alignment of the C-terminal β barrel domain regions of the putative *B. pseudomallei* and *B. mallei* TAAs demonstrates considerable conservation indicative of amplification of these adhesins through gene duplication events (**Figure 2A**). This is potentially significant given the importance of C-terminal regions of TAAs in translocation and trimer stability, as evidenced by the ability of C-terminal domains of YadA family members from diverse bacteria to functionally replace the cognate domain in *Yersinia* (Ackermann et al., 2008). A phylogenetic tree of the β barrel domains is supportive of this idea as the TAAs form two clusters suggesting that these genes may have been amplified from two original ancestral

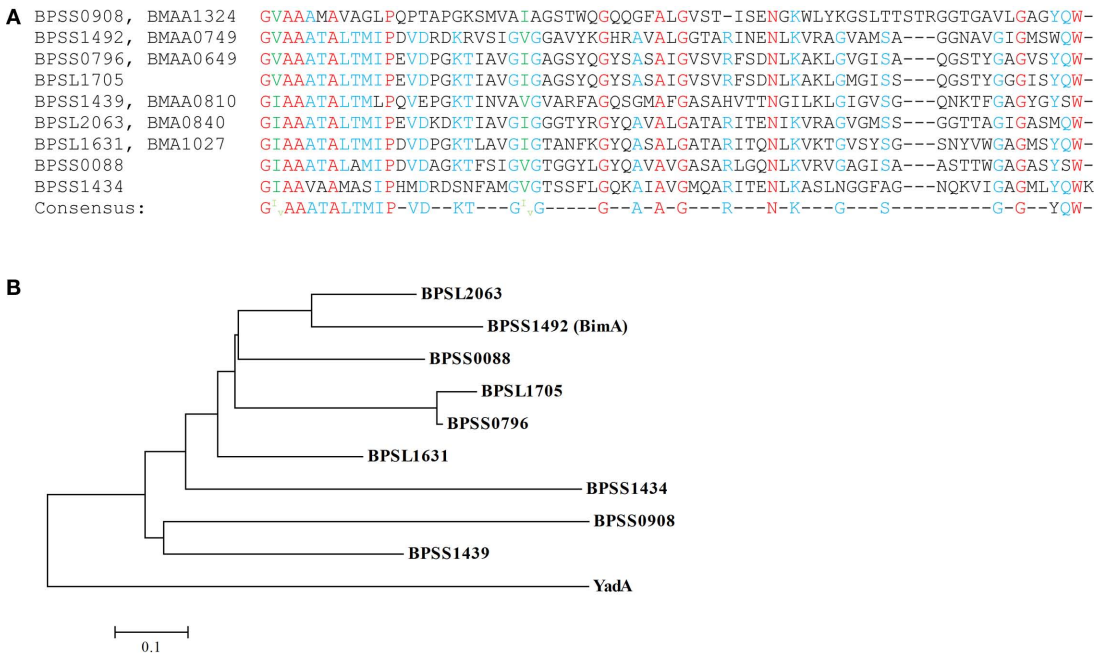

FIGURE 2 | Alignment and phylogenetic analysis of the β barrel domains of the putative *B. pseudomallei* and *B. mallei* TAAs: (A) the nine *B. pseudomallei* C-terminal 70–72 aa β barrel domains (*B. mallei* homologs 100% identical at this region) were aligned; identical residues are highlighted in red, those with high homology (at least 66%) in blue while those with highly conserved substitutions in green. The consensus sequence is listed below. **(B)** The phylogenetic analysis of these domains demonstrates two distinct clusters both of which derived from a common ancestor to the prototypical *Yersinia* YadA TAA.

genes (**Figure 2B**). Both clusters appear to be derived from a common ancestor to the prototypic *Yersinia* YadA TAA. Additionally, the two outliers in the alignment, BPSS0908/BMAA1324 and BPSS1434, display early separation in the phylogenetic tree. Interestingly, of the three unique *B. pseudomallei* TAAs, two (BPSS1434 and BPSS0088) are early branches in the phylogenetic tree suggesting that their absence from *B. mallei* is due to gene loss as later branching genes are present. Meanwhile BPSL1705, which is located within a genomic island (GI8), is very recently branched from BPSS0796/BMAA0649 and has been proposed to have originated as a duplication of BPSS0796/BMAA0649 (Tiyawisutsri et al., 2007). This duplication event may explain why BPSL1705 is the only AT not conserved across the four completed *B. pseudomallei* genomes. Furthermore, the β barrel domains of the *B. pseudomallei* and *B. mallei* TAA homologs show 100% identity although little similarity is seen between the passenger domains. However, the effector domains of TAAs are generally not conserved at a sequence level and the crystal structure analysis of a section of the passenger domain of BPSS1434 (re-annotated as BpaA, *B. pseudomallei* adhesion A) demonstrated quaternary structure similar to that of other TAAs (Edwards et al., 2010). This new annotation gives BPSS1434 the same name as the unrelated Type V two-partner secreted BpaA (Brown et al., 2004) for which no homolog exists in either *B. pseudomallei* K96243 or *B. mallei* ATCC 23344. The *B. pseudomallei* and *B. mallei* genomes contain homologs of BamA, BamB, and SurA which are proposed to assist in translocation of ATs across the OM (Ieva and Bernstein, 2009; Ruiz-Perez et al., 2009; Sauri et al., 2009; Lehr et al., 2010), and further studies are needed to evaluate the role of such factors in AT secretion and pathogenesis.

CONCLUDING REMARKS

On the basis of homology and the precedent of phenotypes for AT mutants in other bacteria, it is reasonable to infer that ATs predicted to be encoded in the genomes of pathogenic *Burkholderia* species may play a role in pathogenesis and immunity. In the short time since annotation of the genomes of *B. pseudomallei* and *B. mallei*, it has been established that several putative ATs mediate bacterial interactions with host cells. For example, BimA mediates intracellular actin-based motility, which in the case of *B. pseudomallei* is necessary for intercellular spread and full virulence, whereas BoaA and BoaB appear to function as adhesins. One should note that significant sequence divergence in effector domains can occur even among closely related species, and within species, as we have noted for BimA (Sitthidet et al., 2008). Such variation in BimA can markedly alter the mode of action (Sitthidet et al., 2011) and future studies will need to consider the extent to which the repertoire and sequence of ATs in prototype strains is typical of wider populations. Very few published studies have probed the role of ATs in pathogenesis or immunity during *B. pseudomallei* and *B. mallei* infection in model hosts, and further studies with defined mutants and complemented strains are needed. Attenuated mutants may be suitable as live-attenuated vaccines, and based on the ability of some ATs to act as B- and T-cell antigens (Tiyawisutsri et al., 2007), purified ATs may have merit as

subunit vaccines or as diagnostic tools. Importantly, the mode of translocation of *Burkholderia* ATs is inferred only from homologous systems, and studies are needed to address outstanding questions regarding their biological role. Future experiments should evaluate the role of AT domains and specific residues in protein folding, oligomerization, interaction and translocation across the OM, with particular reference to the requirement for periplasmic chaperones and the Bam complex. Analysis of the structure of *Burkholderia* ATs may also provide clues to the mechanistic basis of their secretion and function.

REFERENCES

Ackermann, N., Tiller, M., Anding, G., Roggenkamp, A., and Heesemann, J. (2008). Contribution of trimeric autotransporter C-terminal domains of oligomeric coiled-coil adhesin (Oca) family members YadA, UspA1, EibA, and Hia to translocation of the YadA passenger domain and virulence of *Yersinia enterocolitica*. *J. Bacteriol.* 190, 5031–5043.

Balder, R., Lipski, S., Lazarus, J. J., Grose, W., Wooten, R. M., Hogan, R. J., Woods, D. E., and Lafontaine, E. R. (2010). Identification of *Burkholderia mallei* and *Burkholderia pseudomallei* adhesins for human respiratory epithelial cells. *BMC Microbiol.* 10, 250. doi: 10.1186/1471-2180-10-250

Brown, N. F., Logue, C. A., Boddey, J. A., Scott, R., Hirst, R. G., and Beacham, I. R. (2004). Identification of a novel two-partner secretion system from *Burkholderia pseudomallei*. *Mol. Genet. Genomics* 272, 204–215.

Cotter, S. E., Surana, N. K., and St Geme, J. W. R. (2005). Trimeric autotransporters: a distinct subfamily of autotransporter proteins. *Trends Microbiol.* 13, 199–205.

Dautin, N., and Bernstein, H. (2007). Protein secretion in Gram-negative bacteria via the autotransporter pathway. *Annu. Rev. Microbiol.* 61, 89–112.

Desvaux, M., Scott-Tucker, A., Turner, S. M., Cooper, L. M., Huber, D., Nataro, J. P., and Henderson, I. R. (2007). A conserved extended signal peptide region directs posttranslational protein translocation via a novel mechanism. *Microbiology* 153, 59–70.

Dowling, A. J., Wilkinson, P. A., Holden, M. T., Quail, M. A., Bentley, S. D., Reger, J., Waterfield, N. R., Titball, R. W., and Ffrench-Constant, R. H. (2010). Genome-wide analysis reveals loci encoding anti-macrophage factors in the human pathogen *Burkholderia pseudomallei* K96243. *PLoS ONE* 5, e15693. doi: 10.1371/journal.pone.0015693

Edwards, T. E., Phan, I., Abendroth, J., Dieterich, S. H., Masoudi, A., Guo, W., Hewitt, S. N., Kelley, A., Leibly, D., Brittnacher, M. J., Staker, B. L., Miller, S. I., Van Voorhis, W. C., Myler, P. J., and Stewart, L. J. (2010). Structure of a *Burkholderia pseudomallei* trimeric autotransporter adhesin head. *PLoS ONE* 5, e12803. doi: 10.1371/journal.pone.0012803

Felgner, P. L., Kayala, M. A., Vigil, A., Burk, C., Nakajima-Sasaki, R., Pablo, J., Molina, D. M., Hirst, S., Chew, J. S., Wang, D., Tan, G., Duffield, M., Yang, R., Neel, J., Chantratita, N., Bancroft, G., Lertmemongkolchai, G., Davies, D. H., Baldi, P., Peacock, S., and Titball, R.W. (2009). A *Burkholderia pseudomallei* protein microarray reveals serodiagnostic and cross-reactive antigens. *Proc. Natl. Acad. Sci. U.S.A.* 106, 13499–13504.

Galyov, E. E., Brett, P. J., and DeShazer, D. (2010). Molecular insights into *Burkholderia pseudomallei* and *Burkholderia mallei* pathogenesis. *Annu. Rev. Microbiol.* 64, 495–517.

Haglund, C. M., Choe, J. E., Skau, C. T., Kovar, D. R., and Welch, M. D. (2010). *Rickettsia* Sca2 is a bacterial formin-like mediator of actin-based motility. *Nat. Cell Biol.* 12, 1057–1063.

Ieva, R., and Bernstein, H. D. (2009). Interaction of an autotransporter passenger domain with BamA during its translocation across the bacterial outer membrane. *Proc. Natl. Acad. Sci. U.S.A.* 106, 19120–19125.

Jain, S., and Goldberg, M. B. (2007). Requirement for YaeT in the outer membrane assembly of autotransporter proteins. *J. Bacteriol.* 189, 5393–5398.

Kespichayawattana, W., Rattanachetkul, S., Wanun, T., Utaisincharoen, P., and Sirisinha, S. (2000). *Burkholderia pseudomallei* induces cell fusion and actin-associated membrane protrusion: a possible mechanism for cell-to-cell spreading. *Infect. Immun.* 68, 5377–5384.

Kleba, B., Clark, T. R., Lutter, E. I., Ellison, D. W., and Hackstadt, T. (2010). Disruption of the *Rickettsia rickettsii* Sca2 autotransporter inhibits actin-based motility. *Infect. Immun.* 78, 2240–2247.

Lazar Adler, N. R., Govan, B., Cullinane, M., Harper, M., Adler, B., and Boyce, J. D. (2009). The molecular and cellular basis of pathogenesis in melioidosis: how does *Burkholderia pseudomallei* cause disease? *FEMS Microbiol. Rev.* 33, 1079–1099.

Lehr, U., Schütz, M., Oberhettinger, P., Ruiz-Perez, F., Donald, J. W., Palmer, T., Linke, D., Henderson, I. R., and Autenrieth, I. B. (2010). C-terminal amino acid residues of the trimeric autotransporter adhesin YadA of *Yersinia enterocolitica* are decisive for its recognition and assembly by BamA. *Mol. Microbiol.* 78, 932–946.

Nishimura, K., Tajima, N., Yoon, Y. H., Park, S. Y., and Tame, J. R. (2010). Autotransporter passenger proteins: virulence factors with common structural themes. *J. Mol. Med.* 88, 451–458.

Oomen, C. J., Van Ulsen, P., Van Gelder, P., Feijen, M., Tommassen, J., and Gros, P. (2004). Structure of the translocator domain of a bacterial autotransporter. *EMBO J.* 23, 1257–1266.

Peterson, J. H., Szabady, R. L., and Bernstein, H. D. (2006). An unusual signal peptide extension inhibits the binding of bacterial presecretory proteins to the signal recognition particle, trigger factor, and the SecYEG complex. *J. Biol. Chem.* 281, 9038–9048.

Pilatz, S., Breitbach, K., Hein, N., Fehlhaber, B., Schulze, J., Brenneke, B., Eberl, L., and Steinmetz, I. (2006). Identification of *Burkholderia pseudomallei* genes required for the intracellular life cycle and in vivo virulence. *Infect. Immun.* 74, 3576–3586.

Ruiz-Perez, F., Henderson, I. R., Leyton, D. L., Rossiter, A. E., Zhang, Y., and Nataro, J. P. (2009). Roles of periplasmic chaperone proteins in the biogenesis of serine protease autotransporters of Enterobacteriaceae. *J. Bacteriol.* 191, 6571–6583.

Sauri, A., Soprova, Z., Wickström, D., De Gier, J. W., Van Der Schors, R. C., Smit, A. B., Jong, W. S., and Luirink, J. (2009). The Bam (Omp85) complex is involved in secretion of the autotransporter haemoglobin protease. *Microbiology* 155, 3982–3991.

Schell, M. A., Lipscomb, L., and DeShazer, D. (2008). Comparative genomics and an insect model rapidly identify novel virulence genes of *Burkholderia mallei*. *J. Bacteriol.* 190, 2306–2313.

Schell, M. A., Ulrich, R. L., Ribot, W. J., Brueggemann, E. E., Hines, H. B., Chen, D., Lipscomb, L., Kim, H. S., Mrázek, J., Nierman, W. C., and DeShazer, D. (2007). Type VI secretion is a major virulence determinant in *Burkholderia mallei*. *Mol. Microbiol.* 64, 1466–1485.

Sitthidet, C., Korbsrisate, S., Layton, A. N., Field, T. R., Stevens, M. P., and Stevens, J. M. (2011). Identification of motifs of *Burkholderia pseudomallei* BimA required for intracellular motility, actin binding and actin polymerization. *J. Bacteriol.* 193, 1901–1910.

Sitthidet, C., Stevens, J. M., Chantratita, N., Currie, B. J., Peacock, S. J., Korbsrisate, S., and Stevens, M. P. (2008). Prevalence and sequence diversity of a factor required for actin-based motility in natural populations of *Burkholderia* species. *J. Clin. Microbiol.* 46, 2418–2422.

Sitthidet, C., Stevens, J. M., Field, T. R., Layton, A. N., Korbsrisate, S., and Stevens, M. P. (2010). Actin-based motility of *Burkholderia thailandensis* requires a central acidic domain of BimA that recruits and activates the cellular Arp2/3 complex. *J. Bacteriol.* 192, 5249–5252.

Stevens, J. M., Galyov, E. E., and Stevens, M. P. (2006). Actin-dependent movement of bacterial pathogens. *Nat. Rev. Microbiol.* 4, 91–101.

Stevens, J. M., Ulrich, R. L., Taylor, L. A., Wood, M. W., DeShazer, D., Stevens, M. P., and Galyov, E. E. (2005a). Actin-binding proteins from *Burkholderia mallei* and *Burkholderia thailandensis* can functionally compensate for the actin-based motility defect of a *Burkholderia pseudomallei* bimA mutant. *J. Bacteriol.* 187, 7857–7862.

Stevens, M. P., Stevens, J. M., Jeng, R. L., Taylor, L. A., Wood, M. W., Hawes, P., Monaghan, P., Welch, M. D., and Galyov, E. E. (2005b). Identification of a bacterial factor required for actin-based motility of *Burkholderia pseudomallei*. *Mol. Microbiol.* 56, 40–53.

Stevens, M. P., Haque, A., Atkins, T., Hill, J., Wood, M. W., Easton, A., Nelson, M., Underwood-Fowler, C., Titball, R. W., Bancroft, G. J., and Galyov, E. E. (2004). Attenuated virulence and protective efficacy of a *Burkholderia pseudomallei* bsa type III secretion mutant in murine models of melioidosis. *Microbiology* 150, 2669–2676.

Stevens, M. P., Wood, M. W., Taylor, L. A., Monaghan, P., Hawes, P., Jones, P. W., Wallis, T. S., and Galyov, E. E. (2002). An Inv/Mxi-Spa-like type III protein secretion system in *Burkholderia pseudomallei* modulates intracellular behaviour of the pathogen. *Mol. Microbiol.* 46, 649–659.

Suwannasaen, D., Mahawantung, J., Chaowagul, W., Limmathurotsakul, D., Felgner, P. L., Davies, H., Bancroft, G. J., Titball, R. W., and Lertmemongkolchai, G. (2011). Human immune responses to *Burkholderia pseudomallei* characterized by protein microarray analysis. *J. Infect. Dis.* 203, 1001–1011.

Tiyawisutsri, R., Holden, M. T., Tumapa, S., Rengpipat, S., Clarke, S. R., Foster, S. J., Nierman, W. C., Day, N. P., and Peacock, S. J. (2007). *Burkholderia* Hep_Hag autotransporter (BuHA) proteins elicit a strong antibody response during experimental glanders but not human melioidosis. *BMC Microbiol.* 7, 19. doi: 10.1186/1471-2180-7-19

Ulrich, M. P., Norwood, D. A., Christensen, D. R., and Ulrich, R. L. (2006a). Using real-time PCR to specifically detect *Burkholderia mallei. J. Med. Microbiol.* 55, 551–559.

Ulrich, R. L., Ulrich, M. P., Schell, M. A., Kim, H. S., and DeShazer, D. (2006b). Development of a polymerase chain reaction assay for the specific identification of *Burkholderia mallei* and differentiation from *Burkholderia pseudomallei* and other closely related Burkholderiaceae. *Diagn. Microbiol. Infect. Dis.* 55, 37–45.

Van Den Berg, B. (2010). Crystal structure of a full-length autotransporter. *J. Mol. Biol.* 396, 627–633.

Wells, T. J., Tree, J. J., Ulett, G. C., and Schembri, M. A. (2007). Autotransporter proteins: novel targets at the bacterial cell surface. *FEMS Microbiol. Lett.* 274, 163–172.

Whitlock, G. C., Estes, D. M., and Torres, A. G. (2007). Glanders: off to the races with *Burkholderia mallei. FEMS Microbiol. Lett.* 277, 115–122.

Whitmore, A., and Krishnaswami, C. S. (1912). An account of the discovery of a hitherto undescribed infective disease occurring among the population of Rangoon. *Ind. Med. Gaz.* 47, 262–267.

Conflict of Interest Statement: The authors declare that the research was conducted in the absence of any commercial or financial relationships that could be construed as a potential conflict of interest.

Received: 28 April 2011; paper pending published: 31 May 2011; accepted: 28 June 2011; published online: 15 July 2011.
*Citation: Lazar Adler NR, Stevens JM, Stevens MP and Galyov EE (2011) Autotransporters and their role in the virulence of Burkholderia pseudomallei and Burkholderia mallei. Front. Microbio. **2**:151. doi: 10.3389/fmicb.2011.00151*
This article was submitted to Frontiers in Cellular and Infection Microbiology, a specialty of Frontiers in Microbiology.

frontiers in
MICROBIOLOGY

REVIEW ARTICLE
published: 22 August 2011
doi: 10.3389/fmicb.2011.00170

Strategies for intracellular survival of *Burkholderia pseudomallei*

Elizabeth M. Allwood[1], Rodney J. Devenish[2,3], Mark Prescott[2], Ben Adler[1,3]* and John D. Boyce[1,3]

[1] *Department of Microbiology, Monash University, Clayton, VIC, Australia*
[2] *Department of Biochemistry and Molecular Biology, Monash University, Clayton, VIC, Australia*
[3] *Australian Research Council Centre of Excellence in Structural and Functional Microbial Genomics, Monash University, Clayton, VIC, Australia*

Edited by:
Alfredo G. Torres, University of Texas Medical Branch, USA

Reviewed by:
Jonathan Mark Warawa, University of Louisville, USA
Jo Stevens, The University of Edinburgh, UK

****Correspondence:***
Ben Adler, Department of Microbiology, Monash University, Wellington Road, Clayton, VIC 3800, Australia.
e-mail: ben.adler@monash.edu

Burkholderia pseudomallei is the causative agent of melioidosis, a disease with high mortality that is prevalent in tropical regions of the world. A key component of the pathogenesis of melioidosis is the ability of *B. pseudomallei* to enter, survive, and replicate within mammalian host cells. For non-phagocytic cells, bacterial adhesins have been identified both on the bacterial surface and associated with Type 4 pili. Cell invasion involves components of one or more of the three Type 3 Secretion System clusters, which also mediate, at least in part, the escape of bacteria from the endosome into the cytoplasm, where bacteria move by actin-based motility. The mechanism of actin-based motility is not clearly understood, but appears to differ from characterized mechanisms in other bacterial species. A small proportion of intracellular bacteria is targeted by host cell autophagy, involving direct recruitment of LC3 to endosomes rather than through uptake by canonical autophagosomes. However, the majority of bacterial cells are able to circumvent autophagy and other intracellular defense mechanisms such as the induction of inducible nitric oxide synthase, and then replicate in the cytoplasm and spread to adjacent cells via membrane fusion, resulting in the formation of multi-nucleated giant cells. A potential role for host cell ubiquitin in the autophagic response to bacterial infection has recently been proposed.

Keywords: melioidosis, *Burkholderia*, pathogenesis, adhesion, intracellular survival, autophagy, ubiquitination

INTRODUCTION

Burkholderia pseudomallei is a Gram-negative pathogen which is the causative agent of melioidosis, a serious invasive disease of humans and animals. Melioidosis is endemic to northern Australia, Papua New Guinea, Southeast Asia, most of the Indian subcontinent and southern China, Hong Kong, and Taiwan. It is well recognized that *B. pseudomallei* is "highly endemic" to northeast Thailand, northern Australia, Singapore, and Malaysia where many cases of melioidosis are diagnosed each year (Currie et al., 2008). Sporadic cases have also been reported in other regions including Brazil, Puerto Rico, and New Caledonia (Dorman et al., 1998; Aardema et al., 2005; Le Hello et al., 2005; Barth et al., 2007). *B. pseudomallei* is a natural inhabitant of rice paddies, still or stagnant waters, and moist tropical soils (Brett and Woods, 2000). Despite several decades of research on prevention and treatment, mortality from melioidosis remains very high (50% in northeast Thailand and 19% in Australia; Peacock, 2006). Alarmingly, the mortality associated with septic shock remains close to 90% (Stone, 2007). Melioidosis accounts for 20% of all community-acquired septicemias in northeast Thailand (Chaowagul et al., 1989) and 32% of community-acquired bacteremic pneumonia and 6% of all bacteremias in northern Australia (Douglas et al., 2004).

Since the 1990s, it has been well accepted that a key component of the pathogenesis of *B. pseudomallei* is its ability to survive intracellularly in both phagocytic and non-phagocytic cells (Jones et al., 1996). The importance of intracellular survival is paramount, as this remarkable feature allows the bacterium to establish an infection while avoiding host immune responses. Indeed, the ability of *B. pseudomallei* to survive intracellularly explains numerous features of melioidosis, including latency, recrudescence, and treatment difficulty. Latency periods of more than 60 years have been documented (Ngauy et al., 2005). Activation of a latent infection is usually due to a decrease in the individual's immunocompetence and can result in an acute, fulminant, and fatal infection (Koponen et al., 1991). Relapse is common in melioidosis patients; recrudescence of melioidosis following apparent clinical resolution of the primary infection usually results from reactivation rather than reinfection (Haase et al., 1995; Maharjan et al., 2005).

Burkholderia pseudomallei utilizes numerous strategies that enable it to survive in such a specialized niche as the intracellular environment (**Figure 1**). This review will focus on these strategies for intracellular survival, from adhesion, invasion, and endosome escape to actin-based motility, formation of multi-nucleated giant cells (MNGC), evasion of host cell autophagy, and interaction of *B. pseudomallei* with host cell ubiquitination mechanisms.

THE ADHESION OF *B. PSEUDOMALLEI* TO HOST CELLS: AN EARLY STEP IN PATHOGENESIS

It is a *sine qua non* that the internalization of pathogenic bacteria by mammalian cells is preceded by adhesion of the bacteria to the cell surface. It is therefore somewhat surprising that a detailed knowledge at the molecular level of the interaction of *B. pseudomallei* with the eukaryotic cell surface is less developed than that for many

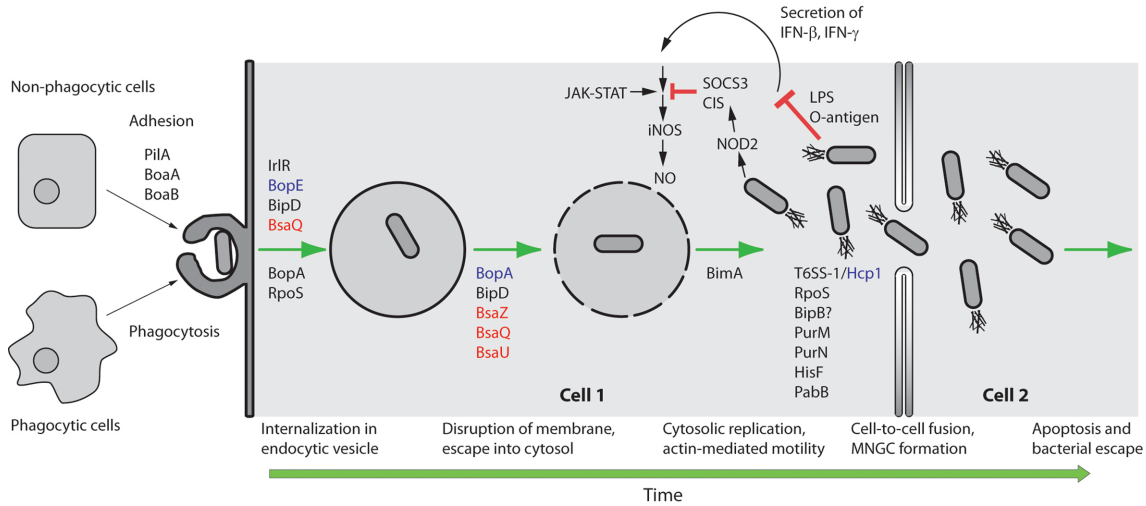

FIGURE 1 | Schematic representation of selected steps in the intracellular lifestyle of *B. pseudomallei*. *B. pseudomallei* can be internalized by either phagocytic or non-phagocytic cells. In non-phagocytic cells PilA and the adhesins BoaA and BoaB are critical for uptake. For the internalization step in non-phagocytic cells the Bsa T3SS structural proteins BipD (translocator), BsaQ (structural component), and BopE (effector) are required. The IrlRS two-component signal transduction system is predicted to regulate the expression of other key gene(s) involved in internalization. For internalization in phagocytic cells the Bsa T3SS putative effector BopA and the alternate sigma factor RpoS play minor roles. The Bsa T3SS structural proteins BsaZ, BsaQ, and BsaU, the translocator protein BipD and the putative effector BopA are critical for membrane disruption and escape from the endocytic vesicle. Once in the cytoplasm *B. pseudomallei* can replicate and move by actin-based motility in a BimA-dependent fashion. *B. pseudomallei* LPS only weakly stimulates IFN secretion, which results in reduced iNOS expression and NO production. Furthermore, *B. pseudomallei* induces expression of suppressor of cytokine signaling 3 (SOCS3) and cytokine-inducible Src homology 2-containing (CIS) proteins which inhibit the Janus kinases – signal transducers and activators of transcription (JAK–STAT) signaling pathway and concomitant iNOS activation. Purine (PurM, PurN), histidine (HisF), and *para*-aminobenzoate (PabB) biosynthetic pathways are important for intracellular replication and survival, while the *B. pseudomallei* T6SS-1 Hcp protein, the alternate sigma factor RpoS, and the Bsa T3SS protein BipB are involved in stimulating cell-to-cell fusion and the formation of MNGC. NOD2 refers to nucleotide-binding oligomerization domain-containing protein 2. Green arrows are used to indicate progression of time. Red T-bar arrows indicate inhibitory interactions. Secretion system components are color coded with effectors in purple, translocators in black, and structural components in red.

other bacterial pathogens. Comparisons between different studies using *B. pseudomallei* are difficult because of the use of different cell lines, bacterial strains, multiplicities of infection, and experimental conditions by different research groups. Nevertheless, the ability to adhere to the cell has been demonstrated to correlate with virulence in a number of studies. Five *B. pseudomallei* strains all adhered more strongly to human A549 lung epithelial cells than did five strains of the non-pathogenic species *B. thailandensis* (Kespichayawattana et al., 2004). The increased adhesion correlated with subsequent increased invasion and cytopathic effect, but, as in many other studies, the molecular basis for the difference was not determined. Likewise, a study which inferred, through inhibition studies, the attachment of *B. pseudomallei* to the GM1–GM2 glycosphingolipid ganglioside on undefined primary human pharyngeal epithelial cells did not investigate the bacterial component(s) involved (Gori et al., 1999).

Based on limited evidence derived from electron microscopy (EM), Ahmed et al. (1999) suggested that the adhesion of *B. pseudomallei* to an undefined population of primary human "pharyngeal" cells involved a bacterial surface structure which was designated, without supporting evidence, as capsular polysaccharide. Paradoxically, a more recent study with a genetically defined acapsular mutant (Reckseidler et al., 2001) found that the lack of capsule resulted in enhanced internalization into A549 and HeLa cells (Phewkliang et al., 2010); there was no effect on intracellular replication or cytotoxicity. Thus, while capsule clearly plays a key role in the ability of *B. pseudomallei* to cause disease (Reckseidler et al., 2001; Lazar Adler et al., 2009), there is no clear evidence for a role in cell adhesion or invasion (**Table 1**).

Type 4 fimbriae (pili) are known to be involved in the adhesion of a large number of bacterial species to a range of cell types, tissues, and other surfaces (Pelicic, 2008). Consequently, these hair-like filaments, or their individual protein components, frequently constitute key adhesins that may be necessary for virulence. In common with many Gram-negative species, *B. pseudomallei*, produces Type 4 pili. Inactivation of the *pilA* gene, which encodes the pilin subunit protein, abrogated the production of pili and resulted in reduced adhesion of *B. pseudomallei* to three different human epithelial cell lines, including A549 cells (Essex-Lopresti et al., 2005). Interestingly, adhesion to A549 and BEAS2-B cells was almost completely abolished, consistent with pili being a major bacterial adhesin, whereas adhesion of the *pilA* mutant to RPMI-2650 cells was approximately 30% that of the wild-type, suggesting the presence of additional adhesins (**Table 1**). The basis for these differences remains unknown. The *pilA* gene can be regulated in response to temperature, with up-regulation at lower temperatures (27–30°C). However, a *pilA B. pseudomallei* mutant showed reduced adhesion to ME-180 cells derived from human cervical tissue (**Table 1**).

Table 1 | Characterization of *B. pseudomallei* mutants with defects in intracellular life cycle.

			Ability for								
Mutant	**Product**	**Strain**	**Adherence**	**Invasion**	**Escape from vesicles**	**Actin-based motility**	**Intracellular survival/ replication**	**MNGC**	**Autophagic processes**	**Attenuated: model**	**Reference**
INVOLVED IN ADHERENCE											
pilA	Pilin subunit	K96243 and 08	↓: A549, BEAS2-B, RPMI-2650, and ME-180	ND	ND	ND	ND	ND	ND	Yes: *C. elegans*, BALB/c (i.n.) No: BALB/c (i.p.)	Essex-Lopresti et al. (2005), Boddey et al. (2006)
boaA	Adhesin	DD503	↓: A549, Hep2	Same as WT: J774A.1	ND	ND	Same as WT: J774A.1	ND	ND	ND	Balder et al. (2010)
boaB	Adhesin	DD503	↓: A549, Hep2	Same as WT: J774A.1	ND	ND	Same as WT: J774A.1	ND	ND	ND	Balder et al. (2010)
boaA/boaB	Adhesins	DD503	↓: A549, Hep2 (similar to single mutants)	Same as WT: J774A.1	ND	ND	↓ Growth: J774A.1 same as WT: epithelial cells	ND	ND	ND	Balder et al. (2010)
INVOLVED IN INVASION AND/OR ESCAPE FROM ENDOCYTIC VESICLES											
irlR	Two-component response regulator	1026b	ND	↓: A549, HeLa, and CHO Not ↓ in macrophages	ND	ND	Same as WT: RAW	ND	ND	No: diabetic rats, hamsters (i.p.), and C57BL/6 (i.n.)	Jones et al. (1997), Wiersinga et al. (2008)
bopE	Bsa T3SS effector	10276 and DD503	ND	Same as WT: J774.2 ↓: HeLa	Same as WT: J774.2 (6 h p.i.)	Yes: 6 h p.i.	Same as WT: J774.2	ND	ND	No: BALB/c (i.n. and i.p.) and hamsters (i.p.)	Stevens et al. (2002), Stevens et al. (2003), Stevens et al. (2004), Warawa and Woods (2005)
bipD	Bsa T3SS translocator	10276 and 576	ND	Same as WT: J774.2 and RAW 264.7 ↓: HeLa	↓: J774.2 (6 h p.i) RAW264.7 (almost none up to 6 h p.i.)	No: J774.2 (6 h p.i.)	Almost no replication: J774.2	No	Increased (RAW 264.7)	Yes: BALB/c (i.n. and i.p.) and C57BL/6 IL-12 $p40^{-/-}$ (i.p.)	Stevens et al. (2002), Stevens et al. (2003), Stevens et al. (2004), Gong et al. (2011)
bsaQ	Bsa T3SS structural component	K96243 and KHW	ND	↓: A549	Delayed: A549 (8 h p.i)	ND	Same as WT: A549, J774A.1 and THP-1 (↓ killing of THP-1 cells)	Delayed: A549 (smaller MNGCs)	ND	ND	Sun et al. (2005), Muangsombut et al. (2008)

(Continued)

Table 1 | Continued

			Ability for								
Mutant	**Product**	**Strain**	**Adherence**	**Invasion**	**Escape from vesicles**	**Actin-based motility**	**Intracellular survival/ replication**	**MNGC**	**Autophagic processes**	**Attenuated: model**	**Reference**
bsaZ	Bsa T3SS structural component	10276 and DD503	ND	Same as WT: J774.2 and RAW 264.7	↓: J774.2 (6 h p.i.) delayed: RAW 264.7 (18 h p.i.)	No: J774.2 (6 h p.i.) delayed: RAW 264.7 (12 h p.i.)	Almost no replication: J774.2 Can survive in RAW264.7	Delayed: RAW 264.7	ND	Yes: BALB/c (i.n.) and hamsters (i.p.)	Stevens et al. (2002), Stevens et al. (2004), Warawa and Woods (2005), Burtnick et al. (2008)
sctU1/ sctU2/ bsaZ triple	Bsa T3SS structural component of clusters 1, 2, and 3	DD503	ND	Same as WT: RAW 264.7	Same as *bsaZ* mutant	Delayed: RAW 264.7	Can survive in RAW264.7	Delayed: RAW 264.7	ND	Yes: hamsters (i.p.)	Warawa and Woods (2005), Burtnick et al. (2008)
bsaU	Bsa T3SS structural component	E8	ND	Same as WT: HeLa	Delayed: HeLa (12 h p.i.)	Delayed: HeLa	Same as WT: HeLa and J774A.1	ND	ND	Yes: BALB/c (i.n.)	Pilatz et al. (2006)
bopA	Bsa T3SS effector	K96243 and DD503	ND	↓: RAW 264.7	↓: RAW 264.7	Delayed: RAW 264.7	↓ Survival	Yes (delayed) (RAW 264.7)	Increased co-localization with LC3 (RAW 264.7)	No: hamsters (i.p.) Mild: BALB/c (i.p.)	Stevens et al. (2004), Warawa and Woods (2005), Cullinane et al. (2008), Gong et al. (2011)
INVOLVED IN INTRACELLULAR SURVIVAL											
purM	Phosphoribo syl-formyl-glycinamidine cyclo-ligase	E8	ND	Same as WT: HeLa	ND	Yes: HeLa	No replication: HeLa	ND	ND	Yes: BALB/c (i.n.)	Pilatz et al. (2006)
purN	Phosphorib osyl-glycinamide formyltrans-ferase	E8	ND	Same as WT: HeLa	ND	Yes: HeLa	↓ Replication: HeLa	ND	ND	Yes: BALB/c (i.n.)	Pilatz et al. (2006)
hisF	Imidazole glycerol phosphate synthase	E8	ND	Same as WT: HeLa	ND	Yes: HeLa	↓ Replication: HeLa	ND	ND	Yes: BALB/c (i.n.)	Pilatz et al. (2006)
pabB	*para*-aminobenzoate synthetase component	E8	ND	Same as WT: HeLa	ND	Yes: HeLa	↓ Replication: HeLa	ND	ND	Yes: BALB/c (i.n.)	Pilatz et al. (2006)

bpsI1528	Putative exported protein	E8	ND	Same as WT: HeLa	ND	Severely impaired: HeLa	↓ Replication: HeLa and J774A.1	ND	ND	Yes: BALB/c (i.n.)	Pilatz et al. (2006)
bpscN	T3SS-1 ATPase	K96243	ND	Yes: RAW 264.7	Same as WT: RAW 264.7	Same as WT: RAW 264.7	↓ Survival: RAW 264.7	ND	Increased co-localization with LC3 (RAW 264.7)	Yes: BALB/c (i.n.)	D'Cruze et al. (2011)
INVOLVED IN ACTIN-BASED MOTILITY											
bimA	Autosecreted	10276	ND	Yes: J774.2	Same as WT: J774.2	No: J774.2	Yes: J774.2	No: J774.2	Not susceptible (unpub-lished)	ND	Stevens et al. (2005b)
INVOLVED IN FORMATION OF MNGCS											
rpoS	Global regulatory factor	844	ND	↓: RAW 264.7	Yes: RAW 264.7	ND	Same as WT: RAW 264.7	↓ MNGC	ND	ND	Utaisincharoen et al. (2006)
bipB	Bsa T3SS translocator	K96243	ND	↓: HeLa and A549	ND	ND	ND	↓: J774A.1	ND	Yes: BALB/c (i.n.)	Suparak et al. (2005)
hcp1	T6SS-1 component	K96243	ND	Same as WT: RAW 264.7	Yes: RAW 264.7	Yes: RAW 264.7 (slightly ↓)	Delayed growth: RAW 264.7	No: RAW 264.7 (18 h p.i)	ND	Yes: hamsters (i.p.)	Burtnick et al. (2011)
OTHERS											
lfpA	Lactonase family protein A	DD503	ND	ND	ND	ND	Same as WT: RAW 264.7	Same as WT: RAW 264.7	ND	Yes: hamsters (i.p.) BALB/c (i.n.)	Boddey et al. (2007)
Capsule (SR1015)	Glycosyltran sferase	1026b	Yes	↑: A549 and HeLa	ND	ND	Same as WT: HeLa, A549	Yes: A549	ND	Yes: hamsters (i.p.)	Reckseidler et al. (2001), Phewkliang et al. (2010)
fliC	Flagellin structural component	Δ*fliC*: KHW Tn*5*–*fliC*: 1026b	Yes: A549	Same as WT: A549	ND	ND	Same as WT: A549	ND	ND	Δ*fliC:* Yes: BALB/c (i.n. and i.p.) No: *C. elegans* Tn*5*–*fliC*: No: diabetic rats/hamsters (i.p.)	DeShazer et al. (1997), Chua et al. (2003)

ND, not determined; WT, wild-type; i.n., intranasal infection route; i.p., intraperitoneal infection route; ↓, reduced; ↑, increased.

Interestingly, PilA does not mediate direct adherence of *B. pseudomallei* strain 08 to eukaryotic cells. Rather, up-regulation of *pilA* at lower temperatures is responsible for the formation of *B. pseudomallei* microcolonies. These microcolonies in turn display a higher level of adherence to eukaryotic cells (Boddey et al., 2006). However, temperature regulation was not observed in strain K96243, the first strain to have its genome sequenced. Adhesion to six different human epithelial cell lines by strain 08 was also enhanced at 30˚C, but the role of pili was not investigated (Brown et al., 2002). These studies again highlight the need for caution in extrapolating data derived with different *B. pseudomallei* strains and different eukaryotic cell lines.

Flagellum-mediated adhesion was a prerequisite for invasion of the free-living ameba *Acanthamoeba astronyxis* (Inglis et al., 2003). However, a defined aflagellar *fliC* mutant was markedly attenuated in BALB/c mice, but was unimpaired in its ability to invade A549 cells (Chua et al., 2003; **Table 1**). These findings suggest that flagellae are required for virulence in mice, but probably do not constitute a major adhesin for mammalian cells.

A recent study identified two novel adhesins in *B. pseudomallei* (Balder et al., 2010). The BoaA protein shares similarity with the YadA autotransporter adhesin of *Yersinia enterocolitica* and is present also in *B. mallei*. Recombinant BoaA expressed in *E. coli* enhanced the adhesion of *E. coli* to A549 and Hep2 cells, while inactivation of the *boaA* gene reduced, but did not abolish, adhesion of *B. pseudomallei* to both cell lines (**Table 1**; **Figure 1**). A second related gene, *boaB*, appears to be unique to *B. pseudomallei*. Expression of BoaB in *E. coli* also increased adhesion to A549 and Hep2 cells and mutation of *boaB* reduced adhesion to epithelial cell lines (**Table 1**; **Figure 1**). Significantly, a similar phenotype was observed with cultured normal human bronchial epithelium. A double *boaA*/*boaB* mutant exhibited levels of adhesion similar to those of either single mutant, with some residual binding remaining (**Table 1**). These findings suggest that multiple adhesins are involved in the adhesion of *B. pseudomallei* to eukaryotic cells. Moreover, different adhesins may be involved in the interaction of bacteria with different cell types.

INTRACELLULAR INVASION, ESCAPE FROM ENDOCYTIC VESICLES, AND SURVIVAL WITHIN THE CYTOPLASM

It is likewise a widely accepted notion that initial adherence of pathogenic bacteria to the external surface of host cells is followed immediately by intracellular invasion. Over the last decade, the pace of research addressing how *B. pseudomallei* gains access to the intracellular environment and how it subsequently escapes from endocytic vesicles into the cytoplasm has accelerated, providing much needed insight into this critical step of pathogenesis. Despite this knowledge, a comprehensive understanding of the precise mechanism of intracellular invasion and subsequent endosomal escape is still lacking.

ENTRY INTO HOST CELLS

Burkholderia pseudomallei is taken up by phagocytic cells such as polymorphonuclear leukocytes (Pruksachartvuthi et al., 1990; Egan and Gordon, 1996; Jones et al., 1996) and macrophages (Pruksachartvuthi et al., 1990; Harley et al., 1994, 1998b; Jones et al., 1996; Kespichayawattana et al., 2000; Utaisincharoen et al., 2001) and can invade non-phagocytic cell lines such as HeLa, CHO, A549, and Vero cultured epithelial cell lines (Jones et al., 1996; Harley et al., 1998a; Kespichayawattana et al., 2000). The invasiveness of *B. pseudomallei* and its avirulent counterpart, *B. thailandensis*, was compared in the human respiratory epithelial cell line A549; the invasive capacity of *B. pseudomallei* was significantly greater than that of *B. thailandensis* (Kespichayawattana et al., 2004).

A *B. pseudomallei* 1026b transposon mutagenesis screen identified a gene encoding a putative two-component response regulator that is involved in the invasion of the epithelial cell line A549, HeLa, and CHO cells, but not macrophages (Jones et al., 1997; **Figure 1**). The transposon mutant exhibited an invasion level only 10% that of the parental strain, 1026b, in epithelial cells. The disrupted two-component response regulator was therefore named *irlR* for invasion-related locus (**Table 1**). A putative two-component sensor, *irlS*, was located downstream of the response regulator. This *irlRS* two-component regulatory system is not involved in virulence, as the mutant remained virulent in diabetic rats, hamsters (Jones et al., 1997), and C57BL/6 mice (Wiersinga et al., 2008), suggesting that the tissue culture invasion defect observed *in vitro* was not related to pathogenesis *in vivo*.

Many diverse Gram-negative pathogenic bacteria use Type 3 Secretion Systems (T3SS) as a conserved, but highly adapted, virulence mechanism. The T3SS apparatus comprises approximately 20 different proteins assembled into a syringe-like structure that spans the bacterial inner and outer membranes, enabling the bacteria to secrete and inject effector molecules into the cytosol of eukaryotic host cells for the subversion of cellular functions (Hueck, 1998; Zhang et al., 2006; Sun and Gan, 2010). Although the components of the T3SS apparatus are conserved between species, the secreted proteins are highly divergent (Hueck, 1998). *B. pseudomallei* encodes three T3SS clusters. Clusters 1 and 2 are similar to the T3SS gene clusters encoding the Hrp secretons of the plant pathogens *Ralstonia* (formerly *Burkholderia*) *solanacearum* and *Xanthomonas* spp. (Winstanley et al., 1999; Rainbow et al., 2002). However, cluster 3 shares homology to the *inv/spa/prg* T3SS of *Salmonella* Typhimurium and the *ipa/mxi/spa* T3SS of *Shigella flexneri* (Attree and Attree, 2001; Stevens et al., 2001; Rainbow et al., 2002) and has been designated the *Burkholderia* secretion apparatus (*bsa*) T3SS (Stevens et al., 2002).

Numerous studies have demonstrated the importance of the Bsa T3SS in the intracellular survival, replication, and virulence of *B. pseudomallei*. Indeed, numerous structural components (BsaQ, BsaU, and BsaZ), translocator (BipD), and effector proteins (BopA and BopE) of the Bsa T3SS have been implicated in various aspects of the intracellular lifecycle of *B. pseudomallei*, including invasion of host cells, escape from endocytic vesicles, and intracellular survival. Studies have shown that the invasion event requires the proteins BopE, BipD (Stevens et al., 2003), and BsaQ (Muangsombut et al., 2008; **Table 1**; **Figure 1**). BopE shares similarity with the *Salmonella* SopE/SopE2 effector proteins which act as guanine nucleotide exchange factors (GEFs) for RhoGTPases that regulate the actin network (Hardt et al., 1998; Rudolph et al., 1999; Stender et al., 2000) and in turn facilitate bacterial invasion (Wood et al., 1996; Bakshi et al., 2000). Likewise, BopE facilitates bacterial invasion of non-phagocytic cells, as a *B. pseudomallei* 10276

bopE mutant displayed a significant reduction in invasion of HeLa cells when compared to the wild-type strain (Stevens et al., 2003). In turn, BopE induces rearrangements in the subcortical actin cytoskeleton and also exhibits GEF activity. It was concluded that in epithelial cells, BopE is likely to be translocated into the host cell cytosol, where it may facilitate membrane ruffling by acting as a GEF for Cdc42 and Rac1 (Stevens et al., 2003). This notion is supported by a subsequent study by Upadhyay et al. (2008) which showed that BopE and SopE/SopE2 catalytic domains adopt similar three-dimensional folds, but that BopE has a more compact conformation. An interaction of the catalytic domain of $BopE_{78–261}$ with Cdc42 was also demonstrated. Interestingly, the SopE residues involved in contacting Cdc42 and the residues that were shown by mutation to be functionally important in SopE are conserved or conservatively substituted in BopE. Taken together, these data suggest that BopE uses the same mechanism as SopE and other Rho GEFs in catalyzing guanine nucleotide exchange in Rho GTPases, despite the fact that BopE possesses a more closed conformation (Upadhyay et al., 2008). The study performed by Stevens et al. (2003) also provided evidence that BipD, a translocator protein located on the tip of the needle (Johnson et al., 2007) and similar to *Salmonella* SipD, is also involved in invasion of non-phagocytic cells, as a 10276 *bipD* mutant was impaired in invasion of HeLa cells and notably, to an even greater extent than the *bopE* mutant described above, implying that several Bsa proteins may act in concert with BopE to facilitate bacterial invasion (Stevens et al., 2003; Stevens and Galyov, 2004).

BsaQ shares a high degree of identity with *Salmonella* Typhimurium InvA (56%; Ginocchio and Galán, 1995) and therefore by analogy, BsaQ is most likely to be a conserved inner-membrane channel protein, located at the base of the T3SS apparatus (Muangsombut et al., 2008). A *B. pseudomallei* K96243 *bsaQ* mutant exhibited a 30% reduction in invasion of A549 cells when compared to wild-type *B. pseudomallei* (Muangsombut et al., 2008). In turn, mutation of the *bsaQ* (Bsa structural component) gene prevented the secretion of at least two T3SS proteins, BopE and BipD (Muangsombut et al., 2008). Taken together, as it has been shown that BopE and BipD are required for invasion of non-phagocytic cells (Stevens et al., 2003), it can be speculated that the impaired invasion efficiency exhibited by the *bsaQ* mutant is a consequence of its inability to secrete the effector protein BopE and the translocator BipD. Interestingly, BopE and BipD do not appear to play a role in invasion of phagocytic cells, namely J774.2 murine macrophage-like cells, as *bopE* and *bipD* mutants were taken up by J774.2 cells in comparable numbers to the wild-type strain *B. pseudomallei* 10276 (Stevens et al., 2002). Likewise, we have shown that BipD is not necessary for invasion of RAW 264.7 macrophage-like cells (Gong et al., 2011; **Table 1**). These data indicate the importance of different T3SS mechanisms for the invasion of non-phagocytic and phagocytic cells.

ESCAPE FROM ENDOCYTIC VESICLES

Once a bacterium gains access to the intracellular environment, it must rapidly invoke strategies to survive within this niche. Accordingly, within 15 min of internalization, *B. pseudomallei* strain 708a can escape from endocytic vesicles into the cytoplasm of RAW 264.7, HeLa, and human macrophage-like U937 cells (MOI of either 1000:1 or 100:1) by lysing endosome membranes thus avoiding degradation through the lysosomal system (Harley et al., 1998b). Several Bsa T3SS proteins play a role in escape of *B. pseudomallei* from endocytic vesicles.

We have recently shown that the putative Bsa T3SS effector protein BopA plays an important role in escape of *B. pseudomallei* from phagosomes (Cullinane et al., 2008; Gong et al., 2011); a *bopA* mutant displayed reduced intracellular survival and significantly increased co-localization with GFP–LC3 in RAW 264.7 cells when compared to cells infected with wild-type K96243 (**Table 1**), indicating the decreased ability of the mutant to escape from the phagosome (Cullinane et al., 2008). The same mutant showed reduced phagosomal escape compared to wild-type when analyzed by transmission electron microscopy (TEM); mutant bacteria that were free in the cytoplasm however, could form actin-tails and stimulate MNGC formation (Gong et al., 2011). These data indicate that BopA is important for efficient escape from phagosomes (**Figure 1**). However, the mechanism by which BopA modulates phagosomal escape is not known. Two possible functional domains have been identified in BopA that may contribute to its function in phagosomal escape. The first is a carboxy-terminal Rho GTPase inactivation domain (RID) which may function as a protease or acyltransferase acting on host molecules (Pei and Grishin, 2009). The second is a cholesterol binding domain (CBD; Kayath et al., 2010). In macrophages infected with *Mycobacterium avium*, cholesterol depletion triggered phagolysosomal or autophagolysosomal formation with consequent bacterial degradation (de Chastellier and Thilo, 2006). Similarly, the binding of cholesterol by BopA may lead to the accumulation of cholesterol on phagosome membranes, thereby limiting lysosomal recognition and/or fusion. The function of both domains is amenable to testing. Notably, BopA from *B. mallei* is important for invasion and intracellular survival within J774A.1 macrophage cells; a *B. mallei bopA* mutant showed reduced phagocytic uptake and reduced intracellular survival (Whitlock et al., 2008). In murine alveolar macrophage (MH-S) cells, a *B. mallei bopA* mutant was recovered at higher levels from intracellular compartments compared to wild-type *B. mallei*, suggesting that the *bopA* mutant remains within intracellular compartments longer than wild-type, resulting in decreased escape (Whitlock et al., 2009).

BsaZ, similar to *Salmonella* SpaS, is the last gene in the *bsa* gene cluster that encodes a structural component of the T3SS apparatus (Stevens et al., 2002). By examining the association of intracellular bacteria with lysosome-associated membrane glycoprotein-1 (LAMP-1) containing vacuoles, it has been shown that *bsaZ* and *bipD* mutants are highly delayed in their ability to escape from endocytic vesicles; 95.1 and 95.9% of *bsaZ* and *bipD* mutant bacteria respectively were LAMP-1 associated in J774.2 cells at 6 h post-infection (p.i.; Stevens et al., 2002). Similarly, in analyses using TEM, the *bsaZ* mutant was consistently observed only within vesicles with fully intact membranes (Stevens et al., 2002) and only 2% of *bipD* mutants were able to escape into the cytoplasm of RAW 264.7 cells by 6 h p.i. (Gong et al., 2011; **Table 1**). A similar study performed by Burtnick et al. (2008) also showed a phagosome escape defect for a *bsaZ* mutant in activated RAW 264.7 murine macrophage-like cells. Using TEM analyses they demonstrated that in concordance with results outlined by Stevens et al.

(2002) at 6 h p.i., the *bsaZ* mutant remained in endocytic vesicles; however, by 12 h p.i. bacteria had begun to escape and by 18 h p.i. the majority of mutant bacteria were located in the cytoplasm (Burtnick et al., 2008). Thus, the *bsaZ* mutant does retain the ability to escape from endocytic vesicles, but this process is delayed by 6 to 12 h compared to the parent strain, DD503 (Burtnick et al., 2008; **Table 1**; **Figure 1**).

In non-phagocytic A549 cells, a *bsaQ* mutant also showed delayed escape from endocytic vesicles with 59.4% of mutant bacteria co-localizing with LAMP-1 positive vacuoles at 6 h p.i.; at 8 h p.i. further escape from vacuoles was observed (Muangsombut et al., 2008; **Table 1**; **Figure 1**). Likewise, a transposon mutant which disrupted the gene *bsaU* (Bsa structural component), which is thought to control needle length and whose product shares ∼20% similarity with Spa32 (Sun and Gan, 2010), was unable to escape from endocytic vesicles 6 h after infection of HeLa cells (Pilatz et al., 2006). The mutant however, retained the ability to multiply within the vacuoles, resulting in the formation of large vesicles containing many bacteria; at 12 h p.i. mutant bacteria began to escape, indicating a delayed escape phenotype for this mutant (Pilatz et al., 2006; **Table 1**; **Figure 1**).

The delayed escape phenotype observed for several Bsa T3SS mutants suggests that mechanisms other than the Bsa T3SS may be involved in escape from endocytic vesicles. It is noteworthy to consider the possibility of "cross-talk" taking place between the three T3SS clusters in *B. pseudomallei*. Interestingly, a triple mutant with stable deletions in the genes *sctU1*, *sctU2,* and *bsaZ*, which all encode the putative major inner-membrane subunits of T3SS clusters 1, 2, and 3 of *B. pseudomallei,* respectively, exhibited the same delayed escape phenotype as the *bsaZ* mutant described above (Burtnick et al., 2008; **Table 1**). This therefore provides evidence that components of the T3SS-1 and T3SS-2 are not responsible for the delayed escape phenotype observed for the *bsaZ* mutant and that other factors are involved in delayed phagosomal escape in RAW 264.7 cells (Burtnick et al., 2008). However, we have recently shown that the T3SS cluster 1 predicted ATPase encoded by *bpscN* is essential for full virulence of *B. pseudomallei* in a BALB/c mouse infection model (D'Cruze et al., 2011). A *bpscN* mutant was highly attenuated for virulence in BALB/c mice, displayed reduced intracellular replication in RAW 264.7 macrophage-like cells and increased co-localization with the autophagy marker protein LC3, but was unimpaired for escape from phagosomes. Thus, the T3SS cluster 1 does play a role in the intracellular survival of *B. pseudomallei*.

INTRACELLULAR SURVIVAL

Subsequent to invasion and escape from endocytic vesicles, the ability of *B. pseudomallei* to survive intracellularly is important for progression of infection. Screening of transposon mutants by Pilatz et al. (2006) identified nine mutants with reduced ability to form plaques on PtK2 cell monolayers, indicating a reduced capacity for intercellular spreading. Inactivation of *bsaU* and its role in escape from endocytic vesicles has been discussed earlier in this review. In addition to *bsaU*, Pilatz et al. (2006) showed that purine (*purM* and *purN*), histidine (*hisF*), and *para*-aminobenzoate (*pabB*) biosynthetic pathway genes and *bpsl1528* are all important for intracellular replication and survival.

Neither *purM*, encoding a putative phosphoribosyl-formylglycinamidine cyclo-ligase, nor *purN*, encoding a putative phosphoribosylglycinamide formyltransferase, were required for invasion of HeLa cells; both mutants displayed wild-type levels of cellular invasion. However, both purine biosynthesis pathway mutants were defective for intracellular growth. Interestingly, the *purM* mutant showed no intracellular replication during the course of the experiment. Similarly, *hisF* (encoding a putative imidazole glycerol phosphate synthase) and *pabB* (encoding a putative *para*-aminobenzoate synthetase component) mutants also retained the ability to invade HeLa cells, but were impaired for intracellular growth. Although intracellular growth was impaired for *purM*, *purN*, *hisF,* and *pabB* mutants, actin-tail formation, and the ability to form membrane protrusions were not affected. These findings contrast with those for a *bpsl1528* mutant (encoding a putative exported protein) that not only displayed severely restricted intracellular growth in HeLa and J774A.1 macrophages, but was also defective in formation of actin-tails and membrane protrusions.

RELEVANCE FOR *IN VIVO* PATHOGENESIS

While studies focusing on intracellular invasion, escape from endocytic vesicles and subsequent intracellular replication and survival using various defined mutants have provided insight into the pathogenesis of *B. pseudomallei* in an *in vitro* setting, it is critical to understand the role of the corresponding gene products for *in vivo* pathogenesis. Numerous virulence studies have been carried out and it appears that, with the exception of the *bopE* (effector) mutant, a correlation exists between the *in vitro* invasion and escape defects observed for various Bsa T3SS structural component and translocator mutants, and their reduced ability to cause disease. The *bsaU* transposon mutant, *bsaZ* and *bipD* mutants described above were all attenuated in BALB/c mice following intranasal infection (Stevens et al., 2004; Pilatz et al., 2006). The *bipD* mutant was also attenuated following intraperitoneal infection and this correlated with reduced bacterial replication in the liver and spleen (Stevens et al., 2004), suggesting a role for BipD during both systemic and mucosal infection. A *bsaZ* triple mutant (with deletions in the *bsaZ* homologs, *sctU*, in clusters 1 and 2 as described above) was significantly attenuated in hamsters; however, double and single mutants in *sctU* of clusters 1 and 2 that did not share the cluster 3 *bsaZ* mutation were not attenuated (Warawa and Woods, 2005). However, a T3SS cluster 1 *bpscN* mutant was attenuated in BALB/c mice (D'Cruze et al., 2011). Taken together, these virulence data indicate that a functional Bsa T3SS apparatus is required for full virulence of *B. pseudomallei*. Further, BipD and therefore the Bsa T3SS, is functionally expressed during infection *in vivo*, as antibodies against BipD have been detected in convalescent melioidosis patient sera (Stevens et al., 2002; Allwood et al., 2008).

Interestingly, the *bopE* mutant was not attenuated in BALB/c mice following either intraperitoneal or intranasal infection (Stevens et al., 2004), indicating that the effector protein BopE, on its own, is not essential for virulence and that other effectors must play a role in subversion of normal cellular processes during both systemic and mucosal infection. In turn, Warawa and Woods (2005) also demonstrated that a *bopE* mutant and other putative effector mutants (*bopA*, *bapA*, and *bapC*) were not attenuated for

virulence in the acute hamster model. However, a *bopA* mutant showed a mild attenuation in the BALB/c mouse model (Stevens et al., 2004). It has been theorized that the *B. pseudomallei* Bsa T3SS functions by delivering a set of effector proteins that target specific host cell pathways and that each individual effector alone may actually contribute little to virulence; however, the contribution of multiple effector proteins working in a cooperative manner may have a significant pathogenic impact (Galyov et al., 2010). As such, the generation of double and/or triple effector mutants would address this issue.

Similarly, a correlation also exists between the ability to replicate intracellularly and the ability to cause disease. All mutants identified by Pilatz et al. (2006) that were defective for intracellular growth (*purM, purN, hisF, pabB,* and *bpsl1528*) were also attenuated for virulence in BALB/c mice following intranasal infection. Interestingly, in the case of the *purM*, *pabB,* and *bpsl1528* mutants, all animals not only survived following challenge with 10^7 CFU, but also showed no signs of disease (Pilatz et al., 2006). This study therefore highlights the important role that the purine, histidine and *para*-aminobenzoate biosynthetic pathways and *bpsl1528* play in pathogenesis.

Taken together, these data indicate the importance of numerous genes and proteins involved in the intracellular life cycle of *B. pseudomallei*, including those involved in T3SS and various biosynthetic pathways. Importantly, the requirement for a functional T3SS with the ability to secrete effector proteins is vital for pathogenesis. Clearly, the secretion of numerous effector proteins that function in a collaborative manner, rather than individually, is critical for effective subversion of host cellular functions and therefore for pathogenesis.

ACTIN-BASED MOTILITY: A CRUCIAL MECHANISM FOR CELL-TO-CELL SPREAD

Members of several genera, including *Burkholderia*, *Listeria*, *Shigella*, *Rickettsia*, and *Mycobacterium*, have the remarkable ability to propel themselves through the cytoplasm by polymerization of the eukaryotic cytoskeletal protein actin at the surface of one pole of the bacterium. The force generated by this actin-based motility propels the bacterium through the cytoplasm, at speeds that range from 3 to 87 μm/min, depending on the pathogen and the cell type (Stevens et al., 2006). This motility facilitates the formation of membrane protrusions into neighboring cells and concomitant cell-to-cell spread (Gouin et al., 2005; Stevens et al., 2006). Since the late 1980s, an abundance of research has furthered the understanding of how such intracellular pathogens manipulate the host actin polymerization machinery for their benefit. Ultimately, actin-based motility facilitates the avoidance of host innate and adaptive immune responses as the pathogen spreads directly from cell-to-cell.

THE Arp2/3 COMPLEX

The majority of pathogens capable of actin-based motility do so by exploiting the Arp2/3 complex. This conserved host protein complex consists of seven polypeptides and is involved in both actin filament nucleation and organization (Cossart, 2000). On its own, the Arp2/3 complex possesses weak biochemical activity. The complex becomes activated by nucleation promoting factors (NPFs), which include members of the Wiskott–Aldrich syndrome protein (WASP) family; this activation leads to a conformational change in the complex (Welch and Mullins, 2002; Goley et al., 2004; Gouin et al., 2005; Goley and Welch, 2006). This change initiates the formation of a new filament that emerges from an existing filament, generating a y-branched actin network (Mullins et al., 1998; Amann and Pollard, 2001; Goley and Welch, 2006). Intracellular bacteria have developed a number of different mechanisms for activating the Arp2/3 complex, thereby exploiting the complex for their own benefit. Research to date has identified two main strategies. These mechanisms include either the expression of mimics of the WASP family NPFs (e.g., *Listeria monocytogenes* ActA/*Listeria ivanovii* IactA, or *Rickettsia* RickA), or surface proteins that function by recruiting host family WASP (N-WASP) proteins (e.g., *S. flexneri* IcsA; Welch et al., 1997, 1998; Egile et al., 1999; May et al., 1999; Boujemaa-Paterski et al., 2001; Gouin et al., 2004, 2005; Jeng et al., 2004). The expression of the bacterial protein, predominately at one pole of the cell, therefore initiates actin polymerization by direct or indirect activation of the Arp2/3 complex at the surface of the pathogen (Stevens et al., 2005b).

BimA AND ITS ROLE IN ACTIN-BASED MOTILITY

Interestingly, it seems that *B. pseudomallei* employs a unique mechanism for activation of actin-based motility. Initial evidence that demonstrated the ability of *B. pseudomallei* to induce cellular actin rearrangement and membrane protrusions in both phagocytic and non-phagocytic cells was provided by Kespichayawattana et al. (2000). Actin rearrangement in a "comet" tail formation, typical of actin-based motility, was observed at one pole of the bacterium after staining *B. pseudomallei*-infected J774A.1 and HeLa cells with rhodamine-conjugated phalloidin. It was later discovered that actin-based motility of *B. pseudomallei* is dependent upon the autosecreted protein, BimA (Stevens et al., 2005b). Mutation of *bimA* abolished actin-based motility of *B. pseudomallei*; importantly however, the mutation did not influence the activity of the Bsa T3SS and the mutant retained the ability to escape from endosomes (Stevens et al., 2005b; **Table 1**; **Figure 1**). Evidence supporting the notion that actin-based motility is a prerequisite for intercellular spread was provided by Stevens et al. (2005b) and Sitthidet et al. (2011). A *bimA* mutant did not form membrane protrusions in J774.2 cells (Stevens et al., 2005b) and did not form plaques in A549 monolayers (Sitthidet et al., 2011), indicating the *bimA* mutant could not spread from cell-to-cell. Reminiscent of ActA and IcsA, BimA was found to localize at one pole of the bacterial cell where actin assembly takes place (Stevens et al., 2005b). Interestingly, BimA homologs in *B. mallei* and *B. thailandensis* (which also possess the ability to induce actin-based motility in J774.2 cells) can restore the actin-based motility defect of a *B. pseudomallei bimA* mutant (Stevens et al., 2005a).

A survey of the prevalence and sequence diversity of BimA in clinical and environmental isolates from endemic areas demonstrated intraspecies conservation of BimA in natural populations of *B. pseudomallei*, *B. mallei*, and *B. thailandensis* (Sitthidet et al., 2008). In addition, tandem WASP homology 2 (WH2) domains, which are predicted to mediate the binding of actin monomers, were conserved in sequenced *B. pseudomallei* strains (Sitthidet et al., 2008). These domains were later found to be required for

actin binding, actin assembly, and therefore, actin-based motility (Sitthidet et al., 2011). A proline-rich motif (IP_7, also known as PRM1) which is known to interact with profilin and functions to funnel actin monomers to the tip of actin filaments, was also conserved in sequenced *B. pseudomallei* strains. In addition, a tandem repeat of 13 amino acids adjacent to the IP_7 motif on the amino-terminal side (NIPVPPPMPGGGA) was conserved in most sequenced *B. pseudomallei* strains (Sitthidet et al., 2008). However, later studies indicated that the 13 amino acid repeat and the IP_7 proline-rich motif are not essential for actin-based motility *in vitro* (Sitthidet et al., 2011). The number of PDASX repeats that are adjacent to the WH2 domains on the carboxyl-terminal side was also found to vary within sequenced *B. pseudomallei* strains, with the number of repeats ranging from 2, 5 to 7 copies (Sitthidet et al., 2008). It was demonstrated that a tract of five PDASX direct repeats was required for actin-based motility and intercellular spread; however, they were not involved in actin binding. Interestingly, the rate of polymerization increased in a stepwise manner as the number of PDASX repeats increased from zero to two to five to seven, indicating that these repeats act in an additive manner to stimulate polymerization of pyrene-actin monomers *in vitro* (Sitthidet et al., 2011).

BURKHOLDERIA PSEUDOMALLEI EMPLOYS A UNIQUE MECHANISM FOR ACTIVATION OF ACTIN-BASED MOTILITY

Burkholderia pseudomallei does not activate actin-based motility via a *Shigella*-like mechanism, as N-WASP is not found on either the surface of *B. pseudomallei* or within actin-tails (Breitbach et al., 2003). This, and the fact that F-actin clustering results from transient expression of BimA, a characteristic that is seen with WASP overexpression (Stevens et al., 2005b), indicate that BimA may function as an NPF mimic to induce actin-based motility in infected cells (Stevens et al., 2006). However, the mechanism appears distinct from that of *Listeria*, as VASP proteins were not detected on the surface of *B. pseudomallei* and only very weakly throughout actin-tails (Breitbach et al., 2003); this is in contrast to *Listeria* where Ena/VASP proteins interact directly with ActA (Laurent et al., 1999). Confirmatory to these results, infection of N-WASP- or Ena/VASP-defective cells with *B. pseudomallei* demonstrated that these proteins are not essential for actin-based motility by *B. pseudomallei* (Breitbach et al., 2003).

Interestingly, while the Arp2/3 complex is strongly incorporated into *B. pseudomallei* actin-tails (Breitbach et al., 2003), its precise function in actin polymerization is not clear. BimA can stimulate actin polymerization *in vitro* in an Arp2/3 independent manner (Stevens et al., 2005b). In addition, overexpression of an Arp2/3 binding WCA (WH2, central, and acidic) domain of Scar1 (NPF), which leads to cytoplasmic sequestration and inhibition of the Arp2/3 complex, and therefore inhibition of motility of *Listeria*, *Shigella*, and *Rickettsia conorii*, had no effect on actin-based motility of *B. pseudomallei* (Breitbach et al., 2003). Based on these data, it appears that the mechanism of actin-based motility of *B. pseudomallei* is distinct from that identified for all other intracellular pathogens studied to date. It has been suggested that BimA alone may be sufficient for intracellular motility of *B. pseudomallei*; however, the requirement for other bacterial co-factors or different post-translational modifications of BimA cannot be ruled out (Stevens et al., 2006).

A POTENTIAL ROLE FOR TYPE VI SECRETION SYSTEM CLUSTER 1 AND OTHER GENE PRODUCTS IN ACTIN-BASED MOTILITY

The *B. pseudomallei* genome encodes six functional Type 6 Secretion Systems originally designated T6SS-1-6 (Schell et al., 2007). A subsequent paper by Shalom et al. (2007) however, assigned the names *tss-5*, *tss-4*, *tss-6*, *tss-3*, *tss-2*, and *tss-1*, respectively, to these same gene clusters. As such, we will refer to the nomenclature used by Schell et al. (2007).

T6SS play a role in virulence in many bacterial pathogens where they function to inject effector proteins into host cells (Pukatzki et al., 2009). New evidence has demonstrated that in *B. mallei*, the T6SS-1 plays an important role in actin-based motility in RAW 264.7 cells; *tssE* mutants were able to undergo vacuolar escape, but once in the cytoplasm the mutants exhibited defects in actin polymerization and intra- and intercellular spread (Burtnick et al., 2010). Importantly, a homologous T6SS expressed in *B. pseudomallei* is similarly induced following uptake by RAW 264.7 cells. This system (T6SS-1; locus tags BPSS1493–BPSS1511) is flanked by *bimA* on one side and the Bsa T3SS locus on the other (Shalom et al., 2007). By analogy with *B. mallei*, it could be speculated that mutation of T6SS-1 in *B. pseudomallei* would also cause actin polymerization defects and raises the question as to whether secreted effectors of the T6SS, such as Hcp and/or VgrG, could interact with BimA. Importantly however, a T6SS-1 *tssH* mutant showed no difference in invasion and survival within RAW 264.7 cells compared to wild-type *B. pseudomallei*; its ability to polymerize actin and undergo actin-based motility was not investigated (Shalom et al., 2007). A subsequent study by Burtnick et al. (2011) has now shown that while a *hcp1* (from T6SS-1) mutant did demonstrate a slightly reduced level of actin-based motility compared to wild-type *B. pseudomallei*, this difference was not as significant as that observed in the *B. mallei tssE* T6SS-1 mutant described above (Burtnick et al., 2010). *tssE* is predicted to encode a component of the T6SS-1 apparatus and appears to be required for Hcp1 secretion (Schell et al., 2007). Therefore, it appears likely that *tssE* is required for secretion of other effector(s) that may play a role in actin polymerization, as mutation of *hcp1* on its own had little effect on actin-based motility. Interestingly however, mutation of *hcp1* resulted in the absence of MNGC formation (discussed elsewhere in this review), delayed intracellular growth, and reduced cytotoxicity in RAW 264.7 cells (Burtnick et al., 2011).

Another gene which has been implicated for its potential role in actin-tail formation is *bpsl1528* which encodes a putative exported protein (Pilatz et al., 2006). As described above, a *bpsl1528* mutant was defective for intracellular growth; immunofluorescence microscopy revealed that actin-tail formation was severely impaired as only rudimentary actin-tails were observed and no protrusions could be detected in HeLa cells. However, the mutant also demonstrated reduced swimming motility. Pilatz et al. (2006) therefore speculated that the pleiotropic phenotype of the *bpsl1528* mutant may be due to a regulatory function of the

encoded protein on numerous virulence factors rather than to a single effector molecule.

In summary, the role of BimA in actin-based motility is widely accepted. However, further evidence has indicated that the process of actin polymerization leading to actin-based motility may occur as a result of a concerted effort involving other bacterial factor(s) that could involve the T6SS cluster 1 and other putative exported proteins. Interestingly, the process of activation of actin-based motility by *B. pseudomallei* is distinct from that observed for other pathogens and further studies are therefore required to address this issue.

CELL FUSION AND THE FORMATION OF MULTI-NUCLEATED GIANT CELLS: IMPORTANT MECHANISMS FOR THE PROGRESSION OF INFECTION

As outlined above, several species of intracellular pathogens are able to move throughout the cell cytoplasm by manipulating actin polymerization. For *Shigella*, actin-based motility is also sufficient for the movement of bacteria from cell-to-cell via membrane protrusions (Monack and Theriot, 2001). Indeed, recombinant *E. coli* cells expressing *S. flexneri* IcsA (required for actin polymerization) were able to produce membrane protrusions in HeLa cells and move into the cytoplasm of adjacent cells (Monack and Theriot, 2001). While actin-based motility is an essential prerequisite for the spread of *B. pseudomallei* from cell-to-cell (Stevens et al., 2005b; Sitthidet et al., 2011), cell fusion, and the production of MNGC also appears to be required. Infection of phagocytic or non-phagocytic cell lines with *B. pseudomallei, B. mallei,* or *B. thailandensis* results in cell-to-cell fusion and the formation of MNGC (Harley et al., 1998a). Furthermore, MNGC have also been observed following histopathological assessment of human tissue samples recovered from melioidosis patients (Wong et al., 1995), suggesting that MNGC formation occurs during *B. pseudomallei* infection. Other infectious agents such as human immunodeficiency virus (HIV; Ciborowski and Gendelman, 2006), cytomegalovirus (CMV; Kinzler and Compton, 2005), herpes simplex virus (HSV; Cole and Grose, 2003), and mycobacterial species (Utermöhlen et al., 2008) also drive the formation of MNGC.

Induction of cell fusion following *B. pseudomallei* infection was confirmed by analysis of co-cultures of J774A.1 cells that had been labeled either with cell tracker green CMFDA or cell tracker red CMTMR prior to mixing (Kespichayawattana et al., 2000). Orange–yellow MNGC were observed within 4–6 h after infection, indicating that some of the eukaryotic cell membranes had fused; no fused cells were observed in mock infected cultures. Similar results were obtained with HeLa and L929 cells, although the rate of cell fusion and MNGC formation was slower. *B. pseudomallei* infection leads to apoptosis of both fused and unfused cells. At 2 h p.i. approximately 3% of cells showed evidence of apoptotic changes and this increased to 43% by 6 h. Interestingly, within MNGC, both normal nuclei and those showing apoptotic changes could be observed (Kespichayawattana et al., 2000).

The molecular mechanisms leading to cell fusion and formation of MNGC following *B. pseudomallei* infection are poorly characterized. Macrophage cell fusion may be associated with chronic inflammation and can be induced *in vitro* by treatment of macrophages with certain cytokines, including macrophage colony-stimulating factor, granulocyte–macrophage colony-stimulating factor, interleukin (IL)-4 and IFN-γ (Kondo et al., 2009). Cell fusion in response to infections with the viruses CMV and HSV is associated with the production of viral glycoproteins (Cole and Grose, 2003; Kinzler and Compton, 2005). In *B. pseudomallei,* the ability to form MNGC has been associated with RpoS, BipB, T6SS-1, and the putative toxin-encoding genes *bpsl0590* and *bpsl0591* (**Figure 1**).

A *B. pseudomallei rpoS* mutant could replicate intracellularly almost indistinguishably from the wild-type strain, but was significantly impaired in its ability to induce MNGC formation; only 3% of cells infected with the *rpoS* mutant formed MNGC compared with 17% for cells infected with the wild-type strain (Utaisincharoen et al., 2006). However, the *rpoS* mutant was not tested for its ability to move intracellularly by actin-based motility (**Table 1**). The RpoS regulon in *B. pseudomallei* has been elucidated by comparing protein expression in wild-type and *rpoS* mutant strains; 70 proteins (derived from 58 unique genes) showed differential expression of >3-fold ($p < 0.05$) between the two strains (Osiriphun et al., 2009). The proteins encoded by these differentially expressed genes included bacterial stress response and cell envelope biogenesis components as well as some putative virulence factors, including a T3SS-1 component. Thus, it is likely that RpoS regulates the expression of a *B. pseudomallei* gene(s) that is directly involved in the stimulation of cell-to-cell fusion, but the exact gene(s) has not yet been identified.

The Bsa T3SS and the effector protein BipB have also been implicated in MNGC formation; a *bipB* mutant was unable to induce MNGC formation in J774A.1 macrophage-like cells at 6 h p.i. and showed 6 to 10-fold reduced MNGC formation at later time-points (Suparak et al., 2005). The ability to form MNGC was restored by complementation with intact *bipB*. However, it is unclear if BipB is specifically involved in cell fusion and MNGC formation, as the *bipB* mutant was also significantly impaired for invasion of HeLa cells and was not tested for its ability to move intracellularly by actin-based motility (**Table 1**).

Hcp proteins are critical components of T6SS. *B. pseudomallei* mutants with deletion of *hcp* genes from each of the six T6SS loci were tested for virulence in a hamster infection model; only the Δ*hcp1* mutant was attenuated for virulence (Burtnick et al., 2011). The Δ*hcp1* mutant was taken up by RAW 264.7 macrophages at a similar rate to the wild-type strain and could escape from phagosomes into the cytosol and move intracellularly by actin-based motility. Although the Δ*hcp1* mutant showed a reduced level of actin-based motility and a delayed intracellular growth phenotype, by 18 h p.i. the levels of intracellular wild-type and Δ*hcp1* mutant bacteria were indistinguishable. Importantly, no MNGC formation was observed in RAW 264.7 cells following infection with the Δ*hcp1* mutant despite high levels of intracellular bacteria (**Table 1**). These data suggest that a secreted effector(s) of the T6SS is critical for the cell fusion of macrophages and for the formation of MNGC. Indeed, Burtnick et al. (2011) proposed that the inability of the Δ*hcp1* mutant to induce MNGC formation may lead directly to its reduced intracellular growth defect, as the fusion with nutrient rich, uninfected macrophages may be critical for the intracellular replication of *B. pseudomallei.*

A genome-wide screen for *B. pseudomallei* products which could damage macrophage cells identified a wide range of *B. pseudomallei* genes, including the putative toxin-encoding genes *bpsl0590* and *bpsl0591* (Dowling et al., 2010). In this analysis, the supernatants from cultures of *E. coli* containing *B. pseudomallei* genomic fragments cloned in BAC or fosmid vectors, were tested for activity against J774-2 macrophage cells. More than 110 genomic regions were identified as conferring some level of anti-macrophage activity; however, the cloned genomic fragments contained multiple genes and the anti-macrophage activity was never localized to single genes. Importantly, treatment of J774-2 cells with supernatant from *E. coli* clones containing an approximately 15 kb region containing the genes *bpsl0590* and *bpsl0591*, directly caused apoptosis and the formation of MNGC, suggesting that the putative toxins encoded by these genes may have a direct role in MNGC formation.

The MNGC formed following *B. pseudomallei* infection of macrophage-like cells show striking similarities to osteoclast cells, which are also MNGC. MNGC resulting from *B. pseudomallei* infection of RAW 264.7 cells express increased levels of mRNA encoding each of the osteoclast markers calcitonin receptor (CTR), cathepsin K (CTSK), and tartrate-resistant acid phosphatase (TRAP) compared to uninfected cells (Boddey et al., 2007). Interestingly, while *B. thailandensis* also induces the formation of MNGC, these cells do not express increased levels of the osteoclast markers CTR and CTSK, and show only a marginal increase in TRAP expression (Boddey et al., 2007). The *B. pseudomallei* gene *lfpA* (lactonase family protein A) was found to be required for maximal stimulation of expression of osteoclast markers in RAW 264.7 cells following *B. pseudomallei* infection; this gene is not present in *B. thailandensis*. Expression of *lfpA* itself was up-regulated approximately 10^7-fold in bacteria that were in contact with RAW 264.7 cells as compared to those growing *in vitro*. A *B. pseudomallei lfpA* mutant was able to replicate at levels indistinguishable from the wild-type strain in RAW 264.7 macrophage-like cells and form actin-tails, but showed reduced virulence in both Syrian hamsters and BALB/c mice (Boddey et al., 2007; **Table 1**). Taken together these data suggest that *B. pseudomallei* specifically induces the formation of MNGC through a number of mechanisms and the induction of these host cell changes may have evolved to benefit the bacteria as a niche for optimal replication and spread.

INHIBITION OF MACROPHAGE ACTIVATION FACILITATES INTRACELLULAR SURVIVAL

The ability of *B. pseudomallei* to survive and replicate in macrophages is at least in part due to the suppression of macrophage killing mechanisms, including the production of the free radical species nitric oxide (NO), although it should be noted that human macrophages produce less NO than rodent macrophages (for review see Carsillo et al., 2009). NO is one of the key antimicrobial molecules produced within macrophages and is important for the clearance of many intracellular pathogens, including *Leishmania*, *Salmonella,* and *Mycobacterium* (for review see Fang, 1997). In macrophages, NO production results from the activity of the inducible nitric oxide synthase (iNOS). Expression of iNOS is stimulated by the cytokines IFN-γ, IFN-β, TNFα, IL-1, and IL-2, and by pathogen-associated products including lipopolysaccharide (LPS) and lipoteichoic acid (Fang, 1997; Jacobs and Ignarro, 2001). However, macrophages infected with *B. pseudomallei* do not activate iNOS expression. This is due, at least in part, to the inability of *B. pseudomallei*-infected macrophages to produce IFN-γ and IFN-β, as stimulation of infected macrophages with either of these interferons results in increased iNOS expression and reduced intracellular survival of *B. pseudomallei* (Utaisincharoen et al., 2003, 2004).

The secretion of IFN-β by macrophages is up-regulated in response to LPS and also infection with Gram-negative, but not Gram-positive, bacteria, suggesting that LPS is critical for production of IFN-β (Utaisincharoen et al., 2003). The inability of macrophages infected with *B. pseudomallei* to produce IFN-β may be a direct consequence of the LPS structure of *B. pseudomallei* (Utaisincharoen et al., 2003), as purified *B. pseudomallei* LPS stimulated reduced NO expression in comparison to macrophages stimulated with *E. coli* or *Salmonella enterica* serovar Typhi LPS (Utaisincharoen et al., 2000). Furthermore, a *B. pseudomallei wbiI* mutant, which is predicted to express LPS lacking O-antigen, stimulated significant levels of iNOS and IFN-β production (Arjcharoen et al., 2007; **Figure 1**).

Both IFN-γ and IFN-β produce a transcriptional response through the Janus kinases-signal transducers and activators of transcription (JAK–STAT) signal transduction pathway. The receptor complexes for each IFN type are related but unique (Decker et al., 2002) and binding of IFN to the appropriate receptor results in STAT phosphorylation and dimerization. IFN-γ binding results in STAT-1 homodimerization, whereas IFN-β results in production of phosphorylated STAT-1 homodimers and STAT-1 and STAT-2 heterodimers. These phosphorylated STAT dimers are then translocated into the nucleus where they mediate changes in expression of a range of IFN-regulated genes including iNOS. However, the suppressor of cytokine signaling (SOCS) and cytokine-inducible Src homology 2-containing (CIS) proteins can inhibit STAT phosphorylation and therefore IFN responses (Ekchariyawat et al., 2005; **Figure 1**). RAW 264.7 macrophages exposed to either live or killed *B. pseudomallei* showed increased expression of SOCS3 and CIS but not SOCS1 and 2 (Ekchariyawat et al., 2005). This activation was specifically due to the presence of intracellular *B. pseudomallei,* rather than a secondary response to macrophage cytokine production, as increased SOCS3 and CIS mRNA was observed even following pretreatment of macrophages with the protein inhibitor cyclohexamide (Ekchariyawat et al., 2005, 2007). Furthermore, up-regulation of SOCS3 mRNA was not observed in a macrophage cell line with reduced nucleotide-binding oligomerization domain-containing protein 2 (NOD2) expression, suggesting that the cytoplasmic pattern recognition receptor NOD2 is critical for SOCS3-mediated inhibition of iNOS expression (Pudla et al., 2010).

EVASION OF HOST CELL AUTOPHAGIC MECHANISMS BY *B. PSEUDOMALLEI*

Autophagy occurs in all eukaryotic cells and is critical for the regulated degradation of cellular components. During autophagy a portion of cytoplasm becomes enclosed within an isolation membrane (phagophore), generating a double-membrane vesicle, the

autophagosome, which then, usually following initial fusion with an endosome, fuses with a lysosome. The material sequestered within the autophagosome is then degraded and the products exported to the cytosol for re-use. Autophagy is important in the context of cellular homeostasis for the removal and recycling of damaged or non-functional organelles and the destruction of certain long-lived proteins and other macromolecules (Ravikumar et al., 2010).

Recently, autophagy has become recognized as an important component of the eukaryotic innate immune system (Schmid and Munz, 2007; Ravikumar et al., 2010). In this context, autophagy can function as a defense mechanism against bacterial pathogens, resulting in their clearance. While some pathogens succumb to autophagic clearance and others modify autophagy to benefit their intracellular survival, it is clear that still other intracellular bacterial pathogens can evade autophagy to aid their survival (Hussey et al., 2009; Shahnazari and Brumell, 2011). Notably, two bacterial species, *L. monocytogenes* and *S. flexneri*, which can disrupt the phagosome membrane to allow escape into the cytosol, can be targeted by autophagy (Ogawa et al., 2005; Birmingham et al., 2007) when free in the cytosol.

AUTOPHAGY AND *B. PSEUDOMALLEI*

Bacterial escape from phagosomes, and the prospect of the escaped bacteria being subject to autophagy, led us to carry out the first analyses of the interaction of *B. pseudomallei* with host cell autophagic processes. In response to infection of macrophage RAW 264.7 cells, only a subset of bacteria co-localized with the autophagy marker protein LC3 (Cullinane et al., 2008). When cells were treated with rapamycin, a pharmacological inducer of autophagy, bacterial co-localization with LC3 was increased significantly and bacterial survival was reduced. Thus, autophagy was implicated as part of the host defense system against *B. pseudomallei* infection, although the mechanism by which most invading bacteria avoided host autophagic attack remained obscure. Moreover, we showed that the predicted bacterial Bsa T3SS effector protein, BopA, is involved in modulating the host cell response, as *bopA* mutant bacteria showed increased co-localization with LC3 and reduced intracellular survival (Cullinane et al., 2008).

Recently it was shown that LC3 can be recruited directly to bacteria-containing phagosomes (Sanjuan et al., 2007) via a process designated LC3-associated phagocytosis (LAP; Sanjuan et al., 2009). In RAW 264.7 cells infected with *E. coli*, LAP was induced by LPS treatment via toll-like receptors (TLRs), and involved the rapid translocation of the autophagic proteins Beclin1 and LC3 to the bacteria-containing phagosomes, leading to an increased level of phagocytosis and bacterial killing (Sanjuan et al., 2007). These reports led us to assess the nature of the compartment in which intracellular *B. pseudomallei* is sequestered. Through an extensive analysis of EM images of infected cells, we demonstrated that intracellular bacteria are either free in the cytosol or sequestered in single-membrane phagosomes, but only extremely rarely contained in double-membrane autophagosomes, suggesting that LC3 is recruited to *B. pseudomallei*-containing phagosomes (Gong et al., 2011; **Figure 2**).

Quantitative analysis of EM images of a *bipD* mutant, lacking a functional Bsa T3SS, indicated that it displayed no escape from phagosomes at 2 and 4 h p.i. However, *bipD* mutant bacteria displayed a high level of co-localization with LC3. Furthermore, *bopA* mutant bacteria that display increased co-localization with LC3 (Cullinane et al., 2008) also showed reduced phagosome escape (Gong et al., 2011). These observations indicate that *B. pseudomallei* co-localization with LC3 occurs as a result of direct recruitment of LC3 to phagosomes that contain bacteria and is not due to engulfment of bacteria by canonical autophagosomes (**Figure 2**).

Recruitment of LC3 to phagosomes in LAP led to their rapid acidification and enhanced killing of ingested *E. coli* in RAW 264.7 cells (Sanjuan et al., 2007, 2009). In our experiments, both *bipD* and *bopA* mutant bacteria showed decreased intracellular survival, enhanced co-localization with LC3 and entrapment in phagosomes (Gong et al., 2011). To confirm that these observations were consistent with LAP, we determined the dual co-localization of bacteria with LC3 and the lysosome marker LAMP-1. Such dual co-localization serves as a measure of the maturation of bacteria-containing $LC3^+$ phagosomes by fusion with lysosomes. The percentage of bacteria co-localized with both LC3 and LAMP-1 was significantly higher for both mutants, suggesting that LC3 recruitment is associated with enhanced levels of phagolysosome maturation. Consistent with this proposal was the observation that only a very low percentage of $LC3^-$ bacteria-containing phagosomes were LAMP-1^+. On the basis of these data we propose that LC3 recruitment to *B. pseudomallei*-containing phagosomes stimulates fusion of phagosomes with lysosomes, leading to enhanced killing of the internalized bacteria. However, this hypothesis remains to be demonstrated directly.

Collectively these observations (Gong et al., 2011) show that LAP, rather than canonical autophagy, is the mechanism which macrophage cells use in defense against *B. pseudomallei* infection. However LAP is relatively ineffective and most bacteria escape to the cytosol where they efficiently evade capture by canonical autophagy (**Figure 2**).

ESCAPE FROM AUTOPHAGY OCCURS BY A MECHANISM DIFFERENT FROM THAT USED BY *SHIGELLA*

Shigella flexneri induces membrane damage to mediate bacterial escape from the phagosome into the cytosol, where it induces actin polymerization, mediated by the bacterial IcsA (VirG) protein (Makino et al., 1986; Goldberg and Theriot, 1995). In some cell types IcsA is specifically targeted by the autophagic membrane protein Atg5, thereby inducing autophagy (Ogawa et al., 2005). However, *S. flexneri* secretes a T3SS effector protein, IcsB, which binds to IcsA and competitively inhibits its interaction with Atg5, thus abrogating the induction of autophagy (Ogawa et al., 2005). Interestingly, *B. pseudomallei* encodes the proteins BimA and BopA which have 11 and 23% amino acid identity respectively to their *S. flexneri* homologs, IcsA and IcsB.

Although BimA mediates actin-based intracellular motility of *B. pseudomallei* (Stevens et al., 2005b), it lacks the IcsA-binding domain targeted by Atg5 (Ogawa et al., 2005). Thus, it would seem that BimA and IcsA are not functional counterparts in the context of autophagy evasion. Furthermore, bacterial two-hybrid analysis (our unpublished data) failed to establish an interaction between

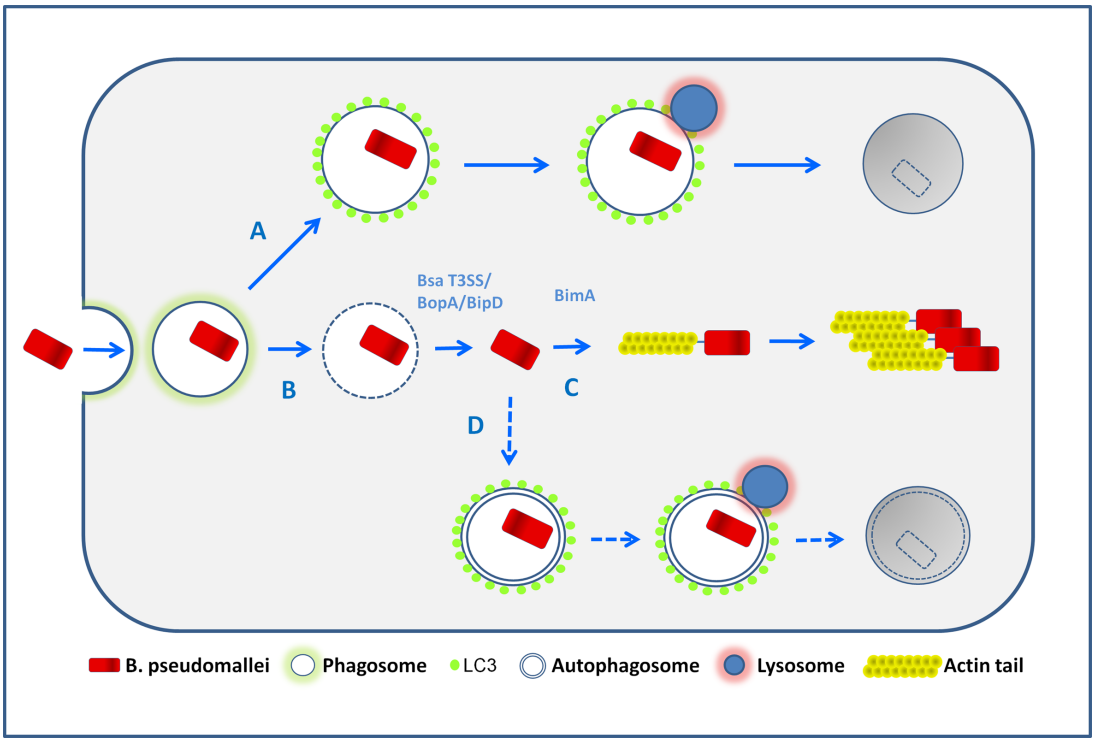

FIGURE 2 | Possible fates of *B. pseudomallei* in infected macrophages. Following phagocytic uptake by macrophages, bacteria are first located within phagosomes. The majority of wild-type bacteria can escape from the phagosome into the cytosol (pathway B) in a process which is largely uncharacterized but involves the Bsa T3SS. Once free in the cytosol bacteria activate BimA-mediated actin-based motility and replicate (pathway C). Potentially some cytosolic bacteria may be sequestered in canonical autophagosomes (pathway D), but the available evidence suggests that this occurs very infrequently. The autophagy marker protein LC3 can be recruited to bacteria-containing phagosomes, a process designated LC3-associated phagocytosis (LAP) which stimulates further phagosomal maturation via recruitment of other proteins, and the subsequent fusion of phagosomes with lysosomes, leading to bacterial killing (pathway A). It is possible that bacteria may escape from LAP, but definitive evidence that this occurs is presently lacking.

BopA and BimA, suggesting that the *B. pseudomallei* proteins do not interact in a manner comparable to their *S. flexneri* counterparts. Thus, we propose that *B. pseudomallei* evades autophagy by an alternative mechanism which currently remains unknown.

UBIQUITINATION-MEDIATED AUTOPHAGY

The specific modification of cellular proteins with polyubiquitin is a fundamental post-translational modification that occurs in all eukaryotic cells and is central to many cellular processes. Depending on the nature of the modification (K48- or K63-linked chains) polyubiquitination can result in altered functional properties, in targeting the protein for degradation by the 26S proteasome, or as shown recently, targeting of the material for lysosomal degradation by the autophagic pathway (for review see Komatsu and Ichimura, 2010).

Ubiquitination involves the conjugation of ubiquitin (Ub) moieties to target proteins. In mammalian cells, ubiquitination involves three enzymatic steps. Ub-activating enzymes (E1) transfer Ub to E2-conjugating enzymes, which then transfer the activated Ub to a lysine of the target protein through E3 ligases (Shabek and Ciechanover, 2010). Deubiquitinases are responsible for removing Ub chains from proteins (Shabek and Ciechanover, 2010).

The ubiquitination pathway does not operate in prokaryotes. Nevertheless, polyubiquitination has been shown in many cases to be important for regulating the host response to pathogens. Exploitation of host ubiquitination signaling pathways by pathogen effectors appears to be a common theme among bacteria (for review see Angot et al., 2007). A number of pathogen tactics has been described; they include effectors secreted by Type III and Type VI systems that (i) use the host ubiquitin proteasome system (UPS) to assure their own destruction; (ii) interfere with the ubiquitination level of key cellular proteins involved in innate immunity, or (iii) mimic E3 ligase subunits to manipulate the UPS to its own advantage.

A recent report suggests that, like a number of other pathogens, *B. pseudomallei* can modulate host ubiquitination to its own advantage. TssM, a secreted product of the T6SS cluster 5 encoded by the *bpss1512* gene, was identified as a virulence factor for *B. pseudomallei* (Tan et al., 2010). In an acute BALB/c mouse infection model, the absence of TssM in *B. pseudomallei* increased the rate of death and inflammation in infected mice. TssM was alone found to be responsible for down-regulating host inflammatory responses by interfering with the ubiquitination of critical signaling intermediates and, in turn, the activation of NF-κB. Overexpression of TssM in HEK293T cells resulted in diminished ubiquitinated forms of TNFR-associated factor-3, TNFR-associated

factor-6 and IκBα. The attenuation of NF-κB activity observed in macrophages infected with wild-type *B. pseudomallei* was restored in macrophages infected with a *tssM* mutant.

BPSS1512 shares 99% identity with TssM of *B. mallei.* In an earlier study it was shown that *tssM* encodes a broad-based deubiquitinase (Shanks et al., 2009). Cleavage of both K48- and K63-linked ubiquitinated substrates was demonstrated in enzymatic assays. In this study no cellular substrates or phenotype in animal models could be identified. Nevertheless, collectively these studies of TssM indicate that *B. pseudomallei* is able to modulate the host ubiquitination system through the action of a secreted deubiquitinase. It remains to be seen whether other host or bacterial substrates exist for the deubiquitinase activity of TssM, or whether *B. pseudomallei* can secrete other effectors capable of modulating the host Ub-pathway. Since several target cytosolic proteins are subject to the deubiquitinase activity of TssM, it seems likely that other cytosolic host proteins may well be susceptible.

It has been suggested that Ub-mediated targeting is a general and major pathway of selective autophagy in mammals. One possible set of targets for the deubiquitinase activity of TssM, yet to be investigated, are ubiquitinated proteins associated with bacteria and recognized by the autophagic pathway. There are several reports describing the co-localization with polyubiquitin of bacteria that have escaped from the phagosome. Species include *Streptococcus pyogenes*, *L. monocytogenes,* and *Mycobacterium marinum* (for review see Shahnazari and Brumell, 2011). A model has been proposed in which host or bacterial proteins associated with the bacterial surface are directly ubiquitinated by the host system. However, the identity of the ubiquitinated proteins has yet to be established. An alternate model has been proposed, based on observations of *S. flexneri* infections. When *S. flexneri* disrupts the phagosome membrane to escape into the cytosol, proteins associated with membrane remnants, including TRAF6 which is involved in NF-κB signaling, are polyubiquitinated, recruit the autophagy marker LC3 and adaptor p62, and are targeted to degradation through autophagy (Dupont et al., 2009). The presence of both P62 and other IKK components trapped in the membrane remnants led to the suggestion that the autophagy pathway is used to regulate the activation of inflammatory responses at early timepoints in infection (Dupont et al., 2009). Notably, in autophagy deficient ($Atg5^{-/-}$) cells and in cells in which autophagosome maturation was blocked (ATG4B dominant negative mutant), polyubiquitinated proteins and P62 accumulated on membrane remnants, and the early inflammatory and cytokine response was exacerbated (Dupont et al., 2009). Our preliminary data show that *B. pseudomallei* in macrophages do not show a high degree of co-localization with poly-Ub, suggesting that the host ubiquitination pathway might be modulated at a number of levels. One intriguing possibility is that the deubiquitinase activity of the TssM effector may play a role in removing Ub from proteins associated with the bacterial surface, thereby allowing the bacteria to avoid detection and elimination from the host cell by autophagy.

Burkholderia pseudomallei K96243 encodes a cyclomodulin (BPSS1385) that displays 26% identity with the cycle inhibiting factor (Cif) cyclomodulin produced by enteropathogenic and enterohemorrhagic *E. coli* (Jubelin et al., 2009; Yao et al., 2009). Cif from pathogenic *E. coli* is an effector which is injected into host cells via the T3SS machinery and provokes an irreversible cytopathic effect which is characterized by G_1 and G_2 cell cycle arrests and reorganization of the actin network (Nougayrède et al., 2001; Marchès et al., 2003; Taieb et al., 2006; Samba-Louaka et al., 2008; Jubelin et al., 2009). The *B. pseudomallei* cyclomodulin, termed CHBP (for Cif homolog in *Burkholderia pseudomallei*), reveals a papain-like fold with a conserved Cys-His-Gln catalytic triad and has been shown to be a functional homolog of Cif from *E. coli* (Jubelin et al., 2009; Yao et al., 2009). Interestingly, it was recently shown that CHBP is a potent inhibitor of the eukaryotic ubiquitination pathway and specifically deamidates Gln^{40} in ubiquitin and NEDD8 (a ubiquitin-like protein) and in turn attenuates ubiquitination both *in vitro* and during *Burkholderia* infection (Cui et al., 2010). Notably, CHBP was recognized by melioidosis patient serum (Felgner et al., 2009). At present there is no evidence to connect these observations concerning CHBP with the function of host autophagic pathways.

In summary, there is a number of intriguing observations that suggest a role for ubiquitin signaling and the avoidance of host autophagy in response to infection by *B. pseudomallei.* However, a more integrated understanding must await further experimentation.

CONCLUDING REMARKS

Burkholderia pseudomallei has evolved a large array of mechanisms to survive and replicate within eukaryotic cells, including mammalian phagocytic and non-phagocytic cells. As we have outlined in this review, the last two decades have seen significant advances in the elucidation of these mechanisms. However, much remains to be uncovered about the detailed interaction of bacterial and host cell factors at the molecular level. The apparently unique mechanism of actin-based motility in *B. pseudomallei* remains obscure. Likewise, many aspects of the roles of the three T3SS clusters in the interaction of bacterial and host cell molecules and their potential cross-talk remain to be defined. The possibility exists that the different clusters are involved in the invasion of, and replication within, different types of mammalian cells. The precise function of the six T6SS clusters also requires further investigation. While it is clear that most *B. pseudomallei* in cells are able to escape autophagic attack, the mechanisms are presently unknown. The possibility of host ubiquitination of the bacterial cell surface and whether *B. pseudomallei* possesses strategies to combat this process are currently under investigation.

ACKNOWLEDGMENTS

Original work in the authors' laboratories was supported by the Australian Research Council and the National Health and Medical Research Council, Australia.

REFERENCES

Aardema, H., Luijnenburg, E. M., Salm, E. F., Bijlmer, H. A., Visser, C. E., and Van't Wout, J. W. (2005). Changing epidemiology of melioidosis? A case of acute pulmonary melioidosis with fatal outcome imported from Brazil. *Epidemiol. Infect.* 133, 871–875.

Ahmed, K., Enciso, H. D., Masaki, H., Tao, M., Omori, A., Tharavichikul, P., and Nagatake, T. (1999). Attachment of *Burkholderia pseudomallei* to pharyngeal epithelial cells: a highly pathogenic bacteria with low attachment ability. *Am. J. Trop. Med. Hyg.* 60, 90–93.

Allwood, E. M., Logue, C. A., Hafner, G. J., Ketheesan, N., Norton, R. E., Peak, I. R., and Beacham, I. R. (2008). Evaluation of recombinant antigens for diagnosis of melioidosis. *FEMS Immunol. Med. Microbiol.* 54, 144–153.

Amann, K. J., and Pollard, T. D. (2001). Direct real-time observation of actin filament branching mediated by Arp2/3 complex using total internal reflection fluorescence microscopy. *Proc. Natl. Acad. Sci. U.S.A.* 98, 15009–15013.

Angot, A., Vergunst, A., Genin, S., and Peeters, N. (2007). Exploitation of eukaryotic ubiquitin signaling pathways by effectors translocated by bacterial type III and type IV secretion systems. *PLoS Pathog.* 3, e3. doi: 10.1371/journal.ppat.0030003

Arjcharoen, S., Wikraiphat, C., Pudla, M., Limposuwan, K., Woods, D. E., Sirisinha, S., and Utaisincharoen, P. (2007). Fate of a *Burkholderia pseudomallei* lipopolysaccharide mutant in the mouse macrophage cell line RAW 264.7: possible role for the O-antigenic polysaccharide moiety of lipopolysaccharide in internalization and intracellular survival. *Infect. Immun.* 75, 4298–4304.

Attree, O., and Attree, I. (2001). A second type III secretion system in *Burkholderia pseudomallei*: who is the real culprit? *Microbiology* 147, 3197–3199.

Bakshi, C. S., Singh, V. P., Wood, M. W., Jones, P. W., Wallis, T. S., and Galyov, E. E. (2000). Identification of SopE2, a *Salmonella* secreted protein which is highly homologous to SopE and involved in bacterial invasion of epithelial cells. *J. Bacteriol.* 182, 2341–2344.

Balder, R., Lipski, S., Lazarus, J. J., Grose, W., Wooten, R. M., Hogan, R. J., Woods, D. E., and Lafontaine, E. R. (2010). Identification of *Burkholderia mallei* and *Burkholderia pseudomallei* adhesins for human respiratory epithelial cells. *BMC Microbiol.* 10, 250. doi: 10.1186/1471-2180-10-250

Barth, A. L., de Abreu, E., Silva, F. A., Hoffmann, A., Vieira, M. I., Zavascki, A. P., Ferreira, A. G., da Cunha, L. G. J., Albano, R. M., and de Andrade Marques, E. (2007). Cystic fibrosis patient with *Burkholderia pseudomallei* infection acquired in Brazil. *J. Clin. Microbiol.* 45, 4077–4080.

Birmingham, C. L., Canadien, V., Gouin, E., Troy, E. B., Yoshimori, T., Cossart, P., Higgins, D. E., and Brumell, J. H. (2007). *Listeria monocytogenes* evades killing by autophagy during colonization of host cells. *Autophagy* 3, 442–451.

Boddey, J. A., Day, C. J., Flegg, C. P., Ulrich, R. L., Stephens, S. R., Beacham, I. R., Morrison, N. A., and Peak, I. R. (2007). The bacterial gene *lfpA* influences the potent induction of calcitonin receptor and osteoclast-related genes in *Burkholderia pseudomallei*-induced TRAP-positive multinucleated giant cells. *Cell. Microbiol.* 9, 514–531.

Boddey, J. A., Flegg, C. P., Day, C. J., Beacham, I. R., and Peak, I. R. (2006). Temperature-regulated microcolony formation by *Burkholderia pseudomallei* requires *pilA* and enhances association with cultured human cells. *Infect. Immun.* 74, 5374–5381.

Boujemaa-Paterski, R., Gouin, E., Hansen, G., Samarin, S., Le Clainche, C., Didry, D., Dehoux, P., Cossart, P., Kocks, C., Carlier, M. F., and Pantaloni, D. (2001). *Listeria* protein ActA mimics WASP family proteins: it activates filament barbed end branching by Arp2/3 complex. *Biochemistry* 40, 11390–11404.

Breitbach, K., Rottner, K., Klocke, S., Rohde, M., Jenzora, A., Wehland, J., and Steinmetz, I. (2003). Actin-based motility of *Burkholderia pseudomallei* involves the Arp 2/3 complex, but not N-WASP and Ena/VASP proteins. *Cell. Microbiol.* 5, 385–393.

Brett, P. J., and Woods, D. E. (2000). Pathogenesis of and immunity to melioidosis. *Acta Trop.* 74, 201–210.

Brown, N. F., Boddey, J. A., Flegg, C. P., and Beacham, I. R. (2002). Adherence of *Burkholderia pseudomallei* cells to cultured human epithelial cell lines is regulated by growth temperature. *Infect. Immun.* 70, 974–980.

Burtnick, M. N., Brett, P. J., Harding, S. V., Ngugi, S. A., Ribot, W. J., Chantratita, N., Scorpio, A., Milne, T. S., Dean, R. E., Fritz, D. L., Peacock, S. J., Prior, J. L., Atkins, T. P., and Deshazer, D. (2011). The cluster 1 type VI secretion system is a major virulence determinant in *Burkholderia pseudomallei*. *Infect. Immun.* 79, 1512–1525.

Burtnick, M. N., Brett, P. J., Nair, V., Warawa, J. M., Woods, D. E., and Gherardini, F. C. (2008). *Burkholderia pseudomallei* type III secretion system mutants exhibit delayed vacuolar escape phenotypes in RAW 264.7 murine macrophages. *Infect. Immun.* 76, 2991–3000.

Burtnick, M. N., DeShazer, D., Nair, V., Gherardini, F. C., and Brett, P. J. (2010). *Burkholderia mallei* cluster 1 type VI secretion mutants exhibit growth and actin polymerization defects in RAW 264.7 murine macrophages. *Infect. Immun.* 78, 88–99.

Carsillo, M., Kutala, V. K., Puschel, K., Blanco, J., Kuppusamy, P., and Niewiesk, S. (2009). Nitric oxide production and nitric oxide synthase type 2 expression by cotton rat (*Sigmodon hispidus*) macrophages reflect the same pattern as human macrophages. *Dev. Comp. Immunol.* 33, 718–724.

Chaowagul, W., White, N. J., Dance, D. A., Wattanagoon, Y., Naigowit, P., Davis, T. M., Looareesuwan, S., and Pitakwatchara, N. (1989). Melioidosis: a major cause of community-acquired septicemia in northeastern Thailand. *J. Infect. Dis.* 159, 890–899.

Chua, K. L., Chan, Y. Y., and Gan, Y. H. (2003). Flagella are virulence determinants of *Burkholderia pseudomallei*. *Infect. Immun.* 71, 1622–1629.

Ciborowski, P., and Gendelman, H. E. (2006). Human immunodeficiency virus-mononuclear phagocyte interactions: emerging avenues of biomarker discovery, modes of viral persistence and disease pathogenesis. *Curr. HIV Res.* 4, 279–291.

Cole, N. L., and Grose, C. (2003). Membrane fusion mediated by herpesvirus glycoproteins: the paradigm of varicella-zoster virus. *Rev. Med. Virol.* 13, 207–222.

Cossart, P. (2000). Actin-based motility of pathogens: the Arp2/3 complex is a central player. *Cell. Microbiol.* 2, 195–205.

Cui, J., Yao, Q., Li, S., Ding, X., Lu, Q., Mao, H., Liu, L., Zheng, N., Chen, S., and Shao, F. (2010). Glutamine deamidation and dysfunction of ubiquitin/NEDD8 induced by a bacterial effector family. *Science* 329, 1215–1218.

Cullinane, M., Gong, L., Li, X., Lazar-Adler, N., Tra, T., Wolvetang, E., Prescott, M., Boyce, J. D., Devenish, R. J., and Adler, B. (2008). Stimulation of autophagy suppresses the intracellular survival of *Burkholderia pseudomallei* in mammalian cell lines. *Autophagy* 4, 744–753.

Currie, B. J., Dance, D. A., and Cheng, A. C. (2008). The global distribution of *Burkholderia pseudomallei* and melioidosis: an update. *Trans. R. Soc. Trop. Med. Hyg.* 102, S1–S4.

D'Cruze, T., Gong, L., Treerat, P., Ramm, G., Boyce, J. D., Prescott, M., Adler, B., and Devenish, R. J. (2011). A role for the *Burkholderia pseudomallei* type three secretion system cluster 1 *bpscN* gene in virulence. *Infect. Immun.* doi: 10.1128/IAI.01351-10. [Epub ahead of print].

de Chastellier, C., and Thilo, L. (2006). Cholesterol depletion in *Mycobacterium avium*-infected macrophages overcomes the block in phagosome maturation and leads to the reversible sequestration of viable Mycobacteria in phagolysosome-derived autophagic vacuoles. *Cell. Microbiol.* 8, 242–256.

Decker, T., Stockinger, S., Karaghiosoff, M., Müller, M., and Kovarik, P. (2002). IFNs and STATs in innate immunity to microorganisms. *J. Clin. Invest.* 109, 1271–1277.

DeShazer, D., Brett, P. J., Carlyon, R., and Woods, D. E. (1997). Mutagenesis of *Burkholderia pseudomallei* with Tn5-OT182: isolation of motility mutants and molecular characterization of the flagellin structural gene. *J. Bacteriol.* 179, 2116–2125.

Dorman, S. E., Gill, V. J., Gallin, J. I., and Holland, S. M. (1998). *Burkholderia pseudomallei* infection in a Puerto Rican patient with chronic granulomatous disease: case report and review of occurrences in the Americas. *Clin. Infect. Dis.* 26, 889–894.

Douglas, M. W., Lum, G., Roy, J., Fisher, D. A., Anstey, N. M., and Currie, B. J. (2004). Epidemiology of community-acquired and nosocomial bloodstream infections in tropical Australia: a 12-month prospective study. *Trop. Med. Int. Health* 9, 795–804.

Dowling, A. J., Wilkinson, P. A., Holden, M. T., Quail, M. A., Bentley, S. D., Reger, J., Waterfield, N. R., Titball, R. W., and Ffrench-Constant, R. H. (2010). Genome-wide analysis reveals loci encoding anti-macrophage factors in the human pathogen *Burkholderia pseudomallei* K96243. *PLoS ONE* 5, e15693. doi: 10.1371/journal.pone.0015693

Dupont, N., Lacas-Gervais, S., Bertout, J., Paz, I., Freche, B., Van Nhieu, G. T., van der Goot, F. G., Sansonetti, P. J., and Lafont, F. (2009). *Shigella* phagocytic vacuolar membrane remnants participate in the cellular response to pathogen invasion and are regulated by autophagy. *Cell Host Microbe* 6, 137–149.

Egan, A. M., and Gordon, D. L. (1996). *Burkholderia pseudomallei* activates complement and is ingested but not killed by polymorphonuclear leukocytes. *Infect. Immun.* 64, 4952–4959.

Egile, C., Loisel, T. P., Laurent, V., Li, R., Pantaloni, D., Sansonetti, P. J., and Carlier, M. F. (1999). Activation of the CDC42 effector N-WASP by the *Shigella flexneri* IcsA protein promotes actin nucleation by Arp2/3 complex and bacterial actin-based motility. *J. Cell Biol.* 146, 1319–1332.

Ekchariyawat, P., Pudla, S., Limposuwan, K., Arjcharoen, S., Sirisinha, S., and Utaisincharoen, P. (2005). *Burkholderia pseudomallei*-induced expression of suppressor of cytokine signaling 3 and cytokine-inducible src homology 2-containing protein in mouse macrophages: a possible mechanism for suppression of the response to gamma interferon stimulation. *Infect. Immun.* 73, 7332–7339.

Ekchariyawat, P., Pudla, S., Limposuwan, K., Arjcharoen, S., Sirisinha, S., and Utaisincharoen, P. (2007). Expression of suppressor of cytokine signaling 3 (SOCS3) and cytokine-inducible Src homology 2-containing protein (CIS) induced in *Burkholderia pseudomallei*-infected mouse macrophages requires bacterial internalization. *Microb. Pathog.* 42, 104–110.

Essex-Lopresti, A. E., Boddey, J. A., Thomas, R., Smith, M. P., Hartley, M. G., Atkins, T., Brown, N. F., Tsang, C. H., Peak, I. R., Hill, J., Beacham, I. R., and Titball, R. W. (2005). A type IV pilin, PilA, contributes to adherence of *Burkholderia pseudomallei* and virulence in vivo. *Infect. Immun.* 73, 1260–1264.

Fang, F. C. (1997). Perspectives series: host/pathogen interactions. Mechanisms of nitric oxide-related antimicrobial activity. *J. Clin. Invest.* 99, 2818–2825.

Felgner, P. L., Kayala, M. A., Vigil, A., Burk, C., Nakajima-Sasaki, R., Pablo, J., Molina, D. M., Hirst, S., Chew, J. S., Wang, D., Tan, G., Duffield, M., Yang, R., Neel, J., Chantratita, N., Bancroft, G., Lertmemongkolchai, G., Davies, D. H., Baldi, P., Peacock, S., and Titball, R. W. (2009). A *Burkholderia pseudomallei* protein microarray reveals serodiagnostic and cross-reactive antigens. *Proc. Natl. Acad. Sci. U.S.A.* 106, 13499–13504.

Galyov, E. E., Brett, P. J., and DeShazer, D. (2010). Molecular insights into *Burkholderia pseudomallei* and *Burkholderia mallei* pathogenesis. *Annu. Rev. Microbiol.* 64, 495–517.

Ginocchio, C. C., and Galán, J. E. (1995). Functional conservation among members of the *Salmonella typhimurium* InvA family of proteins. *Infect. Immun.* 63, 729–732.

Goldberg, M. B., and Theriot, J. A. (1995). *Shigella flexneri* surface protein IcsA is sufficient to direct actin-based motility. *Proc. Natl. Acad. Sci. U.S.A.* 92, 6572–6576.

Goley, E. D., Rodenbusch, S. E., Martin, A. C., and Welch, M. D. (2004). Critical conformational changes in the Arp2/3 complex are induced by nucleotide and nucleation promoting factor. *Mol. Cell* 16, 269–279.

Goley, E. D., and Welch, M. D. (2006). The ARP2/3 complex: an actin nucleator comes of age. *Nat. Rev. Mol. Cell Biol.* 7, 713–726.

Gong, L., Cullinane, M., Treerat, P., Ramm, G., Prescott, M., Adler, B., Boyce, J. D., and Devenish, R. J. (2011). The *Burkholderia pseudomallei* type III secretion system and BopA are required for evasion of LC3-associated phagocytosis. *PLoS ONE* 6, e17852. doi: 10.1371/journal.pone.0017852

Gori, A. H., Ahmed, K., Martinez, G., Masaki, H., Watanabe, K., and Nagatake, T. (1999). Mediation of attachment of *Burkholderia pseudomallei* to human pharyngeal epithelial cells by the asialoganglioside GM1-GM2 receptor complex. *Am. J. Trop. Med. Hyg.* 61, 473–475.

Gouin, E., Egile, C., Dehoux, P., Villiers, V., Adams, J., Gertler, F., Li, R., and Cossart, P. (2004). The RickA protein of *Rickettsia conorii* activates the Arp2/3 complex. *Nature* 427, 457–461.

Gouin, E., Welch, M. D., and Cossart, P. (2005). Actin-based motility of intracellular pathogens. *Curr. Opin. Microbiol.* 8, 35–45.

Haase, A., Melder, A., Smith-Vaughan, H., Kemp, D., and Currie, B. (1995). RAPD analysis of isolates of *Burkholderia pseudomallei* from patients with recurrent melioidosis. *Epidemiol. Infect.* 115, 115–121.

Hardt, W. D., Chen, L. M., Schuebel, K. E., Bustelo, X. R., and Galán, J. E. (1998). *S. typhimurium* encodes an activator of Rho GTPases that induces membrane ruffling and nuclear responses in host cells. *Cell* 93, 815–826.

Harley, V. S., Dance, D. A., Drasar, B. S., and Tovey, G. (1998a). Effects of *Burkholderia pseudomallei* and other *Burkholderia* species on eukaryotic cells in tissue culture. *Microbios* 96, 71–93.

Harley, V. S., Dance, D. A., Tovey, G., McCrossan, M. V., and Drasar, B. S. (1998b). An ultrastructural study of the phagocytosis of *Burkholderia pseudomallei*. *Microbios* 94, 35–45.

Harley, V. S., Dance, D. A., Tovey, G., and Drasar, B. S. (1994). Interaction of *Pseudomonas pseudomallei* with macrophages. *Biochem. Soc. Trans.* 22, 88S.

Hueck, C. J. (1998). Type III protein secretion systems in bacterial pathogens of animals and plants. *Microbiol. Mol. Biol. Rev.* 62, 379–433.

Hussey, S., Travassos, L. H., and Jones, N. L. (2009). Autophagy as an emerging dimension to adaptive and innate immunity. *Semin. Immunol.* 21, 233–241.

Inglis, T. J., Robertson, T., Woods, D. E., Dutton, N., and Chang, B. J. (2003). Flagellum-mediated adhesion by *Burkholderia pseudomallei* precedes invasion of *Acanthamoeba astronyxis*. *Infect. Immun.* 71, 2280–2282.

Jacobs, A. T., and Ignarro, L. J. (2001). Lipopolysaccharide-induced expression of interferon-beta mediates the timing of inducible nitric-oxide synthase induction in RAW 264.7 macrophages. *J. Biol. Chem.* 276, 47950–47957.

Jeng, R. L., Goley, E. D., D'Alessio, J. A., Chaga, O. Y., Svitkina, T. M., Borisy, G. G., Heinzen, R. A., and Welch, M. D. (2004). A *Rickettsia* WASP-like protein activates the Arp2/3 complex and mediates actin-based motility. *Cell. Microbiol.* 6, 761–769.

Johnson, S., Roversi, P., Espina, M., Olive, A., Deane, J. E., Birket, S., Field, T., Picking, W. D., Blocker, A. J., Galyov, E. E., Picking, W. L., and Lea, S. M. (2007). Self-chaperoning of the type III secretion system needle tip proteins IpaD and BipD. *J. Biol. Chem.* 282, 4035–4044.

Jones, A. L., Beveridge, T. J., and Woods, D. E. (1996). Intracellular survival of *Burkholderia pseudomallei*. *Infect. Immun.* 64, 782–790.

Jones, A. L., DeShazer, D., and Woods, D. E. (1997). Identification and characterization of a two-component regulatory system involved in invasion of eukaryotic cells and heavy-metal resistance in *Burkholderia pseudomallei*. *Infect. Immun.* 65, 4972–4977.

Jubelin, G., Chavez, C. V., Taieb, F., Banfield, M. J., Samba-Louaka, A., Nobe, R., Nougayrède, J. P., Zumbihl, R., Givaudan, A., Escoubas, J. M., and Oswald, E. (2009). Cycle inhibiting factors (CIFs) are a growing family of functional cyclomodulins present in invertebrate and mammal bacterial pathogens. *PLoS ONE* 4, e4855. doi: 10.1371/journal.pone.0004855

Kayath, C. A., Hussey, S., El hajjami, N., Nagra, K., Philpott, D., and Allaoui, A. (2010). Escape of intracellular *Shigella* from autophagy requires binding to cholesterol through the type III effector, IcsB. *Microbes Infect.* 12, 956–966.

Kespichayawattana, W., Intachote, P., Utaisincharoen, P., and Sirisinha, S. (2004). Virulent *Burkholderia pseudomallei* is more efficient than avirulent *Burkholderia thailandensis* in invasion of and adherence to cultured human epithelial cells. *Microb. Pathog.* 36, 287–292.

Kespichayawattana, W., Rattanachetkul, S., Wanun, T., Utaisincharoen, P., and Sirisinha, S. (2000). *Burkholderia pseudomallei* induces cell fusion and actin-associated membrane protrusion: a possible mechanism for cell-to-cell spreading. *Infect. Immun.* 68, 5377–5384.

Kinzler, E. R., and Compton, T. (2005). Characterization of human cytomegalovirus glycoprotein-induced cell-cell fusion. *J. Virol.* 79, 7827–7837.

Komatsu, M., and Ichimura, Y. (2010). Selective autophagy regulates various cellular functions. *Genes Cells* 15, 923–933.

Kondo, Y., Yasui, K., Yashiro, M., Tsuge, M., Kotani, N., and Morishima, T. (2009). Multi-nucleated giant cell formation from human cord blood monocytes in vitro, in comparison with adult peripheral blood monocytes. *Clin. Exp. Immunol.* 158, 84–90.

Koponen, M. A., Zlock, D., Palmer, D. L., and Merlin, T. L. (1991). Melioidosis. Forgotten, but not gone! *Arch. Intern. Med.* 151, 605–608.

Laurent, V., Loisel, T. P., Harbeck, B., Wehman, A., Gröbe, L., Jockusch, B. M., Wehland, J., Gertler, F. B., and Carlier, M. F. (1999). Role of proteins of the Ena/VASP family in actin-based motility of *Listeria monocytogenes*. *J. Cell Biol.* 144, 1245–1258.

Lazar Adler, N. R., Govan, B., Cullinane, M., Harper, M., Adler, B., and Boyce, J. D. (2009). The molecular and cellular basis of pathogenesis in melioidosis: how does *Burkholderia pseudomallei* cause disease? *FEMS Microbiol. Rev.* 33, 1079–1099.

Le Hello, S., Currie, B. J., Godoy, D., Spratt, B. G., Mikulski, M., Lacassin, F., and Garin, B. (2005). Melioidosis in New Caledonia. *Emerging Infect. Dis.* 11, 1607–1609.

Maharjan, B., Chantratita, N., Vesaratchavest, M., Cheng, A., Wuthiekanun, V., Chierakul, W., Chaowagul, W., Day, N. P., and Peacock, S. J. (2005). Recurrent melioidosis in patients in northeast Thailand is frequently due to reinfection rather than relapse. *J. Clin. Microbiol.* 43, 6032–6034.

Makino, S., Sasakawa, C., Kamata, K., Kurata, T., and Yoshikawa, M. (1986). A genetic determinant required for continuous reinfection of adjacent cells on large plasmid in *S. flexneri* 2a. *Cell* 46, 551–555.

Marchès, O., Ledger, T. N., Boury, M., Ohara, M., Tu, X., Goffaux, F., Mainil, J., Rosenshine, I., Sugai, M., De Rycke, J., and Oswald, E. (2003). Enteropathogenic and enterohaemorrhagic *Escherichia coli* deliver a novel effector called Cif, which blocks cell cycle G2/M transition. *Mol. Microbiol.* 50, 1553–1567.

May, R. C., Hall, M. E., Higgs, H. N., Pollard, T. D., Chakraborty, T., Wehland, J., Machesky, L. M., and Sechi, A. S. (1999). The Arp2/3 complex is essential for the actin-based motility of *Listeria monocytogenes*. *Curr. Biol.* 9, 759–762.

Monack, D. M., and Theriot, J. A. (2001). Actin-based motility is sufficient for bacterial membrane protrusion formation and host cell uptake. *Cell. Microbiol.* 3, 633–647.

Muangsombut, V., Suparak, S., Pumirat, P., Damnin, S., Vattanaviboon, P., Thongboonkerd, V., and Korbsrisate, S. (2008). Inactivation of *Burkholderia pseudomallei bsaQ* results in decreased invasion efficiency and delayed escape of bacteria from endocytic vesicles. *Arch. Microbiol.* 190, 623–631.

Mullins, R. D., Heuser, J. A., and Pollard, T. D. (1998). The interaction of Arp2/3 complex with actin: nucleation, high affinity pointed end capping, and formation of branching networks of filaments. *Proc. Natl. Acad. Sci. U.S.A.* 95, 6181–6186.

Ngauy, V., Lemeshev, Y., Sadkowski, L., and Crawford, G. (2005). Cutaneous melioidosis in a man who was taken as a prisoner of war by the Japanese during World War II. *J. Clin. Microbiol.* 43, 970–972.

Nougayrède, J. P., Boury, M., Tasca, C., Marchès, O., Milon, A., Oswald, E., and De Rycke, J. (2001). Type III secretion-dependent cell cycle block caused in HeLa cells by enteropathogenic *Escherichia coli* O103. *Infect. Immun.* 69, 6785–6795.

Ogawa, M., Yoshimori, T., Suzuki, T., Sagara, H., Mizushima, N., and Sasakawa, C. (2005). Escape of intracellular *Shigella* from autophagy. *Science* 307, 727–731.

Osiriphun, Y., Wongtrakoongate, P., Sanongkiet, S., Suriyaphol, P., Thongboonkerd, V., and Tungpradabkul, S. (2009). Identification and characterization of RpoS regulon and RpoS-dependent promoters in *Burkholderia pseudomallei*. *J. Proteome Res.* 8, 3118–3131.

Peacock, S. J. (2006). Melioidosis. *Curr. Opin. Infect. Dis.* 19, 421–428.

Pei, J., and Grishin, N. V. (2009). The Rho GTPase inactivation domain in *Vibrio cholerae* MARTX toxin has a circularly permuted papain-like thiol protease fold. *Proteins* 77, 413–419.

Pelicic, V. (2008). Type IV pili: e pluribus unum? *Mol. Microbiol.* 68, 827–837.

Phewkliang, A., Wongratanacheewin, S., and Chareonsudjai, S. (2010). Role of *Burkholderia pseudomallei* in the invasion, replication and induction of apoptosis in human epithelial cell lines. *Southeast Asian J. Trop. Med. Public Health* 41, 1164–1176.

Pilatz, S., Breitbach, K., Hein, N., Fehlhaber, B., Schulze, J., Brenneke, B., Eberl, L., and Steinmetz, I. (2006). Identification of *Burkholderia pseudomallei* genes required for the intracellular life cycle and in vivo virulence. *Infect. Immun.* 74, 3576–3586.

Pruksachartvuthi, S., Aswapokee, N., and Thankerngpol, K. (1990). Survival of *Pseudomonas pseudomallei* in human phagocytes. *J. Med. Microbiol.* 31, 109–114.

Pudla, M., Kananuruk, A., Limposuwan, K., Sirisinha, S., and Utaisincharoen, P. (2010). Nucleotide-binding oligomerization domain-containing protein 2 regulates suppressor of cytokine signaling 3 expression in *Burkholderia pseudomallei*-infected mouse macrophage cell line RAW 264.7. *Innate Immun.* doi: 10.1177/1753425910385484. [Epub ahead of print].

Pukatzki, S., McAuley, S. B., and Miyata, S. T. (2009). The type VI secretion system: translocation of effectors and effector-domains. *Curr. Opin. Microbiol.* 12, 11–17.

Rainbow, L., Hart, C. A., and Winstanley, C. (2002). Distribution of type III secretion gene clusters in *Burkholderia pseudomallei*, *B. thailandensis* and *B. mallei*. *J. Med. Microbiol.* 51, 374–384.

Ravikumar, B., Sarkar, S., Davies, J. E., Futter, M., Garcia-Arencibia, M., Green-Thompson, Z. W., Jimenez-Sanchez, M., Korolchuk, V. I., Lichtenberg, M., Luo, S., Massey, D. C., Menzies, F. M., Moreau, K., Narayanan, U., Renna, M., Siddiqi, F. H., Underwood, B. R., Winslow, A. R., and Rubinsztein, D. C. (2010). Regulation of mammalian autophagy in physiology and pathophysiology. *Physiol. Rev.* 90, 1383–1435.

Reckseidler, S. L., DeShazer, D., Sokol, P. A., and Woods, D. E. (2001). Detection of bacterial virulence genes by subtractive hybridization: identification of capsular polysaccharide of *Burkholderia pseudomallei* as a major virulence determinant. *Infect. Immun.* 69, 34–44.

Rudolph, M. G., Weise, C., Mirold, S., Hillenbrand, B., Bader, B., Wittinghofer, A., and Hardt, W. D. (1999). Biochemical analysis of SopE from *Salmonella typhimurium*, a highly efficient guanosine nucleotide exchange factor for RhoGTPases. *J. Biol. Chem.* 274, 30501–30509.

Samba-Louaka, A., Nougayrède, J. P., Watrin, C., Jubelin, G., Oswald, E., and Taieb, F. (2008). Bacterial cyclomodulin Cif blocks the host cell cycle by stabilizing the cyclin-dependent kinase inhibitors p21 and p27. *Cell. Microbiol.* 10, 2496–2508.

Sanjuan, M. A., Dillon, C. P., Tait, S. W., Moshiach, S., Dorsey, F., Connell, S., Komatsu, M., Tanaka, K., Cleveland, J. L., Withoff, S., and Green, D. R. (2007). Toll-like receptor signalling in macrophages links the autophagy pathway to phagocytosis. *Nature* 450, 1253–1257.

Sanjuan, M. A., Milasta, S., and Green, D. R. (2009). Toll-like receptor signaling in the lysosomal pathways. *Immunol. Rev.* 227, 203–220.

Schell, M. A., Ulrich, R. L., Ribot, W. J., Brueggemann, E. E., Hines, H. B., Chen, D., Lipscomb, L., Kim, H. S., Mrazek, J., Nierman, W. C., and DeShazer, D. (2007). Type VI secretion is a major virulence determinant in *Burkholderia mallei*. *Mol. Microbiol.* 64, 1466–1485.

Schmid, D., and Munz, C. (2007). Innate and adaptive immunity through autophagy. *Immunity* 27, 11–21.

Shabek, N., and Ciechanover, A. (2010). Degradation of ubiquitin: the fate of the cellular reaper. *Cell Cycle* 9, 523–530.

Shahnazari, S., and Brumell, J. H. (2011). Mechanisms and consequences of bacterial targeting by the autophagy pathway. *Curr. Opin. Microbiol.* 14, 68–75.

Shalom, G., Shaw, J. G., and Thomas, M. S. (2007). In vivo expression technology identifies a type VI secretion system locus in *Burkholderia pseudomallei* that is induced upon invasion of macrophages. *Microbiology* 153, 2689–2699.

Shanks, J., Burtnick, M. N., Brett, P. J., Waag, D. M., Spurgers, K. B., Ribot, W. J., Schell, M. A., Panchal, R. G., Gherardini, F. C., Wilkinson, K. D., and Deshazer, D. (2009). *Burkholderia mallei tssM* encodes a putative deubiquitinase that is secreted and expressed inside infected RAW 264.7 murine macrophages. *Infect. Immun.* 77, 1636–1648.

Sitthidet, C., Korbsrisate, S., Layton, A. N., Field, T. R., Stevens, M. P., and Stevens, J. M. (2011). Identification of motifs of *Burkholderia pseudomallei* BimA required for intracellular motility, actin binding, and actin polymerization. *J. Bacteriol.* 193, 1901–1910.

Sitthidet, C., Stevens, J. M., Chantratita, N., Currie, B. J., Peacock, S. J., Korbsrisate, S., and Stevens, M. P. (2008). Prevalence and sequence diversity of a factor required for actin-based motility in natural populations of *Burkholderia* species. *J. Clin. Microbiol.* 46, 2418–2422.

Stender, S., Friebel, A., Linder, S., Rohde, M., Mirold, S., and Hardt, W. D. (2000). Identification of SopE2 from *Salmonella typhimurium*, a conserved guanine nucleotide exchange factor for Cdc42 of the host cell. *Mol. Microbiol.* 36, 1206–1221.

Stevens, J. M., Galyov, E. E., and Stevens, M. P. (2006). Actin-dependent movement of bacterial pathogens. *Nat. Rev. Microbiol.* 4, 91–101.

Stevens, J. M., Ulrich, R. L., Taylor, L. A., Wood, M. W., Deshazer, D., Stevens, M. P., and Galyov, E. E. (2005a). Actin-binding proteins from *Burkholderia mallei* and *Burkholderia thailandensis* can functionally compensate for the actin-based motility defect of a *Burkholderia pseudomallei bimA* mutant. *J. Bacteriol.* 187, 7857–7862.

Stevens, M. P., Stevens, J. M., Jeng, R. L., Taylor, L. A., Wood, M. W., Hawes, P., Monaghan, P., Welch, M. D., and Galyov, E. E. (2005b). Identification of a bacterial factor required for actin-based motility of *Burkholderia pseudomallei*. *Mol. Microbiol.* 56, 40–53.

Stevens, M. P., Brown, P. J., Wood, M. W., Wallis, T. S., and Galyov, E. E. (2001). "Cognate virulence gene clusters in *Salmonella* and *B. pseudomallei*," in *Proceedings of the World Melioidosis Congress*, Perth.

Stevens, M. P., Friebel, A., Taylor, L. A., Wood, M. W., Brown, P. J., Hardt, W. D., and Galyov, E. E. (2003). A *Burkholderia pseudomallei* type III secreted protein, BopE, facilitates bacterial invasion of epithelial cells and exhibits guanine nucleotide exchange factor activity. *J. Bacteriol.* 185, 4992–4996.

Stevens, M. P., and Galyov, E. E. (2004). Exploitation of host cells by *Burkholderia pseudomallei*. *Int. J. Med. Microbiol.* 293, 549–555.

Stevens, M. P., Haque, A., Atkins, T., Hill, J., Wood, M. W., Easton, A., Nelson, M., Underwood-Fowler, C., Titball, R. W., Bancroft, G. J., and Galyov, E. E. (2004). Attenuated virulence and protective efficacy of a *Burkholderia pseudomallei bsa* type III secretion mutant in murine models of melioidosis. *Microbiology* 150, 2669–2676.

Stevens, M. P., Wood, M. W., Taylor, L. A., Monaghan, P., Hawes, P., Jones, P. W., Wallis, T. S., and Galyov, E. E. (2002). An Inv/Mxi-Spa-like type III protein secretion system in *Burkholderia pseudomallei* modulates intracellular behaviour of the pathogen. *Mol. Microbiol.* 46, 649–659.

Stone, R. (2007). Infectious disease. Racing to defuse a bacterial time bomb. *Science* 317, 1022–1024.

Sun, G. W., and Gan, Y. H. (2010). Unraveling type III secretion systems in the highly versatile *Burkholderia pseudomallei*. *Trends Microbiol.* 18, 561–568.

Sun, G. W., Lu, J., Pervaiz, S., Cao, W. P., and Gan, Y. H. (2005). Caspase-1 dependent macrophage death induced by *Burkholderia pseudomallei*. *Cell. Microbiol.* 7, 1447–1458.

Suparak, S., Kespichayawattana, W., Haque, A., Easton, A., Damnin, S., Lertmemongkolchai, G., Bancroft, G. J., and Korbsrisate, S. (2005). Multinucleated giant cell formation and apoptosis in infected host cells is mediated by *Burkholderia pseudomallei* type III secretion protein BipB. *J. Bacteriol.* 187, 6556–6560.

Taieb, F., Nougayrède, J. P., Watrin, C., Samba-Louaka, A., and Oswald, E. (2006). *Escherichia coli* cyclomodulin Cif induces G2 arrest of the host cell cycle without activation of the DNA-damage checkpoint-signalling pathway. *Cell. Microbiol.* 8, 1910–1921.

Tan, K. S., Chen, Y., Lim, Y. C., Tan, G. Y., Liu, Y., Lim, Y. T., Macary, P., and Gan, Y. H. (2010). Suppression of host innate immune response by *Burkholderia pseudomallei* through the virulence factor TssM. *J. Immunol.* 184, 5160–5171.

Upadhyay, A., Wu, H. L., Williams, C., Field, T., Galyov, E. E., van den Elsen, J. M., and Bagby, S. (2008). The guanine-nucleotide-exchange factor BopE from *Burkholderia pseudomallei* adopts a compact version of the *Salmonella* SopE/SopE2 fold and undergoes a closed-to-open conformational change upon interaction with Cdc42. *Biochem. J.* 411, 485–493.

Utaisincharoen, P., Anuntagool, N., Arjcharoen, S., Limposuwan, K., Chaisuriya, P., and Sirisinha, S. (2004). Induction of iNOS expression and antimicrobial activity by interferon (IFN)-beta is distinct from IFN-gamma in *Burkholderia pseudomallei*-infected mouse macrophages. *Clin. Exp. Immunol.* 136, 277–283.

Utaisincharoen, P., Anuntagool, N., Limposuwan, K., Chaisuriya, P., and Sirisinha, S. (2003). Involvement of beta interferon in enhancing inducible nitric oxide synthase production and antimicrobial activity of *Burkholderia pseudomallei*-infected macrophages. *Infect. Immun.* 71, 3053–3057.

Utaisincharoen, P., Arjcharoen, S., Limposuwan, K., Tungpradabkul, S., and Sirisinha, S. (2006). *Burkholderia pseudomallei* RpoS regulates multinucleated giant cell formation and inducible nitric oxide synthase expression in mouse macrophage cell line (RAW 264.7). *Microb. Pathog.* 40, 184–189.

Utaisincharoen, P., Tangthawornchaikul, N., Kespichayawattana, W., Anuntagool, N., Chaisuriya, P., and Sirisinha, S. (2000). Kinetic studies of the production of nitric oxide (NO) and tumour necrosis factor-alpha (TNF-alpha) in macrophages stimulated with *Burkholderia pseudomallei* endotoxin. *Clin. Exp. Immunol.* 122, 324–329.

Utaisincharoen, P., Tangthawornchaikul, N., Kespichayawattana, W., Chaisuriya, P., and Sirisinha, S. (2001). *Burkholderia pseudomallei* interferes with inducible nitric oxide synthase (iNOS) production: a possible mechanism of evading macrophage killing. *Microbiol. Immunol.* 45, 307–313.

Utermöhlen, O., Herz, J., Schramm, M., and Krönke, M. (2008). Fusogenicity of membranes: the impact of acid sphingomyelinase on innate immune responses. *Immunobiology* 213, 307–314.

Warawa, J., and Woods, D. E. (2005). Type III secretion system cluster 3 is required for maximal virulence of *Burkholderia pseudomallei* in a hamster infection model. *FEMS Microbiol. Lett.* 242, 101–108.

Welch, M. D., Iwamatsu, A., and Mitchison, T. J. (1997). Actin polymerization is induced by Arp2/3 protein complex at the surface of *Listeria monocytogenes*. *Nature* 385, 265–269.

Welch, M. D., and Mullins, R. D. (2002). Cellular control of actin nucleation. *Annu. Rev. Cell Dev. Biol.* 18, 247–288.

Welch, M. D., Rosenblatt, J., Skoble, J., Portnoy, D. A., and Mitchison, T. J. (1998). Interaction of human Arp2/3 complex and the *Listeria monocytogenes* ActA protein in actin filament nucleation. *Science* 281, 105–108.

Whitlock, G. C., Estes, D. M., Young, G. M., Young, B., and Torres, A. G. (2008). Construction of a reporter system to study *Burkholderia mallei* type III secretion and identification of the BopA effector protein function in intracellular survival. *Trans. R. Soc. Trop. Med. Hyg.* 102, S127–S133.

Whitlock, G. C., Valbuena, G. A., Popov, V. L., Judy, B. M., Estes, D. M., and Torres, A. G. (2009). *Burkholderia mallei* cellular interactions in a respiratory cell model. *J. Med. Microbiol.* 58, 554–562.

Wiersinga, W. J., de Vos, A. F., de Beer, R., Wieland, C. W., Roelofs, J. J., Woods, D. E., and van der Poll, T. (2008). Inflammation patterns induced by different *Burkholderia* species in mice. *Cell. Microbiol.* 10, 81–87.

Winstanley, C., Hales, B. A., and Hart, C. A. (1999). Evidence for the presence in *Burkholderia pseudomallei* of a type III secretion system-associated gene cluster. *J. Med. Microbiol.* 48, 649–656.

Wong, K. T., Puthucheary, S. D., and Vadivelu, J. (1995). The histopathology of human melioidosis. *Histopathology* 26, 51–55.

Wood, M. W., Rosqvist, R., Mullan, P. B., Edwards, M. H., and Galyov, E. E. (1996). SopE, a secreted protein of *Salmonella dublin*, is translocated into the target eukaryotic cell via a *sip*-dependent mechanism and promotes bacterial entry. *Mol. Microbiol.* 22, 327–338.

Yao, Q., Cui, J., Zhu, Y., Wang, G., Hu, L., Long, C., Cao, R., Liu, X., Huang, N., Chen, S., Liu, L., and Shao, F. (2009). A bacterial type III effector family uses the papain-like hydrolytic activity to arrest the host cell cycle. *Proc. Natl. Acad. Sci. U.S.A.* 106, 3716–3721.

Zhang, L., Wang, Y., Picking, W. L., Picking, W. D., and De Guzman, R. N. (2006). Solution structure of monomeric BsaL, the type III secretion needle protein of *Burkholderia pseudomallei*. *J. Mol. Biol.* 359, 322–330.

Conflict of Interest Statement: The authors declare that the research was conducted in the absence of any commercial or financial relationships that could be construed as a potential conflict of interest.

Received: 18 May 2011; paper pending published: 28 May 2011; accepted: 26 July 2011; published online: 22 August 2011.
Citation: Allwood EM, Devenish RJ, Prescott M, Adler B and Boyce JD (2011) Strategies for intracellular survival of Burkholderia pseudomallei. Front. Microbio. ***2****:170. doi: 10.3389/fmicb.2011.00170*
This article was submitted to Frontiers in Cellular and Infection Microbiology, a specialty of Frontiers in Microbiology.

frontiers in
MICROBIOLOGY

ORIGINAL RESEARCH ARTICLE
published: 26 August 2011
doi: 10.3389/fmicb.2011.00174

In vivo bioluminescence imaging of *Burkholderia mallei* respiratory infection and treatment in the mouse model

Shane Massey[1], Katie Johnston[1], Tiffany M. Mott[1], Barbara M. Judy[2], Brian H. Kvitko[3], Herbert P. Schweizer[3], D. Mark Estes[4] and Alfredo G. Torres[1,2,5]*

[1] Department of Microbiology and Immunology, University of Texas Medical Branch, Galveston, TX, USA
[2] Department of Pathology, University of Texas Medical Branch, Galveston, TX, USA
[3] Department of Microbiology, Immunology and Pathology, Colorado State University, Fort Collins, CO, USA
[4] Department of Infectious Diseases, College of Veterinary Medicine, University of Georgia, Athens, GA, USA
[5] Sealy Center for Vaccine Development and Center for Tropical Diseases, University of Texas Medical Branch, Galveston, TX, USA

Edited by:
Ivo Steinmetz, University of Greifswald, Germany

Reviewed by:
Ifor Beacham, Griffith University, Australia
Paul J. Brett, University of South Alabama, USA

***Correspondence:**
Alfredo G. Torres, Department of Microbiology and Immunology, University of Texas Medical Branch, 301 University Boulevard, Galveston, TX 77555-1070, USA.
e-mail: altorres@utmb.edu

Bioluminescent imaging (BLI) technology is a powerful tool for monitoring infectious disease progression and treatment approaches. BLI is particularly useful for tracking fastidious intracellular pathogens that might be difficult to recover from certain organs. *Burkholderia mallei*, the causative agent of glanders, is a facultative intracellular pathogen and has been classified by the CDC as a Category B select agent due to its highly infectious nature and potential use as a biological weapon. Very little is known regarding pathogenesis or treatment of glanders. We investigated the use of bioluminescent reporter constructs to monitor the dynamics of infection as well as the efficacy of therapeutics for *B. mallei* in real-time. A stable luminescent reporter *B. mallei* strain was created using the pUTmini-Tn*5*::*lux*Km2 plasmid and used to monitor glanders in the BALB/c murine model. Mice were infected via the intranasal route with 5×10^3 bacteria and monitored by BLI at 24, 48, and 72 h. We verified that our reporter construct maintained similar virulence and growth kinetics compared to wild-type *B. mallei* and confirmed that it maintains luminescent stability in the presence or absence of antibiotic selection. The luminescent signal was initially seen in the lungs, and progressed to the liver and spleen over the course of infection. We demonstrated that antibiotic treatment 24 h post-infection resulted in reduction of bioluminescence that can be attributed to decreased bacterial burden in target organs. These findings suggest that BLI can be used to monitor disease progression and efficacy of therapeutics during glanders infections. Finally, we report an alternative method to mini-Tn*5*::*lux*Km2 transposon using mini-Tn*7*-*lux* elements that insert site-specifically at known genomic attachment sites and that can also be used to tag bacteria.

Keywords: bioluminescence, *Burkholderia mallei*, *in vivo* imaging, antibiotic

INTRODUCTION

Burkholderia mallei are Gram negative, facultative intracellular bacteria, and the causative agent for glanders. Horses, mules, and donkeys are the only known natural reservoirs. The disease has been eradicated in the United States, although it remains endemic in the Middle East, Central and South America, and Asia. Among humans, glanders is considered an occupational disease as most individuals who contract the disease are lab workers (Srinivasan et al., 2001) or individuals who come into close contact with infected animals (Sanford, 1995). Typically, human infections occur via contamination of the mucus membranes, wounds or abrasions. *B. mallei* is highly infectious in aerosol form, requiring very few organisms to establish an infection (Lever et al., 2003). *B. mallei* is also regarded as a potential biological threat due to their highly infectious nature and the incapacitating, often fatal disease progression in humans. Despite the history of *B. mallei* as a bio-weapon (Sharrer, 1995; Christopher et al., 1997), little data about the efficacy of vaccinations or antibiotic treatment methods is available. Currently there are no vaccines available for either equine or human *B. mallei* infections. Numerous reports indicate *in vitro* susceptibility to a wide array of antibiotics (Kenny et al., 1999; Heine et al., 2001; Judy et al., 2009) including: aminoglycosides, cephalosporins, sulfonamides, macrolides, and fluoroquinolones; however, the *in vivo* efficacies are not well known. Due to the potential use as a biological weapon and the scarcity of *in vivo* treatment data, further evaluation of glanders progression in response to antibiotic challenge and/or vaccination is of utmost importance.

Bioluminescence imaging (BLI) is a technique based on the detection of visible light produced by luciferase-catalyzed reactions with a specific substrate. There are a variety of bioluminescent systems that have been identified in nature. The application of these as reporter systems can be divided into two strategies. The first one centers on the use of luciferase enzymes alone. Mammalian cells, or bacteria, can be engineered to express a plasmid-borne copy of the luciferase enzyme from organisms such as the firefly (*Photinus pyralis*) or the sea pansy (*Renilla reniformis*). Mammalian cells lack the required luciferin substrate for

the bioluminescent reaction; therefore it must be exogenously supplied. The second strategy involves the use of the entire *lux* operon from a bacterium such as *Photorhabdus luminescens* (formerly *Xenorhabdus luminescens*). A transposon insertion or plasmid vector containing the luciferase enzyme, as well as the components for substrate production can be engineered with a transposon insertion (Flentie et al., 2008). This system will emit light in the range of 495–500 nm. Since the enzyme and substrate are both synthesized, exogenous application of substrate is not necessary. The plasmid vectors or transposon insertions confer a constitutively expressed luminescent phenotype in a bacterial pathogen and permit the real-time *in vivo* monitoring of the organism. BLI has routinely been utilized to track disease progression in mice. *Salmonella enterica* serovar Typhimurium was transformed with the *lux* operon to determine virulence differences between three strains in one of the initial BLI studies on bacterial pathogenesis (Contag et al., 1995). BLI has since been used to monitor bacterial dissemination or to validate antimicrobial treatment regimen in *Escherichia coli* (Rocchetta et al., 2001; Foucault et al., 2010) and *Mycobacterium tuberculosis* (Andreu et al., 2010), as well as the select agents *Francisella tularensis* (Bina et al., 2010) and *Burkholderia pseudomallei* (Owen et al., 2009). Since bioluminescence is related to bacterial load, this property can be used to quantitatively assess the pathogen burden as well as to provide new insights into tissue tropism during infection (Hutchens and Luker, 2007).

Murine glanders has been widely used to study *B. mallei* infections and potential therapeutics (Leakey et al., 1998; Fritz et al., 2000; Lever et al., 2003; Whitlock et al., 2008; Sarkar-Tyson et al., 2009). BALB/c mice are highly susceptible to *B. mallei* infection and provide an excellent model for acute glanders. C57BL/6 mice are more resistant to infection and are better suited for modeling chronic glanders. In this study, we monitored the bacterial infection in BALB/c mice with a strain of *B. mallei* containing a stable, chromosomally integrated copy of the *lux* operon from *P. luminescens*. After intranasal (i.n.) infection, the signal intensity associated with the bioluminescent bacteria increased over time in the lung as the bacteria replicated. Intraperitoneal antibiotic treatment correlated with decrease in bioluminescence, and the infection re-emerged after antibiotic treatment was stopped. This study demonstrates the potential for assessing therapeutic treatments using BLI.

MATERIALS AND METHODS

BACTERIAL STRAINS

Escherichia coli S17-1 (λ*pir*) was used a host for the pUTmini-Tn*5*::*lux*Km2 transfer plasmid described by Winson et al. (1998). The plasmid was maintained in *E. coli* S17-1 (λ*pir*) and was mobilized via conjugation into *B. mallei* ATCC 23344. For conjugation, *E. coli* S17-1 (λ*pir*) harboring the transfer plasmid and *B. mallei* ATCC 23344 were grown overnight at 37°C in 5 ml Luria-Bertani (LB) media (the *E. coli* cultures was supplemented with 50 μg/ml kanamycin). One milliliter of each overnight culture was pelleted and washed with 1 ml LB. Each culture was pelleted again and re-suspended in 500 μl of LB. The two cultures were combined and passed through a 0.45-μM analytical filter. The filter was placed on an LB plate, which was incubated for 6 h at 37°C. The cells were scraped from the surface of the filter and re-suspended in 3 ml of phosphate buffered saline (PBS). Dilutions were spread onto LB plates supplemented with 4% glycerol (LBG) as well as 50 μg/ml kanamycin (Km) and 50 μg/ml polymyxin B. These plates were then incubated at 37°C for 24 h.

Bioluminescent colonies from the *B. mallei lux* strain, henceforth referred to as CSM001, were detected by an *in vitro* imaging system (IVIS) and were maintained on LBG plates with Km. *B. mallei* strain ATCC 23344 was cultured on LBG for 48 h at 37°C. The isolated colonies were cultured in LBG broth shaking for 24 h at 37°C. Optical density readings (OD_{600}) were used to determine bacterial concentrations (CFU/ml). Bacteria were pelleted by centrifugation and re-suspended in LBG broth to obtain the desired concentration for inoculation.

Established protocols were used for isolation of bioluminescent *B. thailandensis* (Choi et al., 2005) and *B. pseudomallei* (Choi et al., 2005). Briefly, pUC18T-mini-Tn*7*T-Zeo-*P1-lux* was introduced in *B. thailandensis* strain E264R [a rifampicin resistant derivative of E264 (Choi et al., 2005)] by biparental mating using *E. coli* mobilizer strain SM10 (λ*pir*) and helper plasmid pTNS3 (Choi et al., 2008). Exconjugants were selected on Lennox LB medium (MO BIO Laboratories, Carlsbad, CA, USA) with 200 μg/ml zeocin (Invitrogen, Carlsbad, CA, USA) and 200 μg/ml rifampicin (Sigma, St. Louis, MO, USA). The pUC18T-mini-Tn*7*T-Gm-*lux* constructs, where the *lux* operon is expressed from endogenous promoters, were transferred to *B. pseudomallei* strain Bp340 (Mima and Schweizer, 2010) using biparental mating with *E. coli* mobilizer strain RHO3 (Lopez et al., 2009). Exconjugants were selected on LB Lennox medium with 15 μg/ml gentamicin (Sigma). The mini-Tn*7* insertion sites were determined using colony PCR and previously described protocols (Choi et al., 2005, 2008). pUC18T-mini-Tn*7*T-Zeo-*P1-lux* is based on pUC18T-mini-Tn*7*T (Choi et al., 2006) and contains a zeocin resistance selection marker and the *P. xenorhabdus luxCDABE* operon from which internal restriction sites were removed (Voisey and Marincs, 1998). The *lux* operon on this plasmid is expressed from the P1 integron promoter (DeShazer and Woods, 1996).

All experiments conducted with *B. mallei* or *B. pseudomallei* were conducted using Select Agent compliant BSL-3/ABSL-3 containment and procedures.

MICE

Female, 6- to 8-week-old, BALB/c mice were obtained from Harlan (Indianapolis, IN, USA). Animal studies were performed in accordance with the Institutional Animal Care and Use Committee's guidelines at UTMB as recommended by the National Institute of Health.

IN VITRO STABILITY

The stability of the mini-Tn*5*::*lux*Km2 transposon insertion in *B. mallei* was assessed by sub-culturing the CSM001 strain every 24 h over a period of 4 days as previously described (Foucault et al., 2010). Briefly, CSM001 was grown for 48 h on LBG agar plates. Isolated colonies were cultured in LBG broth shaking for 24 h at 37°C. The overnight culture was diluted 1:1000 in LBG broth in the presence or absence of antibiotic and incubated with shaking for 24 h at 37°C. Cells from the culture were plated on LBG plates in the presence and absence of antibiotic and incubated for 24–48 h at 37°C.

The plates were screened for bioluminescence and quantified using the IVIS Spectrum imaging system (Caliper Corp., Alameda, CA, USA). Each colony from the patch plate was selected as a region of interest (ROI). The Caliper Life Sciences software quantified the signal intensity for each ROI and an average intensity for each plate was calculated.

GROWTH CURVE

The growth curve for CSM001 ($\log_{10}$ CFU/ml) was performed in LBG broth and compared to the growth of wild-type *B. mallei* ATCC 23344 in three independent experiments. Sampling was performed at approximately 4 h intervals of the assay, from 0 to 16 h, then at 26 and 38 h from the start of the experiment. The growth of *B. mallei* wild-type and CSM001 strains were monitored by plating serial dilutions from the time points on LBG media as well as by OD_{600} readings. Statistical differences were determined using an unpaired *t* test with the significance set at $P < 0.05$. The error bars represent the SEM.

DETERMINATION OF LD_{50}

Groups of 10 animals were i.n. inoculated with 10^2, 10^3, 10^4, or 10^5 CFUs of CSM001 in a total volume of 50 µl LB broth (25 µl/nare). Deaths were recorded over a period of 10 days. The LD_{50} was calculated (Reed and Muench, 1938) based on the dosages of the inocula.

BACTERIAL CHALLENGE AND ANTIBIOTIC TREATMENT

For the BLI experiments, animals were i.n. inoculated with 5×10^3 CFUs of CSM001, unless otherwise indicated, in a total volume of 50 µl of LB broth (25 µl/nare). Treatment with levofloxacin via the intraperitoneal (i.p.) route started 24 h after infection, once a day, up to 96 h. Levofloxacin (Levaquin Injection, GlaxoSmithKline) was purchased from the UTMB Pharmacy and prepared according to the manufacturer's instructions at a dosage of 20 mg/kg/day.

BACTERIAL COLONIZATION

CSM001 was grown on LBG plates for 48 h at 37°C followed by sub-culturing in LBG broth shaking for 24 h at 37°C. The bacterial culture was diluted to a concentration of 5×10^3 CFU per 50 µl (unless otherwise indicated). BALB/c mice were i.n. inoculated with the prepared dosage (25 µl/nare). Animals were imaged and sacrificed at 24, 48, and 72 h post inoculation. The lungs, spleen, and liver (when indicated) were harvested. Bioluminescent signal was analyzed in the intact, extracted organs.

BIOLUMINESCENCE QUANTIFICATION

Bioluminescent images were acquired using an IVIS Spectrum (Caliper Corp., Alameda, CA, USA). This system consists of a heated stage inside a light–tight imaging chamber, a cooled charge-coupled-device camera with controller and refrigeration unit, integrated anesthesia system, and a Windows computer system for data acquisition and management. Bioluminescent signal was measured with no excitation (filters blocked) and an open emission filter.

In preparation for *in vivo* imaging, anesthesia was induced in the mice with 2–3% isoflurane in an oxygen-filled induction chamber. Once anesthetized, the mice were transferred to an isolation chamber, which was then placed in the imaging chamber and connected to the in-chamber anesthesia delivery system and maintained at 1–2% isoflurane. The *ex vivo* images of the lungs, spleen, and liver were acquired at each time point immediately after euthanasia. The organs were placed in a petri dish, and then contained in the isolation chamber (during imaging). Bioluminescent signal is represented in the images with a pseudocolor scale ranging from red (most intense) to violet (least intense) indicating the intensity of the signal. Scales were manually set to the same values for every comparable image (*in vivo* and *ex vivo)* to normalize the intensity of the bioluminescence across time points.

RESULTS

ANALYSIS OF THE CSM001 REPORTER STRAIN

The CSM001 strain, a construct expressing the entire *lux* operon was used to avoid the exogenous addition of luciferase substrate. As a first step toward evaluating the use of bioluminescence for monitoring glanders, we wanted to ensure that the transposon integration was stable by utilizing an *in vitro* stability assay (**Figure 1**). CSM001 was grown in LBG and sub-cultured daily over a period of 4 days in the appropriate media. Bacteria were grown in the presence or absence of antibiotic to ensure that selection was not necessary to maintain the transposon stability. Every

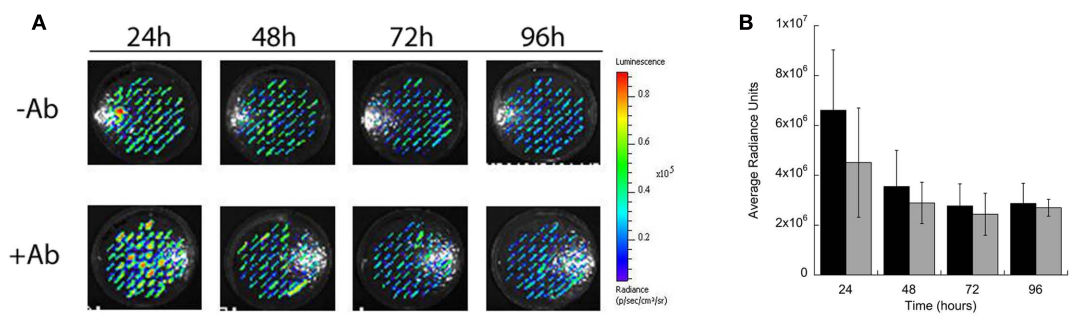

FIGURE 1 | Stability assessment of mini-Tn5::*luxKm2*. (A) The stability of the mini-Tn5::*lux*Km2 transposon insertion in CSM001was assessed by sub-culturing bacteria daily over 4 days in the presence and absence of antibiotic. **(B)** Each colony was selected as a region of interest and quantified using the Living Image software. Insertion stability is expressed as the average radiance units (p/sec/cm²/sr) ± SEM from three independent experiments.

24 h, bacteria from the subculture were plated on the appropriate media, incubated at 37°C and monitored for bioluminescence. The bacteria did not exhibit any apparent difference in the bioluminescent signal on the patch plates (**Figure 1A**) following imaging. There was no significant decrease in the luminescent intensity over the 96-h time course (**Figure 1B**). The CSM001 strain sub-cultured in the presence of antibiotic exhibited the same level of luminescence as those sub-cultured in the absence of antibiotic.

Growth kinetic experiments were performed to ensure that *B. mallei* strain CSM001 grows comparably to the parental *B. mallei* ATCC 23344 strain. First we examined the virulence of our mutant strain compared to the wild-type strain (**Figure 2A**). Four groups of 10 animals were i.n. inoculated with 10^2–10^5 CFUs of bacteria and monitored for survival over the 10-day time period. Following the Reed and Muench method (Reed and Muench, 1938), the 10-day LD_{50} value was calculated to be 6.81×10^2 CFU. Next, we monitored the *in vitro* growth rate of the mutant strain compared to the wild-type strain (**Figure 2B**). Briefly, bacterial cultures were grown in LBG media over 38 h. At the indicated time points the OD_{600} was determined and dilutions of the culture were grown on LBG plates. The growth curves indicate that the growth between the wild-type bacteria and the mutant strain is comparable and not significantly different throughout the time points within the exponential growth phase (4–16 h) stage.

IN VIVO BIOLUMINESCENCE IMAGING

Initial experiments were conducted to determine the threshold detection limits of the CSM001 strain. Groups of mice were i.n. infected with concentrations of bacteria ranging from 10^2 to 10^6 and monitored for daily luminescence analysis. Animals inoculated with the 10^2 and 10^3 doses of bacteria showed no apparent signs of infection 5 days post inoculation. Although luminescence was not detected *in vivo* following a 2-h incubation, a luminescent signal was detected in the lungs of animals infected with 1×10^6 bacteria as soon as 2 h post-infection, indicating a bacterial threshold for detection (**Figure 3**). A number of the animals infected at the higher doses exhibited luminescence signal associated within the brain, and all of these animals expired within 48 h after infection. No luminescence was initially detected with a dosage 5×10^3 CFU (**Figure 3**) although the signal increased over time and the animals survived past 72 h (data not shown). We further tested whether the CSM001 strain could be used as a reporter strain to follow glanders progression in the BALB/c mouse model. Two groups of four BALB/c mice were infected i.n. with 5×10^3 CFUs of the CSM001 strain (**Figure 4**). One group was anesthetized every 24 h and monitored for bioluminescence signal using the IVIS system, collecting, and quantifying the photons emitted by CSM001 within the animals. One animal was sacrificed every 24 h, and the lungs and spleen were harvested for *ex vivo* imaging. Bioluminescence signal was absent at 24 h both *in vivo* and *ex vivo*, but was clearly evident at the 48- and 72-h time points. As predicted, the bioluminescent signal increased over the course of the study (**Figure 4**). CFU determinations confirmed that the observed bioluminescent signal increase. The bacterial burden within the lungs of untreated animals steadily increased from approximately 7.77×10^5 at 24 h to 5.96×10^6 at 48 h and then to 3.17×10^8 at 72 h (**Figure 6A**). When the animals were treated with levofloxacin, the bacterial burden in the lungs was much lower 5.64×10^3 at 48 h and 1.59×10^5 at 72 h (**Figure 6A**). The bacterial burden within the spleen also increased over the course of the infection from approximately 2.15×10^4 at 24 h to 5.72×10^4 at 48 h and then 2.96×10^5 at 72 h (**Figure 6B**). Animals treated with levofloxacin also showed decreased bacterial burden in the spleen with 6.63×10^2 CFU/organ at 48 h and 1.91×10^4 CFU/organ at 72 h (**Figure 6B**).

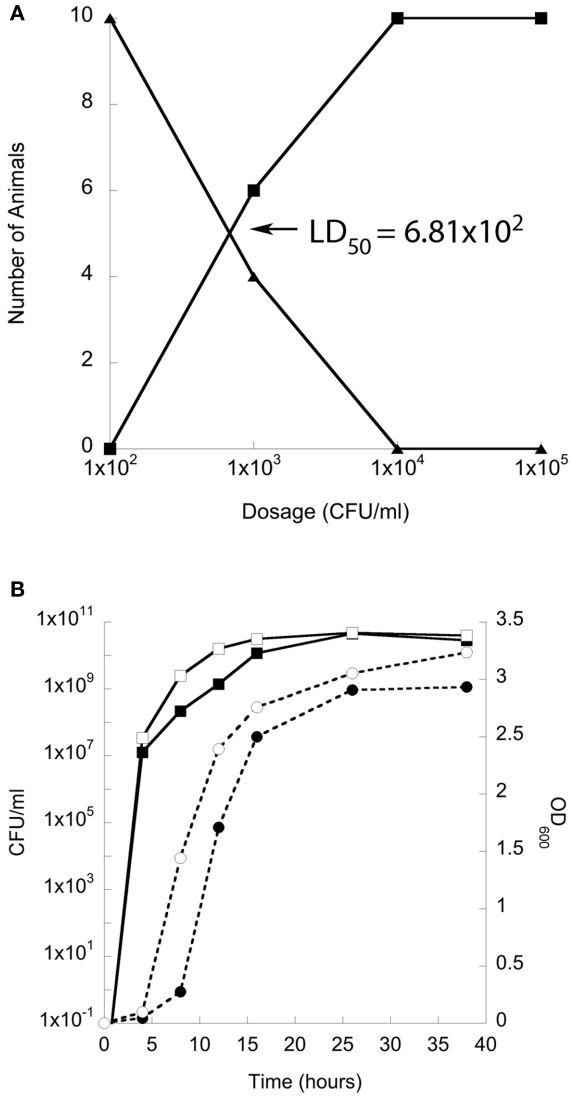

FIGURE 2 | CSM001 comparison to *B. mallei ATCC 23344*. **(A)** The 10-day LD_{50} for CSM001 was determined by infecting groups of 10 animals by i.n. with the indicated doses and monitoring the death (squares) and survival (triangles) of the animals. **(B)** Cultures of CSM001 (open symbols) and *B. mallei* ATCC 23344 (closed symbols) were grown to mid log phase (~12 h) while shaking at 37°C. The cultures were diluted 1:100 and monitored by OD_{600} (circles) and CFU plating (squares) for 38 h at approximately 4 h intervals. Individual data points represent the CFU mean ± SEM of three independent experiments. *, $P < 0.05$.

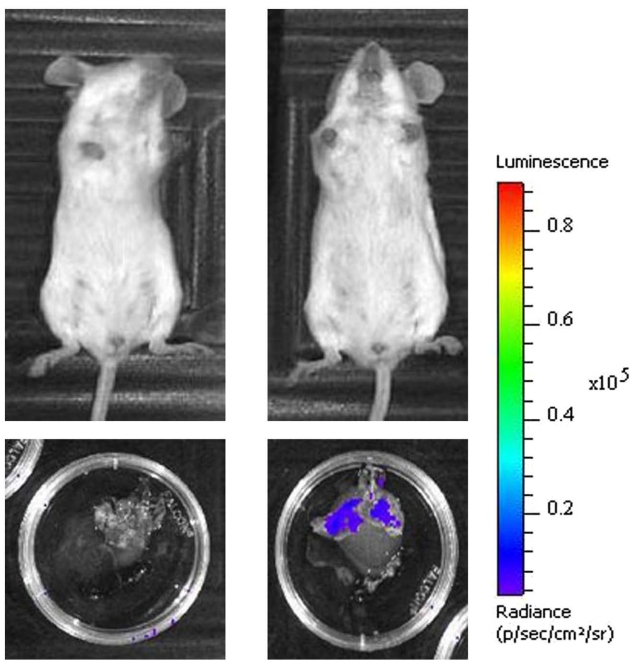

FIGURE 3 | *In vivo imaging confirmation.* CSM001 was i.n. inoculated at the indicated doses. The *in vivo* bioluminescence imaging was performed at 2 h post-infection. The intensity of emission is represented as a pseudocolor image. Each animal was sacrificed and the lungs were harvested for *ex vivo* imaging. Images are representative of replicate experiments.

Our previous studies with the BALB/c mouse model have demonstrated that *B. mallei* is sensitive to levofloxacin both *in vitro* and *in vivo* (Judy et al., 2009). It was shown that treatment with levofloxacin decreased the bacterial burden in the lung and spleen of infected animals. Based on this evidence, we investigated whether the decrease in bacterial burden conferred by levofloxacin treatment could be detected with our bioluminescence system. A second group of animals (**Figure 5A**) received 20 mg/kg/day of levofloxacin 24 h after infection. Every 24 h, the animals were anesthetized and monitored for bioluminescence signal. One animal was sacrificed for *ex vivo* imaging of the lung and spleen, as well as for CFU determination of those organs (data not shown). The levofloxacin treatment resulted in decreased bioluminescence signal over the course of the infection. At the 48-h time point, no signal can be detected *in vivo* or *ex vivo* although bacteria were recovered following organ plating (data not shown). A signal does appear following imaging at 72 h in both the *ex vivo* and *in vivo* images, however compared to the untreated animal the signal intensity is drastically reduced. This observation is consistent with our previous studies, as levofloxacin does not result in clearance of the bacterial infection. In the levofloxacin-treated animals, the antibiotic was discontinued after 96 h. These animals were imaged every 24 h until a bioluminescence signal was detected. The re-emergence of signal occurred at 192 h and revealed apparent bacterial colonization in the brain (**Figure 5B**).

CONSTRUCTION OF STABLE BIOLUMINESCENT *BURKHOLDERIA* STRAINS USING MINI-Tn*7* TRANSPOSONS

As an alternative to tagging with randomly inserting mini-Tn*5-lux* elements, we evaluated mini-Tn*7-lux* elements (**Figure 7A**) that insert site-specifically at known chromosomal attachment sites for tagging of *Burkholderia* spp. To this end, mini-Tn*7-lux* elements were integrated into the genomes of *B. thailandensis* strain E264 and *B. pseudomallei* strain Bp340. The resulting strains emitted light at levels that were comparable to those of *B. mallei* strain ATCC 23344 tagged with a randomly inserted mini-Tn*5-lux* element (**Figure 1A**). The levels of light emitted were somewhat dependent on the promoter used for *lux* operon expression. For example, the constitutive P1 integron promoter driving the *dhfRII* gene from R388 encoding trimethoprim resistance is six times more efficient in *E. coli* than the de-repressed *tac* promoter (DeShazer and Woods, 1996). Consequently, strong light emission was observed in *B. thailandensis* expressing the *lux* operon from this promoter (**Figure 7B**). By comparison, light emission by *B. pseudomallei* where the *lux* operon is preceded by an ∼500 bp DNA fragment which contains at least five predicted (BDGP Neural Network Promoter Prediction; www.fruitfly.org/seq_tools/promoter.html) bacterial promoters with scores of 0.99 to 1.00 was still strong (**Figure 7C**) but less intense than that observed with *B. thailandensis* with a mini-Tn*7-P1-lux* element. Although several mini-Tn*7-lux* constructs with predicted strong promoters were tested in *B. pseudomallei*, cells containing the element with the five random promoters consistently exhibited stable, strong light expression. Promoter screening was by no means exhaustive and, for example, did not include the *ompA* promoter that was previously used to construct a mini-Tn*7-*P_{ompA}*-lux* element that was successfully used to tag a *B. pseudomallei* strain and follow the disease manifestation in a murine melioidosis model (Owen et al., 2009).

DISCUSSION

Burkholderia mallei is a Category B select agent that has been used on a number of occasions as a biological weapon. Infection with *B. mallei* can result in glanders, a disease that affects horses and other equine species, developing into either an acute or chronic infection that ultimately leads to death. Glanders, while eradicated in many countries, remains endemic in a number of areas across the world. Despite the existence of endemic regions and potential threat of *B. mallei* as a bio-weapon, little data is available on the efficacy of glanders treatments. Therefore, there is an urgent need for extensive evaluation of *in vivo* treatment methods. Data collected by other groups has demonstrated that *in vivo* bioluminescence imaging is a valuable tool for providing insights into the mechanisms of pathogenesis and disease progression, with the goal of identifying new therapeutic approaches. In this study, we demonstrate that glanders infection and treatment can be monitored using CSM001, a bioluminescent reporter strain derived from *B. mallei* ATCC 23344.

The CSM001 strain was created to monitor bacterial dissemination by constitutive expression of the *lux* operon from *P. luminescens*. The bacteria are constantly producing a luminescent signal that can be correlated to bacterial burden in affected organs. This simple and quantitative technique provides a number of advantages over current approaches for monitoring bacterial

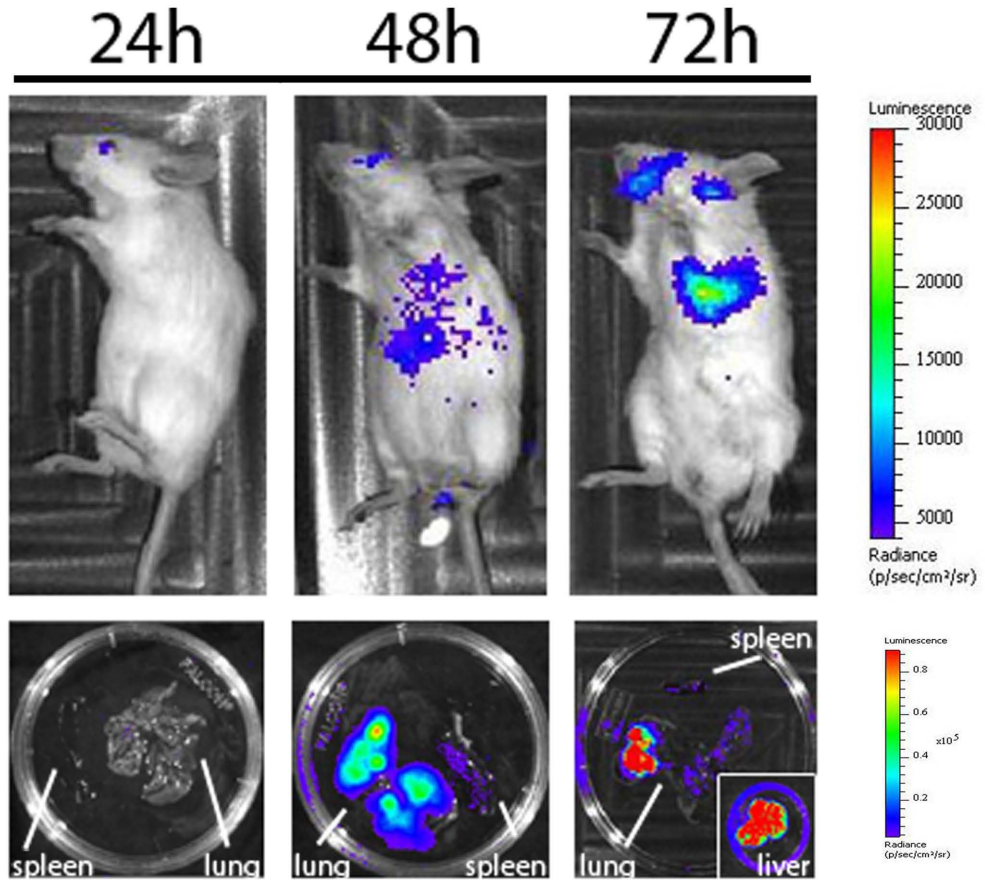

FIGURE 4 | ***In vivo imaging of CSM001 infection.*** CSM001 was i.n. inoculated into mice. The *in vivo* bioluminescence imaging was conducted at 24, 48, and 72 h post-infection. The intensity of emission is represented as a pseudocolor image. At each time point, an animal was sacrificed and organs were harvested for *ex vivo* imaging and bacterial load determination. Images are representative of four replicate experiments.

dissemination and therapeutic efficacies. Traditional methods for determining bacterial localization, colonization, and bacterial burden *in vivo* require that large numbers of experimental animals be euthanized at various time points for assessment of individual organs. The use of bioluminescence allows individual animals to be analyzed at multiple time points. This reduces animal-to-animal variation and ensures that biologically relevant information is not overlooked. In the conventional methods of harvesting organs and CFU plating, it is possible that the infection spreads to unexpected sites and that these infected tissues are not collected. BLI permits monitoring of the bacterial dissemination to these unexpected infection sites. The preferential use of bioluminescent reporters over fluorescent constructs is primarily due to the fact that most mammalian tissues are auto-fluorescent at the same wavelengths as the fluorescent reporter constructs, resulting in a low signal to noise ratio that is not observed when employing bioluminescent reporters.

Bioluminescent imaging has been used to study the mechanisms of pathogenesis and treatment efficacies for a number of infectious bacteria. One of the first investigations using BLI was conducted to monitor the distribution and differences in virulence among three strains of *S. Typhimurium* (Contag et al., 1995). In this study, the authors demonstrated the utility of the bioluminescence system by visualizing the efficacy of antibiotic treatment on infected animals. The *in vivo* bioluminescence has been utilized to detect *E. coli* localization in the neutropenic mouse thigh model where it was shown that bioluminescence was just as effective for determining antibiotic effectiveness as the traditional CFU determination methods (Rocchetta et al., 2001). Also, bioluminescence in *E. coli* has been used to track bacterial colonization in the mouse intestine (Foucault et al., 2010). BLI has also proven useful for monitoring bacterial dissemination in a number of other agents such as *F. tularensis* (Bina et al., 2010) and *M. tuberculosis* (Andreu et al., 2010). Even the colonization routes of *B. pseudomallei*, the closest relative of *B. mallei*, have been monitored using a *lux*-tagged strain (Owen et al., 2009).

Because the *lux* operon was inserted into the chromosome of *B. mallei* via a transposon, it was important to ensure that insertion did not occur in a site that disrupted the virulence or the rate of growth of *B. mallei*. The LD_{50} assay and the growth curve analysis demonstrated that our CSM001 strain mirrored the virulence and growth kinetics of the *B. mallei* ATCC 23344 wild-type strain. If the transposon inserted into a site that increased virulence, it is possible that the infected mice would die prior to reaching a threshold

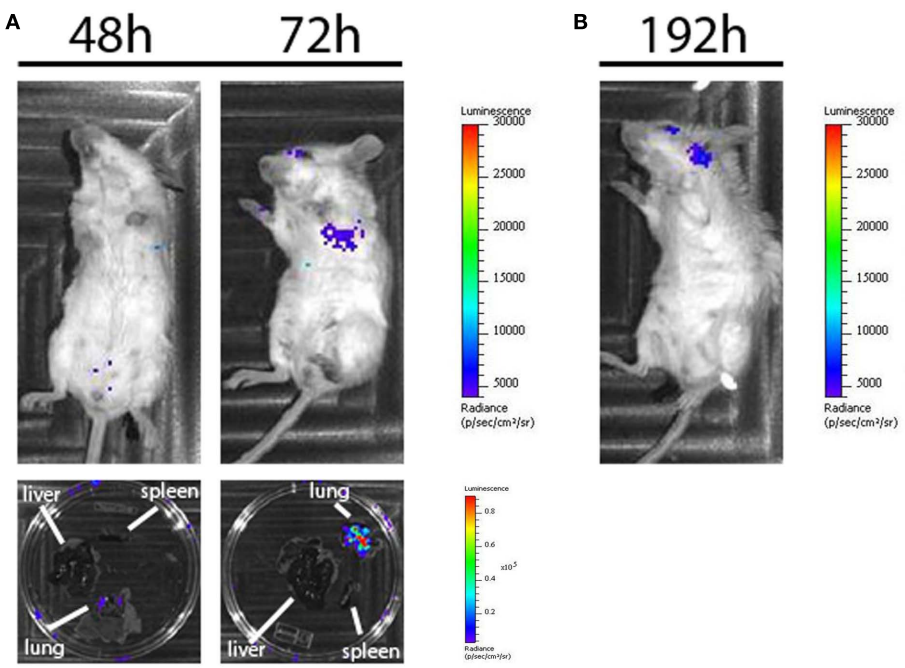

FIGURE 5 | ***In vivo imaging of CSM001 infection post-antibiotic treatment.*** **(A)** CSM001 was i.n. inoculated into mice. The *in vivo* bioluminescence was monitored at 24, 48, and 72 h post-infection. Treatment with 20 mg/kg of levofloxacin was administered after the 24-h time point. At each time point an animal was sacrificed and organs were harvested for *ex vivo* imaging and bacterial load determination. Images are representative of four replicate experiments. **(B)** Antibiotic treatment was suspended following 96 h. Imaging was conducted every 24 h until the luminescence signal returned (192 h time point).

detection limit. It has been previously reported that the LD_{50} for *B. mallei* ATCC 23344 ranges from 1.8×10^3 (Lever et al., 2003) to 2.5×10^5 (Whitlock et al., 2009). We determined the LD_{50} for the CSM001 strain to be 6.81×10^2. Our present study focused on the ability to create a bioluminescent *B. mallei* strain with similar virulence and growth kinetics to the wild-type strain.

As an alternative to tagging with randomly inserting mini-Tn*5-lux* transposons, mini-Tn*7-lux* elements that insert site-specifically at known chromosomal attachment sites can be used to construct reporter bacteria. The attachment sites are generally located in intergenic regions and thus integrants are less likely to be attenuated. Mini-Tn*7* elements offer the added advantage that, unlike "locked in" mini-Tn*5* insertions, they can be readily inserted at the same site in mutant derivatives of the same bacterial strain thereby allowing comparative analyses in isogenic backgrounds. While mini-Tn*7-lux* derivatives have been used to construct bioluminescent *B. pseudomallei* and *B. thailandensis* strains (**Figure 7**; Owen et al., 2009), they have not yet been employed for construction of bioluminescent *B. mallei*. However, this will be easy to achieve since detailed protocols for site- and orientation-specific mini-Tn*7* tagging of *Burkholderia* spp. have been published, including *B. thailandensis* (Choi et al., 2005), *B. pseudomallei* (Choi et al., 2008), and *B. mallei* (Choi et al., 2006). While the *P. luminescens* wild-type *luxCDABE* operon seems to be well expressed in *Burkholderia* spp., there is room for improvement. Stable expression of the *lux* operon can be further optimized by screening of additional promoters known to be well-tolerated and constitutively expressed in *Burkholderia* spp., for example the *s12* ribosomal gene promoter (Choi et al., 2008) or the *ompA* gene promoter (Owen et al., 2009). The *P. luminescens* wild-type *luxCDABE* operon is also very A + T rich (>69%) and it has been proposed that for this and other reasons, e.g., rare codon usage, these genes may not be expressed very well in bacteria with high G + C content genomes. To overcome this potential hurdle, Craney et al. (2007) derived a synthetic *luxCDABE* gene cluster optimized for expression in bacteria with high G + C content. It may be worthwhile considering engineering of mini-Tn*7-lux* elements that exhibit strong, yet stable, light emission using a combination of optimized genus- or species-specific promoter sequences and a *lux* operon optimized for gene expression in bacteria with high G + C content.

The *in vivo* BLI can be used to identify dissemination of bacterial infections in the i.n. mouse model. The BALB/c mouse model has routinely been used to study *B. mallei* infection, as it is highly susceptible (Leakey et al., 1998; Fritz et al., 2000; Lever et al., 2003; Whitlock et al., 2008; Sarkar-Tyson et al., 2009). We monitored BALB/c mice that had been i.n. infected with the CSM001 strain. Over the course of the infection, the bacterial burden in the target organs increased and the infection sites became luminescent and visible with the IVIS. The data collected are consistent with the traditional methods for characterizing bacterial infection. Lever et al. (2003) demonstrated that following aerosol exposure to *B. mallei*, bacterial counts are first detected in the lungs and steadily increased over 5 days, at which point the bacterial

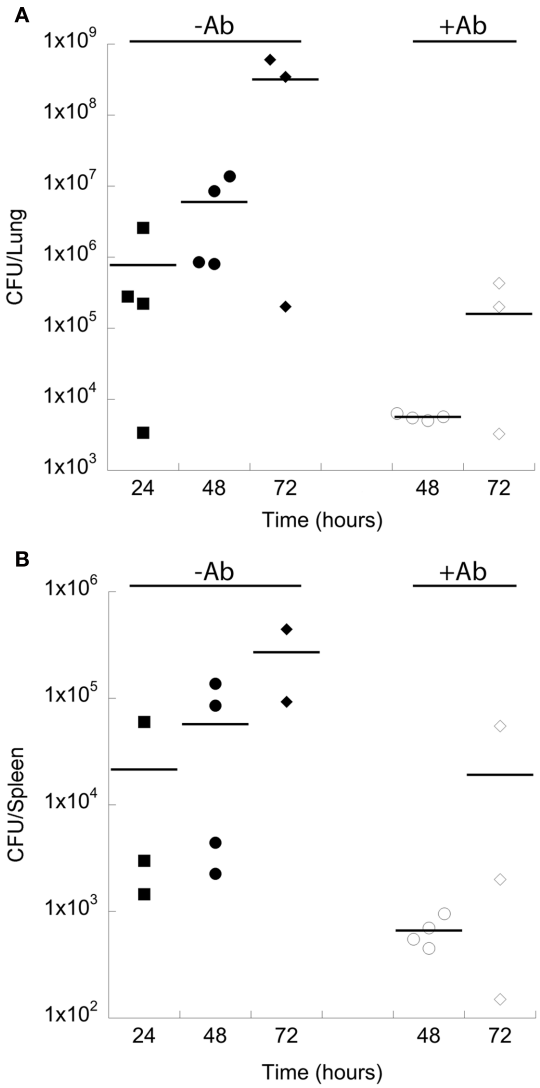

FIGURE 6 | *B. mallei* bacterial burden in treated and untreated *BABLB/c mice.* CSM001 was i.n. inoculated into BALB/c mice as indicated previously for the bioluminescent imaging. At each time point, untreated (closed symbols) or treated (open symbols) animals with 20 mg/kg/day of levofloxacin were sacrificed and the lungs **(A)** and spleen **(B)** were harvested at 24 h (squares), 48 h (circles), 72 h (diamonds) and plated for CFU determination.

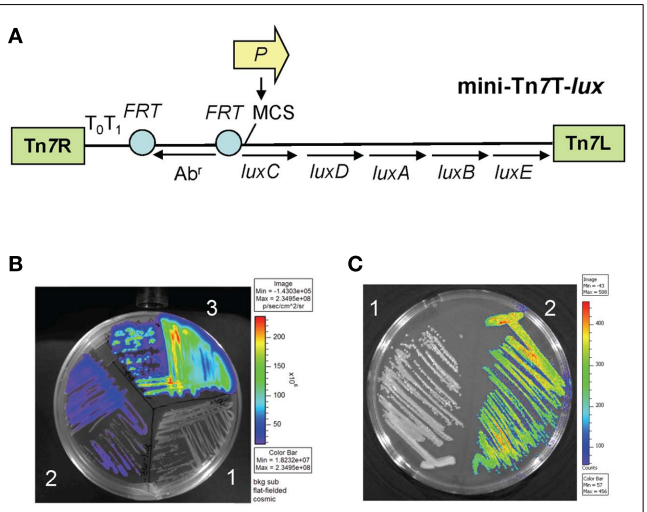

FIGURE 7 | Bioluminescent tagging of *Burkholderia* spp. with mini-Tn *7-lux* elements. (A) Map of a typical mini-Tn*7-lux* element. The basic element contains a promoter-less *P. luminescens luxCDABE* operon that is preceded by a multiple cloning site (MCS). An antibiotic resistance (Ab^r) selection marker inserted upstream of the *lux* operon is preferably flanked by yeast Flp recombinase target (*FRT*) sites that allow optional site-specific excision of the Ab^r marker after site-specific insertion into the bacterial chromosome. Restriction sites in the MCS can also be used to insert customized promoter sequences (arrow labeled *P*). **(B)** A mini-Tn*7-lux* element with a zeocin resistance selection marker was inserted into the *glmS1*-associated insertion site of chromosome 1 of *B. thailandensis* strain E264 (Choi et al., 2005). Bacteria containing either no insertion (1), a promoter-less mini-Tn*7-lux* (2) or a mini-Tn*7-P1-lux* element where the *lux* operon is transcribed from the strong P1 integron promoter (DeShazer and Woods, 1996) were grown overnight on an LB plate and imaged on an IVIS Spectrum imaging system. **(C)** A mini-Tn*7-lux* element with a gentamicin resistance selection marker was inserted into the *glmS3*-associated insertion site on chromosome 2 of *B. pseudomallei* strain Bp340 (Choi et al., 2008; Mima and Schweizer, 2010). Bacteria containing either no insertion (1) or a mini-Tn*7-lux* element where the *lux* operon is transcribed from synthetic promoter sequences active in *B. pseudomallei* (2) were grown overnight on an LB plate and imaged on an IVIS Spectrum imaging system.

burden decreases. We showed that after 24 h of infection there is no bioluminescence signal in the lungs, despite the presence of approximately 1×10^6 bacteria. Presumably this is because a threshold detection limit has not been reached as is evident in **Figure 3**. After 48 h, the bioluminescence signal is visible and this signal increases in intensity at 72 h (**Figure 4**).

Currently, there are no effective vaccines available for glanders infection and very little data exists on the efficacy of antibiotic for treatment of human glanders. One case of human glanders involving an accidental lab exposure was treated with a mixed regimen of antibiotics (Srinivasan et al., 2001). A more standardized course of treatment is necessary however, due to the fact that mixed antibiotic regimen must be administered for a number of days and assumes an accurate and early diagnosis. The antibiotic susceptibility of *B. mallei* is similar to that of *B. pseudomallei* and because of this, most *B. mallei* antibiotic treatments are based on efficacy of treatment regimens for *B. pseudomallei* infections. Levofloxacin inhibits DNA replication and transcription in Gram negative bacteria and has previously been shown to decrease bacterial burden in the lung and spleen of BALB/c mice infected with *B. mallei* (Judy et al., 2009). Here, we demonstrated that the decrease in bacterial burden in the lungs can be visualized using BLI technology. Animals were treated with antibiotic 24 h post-infection, and when the animals were imaged at 72 h, a luminescence signal was visible, although the intensity was markedly reduced. Antibiotic efficacy studies have revealed that *B. mallei* is susceptible to a number of antibiotics *in vitro*, although *in vivo* analysis still needs to be performed; therefore, BLI is a useful tool for assessing various treatments using fewer animals. BLI should also prove useful for monitoring novel therapeutic targets such as new antibiotics, quorum sensing molecules (reviewed in Estes et al., 2010) or virulence

factors associated with the type three (Whitlock et al., 2007) and type six secretion systems (Schell et al., 2007).

A number of our BLI experiments revealed bioluminescence signal associated with the brain of the animals. It was previously reported that the nasal-associated lymphoid tissue (NALT) of BALB/c mice acts as an entryway for *B. pseudomallei* (Owen et al., 2009). The authors concluded that the olfactory nerve served as a route of entry for *B. pseudomallei* to the brain after i.n. infection with 3.6×10^5 CFU. The implication was also made that this route of entry could be responsible for the infections of the CNS often seen in human melioidosis (Currie et al., 2000; Chadwick et al., 2002; White, 2003; Koszyca et al., 2004). Based on our observations (**Figure 5B**), it is possible that *B. mallei* utilizes the same olfactory nerve to reach the brain in mice. Owen et al. (2009) observed localization of *B. pseudomallei* to the brain 48 h after infection. Our experiments with *B. mallei* required at least 72 h before signal could be detected. Further clarification of the role of NALT during glanders infection could provide insights for future vaccination therapies.

In summary, we have developed and validated a BLI technique for the detection of *B. mallei* infection in the BALB/c intranasal model of acute glanders. We demonstrated that this highly sensitive reporter strategy can be used to obtain *in vivo* images of *B. mallei* infection in mice. This BLI method is straightforward and reduces the numbers of animals traditionally required and can be useful for antibiotic efficacy studies as shown by the decrease in luminescent signal of levofloxacin-treated animals. Future studies will verify previously reported *in vitro* antibiotic efficacies and test vaccine candidates.

ACKNOWLEDGMENTS

We thank Dr. Richard Titball from the University of Exeter for the generous gift of the bioluminescent transposon and to Dr. Sonja Lloyd and Dr. Douglas Botkin for critical reading of the manuscript. Grant number U54 AI057156 from the Western Regional Center for Excellence supported this project along with grant number 5U01AI082103-02 and a T32 postdoctoral training grant, number T32A1007536, from the NIAID/NIH. Herbert P. Schweizer was supported by grant AI065357 from the NIAID/NIH. Herbert P. Schweizer acknowledges the contributions of K.-H. Choi, A. Kumar, and D. A. Rholl to work performed with mini-Tn*7-lux* in his laboratory. The contents are solely the responsibility of the authors and do not necessarily represent the official views of the RCE Programs Office, NIAID, or NIH.

REFERENCES

Andreu, N., Zelmer, A., Fletcher, T., Elkington, P. T., Ward, T. H., Ripoll, J., Parish, T., Bancroft, G. J., Schaible, U., Robertson, B. D., and Wiles, S. (2010). Optimisation of bioluminescent reporters for use with mycobacteria. *PLoS ONE* 5, e10777. doi: 10.1371/journal.pone.0010777

Bina, X. R., Miller, M. A., and Bina, J. E. (2010). Construction of a bioluminescence reporter plasmid for *Francisella tularensis*. *Plasmid* 64, 156–161.

Chadwick, D. R., Ang, B., Sitoh, Y. Y., and Lee, C. C. (2002). Cerebral melioidosis in Singapore: a review of five cases. *Trans. R. Soc. Trop. Med. Hyg.* 96, 72–76.

Choi, K. H., Deshazer, D., and Schweizer, H. P. (2006). mini-Tn*7* insertion in bacteria with multiple *glmS*-linked *att*Tn*7* sites: example *Burkholderia mallei* ATCC 23344. *Nat. Protoc.* 1, 162–169.

Choi, K. H., Gaynor, J. B., White, K. G., Lopez, C., Bosio, C. M., Karkhoff-Schweizer, R. R., and Schweizer, H. P. (2005). A Tn7-based broad-range bacterial cloning and expression system. *Nat. Methods* 2, 443–448.

Choi, K. H., Mima, T., Casart, Y., Rholl, D., Kumar, A., Beacham, I. R., and Schweizer, H. P. (2008). Genetic tools for select-agent-compliant manipulation of *Burkholderia pseudomallei*. *Appl. Environ. Microbiol.* 74, 1064–1075.

Christopher, G. W., Cieslak, T. J., Pavlin, J. A., and Eitzen, E. M. Jr. (1997). Biological warfare. A historical perspective. *JAMA* 278, 412–417.

Contag, C. H., Contag, P. R., Mullins, J. I., Spilman, S. D., Stevenson, D. K., and Benaron, D. A. (1995). Photonic detection of bacterial pathogens in living hosts. *Mol. Microbiol.* 18, 593–603.

Craney, A., Hohenauer, T., Xu, Y., Navani, N. K., Li, Y., and Nodwell, J. (2007). A synthetic *luxCDABE* gene cluster optimized for expression in high-GC bacteria. *Nucleic Acids Res.* 35, e46.

Currie, B. J., Fisher, D. A., Howard, D. M., and Burrow, J. N. (2000). Neurological melioidosis. *Acta Trop.* 74, 145–151.

DeShazer, D., and Woods, D. E. (1996). Broad-host-range cloning and cassette vectors based on the R388 trimethoprim resistance gene. *Biotechniques* 20, 762–764.

Estes, D. M., Dow, S. W., Schweizer, H. P., and Torres, A. G. (2010). Present and future therapeutic strategies for melioidosis and glanders. *Expert Rev. Anti. Infect. Ther.* 8, 325–338.

Flentie, K. N., Qi, M., Gammon, S. T., Razia, Y., Lui, F., Marpegan, L., Manglik, A., Piwnica-Worms, D., and Mckinney, J. S. (2008). Stably integrated *luxCDABE* for assessment of *Salmonella* invasion kinetics. *Mol. Imaging* 7, 222–233.

Foucault, M. L., Thomas, L., Goussard, S., Branchini, B. R., and Grillot-Courvalin, C. (2010). In vivo bioluminescence imaging for the study of intestinal colonization by *Escherichia coli* in mice. *Appl. Environ. Microbiol.* 76, 264–274.

Fritz, D. L., Vogel, P., Brown, D. R., Deshazer, D., and Waag, D. M. (2000). Mouse model of sublethal and lethal intraperitoneal glanders (*Burkholderia mallei*). *Vet. Pathol.* 37, 626–636.

Heine, H. S., England, M. J., Waag, D. M., and Byrne, W. R. (2001). *In vitro* antibiotic susceptibilities of *Burkholderia mallei* (causative agent of glanders) determined by broth microdilution and E-test. *Antimicrob. Agents Chemother.* 45, 2119–2121.

Hutchens, M., and Luker, G. D. (2007). Applications of bioluminescence imaging to the study of infectious diseases. *Cell. Microbiol.* 9, 2315–2322.

Judy, B. M., Whitlock, G. C., Torres, A. G., and Estes, D. M. (2009). Comparison of the in vitro and in vivo susceptibilities of *Burkholderia mallei* to ceftazidime and levofloxacin. *BMC Microbiol.* 9, 88. doi: 10.1186/1471-2180-9-88

Kenny, D. J., Russell, P., Rogers, D., Eley, S. M., and Titball, R. W. (1999). In vitro susceptibilities of *Burkholderia mallei* in comparison to those of other pathogenic *Burkholderia* spp. *Antimicrob. Agents Chemother.* 43, 2773–2775.

Koszyca, B., Currie, B. J., and Blumbergs, P. C. (2004). The neuropathology of melioidosis: two cases and a review of the literature. *Clin. Neuropathol.* 23, 195–203.

Leakey, A. K., Ulett, G. C., and Hirst, R. G. (1998). BALB/c and C57Bl/6 mice infected with virulent *Burkholderia pseudomallei* provide contrasting animal models for the acute and chronic forms of human melioidosis. *Microb. Pathog.* 24, 269–275.

Lever, M. S., Nelson, M., Ireland, P. I., Stagg, A. J., Beedham, R. J., Hall, G. A., Knight, G., and Titball, R. W. (2003). Experimental aerogenic *Burkholderia mallei* (glanders) infection in the BALB/c mouse. *J. Med. Microbiol.* 52, 1109–1115.

Lopez, C. M., Rholl, D. A., Trunck, L. A., and Schweizer, H. P. (2009). Versatile dual-technology system for markerless allele replacement in *Burkholderia pseudomallei*. *Appl. Environ. Microbiol.* 75, 6496–6503.

Mima, T., and Schweizer, H. P. (2010). The BpeAB-OprB efflux pump of *Burkholderia pseudomallei* 1026b does not play a role in quorum sensing, virulence factor production, or extrusion of aminoglycosides but is a broad-spectrum drug efflux system. *Antimicrob. Agents Chemother.* 54, 3113–3120.

Owen, S. J., Batzloff, M., Chehrehasa, F., Meedeniya, A., Casart, Y., Logue, C. A., Hirst, R. G., Peak, I. R., Mackay-Sim, A., and Beacham, I. R. (2009). Nasal-associated lymphoid tissue and olfactory epithelium as portals of entry for *Burkholderia pseudomallei* in murine melioidosis. *J. Infect. Dis.* 199, 1761–1770.

Reed, L. J., and Muench, H. (1938). A simple method of estimating fifty per cent endpoints. *Am. J. Hygiene* 27, 493–497.

Rocchetta, H. L., Boylan, C. J., Foley, J. W., Iversen, P. W., Letourneau, D. L., Mcmillian, C. L., Contag, P. R., Jenkins, D. E., and Parr, T. R. Jr. (2001). Validation of a noninvasive, real-time imaging technology using bioluminescent *Escherichia coli* in the neutropenic mouse thigh model of infection. *Antimicrob. Agents Chemother.* 45, 129–137.

Sanford, J. P. (1995). "*Pseudomonas* species (including melioidosis and glanders)," in *Principles and Practice of Infectious Diseases*, 4th Edn, eds G. L. Mandell, J. E. Bennett, and R. Dolin. (New York: Churchill Livingstone), 2003–2009.

Sarkar-Tyson, M., Smither, S. J., Harding, S. V., Atkins, T. P., and Titball, R. W. (2009). Protective efficacy of heat-inactivated *B. thailandensis*, *B. mallei* or *B. pseudomallei* against experimental melioidosis and glanders. *Vaccine* 27, 4447–4451.

Schell, M. A., Ulrich, R. L., Ribot, W. J., Brueggemann, E. E., Hines, H. B., Chen, D., Lipscomb, L., Kim, H. S., Mrazek, J., Nierman, W. C., and Deshazer, D. (2007). Type VI secretion is a major virulence determinant in *Burkholderia mallei*. *Mol. Microbiol.* 64, 1466–1485.

Sharrer, G. T. (1995). The great glanders epizootic, 1861-1866: a civil war legacy. *Agric. Hist.* 69, 79–97.

Srinivasan, A., Kraus, C. N., Deshazer, D., Becker, P. M., Dick, J. D., Spacek, L., Bartlett, J. G., Byrne, W. R., and Thomas, D. L. (2001). Glanders in a military research microbiologist. *N. Engl. J. Med.* 345, 256–258.

Voisey, C. R., and Marincs, F. (1998). Elimination of internal restriction enzyme sites from a bacterial luminescence (*luxCDABE*) operon. *Biotechniques* 24, 56, 58.

White, N. J. (2003). Melioidosis. *Lancet* 361, 1715–1722.

Whitlock, G. C., Estes, D. M., and Torres, A. G. (2007). Glanders: off to the races with *Burkholderia mallei*. *FEMS Microbiol. Lett.* 277, 115–122.

Whitlock, G. C., Lukaszewski, R. A., Judy, B. M., Paessler, S., Torres, A. G., and Estes, D. M. (2008). Host immunity in the protective response to vaccination with heat-killed *Burkholderia mallei*. *BMC Immunol.* 9, 55. doi: 10.1186/1471-2172-9-55

Whitlock, G. C., Valbuena, G. A., Popov, V. L., Judy, B. M., Estes, D. M., and Torres, A. G. (2009). *Burkholderia mallei* cellular interactions in a respiratory cell model. *J. Med. Microbiol.* 58, 554–562.

Winson, M. K., Swift, S., Hill, P. J., Sims, C. M., Griesmayr, G., Bycroft, B. W., Williams, P., and Stewart, G. S. (1998). Engineering the luxCDABE genes from *Photorhabdus luminescens* to provide a bioluminescent reporter for constitutive and promoter probe plasmids and mini-Tn5 constructs. *FEMS Microbiol. Lett.* 163, 193–202.

Conflict of Interest Statement: The authors declare that the research was conducted in the absence of any commercial or financial relationships that could be construed as a potential conflict of interest.

Received: 30 April 2011; accepted: 08 August 2011; published online: 26 August 2011.

Citation: Massey S, Johnston K, Mott TM, Judy BM, Kvitko BH, Schweizer HP, Estes DM and Torres AG (2011) In vivo bioluminescence imaging of Burkholderia mallei respiratory infection and treatment in the mouse model. Front. Microbio. ***2****:174. doi: 10.3389/fmicb.2011.00174*

This article was submitted to Frontiers in Cellular and Infection Microbiology, a specialty of Frontiers in Microbiology.

frontiers in
MICROBIOLOGY

REVIEW ARTICLE
published: 27 September 2011
doi: 10.3389/fmicb.2011.00198

Development of vaccines against *Burkholderia pseudomallei*

Natasha Patel[1]*, Laura Conejero[1], Melanie De Reynal[1], Anna Easton[2], Gregory J. Bancroft[1] and Richard W. Titball[3]

[1] Department of Immunology and Infection, London School of Hygiene and Tropical Medicine, London, UK
[2] Centre for Clinical Microbiology, Department of Infection, Royal Free Campus, University College London, UK
[3] College of Life and Environmental Sciences, University of Exeter, Exeter, UK

Edited by:
Ivo Steinmetz, University of Greifswald, Germany

Reviewed by:
Robert Norton, Townsville Hospital, Australia
Joost Wiersinga, Academic Medical Center, Netherlands

***Correspondence:**
Natasha Patel, Immunology Unit, London School of Hygiene and Tropical Medicine, Keppel Street, London WC1E 7HT, UK.
e-mail: natasha.spink@lshtm.ac.uk

Burkholderia pseudomallei is a Gram-negative bacterium which is the causative agent of melioidosis, a disease which carries a high mortality and morbidity rate in endemic areas of South East Asia and Northern Australia. At present there is no available human vaccine that protects against *B. pseudomallei*, and with the current limitations of antibiotic treatment, the development of new preventative and therapeutic interventions is crucial. This review considers the multiple elements of melioidosis vaccine research including: (i) the immune responses required for protective immunity, (ii) animal models available for preclinical testing of potential candidates, (iii) the different experimental vaccine strategies which are being pursued, and (iv) the obstacles and opportunities for eventual registration of a licensed vaccine in humans.

Keywords: vaccines, melioidosis, *Burkholderia pseudomallei*

BURKHOLDERIA PSEUDOMALLEI AND MELIOIDOSIS

Burkholderia pseudomallei is a Gram-negative, facultative intracellular bacterium which can infect humans and a wide variety of animals (Cheng and Currie, 2005). Natural infection is thought to be primarily via percutaneous inoculation following exposure to muddy soils or surface water, such as in rice paddy fields, in endemic areas (Currie, 2003). It is thought that under certain environmental conditions, such as tropical storms, cyclones, and typhoons, inhalation is the main mode of infection (Currie, 2008). The incidence of melioidosis in endemic areas increases during the monsoon season and is associated with severe infection, pneumonia, and high mortality (Chaowagul et al., 1989; Currie and Jacups, 2003). This is analogous to the fulminant disease and high case fatality rates seen when the bacteria causing anthrax, plague, or tularemia are inhaled rather than inoculated (Inglesby et al., 2000, 2002; Dennis et al., 2001). This shift to more severe melioidosis during the rainy season could be explained by increased exposure to *B. pseudomallei*, possibly due to the heavy rain and winds generating aerosols, causing repeated inhalation of contaminated particles and a greater infection dose (Wiersinga et al., 2006). As this bacterium can cause disease following inhalation and is difficult to treat with antibiotics, it is now considered as a bioterrorism threat and as a potential agent for biological warfare it was added to the list of category B agents by the US Centers for Disease Control and Prevention.

Melioidosis is difficult to treat as *B. pseudomallei* is intrinsically resistant to many antibiotics (Wiersinga et al., 2006). However, this bacterium is susceptible to some newer β-lactam antibiotics and especially ceftazidime (McEniry et al., 1988; Dance et al., 1989; White, 2003). Despite the long course of treatment (typically 20 weeks), the mortality rate in endemic areas remains high (40–50%) and recurrence is common, the overall risk being 10% and rising to 30% if treatment lasts less than 8 weeks (Chaowagul et al., 1993). Of those recurrent infections, 75% are due to bacteria persisting from the original infection, and the remainder are due to re-infection with a different strain (Limmathurotsakul et al., 2006, 2007). Approximately 25% of patients who experience a recurrence die (Chaowagul et al., 1993). At present there is no available human vaccine that protects against *B. pseudomallei*, and with the current limitations of antibiotic treatment, the development of new therapeutic strategies is crucial.

HOST IMMUNE RESPONSES TO *B. PSEUDOMALLEI*

Development of new vaccines against melioidosis will benefit from a thorough understanding of the pathogenesis of infection and the characteristics of naturally occurring immune responses which develop following environmental or experimental exposure to the organism. In this section we review what is known about immune responses generated against *B. pseudomallei*, based primarily on data obtained from mouse models of experimental infection and studies in humans living in the endemic regions of North Eastern (NE) Thailand and Northern Australia.

INNATE IMMUNITY

An efficient host immune response is reliant on both fast acting innate immunity, as well as the more specific but slower adaptive immunity. Innate immunity is a universal and ancient form of host defense, and is essentially the "front line" against infection as it is these effector cells which first come into contact with and respond to invading microorganisms (Janeway and Medzhitov, 2002).

A key element in the initiation of an effective innate immune response and subsequent adaptive immunity is the recognition of microbes by innate cells. Pathogen recognition is mediated

by pattern recognition receptors (PRRs) located on or within host cells, which bind to pathogen associated molecular patterns (PAMPs) expressed by microorganisms (Akira et al., 2006). A large family of well characterized PRRs are the toll-like receptors (TLRs; Akira et al., 2006). *B. pseudomallei* expresses a number of potential PAMPs including, lipopolysaccharide (LPS), lipid-A, peptidoglycan, flagellin, type III secretion system (TTSS), and DNA, which have the potential to be recognized by different TLRs (Wiersinga and van der Poll, 2009). Mice lacking a key TLR adaptor signaling protein (MyD88) are highly susceptible to *B. pseudomallei* infection, partly due to reduced recruitment and activation of neutrophils (Wiersinga et al., 2008). TLR4 is thought to be a key molecule in protection against Gram-negative bacteria, given it is the main receptor for LPS (Akira et al., 2006). However a relatively recent study has shown TLR4 does not contribute to host defense against melioidosis *in vivo* (Wiersinga et al., 2007b). The LPS from *B. pseudomallei* differs from other Gram-negative bacteria, and is much less inflammatory (Matsuura et al., 1996), which may contribute to immune evasion. Surprisingly, evidence suggests that *B. pseudomallei* LPS signals via TLR2 as opposed to TLR4, and that this pathway can in fact exacerbate disease in the host (Wiersinga et al., 2007b). However the mechanism by which TLR2 signaling contributes to *B. pseudomallei* pathogenesis remains to be determined. Furthermore, increased expression of TLR2 and TLR4 can be seen in patients with septic melioidosis (Wiersinga et al., 2007b). Together this data indicates a protective role for TLR-mediated MyD88-dependent cell signaling, but highlights that dysregulation of TLR-mediated immune responses can result in pathogenesis and contribute to the development of septic melioidosis.

The IFNγ response, especially within the first 24 h of *B. pseudomallei* infection, has proven essential for resistance in mice, as demonstrated by the rapid death of IFNγ KO mice and mice treated with neutralizing monoclonal antibodies (mAb) against IFNγ (Santanirand et al., 1999; Haque et al., 2006a; Wiersinga et al., 2007c). These studies also showed the IFNγ-inducing cytokines IL-12, and to a lesser extent IL-18, are essential for resistance to infection (Santanirand et al., 1999; Haque et al., 2006a). The cellular source of IFNγ is primarily NK cells and bystander-activated $CD8^+$ T cells (Lertmemongkolchai et al., 2001), but these cells do not appear to be crucial in early protection suggesting extensive redundancy in the source of IFNγ (Haque et al., 2006a). In the absence of NK cells and T cells, up to 5% of the IFNγ response can still be detected and surprisingly this is still sufficient to initially control the infection. This compensation in IFNγ production has been attributed to non-lymphoid cells such as macrophages (Haque et al., 2006a).

IFNγ activated macrophages contribute to host defense by phagocytosis and killing of microbes via production of reactive oxygen intermediates (ROIs) and reactive nitrogen intermediates (RNIs), as well as cytokine and chemokine production, and antigen-presentation to T cells (Taylor et al., 2005). *In vivo* studies have provided evidence that macrophages are essential for early control of *B. pseudomallei* in both BALB/c and C57BL/6 mice (Breitbach et al., 2006). Although several immune evasion strategies have been described including inhibition of iNOS and TNFα production, upregulation of the suppressor of cytokine signaling 3 (SOCS3) and cytokine-inducible Src homology 2-containing protein (CIS), resulting in reduced IFNγ signaling (Utaisincharoen et al., 2001; Ekchariyawat et al., 2005). Furthermore there may be distinct roles for nitric oxide (NO) between mouse strains as BALB/c mice were more susceptible to early infection when NO was inhibited, whereas C57BL/6 $iNOS^{-/-}$ mice showed the same disease progression as wild-type controls (Breitbach et al., 2006, 2011).

Neutrophils or polymorphonuclear leukocytes (PMNLs) are the first cells to arrive at the site of infection and are potent effectors of innate immune responses, both by direct antimicrobial activity and through the induction of inflammatory responses via immuno-regulatory cytokine and chemokine production (Scapini et al., 2000; Segal, 2004; Martineau et al., 2007). Following intravenous (i.v.) challenge with *B. pseudomallei*, upregulation of the neutrophil chemokines CXCL1 (KC) and CXCL2 (MIP-2) can be detected in mouse spleen and liver tissues, coinciding with neutrophil infiltration to the site of infection (Barnes et al., 2001). *In vivo* depletion of these cells using neutralizing mAb, resulted in exacerbated disease mortality as mice were unable to control bacterial burdens compared to untreated mice, suggesting an essential role for neutrophils in early resistance to experimental pulmonary *B. pseudomallei* infection (Easton et al., 2007). Neutrophils are a major source of ROIs, and this is the principle microbicidal mechanism employed by these cells. There is evidence to suggest ROIs may contribute to resistance as mice lacking NADPH oxidase, an important enzyme in the generation of ROIs, were more susceptible to *B. pseudomallei* infection (Breitbach et al., 2006). Conversely, *in vitro* studies have demonstrated conflicting abilities of isolated human PMNLs to kill *B. pseudomallei* (Egan and Gordon, 1996; Chanchamroen et al., 2009).

Overall the literature involving neutrophils in human melioidosis is limited. Biopsies from melioidosis patients revealed necrotic lesions with extensive neutrophil infiltration and higher numbers of neutrophils have been detected in peripheral blood samples from melioidosis patients compared to healthy controls (Piggott and Hochholzer, 1970; Wong et al., 1995; Ramsay et al., 2002). In accordance with this, expression of the human neutrophil chemokine CXCL8 (IL-8) is induced following the infection of human cells with *B. pseudomallei* and serum levels of IL-8 may be an indicator of poor prognosis in human melioidosis (Friedland et al., 1992; Utaisincharoen et al., 2004; Hii et al., 2008). Defective neutrophil function has been linked to the increased susceptibility seen in diabetic patients, a prominent risk factor of melioidosis, highlighting the importance of these cells in resistance to disease (Chanchamroen et al., 2009). Furthermore, melioidosis has been reported in chronic granulomatous disease (CGD) patients, a condition characterized by defective NADPH oxidase (Dorman et al., 1998; Renella et al., 2006).

From these studies it is clear that early control of *B. pseudomallei* infection is paramount for survival, however the underlying mechanisms of innate protection remain unclear. Considering the important interactions between the innate and adaptive immune systems, further understanding of innate resistance will be beneficial to the development of therapeutic agents against *B. pseudomallei*.

T CELL-MEDIATED IMMUNITY

There is an extensive literature on the role of $CD4^+$ and $CD8^+$ T cells in immunity to other pathogenic bacteria (Coffman and Carty, 1986; Mosmann et al., 1986; Edelson and Unanue, 2000; Flynn and Chan, 2001), but to date such information in the context of melioidosis is limited. Studies using mice have demonstrated that T cell-mediated immunity (CMI) is necessary for protection against disease. Following i.v. *B. pseudomallei* infection in mice, delayed-type hypersensitivity (DTH) responses and lymphocyte proliferation to *B. pseudomallei* were detected, indicating the generation of CMI and memory cells (Barnes and Ketheesan, 2007). A study by Haque et al. found $RAG^{-/-}$ mice, which lack T and B cells, succumbed to infection via the i.p. route more rapidly than C57BL/6 wild-type mice. T cells isolated from infected C57BL/6 mice demonstrated Ag-specific IFNγ production in response to restimulation *in vitro*, suggesting primary infection with *B. pseudomallei* primes populations of memory $CD4^+$ and $CD8^+$ T cells. Further analysis of the T cell compartment by depletion of $CD4^+$ or $CD8^+$ T cells before intraperitoneal (i.p.) challenge and for 50 days post infection, showed mice lacking $CD4^+$ T cells died significantly earlier than controls (Haque et al., 2006a). Mice depleted of $CD8^+$ T cells also had a shorter survival time compared to controls, however the difference was not statistically significant suggesting $CD4^+$ T cells play a more important role in protection against *B. pseudomallei* infection (Haque et al., 2006a). Despite *in vitro* studies showing early $CD8^+$ T cell-derived IFNγ production due to bystander activation (Lertmemongkolchai et al., 2001), the contribution of T cells to resistance is essential only in the later stages of infection. This is demonstrated by the fact that $RAG^{-/-}$ mice were able to control early bacterial growth as efficiently as wild-type controls but still succumbed to infection after 14 days, consistent with the time course of activation of the adaptive immune response (Haque et al., 2006a).

There is increasing evidence of the induction of *B. pseudomallei*-reactive T cells in humans. Lymphocytes from patients who had recovered from clinical melioidosis and patients who were seropositive but had no clinical history of disease, were able to proliferate *in vitro* in response to *B. pseudomallei* (Ketheesan et al., 2002; Barnes et al., 2004; Govan and Ketheesan, 2004). The proliferative response was significantly higher in these patients when compared to seronegative healthy controls. Further analysis of these lymphocytes showed the $CD4^+$ and $CD8^+$ T cells were activated and capable of producing antigenic-specific IFNγ (Ketheesan et al., 2002; Barnes et al., 2004). The percentage of each T cell subtype and IFNγ production was significantly higher in recovered patients compared to controls suggesting the presence of *B. pseudomallei*-reactive memory T cells (Ketheesan et al., 2002; Barnes et al., 2004). In contrast patients with acute melioidosis are known to be lymphocytopenic with low numbers of circulating $CD4^+$ and $CD8^+$ T cells, possibly compromising the development of specific immunity (Tanphaichitra and Srimuang, 1984; Ramsay et al., 2002).

A recent study on Thai patients who had recovered from melioidosis, identified IFNγ-producing $CD4^+$ and $CD8^+$ T cells which recognized LolC, OppA, and PotF, which are members of the *B. pseudomallei* ATP-binding cassette (ABC) transporter family and are known T cell immunogens in mice (Tippayawat et al., 2009). These antigen-specific T cells were responsible for the majority of the total IFNγ generated in the culture, as T cell depletion significantly reduced the IFNγ ELISPOT response. A strong correlation between IFNγ and granzyme B was also observed by ELISPOT, indicating cytotoxic $CD8^+$ T cells are primed in response to *B. pseudomallei* (Tippayawat et al., 2009). Further characterization of these memory T cells revealed the majority were terminally differentiated T effector memory cells (Tippayawat et al., 2009). These data suggest memory T cells are capable of recognizing and rapidly responding to *B. pseudomallei* antigens, but do not prove this response is protective. However, seropositive individuals with no clinical history of disease showed a higher proliferative and IFNγ response than those who had recovered from clinical melioidosis (Barnes et al., 2004). Together these studies indicate that a strong T cell response may be essential for resolution of clinical melioidosis and protection against disease progression (Barnes et al., 2004).

The importance of $CD4^+$ T cells in other pulmonary infections is highlighted by the human immuno-deficiency virus (HIV) epidemic. HIV patients are more susceptible to infection from opportunistic lung pathogens such as *M. tuberculosis*, *Pneumocystis carinii*, and *Streptococcus pneumoniae*, and this increased risk is inversely proportional to the circulating $CD4^+$ T cell count (Phair et al., 1990; Hoover et al., 1993; Gilks et al., 1996; Dworkin et al., 2001; Sharma et al., 2005). Surprisingly, the loss of $CD4^+$ T cells during HIV infection does not appear to be a risk factor for melioidosis (Chierakul et al., 2005), questioning the importance of these cells in protection in human disease despite the clear evidence of their presence in exposed individuals and their role in protection in mouse models. It should also be noted that whilst current literature indicates a role for the Th1 arm of the adaptive immune response, at present the function of other T cell subsets such as T reg and Th17 cells during *B. pseudomallei* infection are unknown.

ANTIBODY-MEDIATED IMMUNITY

In endemic areas a large proportion of the population are seropositive for antibodies against *B. pseudomallei*, though the functions of these antibodies and their roles in protection are unclear (Cheng et al., 2008). High levels of *B. pseudomallei*-specific IgG, IgM, and IgA antibodies have been detected in sera from melioidosis patients, which remained elevated for the duration of infection. Further analysis of the IgG isotype revealed IgG1 to be the predominant subclass produced, indicative of a Th1 response. Yet eradication of *B. pseudomallei* was not evident in these patients as relapse occurred (Vasu et al., 2003). This apparent lack of protective humoral responses during primary infection is also reflected in studies where μMT mice lacking B cells were as susceptible to *B. pseudomallei* infection as wild-type mice (Haque et al., 2006a). Given that *B. pseudomallei* is a facultative intracellular pathogen which can spread from cell-to-cell, it may be that the bacteria is protected from antibody killing by remaining inside host cells. The elevated antibody responses observed in melioidosis patients could be directed against extracellular bacteria before they are taken up into host cells. Therefore the generation of these antibodies is ineffective at preventing disease.

In contrast to the suggestions that antibodies play no role in protection, IgG antibodies to *B. pseudomallei* LPS were

significantly higher in patients who survived melioidosis compared to those who died, and also higher in patients with non-septic melioidosis compared to septic patients (Charuchaimontri et al., 1999). This indicates that antibodies against LPS may be protective against disease. In addition, a number of *in vivo* studies in mice have demonstrated a protective humoral immune response by passive transfer of antibodies to *B. pseudomallei* components, such as LPS, capsular polysaccharide (CPS), and flagellin (Brett and Woods, 1996; Ho et al., 1997; Jones et al., 2002; Nelson et al., 2004). In these studies, protection was incomplete and mice eventually succumbed to infection (Jones et al., 2002). Antibodies against LPS appear to be protective by promoting opsonization-induced phagocytic killing of bacteria *in vitro* (Ho et al., 1997). It is also possible that B cells are required for other functions. For example, it is well known that B cells are efficient at presenting soluble antigens via MHC class II, resulting in the further activation of $CD4^+$ T cells (Janeway et al., 2008). There is evidence that B cells can amplify the IFNγ response by T cells via a TNFα-mediated mechanism during infection (Menard et al., 2007). This could be important in *B. pseudomallei* infection as both these cytokines are required for protection (Santanirand et al., 1997, 1999). Furthermore, B cell-deficient mice infected with lymphocytic choriomeningitis virus (LCMV) experienced a loss of $CD4^+$ T cell memory and were subsequently unable to resolve the chronic infection (Thomsen et al., 1996). At present the interactions of B and T cells during *B. pseudomallei* infection are not known, and it is possible that these cells could contribute to vaccine-mediated immunity or modulation of chronic infections in addition to antibody production. Hence there is conflicting evidence surrounding the role of B cells and antibodies in resistance to primary *B. pseudomallei* infection, and further studies are necessary to resolve this debate.

IS A VACCINE AGAINST *B. PSEUDOMALLEI* POSSIBLE?

Observations of the epidemiology of human melioidosis can provide important clues to guide vaccination strategies and flag some of the potential obstacles that may arise in development of an effective product. In endemic rural areas a large proportion of the population may be exposed to *B. pseudomallei* and will test seropositive for antibodies against the bacteria. For example in NE Thailand, 80% of the population have seroconverted by the age of 4 years (Kanaphun et al., 1993). Yet in spite of constant exposure, only a relatively small fraction of the population develops active disease, mostly if they have underlying risk factors which compromise their immune system, the most prominent of these being diabetes mellitus (Chaowagul et al., 1989; Suputtamongkol et al., 1999; Currie et al., 2000, 2004; Chrispal et al., 2010). A study of individuals with no history of disease from an endemic region of Thailand found a significant correlation between increasing antibody titer and specific IFNγ production by T cells (Tippayawat et al., 2009). Together these factors suggest that those exposed to *B. pseudomallei* and do not develop disease have acquired some form of protective immunity, and this provides grounding for the theory that vaccination against melioidosis is feasible. In further support of this, is the observation that specific IgG antibodies to *B. pseudomallei* LPS were found to be significantly higher in patients who survived melioidosis compared to those who died from disease, and also in patients with non-septic melioidosis compared to septic patients (Charuchaimontri et al., 1999).

On the other hand, there is data to be considered which imply the development of a vaccine against *B. pseudomallei* may be intrinsically difficult. Whilst in Thailand the seroconversion rate is very high, the percentages of seropositive individuals can vary greatly between regions and subpopulations in other endemic areas (Cheng et al., 2008; Adler et al., 2009). For example in Northern Australia just 5% of the population are seropositive and there is no correlation between antibody and IFNγ production as there is in Thailand (Ashdown and Guard, 1984; Lazzaroni et al., 2008). Furthermore, whilst high levels of specific antibody can be detected in sera from melioidosis patients, it is important to note that recovered melioidosis patients are not protected against further episodes of disease (Kanaphun et al., 1993; Vasu et al., 2003; White, 2003; Maharjan et al., 2005). This implies that an effective vaccine will need to work more efficiently and/or in a different manner than the naturally occurring immune response observed in these individuals. However, whilst development of sterilizing immunity by vaccination is the ultimate goal, even a partially effective vaccine may provide clinical benefit if used in combination with other types of intervention to control disease. We have recently shown that combining prophylactic vaccination plus a generic immunostimulant around the time of exposure decreases the risk of sepsis and delays mortality (Easton et al., 2011). It might also be possible to use vaccines in combination with antibiotics. The risk of death in acute melioidosis is strongly related to the presence or absence of bacteremia upon presentation. Furthermore, 50% of patient mortality occurs within 48 h of presentation in a hospital and many individuals die before antibiotic therapy can start. Therefore development of a vaccine which delays the onset of bacteremia and acute disease could extend the window of opportunity for antibiotic treatment and still be of significant clinical benefit.

ANIMAL MODELS OF MELIOIDOSIS FOR VACCINE RESEARCH

Animal models of infection are an essential component of any vaccine development pipeline and are used for defining immune responses that mediate protection, preclinical testing of potential vaccine candidates and generating immune correlates of protection which can then be applied to Phase I and later studies in humans. *B. pseudomallei* is not host specific and can infect a broad range of animal species such as cattle, horses, rodents, sheep, pigs, cats, dogs, goats, camels, dolphins, kangaroos, koalas, deer, and water buffalo (Titball et al., 2008). Due to issues of cost, logistics, and availability of immunological reagents, experimental melioidosis has been primarily studied in rodents, and to date three models of infection have been characterized. Syrian hamsters are highly susceptible to *B. pseudomallei* infection with an LD_{50} (dose required for 50% mortality) of <10 CFU via the i.p route (Jones et al., 1997). This is an extremely acute disease model with most deaths occurring within 48 h post challenge. Another acute model of infection has been developed in diabetic rats. Only infant diabetic rats up to 4 weeks old are susceptible to *B. pseudomallei*, with LD_{50} doses reported to be $<2 \times 10^4$ CFU via the i.p. route. However, the mouse model of infection with *B. pseudomallei* is the most extensively studied and best characterized, and has proved

invaluable to our understanding of the immunopathogenesis of melioidosis.

Currently, there is a highly susceptible model established in the BALB/c mouse representing acute human melioidosis, and a more resistant C57BL/6 mouse model which mimics a chronic human infection (Leakey et al., 1998; Liu et al., 2002). In both cases the intranasal (i.n.) or inhalation (aerosol) route is the most susceptible compared to i.p. or subcutaneous (s.c.), with a typical LD_{50} dose of 5–100 CFU required for acute disease in BALB/c mice (Titball et al., 2008; Lever et al., 2009). C57BL/6 mice consistently show 10- to 100-fold greater resistance to *B. pseudomallei* compared to BALB/c mice, regardless of the route of infection (Leakey et al., 1998; Hoppe et al., 1999; Liu et al., 2002; Tan et al., 2008; Titball et al., 2008). Infection with *B. pseudomallei* in BALB/c mice is characterized by rapid, highly elevated IFNγ, TNFα, IL-1β, and IL-6 production, accompanied by high bacterial burdens in the spleen, lungs, and liver and development of overwhelming bacteremia within 96 h of infection (Leakey et al., 1998; Hoppe et al., 1999; Ulett et al., 2000a; Liu et al., 2002). In contrast C57BL/6 mice demonstrate a slower pro-inflammatory cytokine response of lower magnitude with IFNγ production persisting throughout the infection (Ulett et al., 2000a,b). These mice have very low organ burdens and no detectable bacteria in the blood at 3 days post infection, though still eventually succumb to infection after 2–6 weeks (Leakey et al., 1998). Thus it has been suggested the control and regulation of IFNγ production, and the early down-regulation of other pro-inflammatory cytokines allow C57BL/6 mice to balance the protective cell-mediated immune response conferring resistance, with the development of immunopathology (Ulett et al., 2000a,b; Liu et al., 2002). However the precise genetic differences which control resistance to *B. pseudomallei* in these two mouse strains have not been determined.

Patients with melioidosis have elevated serum TNFα, IL-1β, and IL-6 levels, and increasing concentrations of these cytokines correlate with disease severity and the onset of fatal sepsis (Friedland et al., 1992; Suputtamongkol et al., 1992; Wiersinga et al., 2007a). In addition, patients with severe bacteremic melioidosis have very high serum levels of IFNγ, along with elevated levels of the IFNγ-inducing cytokines IL-12, IL-18, and IL-15 (Brown et al., 1991; Lauw et al., 1999), this further demonstrates the parallels between human melioidosis and mouse models. High serum levels of IL-10 are detected in melioidosis patients, which in conjunction with IL-6 is considered a prognostic indicator of mortality (Simpson et al., 2000; Wiersinga et al., 2007a). Therefore, in some respects, the mouse is a good model of acute melioidosis in humans, and therefore will hopefully predict vaccine efficacy in non-human primates and humans.

Large animal models of experimental melioidosis are rare, yet there are studies which have assessed the susceptibility of various non-human primate species to naturally occurring infection (Trakulsomboon et al., 1994; Sprague and Neubauer, 2004). Many of the symptoms observed during infection in these animals are also prominent in human disease, and the further development of such models may be central to the development of vaccines in the future (Sprague and Neubauer, 2004; Titball et al., 2008).

Finally, recent studies have considered infection models which avoid the use of mammals. Both phagocytic ameba (*Dictyostelium discoideum*) and wax moth larvae (*Galleria mellonella*) models have demonstrated the ability to discriminate between different isolates and genetic mutants of *B. pseudomallei* depending on their virulence (Hasselbring et al., 2011; Wand et al., 2011). Although such models cannot be used to directly assess the protective efficacy of defined experimental vaccines, they do provide novel and inexpensive, high-throughput screening systems with which to determine future virulence factors and thus potential vaccine candidates.

CURRENT VACCINE STRATEGIES

LIVE ATTENUATED VACCINES

Live attenuated (LA) vaccines, such as BCG, measles, mumps, and rubella vaccines, induce strong immunity in the host and often only one immunizing dose is required to elicit protective long-lasting protective immunity. Since LA vaccines replicate *in vivo* before being cleared by the host, this type of vaccine can strongly stimulate both the humoral and cell-mediated arms of the immune system, making them some of the most effective vaccines against human pathogens (Pirofski and Casadevall, 1998; Liljeqvist and Ståhl, 1999; Titball, 2008). Yet there are safety concerns about the development of LA vaccines, involving the possibility of reversion to virulent wild-type strains which can cause disease or whether they are safe for immunocompromised patients, a growing population in society today (Pirofski and Casadevall, 1998). For example the measles vaccine is currently not given to children with defects in CMI (with the exception of asymptomatic HIV patients) and there have been several reported cases of disseminated infection following vaccination in the past (Mitus et al., 1962; Monafo et al., 1994; Pirofski and Casadevall, 1998). Reports have also demonstrated similar results following BCG vaccination, and hence this vaccine is not recommended for use in patients with impaired immunity (Pirofski and Casadevall, 1998). For example, with the now acknowledged risks of giving BCG to HIV infected children, new LA TB vaccines will need to show significantly less virulence than BCG in immunocompromised mice before being accepted into Phase I trials.

In the case of *B. pseudomallei*, a number of naturally attenuated or genetically altered bacteria have been tested for protective efficacy, starting with pioneering studies by Dannenberg and Scott (1958a,b, 1960). More recently, Stevens et al. (2004) used an attenuated *B. pseudomallei bip D* mutant, which has a dysfunctional TTSS, to immunize mice. Partial protection was seen in vaccinated mice after challenge with virulent wild-type *B. pseudomallei*, but immunization with the purified Bip D protein was not protective (Stevens et al., 2004; Druar et al., 2008). An attenuated acapsular mutant of *B. pseudomallei* was considered a potential vaccination candidate, however i.p. immunization did not protect mice against subsequent challenge with virulent *B. pseudomallei* (Atkins et al., 2002b). *B. pseudomallei purN*$^-$ and *purM*$^-$ mutants, which have defects in the purine biosynthesis pathway, important for RNA and DNA synthesis and consequently bacterial replication have also been tested (Pilatz et al., 2006; Breitbach et al., 2008). These were able to protect BALB/c mice against acute challenge with virulent *B. pseudomallei*, however immunization could not prevent the chronic stages of melioidosis (Breitbach et al., 2008). Protection was incomplete and when any surviving mice were examined,

abscesses were observed and bacteria could be isolated from multiple organs (Breitbach et al., 2008). It should be noted that at present there is no vaccine model which has shown protection against chronic melioidosis.

Atkins et al. (2002a) identified a *B. pseudomallei ilvI* mutant, termed 2D2. The *ilvI* gene encodes part of an enzyme required for the biosynthesis of branched chain amino acids (leucine, isoleucine, and valine), and interruption in this gene renders the bacteria auxotrophic for these essential amino acids. Hence, *B. pseudomallei* 2D2 was highly attenuated in mice and effectively cleared from multiple organs after 30 days (Atkins et al., 2002a). Immunization via the i.p. route protected susceptible BALB/c mice from subsequent challenge with virulent *B. pseudomallei* strain 576, with a significant reduction in bacterial loads in the spleen compared to unvaccinated controls (Atkins et al., 2002a; Haque et al., 2006b). However protection was incomplete and mice eventually succumbed to infection around day 50 post challenge (Haque et al., 2006b). Vaccinated mice were also protected against challenge with the heterologous strain *B. pseudomallei* BRI, yet protection was specific to *B. pseudomallei* as when challenged with the facultative intracellular human pathogen *F. tularensis* no protection was seen (Atkins et al., 2002a). *In vitro* stimulation of splenocytes from 2D2-immunized mice showed increased T cell proliferation and IFNγ production in response to irradiated *B. pseudomallei* 576 and TTSS antigens Bop E and Bip D, compared to controls, indicating 2D2 can efficiently prime T cells (Haque et al., 2006b). Adoptive transfer of T cells from 2D2-immunized mice into severe combined immune deficient (SCID) mice, which have no T or B cells, was able to protect these highly susceptible mice against *B. pseudomallei* infection (Haque et al., 2006b). The addition of immune sera to T cell transfer further enhanced the protection, indicating that 2D2 elicits a humoral and cell-mediated immune response (Haque, unpublished observation). Antibody depletion experiments in 2D2-immunized mice demonstrated the importance of $CD4^+$ T cells, rather than $CD8^+$ T cells, in conferring the protection seen in this mouse model (Haque et al., 2006b).

The concerns over safety of LA vaccines and potential latency associated with this bacterium make it unlikely the *B. pseudomallei* mutants discussed above will progress further in vaccine development. However there is evidence to suggest LA *M. tuberculosis* vaccines, such as MTBVAC01 which has disruptions in the associated-virulence regulator gene *phoP*, will enter clinical trials in the next few years (Verreck et al., 2009; Kaufmann et al., 2010). Thus there may be hope for LA *B. pseudomallei* vaccine development in the future if additional mutations were introduced which limit the potential of the bacterium to persist in the host. Nonetheless, an alternative and more feasible approach is the development of a vaccine using dead *B. pseudomallei*, otherwise known as killed whole cell (KWC) vaccines.

KILLED WHOLE CELL VACCINES

Killed whole cell vaccines cannot replicate and are therefore non-infectious, and this type of vaccine has been licensed for human use against bacteria such as *Bacillus anthracis*, *Vibrio cholerae*, *Bordetella pertussis*, and *Yersinia pestis* (Pirofski and Casadevall, 1998). However, whilst this type of vaccine is undoubtedly safer compared to live vaccines, the protective immunity induced is weaker, possibly due to lack of CMI responses or the destruction of antigens during the killing process (Ivanoff et al., 1994; Griffin et al., 2007; Titball, 2008). On the other hand, KWC vaccines can induce strong antibody-specific responses which can mediate protection: for example the pertussis vaccines generate neutralizing antibodies against the pertussis toxin and this is a key element in their protective efficacy (Hewlett, 1997). Hence KWC vaccines are generally more protective against extracellular compared to intracellular bacteria.

There are concerns associated with KWC vaccines as well. In most cases protection requires multiple immunization doses, and there are clear risks of reactogenicity and adverse effects in the recipient. This has been observed with the current KWC *Y. pestis* vaccine, as well as a *B. pertussis* vaccine (Pw) which has now been replaced with a safer but less immunogenic acellular vaccine (Pa; Higgins et al., 2006; Williamson, 2009). Interestingly the route of vaccination can influence the reactogenicity of KWC vaccines. Parenteral immunization with a KWC vaccine against cholera or typhoid induces adverse reactions in the recipient, however if these vaccines are delivered orally they are well tolerated and much less reactogenic (Ivanoff et al., 1994; Hill et al., 2006).

The few studies which have evaluated this type of vaccine regimen against experimental melioidosis demonstrate conflicting results. Following vaccination of BALB/c mice with multiple low doses of heat-killed *B. pseudomallei* (HkBps) via the s.c. route, significant increases in serum IgG2a and IgG1 were seen compared to control mice, yet only a low level of proliferation was detected following stimulation of splenocytes with antigen (Barnes and Ketheesan, 2007). In accordance with this observation, barely detectable amounts of IFNγ were detected via ELISPOT analysis although significantly enhanced levels of IL-10 were observed in HkBps vaccinated mice compared to controls (Barnes and Ketheesan, 2007). When challenged via the i.v. route with virulent *B. pseudomallei*, vaccinated mice were not protected compared to control mice, showing similar bacterial loads in the spleen and 100% mortality before day 5 post challenge (Barnes and Ketheesan, 2007). On the contrary to this data, one of the first melioidosis vaccine studies demonstrated complete protection for 7 days post challenge using HkBps and partially purified toxic material to vaccinate mice (Razak et al., 1986). Another publication used high doses of HkBps (more consistent with that of other killed vaccines such as plague and typhoid) to vaccinate BALB/c mice via the i.p. route and demonstrated significant protection against subsequent i.p. challenge with homologous and heterologous virulent *B. pseudomallei* strains, with 80–100% of mice alive after 3 weeks post challenge (Sarkar-Tyson et al., 2009). Due to the threat of infection via inhalation in both a natural and biological warfare situation, protection against aerosol challenge was also evaluated. Vaccinated mice were protected against aerosol challenge, as evidenced by a delayed time to death compared to control mice, but the window of protection was greatly reduced compared to i.p. challenge. Therefore the protection was only partial and surviving mice all had heavy bacterial loads detected in the spleen. More recently, Henderson et al. (2011) vaccinated mice i.n. with HkBps in combination with cationic liposomes complexed with non-coding plasmid DNA (CLDC) as an adjuvant,

and demonstrated significant protection against pulmonary challenge up to day 40 post challenge. Whilst there was no evaluation of the immune response in vaccinated mice in these publications, these data clearly demonstrate that vaccination with HkBps can be protective though the route of immunization and challenge can affect the outcome.

Dendritic cells (DCs) play a key role in the generation of adaptive immune responses during infection via antigen-presentation and activation of T cells. Depending on the nature of the microbial stimulus DCs can direct the development of polarized T cell responses to either a Th1 or Th2 phenotype (Janeway et al., 2008). Accordingly these cells have been utilized as a vaccine-delivery vector to generate CMI responses to *B. pseudomallei* (Healey et al., 2005; Elvin et al., 2006). Healey et al. employed a "prime–boost" vaccination regimen, the concept of which is to prime with an antigen delivered by one method and then boost with the same antigen given via a different vector/adjuvant, and in doing so induce high quality immune responses by different T cell subsets (Liljeqvist and Ståhl, 1999; Lu, 2009). This has become a common approach for vaccine development against the most challenging diseases such as HIV, malaria, and tuberculosis (Cai et al., 2006; Magalhaes et al., 2008; Lu, 2009; Sander et al., 2009; Kaufmann et al., 2010). In this case, BALB/c mice were primed with purified DCs pulsed with HkBps and then after 28 days, mice were boosted with HkBps administered with adjuvant. Following vaccination, small but significant increases in antigen-specific IgG antibodies were detected in the serum. However, strong CMI responses were induced as determined by proliferation and IFNγ production by splenocytes from immunized mice in response to restimulation with HkBps. Vaccinated mice were protected against challenge with virulent *B. pseudomallei* with 60% survival at day 35, however bacteria were detected in tissues of surviving mice suggesting that sterilizing immunity was not achieved (Healey et al., 2005). Whilst this vaccination regimen enhanced CMI responses, it induced relatively low antibody production. A further study however, found adding CpG ODN to the DC culture conditions increased antibody production and correlated with a significant increase in survival after challenge (Elvin et al., 2006). This data highlights the need for vaccines to incorporate targets of both humoral and CMI responses.

SUBUNIT VACCINES

The focus of new vaccine development in recent years has largely been directed toward the use of discrete bacterial components known as subunits. Indeed there are several subunit vaccines available for human use, such as toxoid vaccines (inactivated bacterial toxins) against diphtheria and tetanus, and CPS vaccines against meningococcal or pneumococcal diseases (Pirofski and Casadevall, 1998; Fry et al., 2002). In accordance with this, a number of subunit vaccine candidates have been evaluated for use against *B. pseudomallei* and are summarized in **Table 1**. The subunits purified from pathogenic organisms are generally safe to use providing the extraction procedure or detoxifying method can separate them from potentially reactogenic material (Liljeqvist and Ståhl, 1999). However, the production of such vaccines often requires the cultivation of pathogenic organisms on a large scale which can be costly and hazardous (Liljeqvist and Ståhl, 1999). An alternative to this method is the generation of recombinant subunits, in which the gene encoding the subunit is isolated from the host organism and transferred into a different organism which is non-pathogenic,

Table 1 | Subunit vaccine candidates tested to date.

Antigen	Composition	Protection	References
LPS	Lipopolysaccharide	80% Survival at day 14 after 4,300 MLD challenge	Nelson et al. (2004)
CPS	Polysaccharide	40% Survival at day 14 after 4,300 MLD challenge	Nelson et al. (2004)
Flagellin	Naked DNA	80–90% Survival at day 14 after up to 100 LD_{50} challenge	Chen et al. (2006a,b), Brett et al. (1994)
Flagellin	Protein	50% Survival at day 7 after up to 100 LD_{50} challenge	Chen et al. (2006a), Brett et al. (1994)
Flagellin-O-antigen conjugate	Protein–polysaccharide	Passive transfer of sera protected 40% of diabetic rats from 400 LD_{50} challenge at day 8	Brett and Woods (1996)
BipB, BipC, BipD	Protein	None at day 5 after 30 LD_{50} challenge	Druar et al. (2008)
Omp85	Protein	70% Survival at day 15 after 10 × LD_{50} challenge	Su et al. (2010)
EF-TU	Protein	Reduced colonization after aerosol challenge with 1 × LD_{50} *B. thailandensis*	Nieves et al. (2010)
BPSL2522 (Omp3)	Protein	50% Survival at day 14 after 10 × LD_{50} challenge	Hara et al. (2009)
BPSL2765 (Omp7)	Protein	75% Survival at day 14 after 10 × LD_{50} challenge	Hara et al. (2009)
LolC	Protein	80% Survival at day 14 after 153 MLD challenge i.p.	Harland et al. (2007b)

The antigens listed were purified from B. pseudomallei (LPS and CPS), or produced as recombinant proteins in E. coli and then purified. The ability of these antigens to induce protective immunity in mice toward an intraperitoneal (i.p.) challenge (aerosol challenge for EF-Tu) with B. pseudomallei (B. thailandensis for EF-Tu) is summarized as the proportion of surviving mice on the day indicated post challenge. Protection studies with the flagellin-O-antigen conjugate were carried out after the passive transfer of sera into diabetic rats which were then challenged with B. pseudomallei. Lethal dose 50% (LD_{50}) and median lethal dose (MLD) are broadly equivalent.

such as *E. coli*. The recombinant subunit is then produced by the heterologous host and can be designed to be delivered as a purified immunogen, or as purified DNA encoding the immunogen (Liljeqvist and Ståhl, 1999).

Purified CPS have been investigated as subunit vaccines and have demonstrated protection against several pathogens, however this approach does have some limitations. CPS are type II antigens, meaning they stimulate antibody production by B cells independently of MHC Class II-restricted T cell help, hence a predominantly IgM antibody response is induced with suboptimal memory (Pirofski and Casadevall, 1998). In the case of licensed CPS vaccines, booster immunizations are often required to maintain antibody titers (Jones, 2005). Conjugation of CPS to immunogenic proteins (such as tetanus toxoid) overcomes these problems by providing potent T cell help and has revolutionized the prevention of *Haemophilus influenza* type B, pneumococcal and meningococcal infections among others (Danzig, 2004; Bernatoniene and Finn, 2005; Eskola, 2010).

Administration of purified LPS has also been explored as a vaccine. In an experimental model of *K. pneumonia* infection, vaccination with purified LPS protected mice against subsequent challenge (Clements et al., 2008). This has also been seen with *Brucella melitensis* and *P. aeruginosa* (Preston et al., 1997; Bhattacharjee et al., 2006). However, as with CPS vaccines, lack of CMI induction by LPS vaccines can result in limited protection against intracellular bacteria such as *Francisella tularensis* (Fulop et al., 2001).

Following the discovery that antibodies to *B. pseudomallei* LPS were more prominent in patients who survived melioidosis compared to those who died (Charuchaimontri et al., 1999), the use of monoclonal antibodies against LPS and CPS as potential vaccines were evaluated in BALB/c mice (Jones et al., 2002). Following passive immunization via the i.v. route, mice showed a significantly delayed time to death yet still succumbed to infection, demonstrating incomplete protection against the subsequent i.p. challenge with virulent *B. pseudomallei* (Jones et al., 2002). Another study by Nelson et al. (2004) evaluated these two surface polysaccharides as subunit vaccines and conducted active immunization experiments in BALB/c mice. Mice vaccinated i.p. with LPS developed strong IgM and IgG3 antibody responses, whilst CPS induced a predominately IgG2b antibody response and minimal IgM and IgG3 responses (Nelson et al., 2004). Protection against *B. pseudomallei* challenge was demonstrated following vaccination with both antigens, however this was only the case against i.p. challenge as when mice were challenged via the aerosol route no protection was observed (Nelson et al., 2004). The addition of adjuvant enhanced the protection seen with CPS but this was not the case with LPS (Nelson et al., 2004). As with passive immunization, the protection afforded by this method was again only partial and mice eventually succumbed to infection (Nelson et al., 2004). A recent study used HkBps mutants which had disruptions in the type I O-PS (capsule), type II O-PS (LPS), type III O-PS, and type IV O-PS surface polysaccharide gene clusters (Sarkar-Tyson et al., 2007). Immunization of BALB/c mice with all four HkBps mutant strains resulted in delayed time to death compared to naive controls when challenged i.p. with virulent *B. pseudomallei*, however the protection afforded by each strain varied, possibly highlighting the importance of each polysaccharide in protection (Sarkar-Tyson et al., 2007).

The related bacterium *B. thailandensis* which is considered to be avirulent in humans can often be isolated from soil in endemic areas of Thailand (Smith et al., 1997). Studies have shown the LPS structure of this organism to be similar to that of *B. pseudomallei*, yet it elicits stronger immune responses from human and murine macrophage cell lines *in vitro* compared to its virulent counterpart (Anuntagool et al., 1998; Brett et al., 2003; Qazi et al., 2008; Novem et al., 2009; Ngugi et al., 2010). Recently LPS isolated from *B. thailandensis* was evaluated as a potential vaccine candidate. Immunized mice were protected from subsequent challenge with *B. pseudomallei* with 50% survival at day 35, however bacteria could be detected in the tissues of these surviving mice suggesting sterilizing immunity was not achieved and the infection would ultimately prove fatal (Ngugi et al., 2010). The use of *B. thailandensis* as a vaccine against melioidosis has not been widely explored to date but there are reports of live and heat-killed *B. thailandensis* also providing protection against *B. pseudomallei* infection (Iliukhin et al., 2002; Sarkar-Tyson et al., 2009). Considering the financial and safety benefits of working with a Containment Level 2 organism this is an area of melioidosis vaccine research which should continue to be explored.

Antibodies against other known *B. pseudomallei* virulence factors such as flagella have also been investigated as vaccine candidates. Anti-flagellin antibodies are known to reduce bacterial motility and have shown some passive protection against infection in diabetic rats (Brett et al., 1994). A subsequent publication by the same authors attempted to enhance the immunological repertoire of the vaccine recipient by conjugating flagellin proteins to the O-PS moiety of LPS isolated from the same strain, thereby developing the first conjugate vaccine for this infection (Brett and Woods, 1996). Passive immunization with the flagellin-polysaccharide conjugate still only provided partial protection in diabetic rats (Brett and Woods, 1996). To date conjugate vaccines against *B. pseudomallei* using better defined protein carriers such as those found in pneumococcal vaccines have not been reported.

The limited success of these vaccine studies, which universally resulted in only partial protection, is thought to be due to the lack of T cell stimulation afforded by these strategies. Thus, some attempts to resolve these problems have involved the evaluation of DNA vaccines. These consist of small circular bacterial DNA (plasmid) expression vectors, which encode candidate vaccine antigens under the control of strong viral promoters which are recognized by the host (Liljeqvist and Ståhl, 1999). Following plasmid DNA vaccination, the antigen is expressed by the host cells and delivered to antigen-presenting cells, resulting in strong T CMI (Plotkin, 2009). A significant potential advantage of DNA vaccines is the ability to induce $CD8^+$ T cell responses via MHC class I presentation, which is important for protection against other intracellular pathogens (Kaufmann et al., 2010). Parenteral vaccinations via injection or gene gun delivery are the most common modes of DNA vaccine delivery. However this is less advantageous in targeting the mucosal surfaces. Furthermore, whilst DNA vaccines have achieved success in most animal models, only modest immunogenicity has been observed in higher primates and human clinical trials posing an ongoing challenge of formulating DNA vaccines

for use in humans (Coban et al., 2008). In attempts to improve the efficacy of DNA vaccines the genetic manipulation of live vectors, primarily bacteria or viruses, expressing pathogen-specific DNA has also been investigated. A prime example of this technique can be seen in *M. tuberculosis* vaccines, where a number of candidates have been generated using recombinant, replication-deficient vaccinia virus or adenoviruses which express the mycobacterial Ag85A (termed MVA85A and AdAg85A respectively; McShane et al., 2004; Santosuosso et al., 2006; Radosevic et al., 2007; Sander et al., 2009). These can induce strong Th1 immunity, including $CD8^+$ T cell responses, and are being evaluated in clinical trials for further development (Kaufmann et al., 2010). A limitation of these vaccines however, is reduced efficacy following previous exposure to the vector, such as previous vaccination with vaccinia or natural exposure to cross-reacting strains of adenovirus (reviewed in Bangari and Mittal, 2006).

DNA vaccines have also been investigated to a limited degree in melioidosis. Chen et al. evaluated a DNA vaccine encoding the *fliC* gene and demonstrated protection against *B. pseudomallei* infection in BALB/c mice. Intramuscular (i.m.) vaccination with this construct elicited both humoral and cell-mediated immune responses, demonstrated by increased IgG production and enhanced proliferation of splenocytes in response to *B. pseudomallei* flagellin (Chen et al., 2006b). IgG2a was the dominant antibody subclass detected, and a higher number of IFNγ-secreting cells were found in the spleens of immunized mice, indicating the induction of a Th1 phenotype (Chen et al., 2006b). Immunized mice showed better control of bacterial burden in organs and increased survival after i.v. challenge compared to controls (Chen et al., 2006b). Addition of the immunoadjuvant, cytosine preceding a guanosine motif oligodeoxynucleotide (CpG ODN), to the plasmid DNA encoding flagellin further enhanced the protective effects elicited by this vaccination strategy (Chen et al., 2006a).

Purified proteins have had some success as potential vaccine candidates against other bioterrorism agents. For example, *Y. pestis* secretes a number of virulence factors which include Fraction 1 (F1) and V (virulence) proteins. These have been formulated together in recombinant subunit vaccines, and can induce protective immunity against plague (Williamson, 2009). However the use of single proteins or peptides as vaccines has had limited success due to restricted immunogenicity within the host, and often must be delivered with adjuvants to elicit protection. Furthermore, this approach requires the identification of virulence determinants or immunogenic epitopes as potential vaccine candidates, which in the case of intracellular bacteria can prove challenging (Titball, 2008). Nonetheless, in an attempt to identify novel vaccine antigens for *B. pseudomallei*, Harland et al. (2007b) evaluated proteins of the ABC systems. ABC systems are widespread among living organisms and are thought to have roles in nutrient uptake and survival, as well as drug resistance and virulence (Garmory and Titball, 2004). Comprising one of the largest protein families in prokaryotes, ABC systems are characterized by a highly conserved ATPase domain which binds ATP and provides energy for the conserved ABC proteins to import and export a wide variety of substrates across the membrane (Garmory and Titball, 2004). Given the location of the ABC transporters it is possible that some protein components of the system are exposed to the immune system during infection, making them attractive as potential vaccine candidates. Three *B. pseudomallei* ABC transporter proteins, namely LolC, PotF, and OppA, were selected as candidate vaccine antigens following annotation of the reference strain *B. pseudomallei* K96423 (Harland et al., 2007a,b). Immunization of BALB/c mice with each protein mixed with adjuvant generated protein-specific IgG responses which were biased toward the IgG2a isotype and therefore a Th1 phenotype (Harland et al., 2007b). In addition, restimulation assays using T cells from spleens of immunized mice, detected protein-specific IFNγ production in culture supernatants (Harland et al., 2007b).

This work indicated that all three proteins were capable of inducing both antigen-specific humoral and CMI responses. When mice were challenged i.p. with virulent *B. pseudomallei* K96423, PotF, and LolC vaccinated mice were significantly protected compared to naive mice, whilst vaccination with OppA showed no protection (Harland et al., 2007b). LolC was the most protective protein and when combined with immune stimulating complexes (ISCOMS) adjuvant in a complex with CpG ODN, the protection afforded by this vaccine was enhanced (Harland et al., 2007b). Mice immunized with LolC were also significantly protected against challenge with the heterologous strain *B. pseudomallei* 576 (Harland et al., 2007b). However despite the relative success of this candidate vaccine, protection against melioidosis was still incomplete as mice eventually succumbed to infection.

A recent study highlighted the *B. pseudomallei* outer membrane protein A family (OmpA) as being immunogenic in mice as well as melioidosis patients (Hara et al., 2009). Evaluation of the *B. pseudomallei* whole genome sequence identified 12 OmpA domains. Following annotation of the relevant open reading frames (ORFs) two of these OmpAs, namely Omp3 and Omp7, were successfully expressed as soluble protein and subsequently purified. Immunization of BALB/c mice with either Omp3 or Omp7 administered with adjuvant, significantly enhanced survival time following subsequent challenge with *B. pseudomallei.* Another study considered the Omp85 protein family as potential vaccine candidates (Su et al., 2010). As with the OmpAs, BALB/c mice immunized with recombinant Omp85 demonstrated increased survival as well as reduced bacterial burdens in tissues compared to unvaccinated controls (Su et al., 2010). Thus pilot experiments with Omp family proteins have demonstrated protective efficacy in animal models of melioidosis and studies with these proteins continue (Hara et al., 2009; Su et al., 2010). However it should be noted that the protection afforded was no greater than that observed previously with other strategies. Another abundant protein family which could be considered for vaccine research are the autotransporter proteins. These outer membrane/secreted proteins facilitate transport across the bacterial cell membrane and to the cell surface, and have been implicated in virulence of some Gram-negative bacteria (Henderson et al., 2004; Wells et al., 2007). Investigation of this system in *B. pseudomallei* could provide more candidate proteins for vaccine development against melioidosis. Thus, the search for novel vaccine antigens against *B. pseudomallei* is continuing.

In summary it is clear that a number of different strategies are under investigation for the development of new vaccines against melioidosis. However better understanding of specific pathogen–host interactions *in vivo*, as well as identification of key virulence determinants and correlates of protection, are needed to enhance vaccine research and development in the future.

DISCUSSION

A subunit vaccine based on a combination of protein and polysaccharide seems the most promising candidate melioidosis vaccine. Although there are some studies from the 1990s which demonstrate the feasibility of such a vaccine, there is no material currently available for testing, and no robust and reliable process for producing such a vaccine. The further development of a vaccine is also likely to depend on the nature of the population to be protected. For example, in South East (SE) Asia most of the individuals who develop melioidosis have an underlying condition that increases their susceptibility to disease. Thus individuals are effectively imunosuppressed, meaning that vaccines may be less effective in this group. The current assumption is that many of these individuals contract the disease via cuts and abrasions but it is possible that some cases are the consequence of the ingestion or inhalation of bacteria. In contrast a biodefense vaccine would need to protect the general population against an airborne challenge and would need to protect healthy individuals in addition to those with an underlying condition which pre-disposes them to disease. Ideally, a vaccine would be able to protect both of these groups and this linkage has several clear potential benefits. Firstly, it seems unlikely that a melioidosis vaccine for use in endemic areas in SE Asia would be economically viable without the ability to also use this vaccine for biodefense purposes. Secondly, the ability to identify at-risk groups in Thailand, or indeed other parts of SE Asia, would allow meaningful clinical trials to be carried out.

There is still considerable debate over the most appropriate animal model for testing vaccine candidates. Many of the studies carried out to date are in highly susceptible BALB/c mice and this model is more suitable to the study of acute melioidosis. In contrast C57BL/6 mice develop either acute or chronic disease depending on the challenge dose. The characteristic clinical features of human melioidosis such as acute versus chronic disease, pneumonia, and abscess formation in the liver and spleen are therefore mirrored in the C57BL/6 model. In studies we have carried out, the degree of protection offered by various immunogens has been greater in C57BL/6 than in BALB/c mice. Whilst a large proportion of an endemic population is exposed to *B. pseudomallei* only relatively few develop clinical disease, suggesting the majority of people have some form of resistance against melioidosis. Alternatively given the risk factors associated with melioidosis, the organism may only be capable of causing disease in an immunocompromised host. Nonetheless the immune responses elicited by patients who develop clinical infection are likely to be different to those who remain asymptomatic, so identifying immune responses under conditions of the strongest vaccine protection in resistant mice may provide insights into what is required from future vaccine designs. Our laboratories have addressed this problem and preliminary data demonstrated that following i.n. vaccination with 2D2, C57BL/6 mice were significantly protected against i.n. challenge with *B. pseudomallei* 576 with 60% of mice still alive 250 days post challenge (A. Easton, unpublished data). To determine if the surviving mice had completely cleared the infection, they were treated with dexamethasone which suppresses the immune system and consequently reactivation of acute infection can occur due to the presence of persistent bacteria. However all mice survived the dexamethasone treatment and no bacteria were detected in the spleen, lung, or liver indicating that these mice had in fact achieved sterilizing immunity following 2D2 vaccination (A. Easton, unpublished data). This vaccine strategy thus provides the best protection against experimental melioidosis to date, and further investigation using the resistant C57BL/6 model in vaccination studies is ongoing.

Whilst the i.p. route is commonly used in experimental animal models, the s.c. or i.n. route of infection could be considered more physiologically relevant model for melioidosis. In human *B. pseudomallei* infection, inhalation is an important route of exposure in both endemic regions and in a potential bioterrorism situation. Involvement of the lung is often associated with severe disease with pneumonia being the most prominent clinical presentation of melioidosis in all studies (Howe et al., 1971; Guard et al., 1984; Chaowagul et al., 1989; Puthucheary et al., 1992; Simpson et al., 1999; Currie et al., 2000; Chrispal et al., 2010). Despite the importance of pulmonary *B. pseudomallei* infection, very few studies have investigated vaccine-mediated protection against respiratory challenge. Studies of other respiratory infections such as influenza, tuberculosis, and tularemia, have demonstrated that to effectively generate protective mucosal immune responses, the vaccine should be delivered directly to the target mucosa rather than systemically (Hornick and Eigelsbach, 1966; Conlan et al., 2005; Santosuosso et al., 2006; Perrone et al., 2009). Consequently our laboratory has developed an i.n. model of vaccination in BALB/c mice using the *B. pseudomallei* mutant 2D2. Vaccinated mice were protected against subsequent i.n. challenge, as determined by enhanced survival and reduced bacterial burdens in the spleen and lung (Easton et al., 2011). Of note is the observation that protection against pulmonary *B. pseudomallei* challenge was significantly greater following i.n. vaccination as opposed to i.p. vaccination (Easton et al., 2011). This phenomenon was also seen in experiments by Breitbach et al. (2008) in which vaccination with attenuated *B. pseudomallei* purine mutants was most effective against pulmonary challenge when administered via the i.n. route. Furthermore a recent study demonstrated i.n. vaccination with HkBps administered with a potent mucosal adjuvant, was significantly more protective against i.n. challenge compared to HkBps alone (Henderson et al., 2011). Together these data highlight the need to consider the efficacy of pulmonary vaccination and mucosal targeting in the future of melioidosis vaccine design and development.

Finally, since it may be possible to carry our clinical trials with a candidate melioidosis vaccine, there may be a less urgent need for non-human primate models of disease than is the case for other infections caused by bioterrorism agents. Nevertheless, it would be highly desirable to have also tested such a candidate in a suitable non-human primate model. To our knowledge, marmoset,

rhesus macaque, and African Green monkey models of melioidosis are currently being evaluated and we await the results of these studies.

ACKNOWLEDGMENTS

Work in the authors laboratory was supported by National Institute of Health Grant U01AI061363.

REFERENCES

Adler, N. R., Govan, B., Cullinane, M., Harper, M., Adler, B., and Boyce, J. D. (2009). The molecular and cellular basis of pathogenesis in melioidosis: how does *Burkholderia pseudomallei* cause disease? *FEMS Microbiol. Rev.* 33, 1079–1099.

Akira, S., Uematsu, S., and Takeuchi, O. (2006). Pathogen recognition and innate immunity. *Cell* 124, 783–801.

Anuntagool, N., Intachote, P., Wuthiekanun, V., White, N. J., and Sirisinha, S. (1998). Lipopolysaccharide from nonvirulent Ara+*Burkholderia pseudomallei* isolates is immunologically indistinguishable from lipopolysaccharide from virulent Ara- clinical isolates. *Clin. Diagn. Lab. Immunol.* 5, 225–229.

Ashdown, L. R., and Guard, R. W. (1984). The prevalence of human melioidosis in Northern Queensland. *Am. J. Trop. Med. Hyg.* 33, 474–478.

Atkins, T., Prior, R. G., Mack, K., Russell, P., Nelson, M., Oyston, P., Dougan, G., and Titball, R. W. (2002a). A mutant of *Burkholderia pseudomallei*, auxotrophic in the branched chain amino acid biosynthetic pathway, is attenuated and protective in a murine model of melioidosis. *Infect. Immun.* 70, 5290–5294.

Atkins, T., Prior, R., Mack, K., Russell, P., Nelson, M., Prior, J., Ellis, J., Oyston, P. C. F., Dougan, G., and Titball, R. W. (2002b). Characterisation of an acapsular mutant of *Burkholderia pseudomallei* identified by signature tagged mutagenesis. *J. Med. Microbiol.* 51, 539–553.

Bangari, D. S., and Mittal, S. K. (2006). Development of nonhuman adenoviruses as vaccine vectors. *Vaccine* 24, 849–862.

Barnes, J. L., and Ketheesan, N. (2007). Development of protective immunity in a murine model of melioidosis is influenced by the source of *Burkholderia pseudomallei* antigens. *Immunol. Cell Biol.* 85, 551–557.

Barnes, J. L., Ulett, G. C., Ketheesan, N., Clair, T., Summers, P. M., and Hirst, R. G. (2001). Induction of multiple chemokine and colony-stimulating factor genes in experimental *Burkholderia pseudomallei* infection. *Immunol. Cell Biol.* 79, 490–501.

Barnes, J. L., Warner, J., Melrose, W., Durrheim, D., Speare, R., Reeder, J. C., and Ketheesan, N. (2004). Adaptive immunity in melioidosis: a possible role for T cells in determining outcome of infection with *Burkholderia pseudomallei*. *Clin. Immunol.* 113, 22–28.

Bernatoniene, J., and Finn, A. (2005). Advances in pneumococcal vaccines: advantages for infants and children. *Drugs* 65, 229–255.

Bhattacharjee, A. K., Izadjoo, M. J., Zollinger, W. D., Nikolich, M. P., and Hoover, D. L. (2006). Comparison of protective efficacy of subcutaneous versus intranasal immunization of mice with a *Brucella melitensis* lipopolysaccharide subunit vaccine. *Infect. Immun.* 74, 5820–5825.

Breitbach, K., Klocke, S., Tschernig, T., van Rooijen, N., Baumann, U., and Steinmetz, I. (2006). Role of inducible nitric oxide synthase and NADPH oxidase in early control of *Burkholderia pseudomallei* infection in mice. *Infect. Immun.* 74, 6300–6309.

Breitbach, K., Köhler, J., and Steinmetz, I. (2008). Induction of protective immunity against *Burkholderia pseudomallei* using attenuated mutants with defects in the intracellular life cycle. *Trans. R. Soc. Trop. Med. Hyg.* 102, S89–S94.

Breitbach, K., Wongprompitak, P., and Steinmetz, I. (2011). Distinct roles for nitric oxide in resistant C57BL/6 and susceptible BALB/c mice to control *Burkholderia pseudomallei* infection. *BMC Immunol.* 12, 20. doi: 10.1186/1471-2172-12-20

Brett, P., and Woods, D. E. (1996). Structural and immunological characterization of *Burkholderia pseudomallei* O-polysaccaride-flagellin protein conjugates. *Infect. Immun* 64, 2824–2828.

Brett, P. J., Burtnick, M. N., and Woods, D. E. (2003). The wbiA locus is required for the 2-O-acetylation of lipopolysaccharide expressed by *Burkholderia pseudomallei* and *Burkholderia thailandensis*. *FEMS Microbiol. Lett.* 218, 323–328.

Brett, P. J., Mah, D. C., and Woods, D. E. (1994). Isolation and characterization of *Pseudomonas pseudomallei* flagellin proteins. *Infect. Immun.* 62, 1914–1919.

Brown, A. E., Dance, D. A., Suputtamongkol, Y., Chaowagul, W., Kongchareon, S., Webster, H. K., and White, N. J. (1991). Immune cell activation in melioidosis: increased serum levels of interferon-gamma and soluble interleukin-2 receptors without change in soluble CD8 protein. *J. Infect. Dis.* 163, 1145–1148.

Cai, H., Yu, D. H., Hu, X. D., Li, S. X., and Zhu, Y. X. (2006). A combined DNA vaccine-prime, BCG-boost strategy results in better protection against *Mycobacterium bovis* challenge. *DNA Cell Biol.* 25, 438–447.

Chanchamroen, S., Kewcharoenwong, C., Susaengrat, W., Ato, M., and Lertmemongkolchai, G. (2009). Human polymorphonuclear neutrophil responses to *Burkholderia pseudomallei* in healthy and diabetic subjects. *Infect. Immun.* 77, 456–463.

Chaowagul, W., Suputtamongkol, Y., Dance, D. A., Rajchanuvong, A., Pattara-arechachai, J., and White, N. J. (1993). Relapse in melioidosis: incidence and risk factors. *J. Infect. Dis.* 168, 1181–1185.

Chaowagul, W., White, N. J., Dance, D. A., Wattanagoon, Y., Naigowit, P., Davis, T. M., Looareesuwan, S., and Pitakwatchara, N. (1989). Melioidosis: a major cause of community-acquired septicemia in northeastern Thailand. *J. Infect. Dis.* 159, 890–899.

Charuchaimontri, C., Suputtamongkol, Y., Nilakul, C., Chaowagul, W., Chetchotisakd, P., Lertpatanasuwun, N., Intaranongpai, S., Brett, P. J., and Woods, D. E. (1999). Antilipopolysaccharide II: an antibody protective against fatal melioidosis. *Clin. Infect. Dis.* 29, 813–818.

Chen, Y.-S., Hsiao, Y.-S., Lin, H.-H., Liu, Y., and Chen, Y.-L. (2006a). CpG-modified plasmid DNA encoding flagellin improves immunogenicity and provides protection against *Burkholderia pseudomallei* infection in BALB/c mice. *Infect. Immun.* 74, 1699–1705.

Chen, Y.-S., Hsiao, Y.-S., Lin, H.-H., Yen, C.-M., Chen, S.-C., and Chen, Y.-L. (2006b). Immunogenicity and anti-*Burkholderia pseudomallei* activity in Balb/c mice immunized with plasmid DNA encoding flagellin. *Vaccine* 24, 750–758.

Cheng, A., and Currie, B. (2005). Melioidosis: epidemiology, pathophysiology, and management. *Clin. Microbiol. Rev.* 18, 383–416.

Cheng, A. C., Wuthiekanun, V., Limmathurotsakul, D., Chierakul, W., and Peacock, S. J. (2008). Intensity of exposure and incidence of melioidosis in Thai children. *Trans. R. Soc. Trop. Med. Hyg.* 102, S37–S39.

Chierakul, W., Wuthiekanun, V., Chaowagul, W., Amornchai, P., Cheng, A. C., White, N. J., Day, N. P. J., and Peacock, S. J. (2005). Disease severity and outcome of melioidosis in HIV coinfected individuals. *Am. J. Trop. Med. Hyg.* 73, 1165–1166.

Chrispal, A., Rajan, S. J., and Sathyendra, S. (2010). The clinical profile and predictors of mortality in patients with melioidosis in South India. *Trop. Doct.* 40, 36–38.

Clements, A., Jenney, A. W., Farn, J. L., Brown, L. E., Deliyannis, G., Hartland, E. L., Pearse, M. J., Maloney, M. B., Wesselingh, S. L., Wijburg, O. L., and Strugnell, R. A. (2008). Targeting subcapsular antigens for prevention of *Klebsiella pneumoniae* infections. *Vaccine* 26, 5649–5653.

Coban, C., Koyama, S., Takeshita, F., Akira, S., and Ishii, K. J. (2008). Molecular and cellular mechanisms of DNA vaccines. *Hum. Vaccin.* 4, 453–457.

Coffman, R. L., and Carty, J. (1986). A T cell activity that enhances polyclonal IgE production and its inhibition by interferon-gamma. *J. Immunol.* 136, 949–954.

Conlan, J. W., Shen, H., KuoLee, R., Zhao, X., and Chen, W. (2005). Aerosol-, but not intradermal-immunization with the live vaccine strain of *Francisella tularensis* protects mice against subsequent aerosol challenge with a highly virulent type A strain of the pathogen by an αβ T cell- and interferon gamma-dependent mechanism. *Vaccine* 23, 2477–2485.

Currie, B. (2003). Melioidosis: an important cause of pneumonia in residents of and travellers returned from endemic regions. *Eur. Respir. J.* 22, 542–550.

Currie, B. J. (2008). Advances and remaining uncertainties in the epidemiology of *Burkholderia pseudomallei* and melioidosis. *Trans. R. Soc. Trop. Med. Hyg.* 102, 225–227.

Currie, B. J., Fisher, D. A., Howard, D. M., Burrow, J. N., Lo, D., Selva-Nayagam, S., Anstey, N. M., Huffam, S. E., Snelling, P. L., Marks, P. J., Stephens, D. P., Lum, G. D., Jacups, S. P., and Krause, V. L. (2000). Endemic melioidosis in tropical northern Australia: a 10-year prospective study and review of the literature. *Clin. Infect. Dis.* 31, 981–986.

Currie, B. J., and Jacups, S. P. (2003). Intensity of rainfall and severity of melioidosis, Australia. *Emerg. Infect. Dis.* 9, 1538–1542.

Currie, B. J., Jacups, S. P., Cheng, A. C., Fisher, D. A., Anstey, N. M., Huffam, S. E., and Krause, V. L. (2004). Melioidosis epidemiology and risk factors from a prospective whole-population study in northern Australia. *Trop. Med. Int. Health* 9, 1167–1174.

Dance, D. A. B., Wuthiekanun, V., Chaowagul, W., and White, N. J. (1989). The antimicrobial susceptibility of *Pseudomonas pseudomallei*. Emergence of resistance in vitro and during treatment. *J. Antimicrob. Chemother.* 24, 295–309.

Dannenberg, A. M. Jr., and Scott, E. M. (1958a). Melioidosis: pathogenesis and immunity in mice and hamsters. I. Studies with virulent strains of *Malleomyces pseudomallei*. *J. Exp. Med.* 107, 153–166.

Dannenberg, A. M. Jr., and Scott, E. M. (1958b). Melioidosis: pathogenesis and immunity in mice and hamsters. II. Studies with avirulent strains of *Malleomyces pseudomallei*. *Am. J. Pathol.* 34, 1099–1121.

Dannenberg, A. M. Jr., and Scott, E. M. (1960). Melioidosis: pathogenesis and immunity in mice and hamsters: III. Effect of vaccination with avirulent strains of *Pseudomonas pseudomallei* on the resistance to the establishment and the resistance to the progress of respiratory melioidosis caused by virulent strains; all-or-none aspects of this disease. *J. Immunol.* 84, 233–246.

Danzig, L. (2004). Meningococcal vaccines. *Pediatr. Infect. Dis. J.* 23, S285–S292.

Dennis, D. T., Inglesby, T. V., Henderson, D. A., Bartlett, J. G., Ascher, M. S., Eitzen, E., Fine, A. D., Friedlander, A. M., Hauer, J., Layton, M.,Lillibridge, S. R., McDade, J. E., Osterholm, M. T., O'Toole, T., Parker, G., Perl, T. M., Russell, P. K., Tonat, K., and for the Working Group in Civilian Biodefense. (2001). Tularemia as a biological weapon: medical and public health management. *JAMA* 285, 2763–2773.

Dorman, S. E., Gill, V. J., Gallin, J. I., and Holland, S. M. (1998). *Burkholderia pseudomallei* infection in a Puerto Rican patient with chronic granulomatous disease: case report and review of occurrences in the Americas. *Clin. Infect. Dis.* 26, 889–894.

Druar, C., Yu, F., Barnes, J. L., Okinaka, R. T., Chantratita, N., Beg, S., Stratilo, C. W., Olive, A. J., Soltes, G., Russell, M. L., Limmathurotsakul, D., Norton, R. E., Ni, S. X., Picking, W. D., Jackson, P. T., Stewart, D. I. H., Tsvetnitsky, V., Picking, W. L., Cherwonogrodzky, J. W., Ketheesan, N., Peacock, S. J., and Wiersma, E. J. (2008). Evaluating *Burkholderia pseudomallei* Bip proteins as vaccines and Bip antibodies as detection agents. *FEMS Immunol. Med. Microbiol.* 52, 78–87.

Dworkin, M. S., Ward, J. W., Hanson, D. L., Jones, J. L., and Kaplan, J. E. (2001). Pneumococcal disease among human immunodeficiency virus-infected persons: incidence, risk factors, and impact of vaccination. *Clin. Infect. Dis.* 32, 794–800.

Easton, A., Haque, A., Chu, K., Lukaszewski, R., and Bancroft, G. J. (2007). A critical role for neutrophils in resistance to experimental infection with *Burkholderia pseudomallei*. *J. Infect. Dis.* 195, 99–107.

Easton, A., Haque, A., Chu, K., Patel, N., Lukaszewski, R., Krieg, A. M., Titball, R. W., and Bancroft, G. J. (2011). Combining vaccination and postexposure CpG therapy provides optimal protection against lethal sepsis in a biodefense model of human melioidosis. *J. Infect. Dis.* 204, 636–644.

Edelson, B. T., and Unanue, E. R. (2000). Immunity to *Listeria* infection. *Curr. Opin. Immunol.* 12, 425–431.

Egan, A. M., and Gordon, D. L. (1996). *Burkholderia pseudomallei* activates complement and is ingested but not killed by polymorphonuclear leukocytes. *Infect. Immun.* 64, 4952–4959.

Ekchariyawat, P., Pudla, S., Limposuwan, K., Arjcharoen, S., Sirisinha, S., and Utaisincharoen, P. (2005). *Burkholderia pseudomallei*-induced expression of suppressor of cytokine signaling 3 and cytokine-inducible Src homology 2-containing protein in mouse macrophages: a possible mechanism for suppression of the response to gamma interferon stimulation. *Infect. Immun.* 73, 7332–7339.

Elvin, S., Healey, G., Westwood, A., Knight, S., Eyles, J., and Williamson, E. (2006). Protection against heterologous *Burkholderia pseudomallei* strains by dendritic cell immunization. *Infect. Immun.* 74, 1706–1711.

Eskola, J. (2010). Foresight in medicine: current challenges with *Haemophilus influenzae* type b conjugate vaccines. *J. Intern. Med.* 267, 241–250.

Flynn, J., and Chan, J. (2001). Immunology of tuberculosis. *Annu. Rev. Immunol.* 19, 93–129.

Friedland, J. S., Suputtamongkol, Y., Remick, D. G., Chaowagul, W., Strieter, R. M., Kunkel, S. L., White, N. J., and Griffin, G. E. (1992). Prolonged elevation of interleukin-8 and interleukin-6 concentrations in plasma and of leukocyte interleukin-8 mRNA levels during septicemic and localized *Pseudomonas pseudomallei* infection. *Infect. Immun.* 60, 2402–2408.

Fry, A. M., Zell, E. R., Schuchat, A., Butler, J. C., and Whitney, C. G. (2002). Comparing potential benefits of new pneumococcal vaccines with the current polysaccharide vaccine in the elderly. *Vaccine* 21, 303–311.

Fulop, M., Mastroeni, P., Green, M., and Titball, R. W. (2001). Role of antibody to lipopolysaccharide in protection against low- and high-virulence strains of *Francisella tularensis*. *Vaccine* 19, 4465–4472.

Garmory, H. S., and Titball, R. W. (2004). ATP-binding cassette transporters are targets for the development of antibacterial vaccines and therapies. *Infect. Immun.* 72, 6757–6763.

Gilks, C. F., Ojoo, S. A., Ojoo, J. C., Brindle, R. J., Paul, J., Batchelor, B. I., Kimari, J. N., Newnham, R., Bwayo, J., Plummer, F. A., and Warrell, D. A. (1996). Invasive pneumococcal disease in a cohort of predominantly HIV-1 infected female sex-workers in Nairobi, Kenya. *Lancet* 347, 718–723.

Govan, B., and Ketheesan, N. (2004). Exposure to *Burkholderia pseudomallei* induces cell-mediated immunity in healthy individuals. *Clin. Microbiol. Infect.* 10, 585–587.

Griffin, K. F., Oyston, P. C., and Titball, R. W. (2007). *Francisella tularensis* vaccines. *FEMS Immunol. Med. Microbiol.* 49, 315–323.

Guard, R. W., Khafagi, F. A., Brigden, M. C., and Ashdown, L. R. (1984). Melioidosis in far north Queensland: a clinical and epidemiological review of twenty cases. *Am. J. Trop. Med. Hyg.* 33, 467–473.

Haque, A., Easton, A., Smith, D., O'Garra, A., Van Rooijen, N., Lertmemongkolchai, G., Titball, R. W., and Bancroft, G. J. (2006a). Role of T cells in innate and adaptive immunity against murine *Burkholderia pseudomallei* infection. *J. Infect. Dis.* 193, 370–379.

Haque, A., Chu, K., Easton, A., Stevens, M. P., Galyov, E. E., Atkins, T., Titball, R., and Bancroft, G. J. (2006b). A live experimental vaccine against *Burkholderia pseudomallei* elicits CD4+ cell-mediated immunity, priming T cells specific for 2 type III secretion system proteins. *J. Infect. Dis.* 194, 1241–1248.

Hara, Y., Mohamed, R., and Nathan, S. (2009). Immunogenic *Burkholderia pseudomallei* outer membrane proteins as potential candidate vaccine targets. *PLoS ONE* 4, e6496. doi: 10.1371/journal.pone.0006496

Harland, D., Dassa, E., Titball, R., Brown, K., and Atkins, H. (2007a). ATP-binding cassette systems in *Burkholderia pseudomallei* and *Burkholderia mallei*. *BMC Genomics* 8, 83. doi: 10.1186/1471-2164-8-83

Harland, D. N., Chu, K., Haque, A., Nelson, M., Walker, N. J., Sarkar-Tyson, M., Atkins, T. P., Moore, B., Brown, K. A., Bancroft, G., Titball, R. W., and Atkins, H. S. (2007b). Identification of a LolC homologue in *Burkholderia pseudomallei*, a novel protective antigen for melioidosis. *Infect. Immun.* 75, 4173–4178.

Hasselbring, B. M., Patel, M. K., and Schell, M. A. (2011). *Dictyostelium discoideum* as a model system for identification of *Burkholderia pseudomallei* virulence factors. *Infect. Immun.* 79, 2079–2088.

Healey, G. D., Elvin, S. J., Morton, M., and Williamson, E. D. (2005). Humoral and cell-mediated adaptive immune responses are required for protection against *Burkholderia pseudomallei* challenge and bacterial clearance postinfection. *Infect. Immun.* 73, 5945–5951.

Henderson, A., Propst, K., Kedl, R., and Dow, S. (2011). Mucosal immunization with liposome-nucleic acid adjuvants generates effective humoral and cellular immunity. *Vaccine* 29, 5304–5312.

Henderson, I. R., Navarro-Garcia, F., Desvaux, M., Fernandez, R. C., and Ala'Aldeen, D. (2004). Type V protein secretion pathway: the autotransporter story. *Microbiol. Mol. Biol. Rev.* 68, 692–744.

Hewlett, E. L. (1997). Preparation and composition of acellular *pertussis* vaccines. Consideration of potential effects on vaccine efficacy. *Dev. Biol. Stand.* 89, 143–151.

Higgins, S. C., Jarnicki, A. G., Lavelle, E. C., and Mills, K. H. G. (2006). TLR4 mediates vaccine-induced protective cellular immunity to *Bordetella pertussis*: role of IL-17-producing T cells. *J. Immunol.* 177, 7980–7989.

Hii, C. S., Sun, G. W., Goh, J. W. K., Lu, J., Stevens, M. P., and Gan, Y. H. (2008). Interleukin-8 induction by *Burkholderia pseudomallei* can occur without Toll-like receptor signaling but requires a functional type III secretion system. *J. Infect. Dis.* 197, 1537–1547.

Hill, D. R., Ford, L., and Lalloo, D. G. (2006). Oral cholera vaccines: use in clinical practice. *Lancet Infect. Dis.* 6, 361–373.

Ho, M., Schollaardt, T., Smith, M. D., Perry, M. B., Brett, P. J., Chaowagul, W., and Bryan, L. E. (1997). Specificity and functional activity of anti-*Burkholderia pseudomallei* polysaccharide antibodies. *Infect. Immun.* 65, 3648–3653.

Hoover, D. R., Saah, A. J., Bacellar, H., Phair, J., Detels, R., Anderson, R., Kaslow, R. A., and The Multicenter AIDS Cohort Study (1993). Clinical manifestations of AIDS in the era of Pneumocystis prophylaxis. *N. Engl. J. Med.* 329, 1922–1926.

Hoppe, I., Brenneke, B., Rohde, M., Kreft, A., Häußler, S., Reganzerowski, A., and Steinmetz, I. (1999). Characterization of a murine model of melioidosis: comparison of different strains of mice. *Infect. Immun.* 67, 2891–2900.

Hornick, R. B., and Eigelsbach, H. T. (1966). Aerogenic immunization of man with live Tularemia vaccine. *Microbiol. Mol. Biol. Rev.* 30, 532–538.

Howe, C., Sampath, A., and Spotnitz, M. (1971). The pseudomallei group: a review. *J. Infect. Dis.* 124, 598–606.

Iliukhin, V. I., Senina, T. V., Plekhanova, N. G., Antonov, V. A., Merinova, L. K., and Seimova, I. K. (2002). *Burkholderia thailandensis*: biological properties, identification and taxonomy. *Mol. Gen. Mikrobiol. Virusol.* 1, 7–11.

Inglesby, T. V., Dennis, D. T., Henderson, D. A., Bartlett, J. G., Ascher, M. S., Eitzen, E., Fine, A. D., Friedlander, A. M., Hauer, J., Koerner, J. F., McDade, J., Osterholm, M. T., O'Toole, T., Parker, G., Perl, T. M., Russell, P. K., Schoch-Spana, M., Tonat, K., and for the Working Group in Civilian Biodefense. (2000). Plague as a biological weapon: medical and public health management. *JAMA* 283, 2281–2290.

Inglesby, T. V., O'Toole, T., Henderson, D. A., Bartlett, J. G., Ascher, M. S., Eitzen, E., Friedlander, A. M., Gerberding, J., Hauer, J., Hughes, J., McDade, J., Osterholm, M. T., Parker, G., Perl, T. M., Russell, P. K., Tonat, K., and for the Working Group in Civilian Biodefense. (2002). Anthrax as a biological weapon, 2002: updated recommendations for management. *JAMA* 287, 2236–2252.

Ivanoff, B., Levine, M. M., and Lambert, P. H. (1994). Vaccination against typhoid fever: present status. *Bull. World Health Organ.* 72, 957–971.

Janeway, C. A., and Medzhitov, R. (2002). Innate immune recognition. *Annu. Rev. Immunol.* 20, 197–216.

Janeway, C.A. Jr., Murphy, K., Travers, P., and Walport, M. (2008). *Janeway's Immunobiology: T Cell-Mediated Immunity*, Chapter 8, 7th Edn. New York: Garland Science, 340–341.

Jones, A., DeShazer, D., and Woods, D. (1997). Identification and characterization of a two-component regulatory system involved in invasion of eukaryotic cells and heavy-metal resistance in *Burkholderia pseudomallei. Infect. Immun.* 65, 4972–4977.

Jones, C. (2005). Vaccines based on the cell surface carbohydrates of pathogenic bacteria. *An. Acad. Bras. Cienc.* 77, 293–324.

Jones, S., Ellis, J., Russell, P., Griffin, K., and Oyston, P. (2002). Passive protection against *Burkholderia pseudomallei* infection in mice by monoclonal antibodies against capsular polysaccharide, lipopolysaccharide or proteins. *J. Med. Microbiol.* 51, 1055–1062.

Kanaphun, P., Thirawattanasuk, N., Suputtamongkol, Y., Naigowit, P., Dance, D. A., Smith, M. D., and White, N. J. (1993). Serology and carriage of *Pseudomonas pseudomallei*: a prospective study in 1000 hospitalized children in northeast Thailand. *J. Infect. Dis.* 167, 230–233.

Kaufmann, S. H. E., Hussey, G., and Lambert, P.-H. (2010). New vaccines for tuberculosis. *Lancet* 375, 2110–2119.

Ketheesan, N., Barnes, J. L., Ulett, G. C., VanGessel, H. J., Norton, R. E., Hirst, R. G., and LaBrooy, J. T. (2002). Demonstration of a cell-mediated immune response in melioidosis. *J. Infect. Dis.* 186, 286–289.

Lauw, F. N., Simpson, A. J., Prins, J. M., Smith, M. D., Kurimoto, M., van Deventer, S. J., Speelman, P., Chaowagul, W., White, N. J., and van der Poll, T. (1999). Elevated plasma concentrations of interferon (IFN)-gamma and the IFN-gamma-inducing cytokines interleukin (IL)-18, IL-12, and IL-15 in severe melioidosis. *J. Infect. Dis.* 180, 1878–1885.

Lazzaroni, S. M., Barnes, J. L., Williams, N. L., Govan, B. L., Norton, R. E., LaBrooy, J. T., and Ketheesan, N. (2008). Seropositivity to *Burkholderia pseudomallei* does not reflect the development of cell-mediated immunity. *Trans. R. Soc. Trop. Med. Hyg.* 102, S66–S70.

Leakey, A. K., Ulett, G. C., and Hirst, R. G. (1998). BALB/c and C57Bl/6 mice infected with virulent *Burkholderia pseudomallei* provide contrasting animal models for the acute and chronic forms of human melioidosis. *Microb. Pathog.* 24, 269–275.

Lertmemongkolchai, G., Cai, G., Hunter, C. A., and Bancroft, G. J. (2001). Bystander activation of CD8+ T cells contributes to the rapid production of IFN-gamma in response to bacterial pathogens. *J. Immunol.* 166, 1097–1105.

Lever, M. S., Michelle, N., Anthony, J. S., Richard, J. B., and Andrew, J. H. S. (2009). Experimental acute respiratory *Burkholderia pseudomallei* infection in BALB/c mice. *Int. J. Exp. Pathol.* 90, 16–25.

Liljeqvist, S., and Ståhl, S. (1999). Production of recombinant subunit vaccines: protein immunogens, live delivery systems and nucleic acid vaccines. *J. Biotechnol.* 73, 1–33.

Limmathurotsakul, D., Chaowagul, W., Chierakul, W., Stepniewska, K., Maharjan, B., Wuthiekanun, V., White, N., Day, N., and Peakcock, S. (2006). Risk factors for recurrent melioidosis. *Clin. Infect. Dis.* 43, 979–986.

Limmathurotsakul, D., Wuthiekanun, V., Chantratita, N., Wongsuvan, G., Thanwisai, A., Biaklang, M., Tumapa, S., Lee, S., Day, N. P. J., and Peacock, S. J. (2007). Simultaneous infection with more than one strain of *Burkholderia pseudomallei* is uncommon in human melioidosis. *J. Clin. Microbiol.* 45, 3830–3832.

Liu, B., Koo, G. C., Yap, E. H., Chua, K. L., and Gan, Y.-H. (2002). Model of differential susceptibility to mucosal *Burkholderia pseudomallei* infection. *Infect. Immun.* 70, 504–511.

Lu, S. (2009). Heterologous prime-boost vaccination. *Curr. Opin. Immunol.* 21, 346–351.

Magalhaes, I., Sizemore, D. R., Ahmed, R. K., Mueller, S., Wehlin, L., Scanga, C., Weichold, F., Schirru, G., Pau, M. G., Goudsmit, J., Kühlmann-Berenzon, S., Spångberg, M., Andersson, J., Gaines, H., Thorstensson, R., Skeiky, Y. A. W., Sadoff, J., and Maeurer, M. (2008). rBCG induces strong antigen-specific T cell responses in Rhesus macaques in a prime-boost setting with an adenovirus 35 tuberculosis vaccine vector. *PLoS ONE* 3, e3790. doi: 10.1371/journal.pone.0003790

Maharjan, B., Chantratita, N., Vesaratchavest, M., Cheng, A., Wuthiekanun, V., Chierakul, W., Chaowagul, W., Day, N. P. J., and Peacock, S. J. (2005). Recurrent melioidosis in patients in northeast Thailand is frequently due to reinfection rather than relapse. *J. Clin. Microbiol.* 43, 6032–6034.

Martineau, A. R., Newton, S. M., Wilkinson, K. A., Kampmann, B., Hall, B. M., Nawroly, N., Packe, G. E., Davidson, R. N., Griffiths, C. J., and Wilkinson, R. J. (2007). Neutrophil-mediated innate immune resistance to mycobacteria. *J. Clin. Invest.* 117, 1988–1994.

Matsuura, M., Kawahara, K., Ezaki, T., and Nakano, M. (1996). Biological activities of lipopolysaccharide of *Burkholderia* (*Pseudomonas*) *pseudomallei. FEMS Microbiol. Lett.* 137, 79–83.

McEniry, D. W., Gillespie, S. H., and Felmingham, D. (1988). Susceptibility of *Pseudomonas pseudomallei* to new beta-lactam and aminoglycoside antibiotics. *J. Antimicrob. Chemother.* 21, 171–175.

McShane, H., Pathan, A. A., Sander, C. R., Keating, S. M., Gilbert, S. C., Huygen, K., Fletcher, H. A., and Hill, A. V. S. (2004). Recombinant modified vaccinia virus Ankara expressing antigen 85A boosts BCG-primed and naturally acquired antimycobacterial immunity in humans. *Nat. Med.* 10, 1240–1244.

Menard, L. C., Minns, L. A., Darche, S., Mielcarz, D. W., Foureau, D. M., Roos, D., Dzierszinski, F., Kasper, L. H., and Buzoni-Gatel, D. (2007). B cells amplify IFN-gamma production by T cells via a TNF-alpha-mediated mechanism. *J. Immunol.* 179, 4857–4866.

Mitus, A., Holloway, A., Evans, A. E., and Enders, J. F. (1962). Attenuated measles vaccine in children with acute leukemia. *Am. J. Dis. Child.* 103, 413–418.

Monafo, W. J., Haslam, D. B., Roberts, R. L., Zaki, S. R., Bellini, W. J., and Coffin, C. M. (1994). Disseminated measles infection after vaccination in a child with a congenital immunodeficiency. *J. Pediatr.* 124, 273–276.

Mosmann, T. R., Cherwinski, H., Bond, M. W., Giedlin, M. A., and Coffman, R. L. (1986). Two types of murine helper T cell clone. I. Definition according to profiles of lymphokine activities and secreted proteins. *J. Immunol.* 136, 2348–2357.

Nelson, M., Prior, J. L., Lever, M. S., Jones, H. E., Atkins, T. P., and Titball, R. W. (2004). Evaluation of lipopolysaccharide and capsular polysaccharide as subunit vaccines against experimental melioidosis. *J. Med. Microbiol.* 53, 1177–1182.

Ngugi, S. A., Ventura, V. V., Qazi, O., Harding, S. V., Kitto, G. B., Estes, D. M., Dell, A., Titball, R. W., Atkins, T. P., Brown, K. A., Hitchen, P. G., and Prior, J. L. (2010). Lipopolysaccharide from *Burkholderia thailandensis* E264 provides protection in a murine model of melioidosis. *Vaccine* 28, 7551–7555.

Nieves, W., Heang, J., Asakrah, S., Höner zu Bentrup, K., Roy, C. J., and Morici, L. A. (2010). Immunospecific responses to bacterial elongation factor Tu during *Burkholderia* infection and immunization. *PLoS ONE* 17, e14361. doi: 10.1371/journal.pone.0014361

Novem, V., Shui, G., Wang, D., Bendt, A. K., Sim, S. H., Liu, Y., Thong, T. W., Sivalingam, S. P., Ooi, E. E., Wenk, M. R., and Tan, G. (2009). Structural and biological diversity of lipopolysaccharides from *Burkholderia pseudomallei* and *Burkholderia thailandensis*. *Clin. Vaccine Immunol.* 16, 1420–1428.

Perrone, L. A., Ahmad, A., Veguilla, V., Lu, X., Smith, G., Katz, J. M., Pushko, P., and Tumpey, T. M. (2009). Intranasal vaccination with 1918 influenza virus-like particles protects mice and ferrets from lethal 1918 and H5N1 influenza virus challenge. *J. Virol.* 83, 5726–5734.

Phair, J., Munoz, A., Detels, R., Kaslow, R., Rinaldo, C., and Saah, A. (1990). The risk of *Pneumocystis carinii* pneumonia among men infected with human immunodeficiency virus type 1. *N. Engl. J. Med.* 322, 161–165.

Piggott, J. A., and Hochholzer, L. (1970). Human melioidosis. A histopathologic study of acute and chronic melioidosis. *Arch. Pathol.* 90, 101–111.

Pilatz, S., Breitbach, K., Hein, N., Fehlhaber, B., Schulze, J., Brenneke, B., Eberl, L., and Steinmetz, I. (2006). Identification of *Burkholderia pseudomallei* genes required for the intracellular life cycle and in vivo virulence. *Infect. Immun.* 74, 3576–3586.

Pirofski, L. A., and Casadevall, A. (1998). Use of licensed vaccines for active immunization of the immunocompromised host. *Clin. Microbiol. Rev.* 11, 1–26.

Plotkin, S. A. (2009). Vaccines: the fourth century. *Clin. Vaccine Immunol.* 16, 1709–1719.

Preston, M. J., Gerceker, A. A., Koles, N. L., Pollack, M., and Pier, G. B. (1997). Prophylactic and therapeutic efficacy of immunoglobulin G antibodies to *Pseudomonas aeruginosa* lipopolysaccharide against murine experimental corneal infection. *Invest. Ophthalmol. Vis. Sci.* 38, 1418–1425.

Puthucheary, S. D., Parasakthi, N., and Lee, M. K. (1992). Septicaemic melioidosis: a review of 50 cases from Malaysia. *Trans. R. Soc. Trop. Med. Hyg.* 86, 683–685.

Qazi, O., Prior, J. L., Judy, B. M., Whitlock, G. C., Kitto, G. B., Torres, A. G., Estes, D. M., and Brown, K. A. (2008). Sero-characterization of lipopolysaccharide from *Burkholderia thailandensis*. *Trans. R. Soc. Trop. Med. Hyg.* 102, S58–S60.

Radosevic, K., Wieland, C. W., Rodriguez, A., Weverling, G. J., Mintardjo, R., Gillissen, G., Vogels, R., Skeiky, Y. A. W., Hone, D. M., Sadoff, J. C., van der Poll, T., Havenga, M., and Goudsmit, J. (2007). Protective immune responses to a recombinant adenovirus type 35 tuberculosis vaccine in two mouse strains: CD4 and CD8 T-cell epitope mapping and role of gamma interferon. *Infect. Immun.* 75, 4105–4115.

Ramsay, S. C., Ketheesan, N., Norton, R., Watson, A. M., and LaBrooy, J. (2002). Peripheral blood lymphocyte subsets in acute human melioidosis. *Eur. J. Clin. Microbiol. Infect. Dis.* 21, 566–568.

Razak, C. E., Ismail, G., Embim, N., and Omar, O. (1986). Protection studies using whole cells and partially purified toxic material (PPTM) of *Pseudomonas pseudomallei*. *Malays. Appl. Biol.* 15, 105.

Renella, R., Perez, J. M., Chollet-Martin, S., Sarnacki, S., Fischer, A., Blanche, S., Casanova, J. L., and Picard, C. (2006). *Burkholderia pseudomallei* infection in chronic granulomatous disease. *Eur. J. Pediatr.* 165, 175–177.

Sander, C. R., Pathan, A. A., Beveridge, N. E. R., Poulton, I., Minassian, A., Alder, N., Van Wijgerden, J., Hill, A. V. S., Gleeson, F. V., Davies, R. J. O., Pasvol, G., and McShane, H. (2009). Safety and immunogenicity of a new tuberculosis vaccine, MVA85A, in *Mycobacterium* tuberculosis-infected individuals. *Am. J. Respir. Crit. Care Med.* 179, 724–733.

Santanirand, P., Harley, V., Dance, D., Drasar, B., and Bancroft, G. J. (1999). Obligatory role of gamma interferon for host survival in a murine model of infection with *B. pseudomallei*. *Infect. Immun.* 67, 3593–3600.

Santanirand, P., Harley, V. S., Dance, D. A., Raynes, J. G., Drasar, B. S., and Bancroft, G. J. (1997). Interferon-gamma mediates host resistance in a murine model of melioidosis. *Biochem. Soc. Trans.* 25, 287S.

Santosuosso, M., McCormick, S., Zhang, X., Zganiacz, A., and Xing, Z. (2006). Intranasal boosting with an adenovirus-vectored vaccine markedly enhances protection by parenteral *Mycobacterium bovis* BCG immunization against pulmonary tuberculosis. *Infect. Immun.* 74, 4634–4643.

Sarkar-Tyson, M., Smither, S. J., Harding, S. V., Atkins, T. P., and Titball, R. W. (2009). Protective efficacy of heat-inactivated *B. thailandensis, B. mallei or B. pseudomallei* against experimental melioidosis and glanders. *Vaccine* 27, 4447–4445.

Sarkar-Tyson, M., Thwaite, J. E., Harding, S. V., Smither, S. J., Oyston, P. C. F., Atkins, T. P., and Titball, R. W. (2007). Polysaccharides and virulence of *Burkholderia pseudomallei*. *J. Med. Microbiol.* 56, 1005–1010.

Scapini, P., Lapinet-Vera, J. A., Gasperini, S., Calzetti, F., Bazzoni, F., and Cassatella, M. A. (2000). The neutrophil as a cellular source of chemokines. *Immunol. Rev.* 177, 195–203.

Segal, A. W. (2004). How neutrophils kill microbes. *Annu. Rev. Immunol.* 23, 197–223.

Sharma, S. K., Mohan, A., and Kadhiravan, T. (2005). HIV-TB co-infection: epidemiology, diagnosis and management. *Indian J. Med. Res.* 121, 550–567.

Simpson, A. J., Smith, M. D., Weverling, G. J., Suputtamongkol, Y., Angus, B. J., Chaowagul, W., White, N. J., van Deventer, S. J., and Prins, J. M. (2000). Prognostic value of cytokine concentrations (tumor necrosis factor-alpha, interleukin-6, and interleukin-10) and clinical parameters in severe melioidosis. *J. Infect. Dis.* 181, 621–625.

Simpson, A. J., Suputtamongkol, Y., Smith, M. D., Angus, B. J., Rajanuwong, A., Wuthiekanun, V., Howe, P. A., Walsh, A. L., Chaowagul, W., and White, N. J. (1999). Comparison of imipenem and ceftazidime as therapy for severe melioidosis. *Clin. Infect. Dis.* 29, 381–387.

Smith, M. D., Angus, B. J., Wuthiekanun, V., and White, N. J. (1997). Arabinose assimilation defines a nonvirulent biotype of *Burkholderia pseudomallei*. *Infect. Immu.* 65, 4319–4321.

Sprague, L. D., and Neubauer, H. (2004). Melioidosis in animals: a review on epizootiology, diagnosis and clinical presentation. *J. Vet. Med. Ser. B Infect. Dis. Vet. Public Health* 51, 305–320.

Stevens, M. P., Haque, A., Atkins, T., Hill, J., Wood, M. W., Easton, A., Nelson, M., Underwood-Fowler, C., Titball, R. W., Bancroft, G. J., and Galyov, E. E. (2004). Attenuated virulence and protective efficacy of a *Burkholderia pseudomallei* bsa type III secretion mutant in murine models of melioidosis. *Microbiology* 150, 2669–2676.

Su, Y.-C., Wan, K.-L., Mohamed, R., and Nathan, S. (2010). Immunization with the recombinant *Burkholderia pseudomallei* outer membrane protein Omp85 induces protective immunity in mice. *Vaccine* 28, 5005–5011.

Suputtamongkol, Y., Chaowagul, W., Chetchotisakd, P., Lertpatanasuwun, N., Intaranongpai, S., Ruchutrakool, T., Budhsarawong, D., Mootsikapun, P., Wuthiekanun, V., Teerawatasook, N., and Lulitanond, A. (1999). Risk factors for melioidosis and bacteremic melioidosis. *Clin. Infect. Dis.* 29, 408–413.

Suputtamongkol, Y., Kwiatkowski, D., Dance, D. A., Chaowagul, W., and White, N. J. (1992). Tumor necrosis factor in septicemic melioidosis. *J. Infect. Dis.* 165, 561–564.

Tan, G.-Y. G., Liu, Y., Sivalingam, S. P., Sim, S.-H., Wang, D., Paucod, J.-C., Gauthier, Y., and Ooi, E.-E. (2008). *Burkholderia pseudomallei* aerosol infection results in differential inflammatory responses in BALB/c and C57Bl/6 mice. *J. Med. Microbiol.* 57, 508–515.

Tanphaichitra, D., and Srimuang, S. (1984). Cellular immunity (T-cell subset using monoclonal antibody) in tuberculosis, melioidosis, pasteurellosis, penicilliosis; and role of levamisole and isoprinosine. *Dev. Biol. Stand.* 57, 117–123.

Taylor, P. R., Martinez-Pomares, L., Stacey, M., Lin, H. H., Brown, G. D., and Gordon, S. (2005). Macrophage receptors and immune recognition. *Annu. Rev. Immunol.* 23, 901–944.

Thomsen, A. R., Johansen, J., Marker, O., and Christensen, J. P. (1996). Exhaustion of CTL memory and recrudescence of viremia in lymphocytic choriomeningitis virus-infected MHC class II-deficient mice and B cell-deficient mice. *J. Immunol.* 157, 3074–3080.

Tippayawat, P., Saenwongsa, W., Mahawantung, J., Suwannasaen, D., Chetchotisakd, P., Limmathurotsakul, D., Peacock, S. J., Felgner, P. L., Atkins, H. S., Titball, R. W., Bancroft, G. J., and Lertmemongkolchai, G. (2009). Phenotypic and functional characterization of human memory T cell responses to *Burkholderia pseudomallei*. *PLoS Negl. Trop. Dis.* 3, e407. doi: 10.1371/journal.pntd.0000407

Titball, R. W. (2008). Vaccines against intracellular bacterial pathogens. *Drug Discov. Today* 13, 596–600.

Titball, R. W., Russell, P., Cuccui, J., Easton, A., Haque, A., Atkins, T., Sarkar-Tyson, M., Harley, V., Wren, B., and Bancroft, G. J. (2008). *Burkholderia pseudomallei*: animal models of infection. *Trans. R. Soc. Trop. Med. Hyg.* 102, S111–S116.

Trakulsomboon, S., Pitt, T. L., and Dance, D. A. (1994). Molecular typing of *Pseudomonas pseudomallei* from imported primates in Britain. *Vet. Rec.* 135, 65–66.

Ulett, G. C., Ketheesan, N., and Hirst, R. G. (2000a). Cytokine gene expression in innately susceptible BALB/c mice and relatively resistant C57BL/6 mice during infection with virulent *Burkholderia pseudomallei*. *Infect. Immun.* 68, 2034–2042.

Ulett, G. C., Ketheesan, N., and Hirst, R. G. (2000b). Proinflammatory cytokine mRNA responses in experimental *Burkholderia pseudomallei* infection in mice. *Acta Trop.* 74, 229–234.

Utaisincharoen, P., Anuntagool, N., Arjcharoen, S., Lengwehasatit, I., Limposuwan, K., Chaisuriya, P., and Sirisinha, S. (2004). *Burkholderia pseudomallei* stimulates low interleukin-8 production in the human lung epithelial cell line A549. *Clin. Exp. Immunol.* 138, 61–65.

Utaisincharoen, P., Tangthawornchaikul, N., Kespichayawattana, W., Chaisuriya, P., and Sirisinha, S. (2001). *Burkholderia pseudomallei* interferes with inducible nitric oxide synthase (iNOS) production: a possible mechanism of evading macrophage killing. *Microbiol. Immunol.* 45, 307–313.

Vasu, C., Vadivelu, J., and Puthucheary, S. D. (2003). The humoral immune response in melioidosis patients during therapy. *Infection* 31, 24–30.

Verreck, F. A. W., Vervenne, R. A. W., Kondova, I., van Kralingen, K. W., Remarque, E. J., Braskamp, G., van der Werff, N. M., Kersbergen, A., Ottenhoff, T. H. M., Heidt, P. J., Gilbert, S. C., Gicquel, B., Hill, A. V. S., Martin, H., McShane, H., and Thomas, A. W. (2009). MVA.85A boosting of BCG and an attenuated, phoP deficient *M. tuberculosis* vaccine both show protective efficacy against tuberculosis in Rhesus macaques. *PLoS ONE* 4, e5264. doi: 10.1371/journal.pone.0005264

Wand, M., Muller, C., Titball, R., and Michell, S. (2011). Macrophage and *Galleria mellonella* infection models reflect the virulence of naturally occurring isolates of *B. pseudomallei, B. thailandensis* and *B. oklahomensis*. *BMC Microbiol.* 11, 11. doi: 10.1186/1471-2180-11-11

Wells, T. J., Tree, J. J., Ulett, G. C., and Schembri, M. A. (2007). Autotransporter proteins: novel targets at the bacterial cell surface. *FEMS Microbiol. Lett.* 274, 163–172.

White, N. (2003). Melioidosis. *Lancet* 361, 1715–1722.

Wiersinga, W., van der Poll, T., White, N., Day, N., and Peacock, S. (2006). Melioidosis: insights into the pathogenicity of *Burkholderia pseudomallei*. *Nat. Rev. Microbiol.* 4, 272–282.

Wiersinga, W. J., Dessing, M. C., Kager, P. A., Cheng, A. C., Limmathurotsakul, D., Day, N. P., Dondorp, A. M., van der Poll, T., and Peacock, S. J. (2007a). High-throughput mRNA profiling characterizes the expression of inflammatory molecules in sepsis caused by *Burkholderia pseudomallei*. *Infect. Immun.* 75, 3074–3079.

Wiersinga, W. J., Wieland, C. W., Dessing, M. C., Chantratita, N., Cheng, A. C., Limmathurotsakul, D., Chierakul, W., Leendertse, M., Florquin, S., de Vos, A. F.,White, N., Dondorp, A. M., Day, N. P., Peacock, S. J., and van der Poll, T. (2007b). Toll-like receptor 2 impairs host defense in Gram-negative sepsis caused by *Burkholderia pseudomallei* (melioidosis). *PLoS Med.* 4, e248. doi: 10.1371/journal.pmed.0040248

Wiersinga, W. J., Wieland, C. W., van der Windt, G. J. W., de Boer, A., Florquin, S., Dondorp, A., Day, N. P., Peacock, S. J., and van der Poll, T. (2007c). Endogenous interleukin-18 improves the early antimicrobial host response in severe melioidosis. 75, 3739–3746.

Wiersinga, W. J., and van der Poll, T. (2009). Immunity to *Burkholderia pseudomallei*. *Curr. Opin. Infect. Dis.* 22, 102–108.

Wiersinga, W. J., Wieland, C. W., Roelofs, J. J. T. H., and van der Poll, T. (2008). MyD88 dependent signaling contributes to protective host defense against *Burkholderia pseudomallei*. *PLoS ONE* 3, e3494. doi: 10.1371/journal.pone.0003494

Williamson, E. D. (2009). Plague. *Vaccine* 27, D56–D60.

Wong, K. T., Puthucheary, S. D., and Vadivelu, J. (1995). The histopathology of human melioidosis. *Histopathology* 26, 51–55.

Conflict of Interest Statement: The authors declare that the research was conducted in the absence of any commercial or financial relationships that could be construed as a potential conflict of interest.

Received: 11 July 2011; accepted: 06 September 2011; published online: 27 September 2011.

Citation: Patel N, Conejero L, De Reynal M, Easton A, Bancroft GJ and Titball RW (2011) Development of vaccines against Burkholderia pseudomallei. Front. Microbio. ***2****:198. doi: 10.3389/fmicb.2011.00198*

This article was submitted to Frontiers in Cellular and Infection Microbiology, a specialty of Frontiers in Microbiology.

frontiers in
MICROBIOLOGY

ORIGINAL RESEARCH ARTICLE
published: 21 November 2011
doi: 10.3389/fmicb.2011.00227

Protective antigens against glanders identified by expression library immunization

Gregory C. Whitlock[1†‡], Mark D. Robida[2‡], Barbara M. Judy[3], Omar Qazi[4], Katherine A. Brown[4,5], Arpaporn Deeraksa[3], Katherine Taylor[3], Shane Massey[1,3], Andrey Loskutov[2], Alex Y. Borovkov[2†], Kevin Brown[2], Jose A. Cano[2†], D. Mitchell Magee[2], Alfredo G. Torres[1,3,6], D. Mark Estes[1†] and Kathryn F. Sykes[2,7]*

[1] Department of Microbiology and Immunology, University of Texas Medical Branch, Galveston, TX, USA
[2] Center for Innovations in Medicine in the Biodesign Institute, Arizona State University, Tempe, AZ, USA
[3] Department of Pathology, University of Texas Medical Branch, Galveston, TX, USA
[4] Institute for Cellular and Molecular Biology, University of Texas, Austin, TX, USA
[5] Department of Chemistry and Biochemistry, University of Texas, Austin, TX, USA
[6] Sealy Center for Vaccine Development, University of Texas Medical Branch, Galveston, TX, USA
[7] School of Life Sciences, Arizona State University, Tempe, AZ, USA

Edited by:
Ivo Steinmetz, University of Greifswald, Germany

Reviewed by:
Shu-Lin Liu, Harbin Medical University, China
Baolin Sun, University of Science and Technology of China, China

***Correspondence:**
Kathryn F. Sykes, Center for Innovations in Medicine, Biodesign Institute, School of Life Sciences, Arizona State University, 1001 McAllister Avenue, Tempe, AZ 85287-5901, USA.
e-mail: kathryn.sykes@asu.edu

†Present address:
Gregory C. Whitlock, Roche Diagnostics, Inc., Indianapolis, IA 46250, USA;
Alex Y. Borovkov, Synbuild LLC, Mesa, AZ 85201, USA;
Jose A. Cano, Universidad Politecnica del Estado de Morelos, Biotecnologia, Jiutepec, Morelos Mexico, Mexico;
D. Mark Estes, Department of Infectious Diseases, College of Veterinary Medicine, Univerity of Georgia, Athens, GA 30602, USA.

‡*Gregory C. Whitlock and Mark D. Robida have contributed equally to this work.*

Burkholderia are highly evolved Gram-negative bacteria that primarily infect solipeds but are transmitted to humans by ingestion and cutaneous or aerosol exposures. Heightened concern over human infections of *Burkholderia mallei* and the very closely related species *B. pseudomallei* is due to the pathogens' proven effectiveness as bioweapons, and to the increased potential for natural opportunistic infections in the growing diabetic and immunocompromised populations. These *Burkholderia* species are nearly impervious to antibiotic treatments and no vaccine exists. In this study, the genome of the highly virulent *B. mallei* ATCC23344 strain was examined by expression library immunization for gene-encoded protective antigens. This protocol for genomic-scale functional screening was customized to accommodate the unusually large complexity of *Burkholderia*, and yielded 12 new putative vaccine candidates. Five of the candidates were individually tested as protein immunogens and three were found to confer significant partial protection against a lethal pulmonary infection in a murine model of disease. Determinations of peripheral blood cytokine and chemokine profiles following individual protein immunizations show that interleukin-2 (IL-2) and IL-4 are elicited by the three confirmed candidates, but unexpectedly interferon-γ and tumor necrosis factor-α are not. We suggest that these pathogen components, discovered using genetic immunization and confirmed in a conventional protein format, will be useful toward the development of a safe and effective glanders vaccine.

Keywords: *Burkholderia, B. mallei*, glanders vaccine, expression library immunization, functional genomics, genetic immunization, DNA vaccine, subunit vaccine

INTRODUCTION

Burkholderia mallei remains an endemic pathogen in many parts of the world including Africa, Asia, the Middle East, and South America (Elschner et al., 2011). This Gram-negative, facultative aerobic bacillus primarily infects solipeds, with horses considered the natural reservoir; however, human infections occur zoonotically. The course of disease depends on the route of infection. Direct contact with the skin leads to a localized cutaneous infection called farcy. Contact with nasal or oral mucosal surfaces or inhalation lead to a highly infectious, painful, and incapacitating disease called glanders (Nierman et al., 2004). Acute symptoms include coughing, fever, and the release of infectious nasal discharge. Nodular lesions form in the lungs and ulcers develop in the mucous membranes of the upper respiratory tract. Without aggressive antibiotic treatment disease progresses to septicemia and is nearly 100% fatal (Waag et al., 2005). Survivors can suffer chronic infections of the muscle liver and spleen for up to 20 years, and remain carriers (Whitlock et al., 2008). Even if quickly diagnosed, antibiotic treatments have shown low efficacy and require long regimens with multiple drugs. Moreover, no vaccine candidate has even progressed to a clinical trial (Kenny et al., 1999; Leelarasamee, 2004; Bondi and Goldberg, 2008). These therapeutic hurdles arise from a number of pathogen characteristics including its ability to reside in the vacuoles of eukaryotic cells. Other immune evading tactics, including high genomic variability (Nierman et al., 2004), have rendered the performance of even live

vaccines disappointing (Ulrich et al., 2005). In addition to being a naturally occurring disease, glanders has been used as a bioweapon against cavalry in the American Civil War, World War I, and World War II (Nierman et al., 2004). The severe nature of the disease and the lack of treatment options, combined with the potential for microbe aerosolization, have made *B. mallei* a member of the Center for Disease Control and Prevention category B Priority Agent list.

Immune correlates of protection for *B. mallei* are not well developed. Its capacity to replicate inside host cells suggests that cell-mediated responses are likely to be linked to protection. However, vaccine studies with heat-killed (HK) *B. mallei* strains, either encapsulated or not, elicited mixed T helper cell type 1/type 2 responses in mice that were only weakly protective (Amemiya et al., 2002; Whitlock et al., 2008). A live capsule-deficient *B. mallei* mutant was not protective; however, aerosol immunization with a live-attenuated auxotrophic mutant conferred 50% survival against aerosol challenge, although the mice were unable to clear the infection. This strain was shown to elicit a Th1-skewed antibody response (IgG2a > to IgG1; Ulrich et al., 2005). In a recent study, the type III secretion system protein BopA was shown to improve survival rate, but also failed to provide sterilizing immunity. It generated a strong Th1-skewed antibody response and T cells that produced γ-interferon (IFNγ; Whitlock et al., 2010).

Although not optimal, the protection conferred by the live *B. mallei* strain and BopA indicate that developing a *Burkholderia* vaccine is possible. The inherent advantage of a live-attenuated vaccine is that no antigen identification or development is required, and broad antigenic diversity is possible because all components are delivered. Molecular component vaccines are an alternative to the use of live or killed preparations. A component design enables immense control relative to whole-pathogen compositions for improving manufacture, product safety and consistency, and vaccine efficacy; however, antigen discovery is required. Discovery is a considerable challenge for *Burkholderia* species because of the unusual fluidity and large size of their genomes, the functional and antigenic diversity of isolates, and the exceptional complexities of the immune responses that infection can elicit (Holden et al., 2004; Nierman et al., 2004; U'Ren et al., 2007). These factors suggest that if a component design is pursued, multiple components will need to be discovered to confer robust protection. Toward this purpose, over 1500 complete bacterial genome sequences are currently published (Relman, 2011). However, the characteristics of a pathogen component that make it protective are poorly understood. Furthermore, a substantial portion of the open reading frames (ORFs) in microbial databases remain without known function (Cui et al., 2005), thereby restricting sequence-based analyses as a method of candidate discovery.

In addition to *in silico* analyses, the large microbial sequence databases can be used for the design and construction of genes and proteins for empirical testing as antigens. New molecular technologies have begun to provide solutions for making production and testing possible on genomic scales. For example, through genetic immunization (Tang et al., 1992) libraries of constructed genes expressing the full coding capacity of a pathogen genome can be delivered into an animal to elicit immune responses to the pathogen proteome in a process termed expression library immunization (ELI; Barry et al., 1995). These libraries are introduced into animals as organized sub-library pools from which individual ORFs are identified for further study based on their ability to stimulate immunity against pathogen challenge. To avoid thousands of time-consuming and bias-ridden cloning steps, we developed linear expression elements (LEEs) that can be rendered genetically active by simply attaching desired expression sequences such as a promoter and terminator (Sykes and Johnston, 1999b). This study demonstrates the utility of a modified ELI method for the discovery of *B. mallei* component vaccine candidates. BALB/c mice were immunized with LEE pools expressing the *B. mallei* ATCC23344 ORF-eome. To address the individual dose diluting effects of the highly mixed ORF pools, a two-dimensional pooling strategy with divergent complexities was applied. In addition, LEEs were gene gun administered using a modified DNA/gold-particle formulation that prevented DNA loss during bombardment. Challenge–protection assays identified 12 ORFs as potential vaccine candidates. Testing of 5 of these 12 candidates individually in a protein subunit format confirmed that three confer significant partial protection against pulmonary challenge and showed that they elicit a CD4-like T cell cytokine response.

MATERIALS AND METHODS

B. MALLEI CULTURING AND GENOMIC DNA ISOLATION

Burkholderia mallei strain ATCC 23344 (China 7) was cultured on Luria–Bertani (LB) agar plates supplemented with 4% glycerol agar plates for 48 h at 37°C. Isolated colonies were sub-cultured to LB broth with 4% glycerol, and incubated at 37°C until exponential growth phase was reached. To obtain HK inoculums, bacterial suspensions were incubated at 85°C for 3 h and stored at 4°C until use. The absence of live *B. mallei* organisms in the HK preparations was confirmed by plating 10% of the total inoculums (v/v) and incubating these at 37°C for 48 h. All procedures were performed under biosafety level-3 containment.

To isolate genomic DNA, bacilli were cultured at 37°C in LB broth for 18 h and then pelleted at 3000–5000 g for 5–10 min at room temperature. The cells were resuspended in 1 ml of buffer B1 (with RNase A; Qiagen, Valencia, CA, USA) to obtain efficient lysis of the bacteria, then 20 μl of lysozyme stock solution and 45 μl of Proteinase K solution were added and the samples were incubated at 37°C for at least 30 min. Buffer 2 (0.35 ml) was added and tubes were mixed and incubated at 50°C for 30 min in a heatblock. Lysates were added to a Qiagen Genomic-tip 500/G purification column and genomic DNA was extracted following manufacturer's instructions.

ORF AMPLIFICATION, LEE ASSEMBLY, AND GENETIC ADJUVANT PREPARATION

The genomic sequence of the two chromosomes of *B. mallei* ATCC23344 were downloaded from GenBank (accession no. CP000010; CP000011). The genome contains a predicted total of 5535 genes (Nierman et al., 2004). In-house software (GeneSplitter) was used to confirm coding sequence annotations and assign a project number to each gene. To design the project's ORF-eome, all genes of 1 kb or less were generated as full length gene ORFs; genes longer than 1 kb were generated as a set of ∼800 bp long sub-genes overlapping by approximately 100 bp, thereby increasing the number of total ORFs in the library. If no primers could be designed to specifically amplify individual

members of a gene family, then the whole family was permitted to be amplified with a single oligo pair and this was recorded. The resulting mixed PCR product was designated with a single ORF number, thereby decreasing the total number of numerically defined ORFs relative to the annotation. Using these rules, a total of 6630 unique *B. mallei* ORFs were electronically defined; a corresponding number of ORF specific primer pairs were predicted and obtained containing a 5′ common forward or reverse region in addition to the ORF specific sequences. In a first step PCR, ORFs were amplified by 20 cycles of denaturation at 98°C, 40 s of annealing at 66°C, and 2 min of extension at 72°C from ∼100 to 150 ng of *B. mallei* ATCC23344 genomic DNA. The MasterTaq Kit (5′) was used with 1× Taq buffer with $MgCl_2$, 1× Taq Master PCR Enhancer, 0.5 units of Taq, 200 μM dNTPs, and 200 nM of ORF specific primers with a common adapter region (forward primers: GGTATAGGCGGAAGCGGATTG; reverse primers: GTGGGAGGGAGGTTAGGT) in a total volume of 10 μl. Universal primers were designed for use in a second step PCR with the common adapter region preceded by a region containing deoxyuracil (dU) phosphoramidite bases at intervals of three within a short 5′ stretch of the ORFs (forward primer: *AGUAGUA GUAGUAGU*GGTATAGGCGGAAGCGGATTG; reverse primer: *AUGAUGAUGAUGAUGAU*GTGGGAGGGAGGTTAGGT). This reaction was set up as a 90-μl master mix containing 1× Taq buffer with $MgCl_2$, 1× Taq Master PCR Enhancer, five units of Taq (Invitrogen), 200 μM dNTPs, and 250 nM of the dU-universal primers, which was then added to the 10-μl first step PCR reaction product. Amplification was conducted with 5 cycles of 30 s denaturation at 98°C, 40 s of annealing at 50°C, and 2 min of extension at 72°C followed by 2 min of extension at 72°C, followed by 15 cycles of denaturation at 98°C, 40 s of annealing at 66°C, and 2 min of extension at 72°C. This dU extension of the ORFs rendered them sensitive to uracil-DNA glycosylase (UDG). This two-step amplification protocol was developed after many optimization tests in which a large number of protocols, kits, and reagents for amplifying ORFs from high-GC genomes were evaluated. Using this protocol 5760 of the 6630 *B. mallei* ORFs were amplified (87%) as high quality products (specific, correct molecular weight) of sufficient yield for LEE construction. ORF yields were quantified fluorimetrically using PicoGreen (Invitrogen). At least 1 pmol of each ORF was generated for use in the library screen.

The cytomegalovirus (CMV) promoter and murine ubiquitin (UB) gene sequences (1.3 kb) and the human growth hormone (hGH) gene terminator sequence (0.6 kb) from pCMVi–UB (Sykes and Johnston, 1999a) were amplified by PCR as two separate fragments, in bulk, with primers carrying dU stretches complementary to those present within the ORF end sequences. These sequence-compatible PCR fragments would serve as upstream and downstream elements for attachment to the ORFs. In preparation, the fragments were gel-fractionated and then purified from preparative agarose gels using QIAquick Gel extraction Kit (Qiagen), and stored at −20°C until LEEs were ready to be non-covalently assembled.

In addition to this library of ORFs, two non *B. mallei* ORFs were similarly prepared in the two-step protocol for use in control group immunizations. The firefly luciferase (LUC) and human α1-antitrypsin gene (AAT) genes were amplified in the first step from pCMViLUC+ and pCMViAAT (Sykes and Johnston, 1999b). The same universal primers described for the library were used in the second step amplification. The LUC and AAT-expressing LEEs would serve as irrelevant antigens for the challenge–protection assays; however, the LUC and AAT LEEs would also be positive controls for gene and genetic immunization activity, respectively. An extra group of mice were bombarded with the LUC-expressing LEEs prepared from the same batch of gene gun cartridges (bullets) as used for the immunizations. Mice were culled 24 h later and ears were harvested to assay LUC activity (Promega, Inc.; Svarovsky et al., 2008). The AAT-expressing LEE served as a positive control for genetic immunization efficiency, as immune sera was later tested for anti-AAT reactivity by ELISA (Sykes and Johnston, 1999b).

The genetic adjuvants heat-labile toxin subunit A (LTA) and subunit B (LTB) of *E. coli* were generated by cloning the respective subunit-encoding genes into the *Bgl*II and *Hin*dIII sites in the multi-cloning site of pCMVi (Sykes and Johnston, 1999a). LTA- and LTB-expressing covalently prepared LEEs containing the promoter, the LTA or LTB ORF, and terminator sequences were generated by digesting the pCMVi–LTA and pCMVi–LTB plasmids with *Dra*I and *Pvu*II. These enzymes serve to linearize the plasmid and cleave most of the plasmid backbone from the gene expression sequences. The LT-expressing LEE fragments were purified from the pCMVi backbone by fractionation using a size-exclusion (Sepharose) column. Fractions were analyzed on a 0.8% agarose gel to identify the LEE fragments, and these fractions were pooled. These plasmid sub-fragments were used for this large scale production of elements for the library of LEEs because large scale production of DNA by PCR is less efficient than that by standard plasmid production.

ORF POOLING, LEE ASSEMBLY, AND BIOLISTIC PARTICLE PREPARATION

The 5760 *B. mallei* ORFs were concentration normalized and then pooled as ORFs using a two-dimensional 96 × 48 pool grid design, such that each dimension held all ORFs of the library. Therefore each ORF was present once per dimension and twice within the full grid. The ORFs within the X-dimension were partitioned into pools by a different sorting method than the ORFs in the Y-dimension such that each ORF resided in a pool of different co-resident ORFs within one dimension relative to the other and these pools were of different ORF complexities in one dimension relative to the other. Since the total DNA dose per gene gun bombardment (shot) was constant, the effect of altering the pool complexity was to alter the dose per ORF. The X-dimension pools delivered 10.5 fmol of each ORF per shot and the Y-dimension pools delivered 5.25 fmole of each ORF per shot. This was accomplished as follows: The ORFs were arrayed into the B–G rows of 80 separate 96-well plates. The 96 X-dimension pools were comprised of 60 ORF components that were pooled by taking all of the ORFs from a specific column from each of 10 plates (for example column 1 of plates 1–10; 1 column/plate × 6 ORFs/column × 10 plates/pool = 60 ORFs/pool). The 48 Y-dimension pools consisted of 120 ORFs that were pooled by taking all of the ORFs from a specific row from each of 10 plates (for example the B row of plates 1–10; 1 row/plate × 12 ORFs/row × 10 plates/pool = 120 ORFs/pool). Upstream and downstream expression elements were added to each pool to equimolar ratio to total 40.3 pmol ORFs per pool. The LTA and LTB adjuvant expressing ORFs were added to

each pool in 1:9 ratio. The combined DNA mixtures representing each pool were ethanol precipitated, dissolved in water and 200 μl aliquots (3 + 1 tubes) were stores at −20°C until genetic immunization was scheduled. UDG (NEB) treatment of DNA in each pool was performed immediately prior to the preparation of gene gun cartridges. For each mixture, 1.25 U of UDG enzyme was added per picomole of dU ends in pool (200 U for 200 μl aliquot). Incubation of UDG reaction was carried out for 45 min at 37°C then 10 min at 60°C and cooling down to room temperature. The reaction mixtures were ethanol precipitated and dissolved in 100 μl water.

For biolistic immunization, LEE pools were loaded onto positively charged (polyethyleneimine, PEI)-gold micro/nano particles as previously described (Svarovsky et al., 2008, 2009) and prepared onto gene gun cartridges for gene gun discharge.

GENETIC IMMUNIZATION AND *B. MALLEI* CHALLENGE

Female, 6- to 8-week-old, BALB/c mice (Harlan Sprague Dawley, Inc., Indianapolis, IN, USA) were acquired and housed under specific-pathogen-free-conditions with food and water *ad libitum* on a 12-h dark/light schedule for 1 week before use. The mice were organized into groups of eight mice genetically vaccinated in the ear skin pinnae with a Helios Gene Gun (Bio-Rad, Hercules, CA, USA) loaded with DNA coated gold particles (Svarovsky et al., 2009) and delivery at a helium pressure of 350 p.s.i. Two shots were delivered to each mouse, one in each ear. Genetic boosts with identical genetic inocula were administered at week 6 post-prime. Negative control mice were either unimmunized or immunized with a LEE expressing the irrelevant (non *B. mallei*) AAT antigen. Vaccine control mice were vaccinated with 0.5 μg of HK *B. mallei* [with Interleukin-12 (IL-12)] by intraparenteral (i.p.) injection using a 25-gage syringe. Mice were challenged with 5×10^5 CFU/50 μl of live *B. mallei* (∼2 LD_{50}) by intranasal (i.n.) delivery 12–13 weeks following the boost. Aliquots from the inocula were plated to confirm the infecting dose. The challenge experiment was carried out in four cascaded sub-experiments due to animal housing limits; however, the same naïve, irrelevant LEE, and positive vaccine controls were included in each sub-experiment. All procedures and animal protocols used in this study were approved by the Biosafety and IACUC committees at UTMB and conducted in either BSL-3 or ABSL-3 laboratories. Survival of mice was monitored at 12 h intervals over time. Survival readouts were analyzed as detailed in the Section "Results." In the sub-experiment testing X1 through X40, no mice died from challenge including the unimmunized controls, indicating a sublethal dose had been administered. Since survival could not be scored as a valid readout for these groups, mice were sacrificed and lungs were weighed as a measure of the severity of inflammatory disease. Challenge results are provided in **Table A1** in Appendix. Lung weight increase has been associated with increased disease (Huppert et al., 1976). However since these readouts could not be combined statistically with the survival data, these groups were excluded from the protection score grid analyses.

RECOMBINANT PROTEIN PRODUCTION OF A SUBSET OF *B. MALLEI* CANDIDATES

Cloning and protein expression protocols were followed as described previously (Whitlock et al., 2010). Briefly, target sequences were subjected to bioinformatics analysis using SignalP v.3.0 (Bendtsen et al., 2004), TMHMM v.2.0 (Krogh et al., 2001), and PHYRE v.0.2 (Kelley et al., 2009) to identify putative N-terminal amino acid (AA) secretion sequences, transmembrane domains, and homologies to published crystal structures, respectively. Protein subcellular localization was predicted using PSORTb v.3.0.2 (Yu et al., 2010) and CELLO v.2.5 (Yu et al., 2004). Informatically predicted signal peptides and transmembrane sequences were identified so as to avoid them if possible in the design of the ORFs for cloning into bacterial expression constructs. This was intended to facilitate recombinant production. The redesigned ORFs were PCR-amplified from genomic *B. mallei* DNA and cloned into pET28a(+) (Novagen), or pcDNA3.1 (Invitrogen) expression vector, in frame with either an N- or C-terminal 6× His affinity tag, or both. Oligo primers introducing specific restriction enzyme sites were purchased from Integrated DNA Technologies. In addition to the new targets, the GroEL gene (BMA_2001) was cloned to be produced and purified for use as a previously characterized immunogen (Amemiya et al., 2007).

For target protein production, *E. coli* host Rosetta (λDE3) was transformed with the expression constructs. Expression was induced by growth in Overnight Express instant TB medium (Novagen) for 18–20 h. Bacterial pellets were lysed using 10× CelLytic B (Sigma), and 6× His-tagged proteins purified by Ni^{2+} affinity chromatography. Purified proteins were dialyzed against two changes of 10 mM HEPES/150 mM NaCl, pH 7.4, aliquoted and stored at −80°C. Protein concentrations were determined using the BCA kit (Pierce) using bovine serum albumin (BSA) as a standard. Five of the 12 candidates and the previously identified antigen GroEL (hsp60) protein were sufficiently produced, with either an N- or C-terminal tag, or both, for vaccine testing. BMA_2001/GroEL (residues 1–550) and BMA_2821 (residues 418–753) were produced with both N- and C-terminal His tags. BMA_2804 (residues 17–370), BMA_A0768 (residues 20–489), and BMA_0816 were produced with C-terminal tags. BMA_0816 was produced in three sub-fragments (residues 43–334, 35–668, and 669–930) with C-terminal tags.

PROTEIN IMMUNIZATION AND VACCINE TESTING OF INDIVIDUAL CANDIDATES

Female, 6- to 8-week-old, BALB/c mice (groups of 12) were immunized by intramuscular (i.m.) injection with 10 μg of one of the purified candidate or control proteins, each formulated with 12.5 μg immune stimulating complexes (ISCOMs) AbISCO 100 (Isconova AB, Sweden) and 12.5 μg murine class C CpG motif oligos (ODN 2395; Coley Pharmaceuticals, Wellesley, MA, USA) in HEPES buffer (pH 7.4). A negative control group was administered the adjuvants only. Mice were boosted at week 4 post-prime with identical inocula and then challenged at week 7 by i.n. route with 2 LD_{50} (1×10^5) *B. mallei* ATCC23344. Deaths were recorded twice daily. Survival results were analyzed by a log-rank statistic test; Mantel–Haenszel survival curves were generated and plotted (PRISM, Graphpad, Inc.). The results from the groups of mice immunized with the same antigen but with an N versus a C-terminal tag were similar; therefore, these data were combined for analysis creating groups of 24 mice. The results from the N-terminal and the central sub-proteins of BMA_816 were similarly protective (the C-terminal sub-protein conferred no protection);

therefore, the results from these two groups were combined for analysis creating a group of 24 mice.

BIOPLEX ANALYSES OF CYTOKINE AND CHEMOKINE EXPRESSION

Peripheral blood sera levels of 23 cytokines and chemokines (IL-1α, IL-1β, IL-2, IL-3, IL-4, IL-5, IL-6, IL-9, IL-10, IL-12p40, IL-12p70, IL-13, IL-17, Eotaxin, G-CSF, GM-CSF, IFN-γ, KC, MCP-1, MIP-1α, MIP-1β, RANTES, and TNF-α) were determined using CD4 Pro Mouse Cytokine 23-plex Assay (Bio-Rad #M60-009RDPD). Blood samples from mice were collected 1 week prior to initial immunization (week −1) and 1 week after the second immunization (week 5 post-prime), and sera were analyzed as per manufacturer's instructions. Replicates of three animals per group per time point were used to determine cytokine and chemokine levels in the blood sera. An unpaired Student's t-test was used to evaluate significance ($p < 0.05$).

RESULTS

DESIGN AND VALIDATION OF LINEAR EXPRESSION ELEMENTS FOR MURINE GENETIC IMMUNIZATIONS

The *B. mallei* ATCC23344 genomic sequence was used to construct a library of 5760 unique ORFs for construction into LEEs. The upstream expression element carries both a CMV promoter and the short coding sequence of a mouse ubiquitin (UB) subunit for proteosome targeting and efficient antigen processing (Sykes and Johnston, 1999a). The downstream element carries a stop codon in all three frames and the efficient transcriptional terminator from hGH gene. The tripartite molecules are annealed to form functional LEEs (**Figure 1** inset).

Before large scale library production, pilot constructs were prepared as described above in order to validate gene vaccine activity in mice. The genes encoding five *B. mallei* proteins predicted to be secreted via the type III secretion system (Whitlock et al., 2007) were used; one of these was recently tested as a protective antigen (Whitlock et al., 2010). BopA (BMA_A1521), BopE (BMA_A1523), BipD (BMA_A1528), BipC (BMA_A1530), and BipB (BMA_A1531) were constructed and prepared as LEEs for mammalian expression. They were individually delivered into groups of five mice by gene gun together with LEEs encoding both subunits A and B of *E. coli* lethal enterotoxin (LTA/B) as genetic adjuvant (Peppoloni et al., 2003). One control group was immunized with LEEs expressing the non-glanders (irrelevant) luciferase (LUC) antigen with LTA/B; another control group was not immunized. Mice were genetically immunized at weeks 0, 3, and 6 followed by blood draws for evaluation of sera reactivity to recombinantly produced antigens. At week 9, i.p. challenges with 6×10^7 *B. mallei* were conducted. Survival results indicated several of the antigens conferred extended time to death; BopA and BipD provided 20% endpoint survival from the i.p. challenge (**Figure 1**). These results confirm that the LEE genetic immunization constructs are immunologically functional *in vivo*.

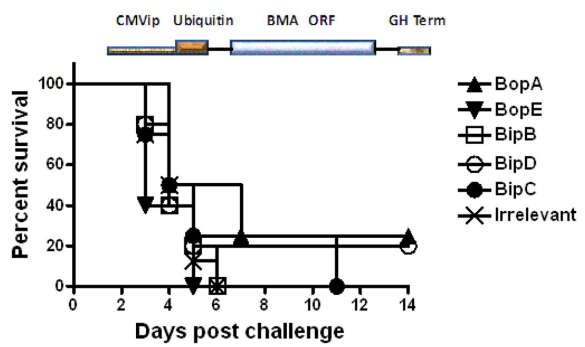

FIGURE 1 | Validation of ORF construction and expression *in vivo*. A set of five genes encoding *B. mallei* proteins predicted to be secreted were generated and constructed as linear expression elements (LEEs). These LEEs were constructed by the same protocols as intended for use in preparing and testing the *B. mallei* ORF library for vaccine candidates. Inset cartoon shows LEE design. These five LEEs were co-delivered with LEEs encoding the *E. coli* heat-labile enterotoxin subunits A and B (LTA/B) as adjuvant by gene gun at weeks 0, 3, and 6 into groups of five mice. At week 9, mice were evaluated immunologically in challenge–protection assays. Survival curves of immunized animals are plotted following i.n. delivery of 1×10^5 bacteria (2 LD_{50} *B. mallei* strain ATCC23344). The irrelevant group was immunized similarly but with a LEE expressing the luciferase (LUC) as a negative control for vaccine activity. This construct also served as a positive control for LEE gene expression activity (data not shown).

B. MALLEI EXPRESSION LIBRARY CONSTRUCTION AND STRATEGY FOR PROTECTIVE ANTIGEN SCREENING

Bioinformatic analyses of the genome identified a number of challenges for gene production relative to standard PCR amplification, including the high-GC content (70%) of the genome's coding sequences. In addition, several gene sequences displayed high homology; specific PCR amplification of these ORFs required detailed analyses of gene flanking sequences and individualized reaction conditions. Further design hurdles included the large number of transposable elements, bacterial introns, and overlapping transcripts that are found throughout the genome. Using the optimized reagents and protocol conditions, 5760 of the 6630 enumerated ORFs were amplified and constructed into LEEs, representing 87% of the coding capacity of *B. mallei*.

The ELI screen was designed to assay the vaccine potential of each *B. mallei* library component twice. This was done by distributing the complete library of 5760 ORFs into two immunization pools, by independent strategies that were designated X and Y. The feasibility of performing this multiplexed protection experiment design for antigen discovery was previously demonstrated (Stemke-Hale et al., 2005; Borovkov et al., 2009). For this project, each of the X-pools held 60 ORFs, creating 96 X's; each of the Y-pools held 120 ORFs, creating 48 Y's. Every ORF resided once in the X library and once in the Y library, but at doses that differed by twofold. Unlike earlier strategies, this enabled sensitivity to be optimized in the X-dimension and screening efficiency to be optimized in the Y-dimension. Two-dimensional matrix analyses of these organized distributions of ORFs would enable a single animal experiment of 144 groups to be used to infer which individual ORFs were responsible for disease protection.

GLANDERS ELI SCREEN

The inocula comprising the X and Y LEE pools were co-delivered with the LTA/B genetic adjuvant into groups of eight BALB/c mice by gene gun on charged-gold micro/nanoparticles (Svarovsky et al., 2009). Genetic boosts were delivered at week 6 post-prime using the same inocula. At week 18 post-prime, a lethal i.n. challenge of *B. mallei* (2 LD_{50}) was administered; mice were monitored

and deaths were recorded twice daily. As negative controls, naïve mice were not immunized and an irrelevant antigen group was administered an AAT-expressing LEE. As a positive control for protection, a group of mice was i.p. immunized with a HK *B. mallei* preparation with IL-12p70 as adjuvant.

Protection scores for all of the test and control groups were determined by recording the hours survived by each mouse, then deriving an average survival time for each group (**Table A1**). Confidence intervals (95%) and ANOVA scores were calculated to generate corresponding *p*-values for each test group relative to controls. In the X library of ORF-expressing LEE pools, X57, X59, and X89 conferred significantly extended times to death; within the Y library pools Y15 and Y19 were significantly protective ($p < 0.05$). These results are detailed in **Table 1**. In addition to the protection score analysis, log-rank Mantel–Haenszel survival curves were generated, with respective *p*-values calculated relative to controls (Prism 4.0, Graphpad Software, San Diego, CA, USA). This analysis indicated that mice immunized with pool Y24 also displayed significant extended time to death. Endpoint group survival rates are shown alongside each group's survival curve statistic in **Table 1**. Animals immunized with pool X89 showed 87.5% endpoint survival following lethal i.n. infection. Immunization with pools X57 and X59 provided animals 75% endpoint survival following the i.n. challenge. The mouse groups administered the positive vaccine control (HK *B. mallei* with IL-12p) displayed 100 and 62.5% survival rates in the X and Y challenge assays, respectively; the irrelevant antigen groups showed 25 and 0% survival in X and Y experiments, respectively. These survival curves are displayed in **Figure 2**; the top panel displays significantly different test group and also control group survival curves from the X challenge assay and the bottom panel similarly shows the Y challenge assay survival curves.

Together, the protection score and survival curve analyses indicated that three X-pools and three Y-pools were significantly protective. However, the pooling strategy of the two-dimensional screen designated Y-pools with twice the ORF complexity of the X-pools (120 versus 60 ORFs). Since a matrix analysis would be most informative if a similar number of ORFs were crossed from each dimension (library), the X-pools ranked 4, 5, and 6 (X75, X76, and X95 with *p*-values of 0.17, 0.20, and 0.018, respectively) were taken into the cross-hair analyses. Their protection scores, survival rates, and statistics are provided in **Table 1**.

Table 1 | Analyses of ELI challenge–protection screen.

	Protection score (*p*-value)	Protection rank	Endpoint survival (%) (*p*-value)
X-POOLS			
X89	423 (0.003)	1	87.5 (0.006)
X57	372 (0.03)	2	75 (0.029)
X59	365 (0.04)	3	75 (0.05)
X75	321 (0.17)	4	62.5 (0.137)
X95	318 (0.18)	5	62.5 (0.158)
X76	317 (0.20)	6	62.5 (0.156)
Irrelevant	126 (0.59)		25
HK + IL-12	456 (0.0005)		100
Y-POOLS			
Y19	270 (0.02)	1	50 (0.027)
Y15	269 (0.02)	2	50 (0.08)
Y24	233 (0.10)	3	37.5 (0.05)
Irrelevant	146 (0.89)		0
HK + IL-12	336 (0.0003)		62.5

IDENTIFICATION AND TESTING OF SCREEN-INFERRED PROTECTIVE ANTIGENS

A matrix analysis was performed to pinpoint any antigens that conferred protection as a constituent within both its X-pool and Y-pool inocula. This was done by comparing the list of ORFs comprising the subset of X-pools selected for further evaluation

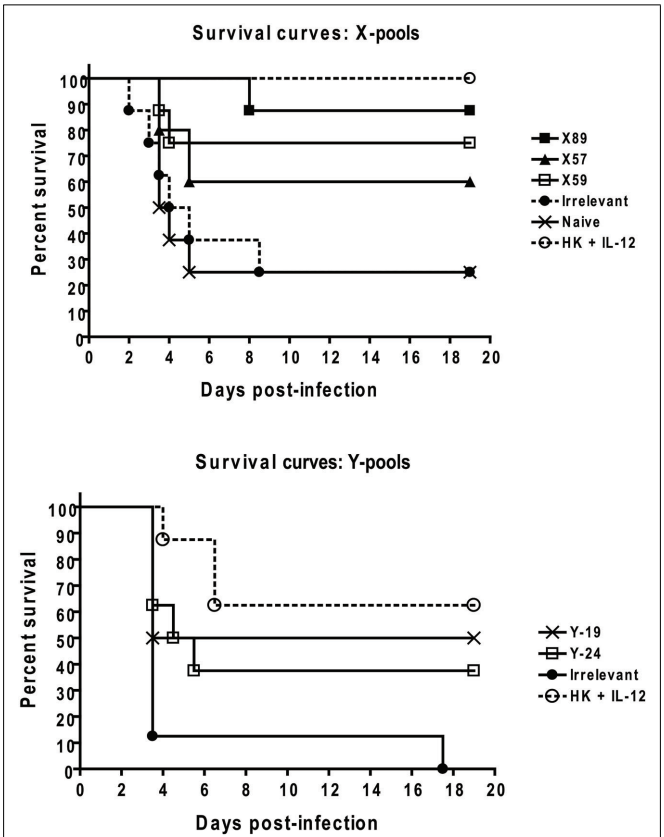

FIGURE 2 | Screening of the *B. mallei* ORF-ome for vaccine candidates by ORF-pool immunization and challenge–protection assay. Groups of eight mice were immunized once in each ear pinna with 1 μg dose by gene gun. Each discharge carried a pool of *B. mallei* ORFs as LEEs (0.9 μg) and the genetic adjuvant LTA/B (0.1 μg). The LTA and LTB-expressing LEEs were mixed 1:5 (0.08 and 0.02 μg, respectively). Two libraries of 5750 ORFs, labeled X and Y, were partitioned into 96 pools of 60 ORFs (X-pools) or 48 pools of 120 ORFs (Y-pools). Controls were heat-killed (HK) *B. mallei*, the non *B. mallei* antigen α1-antitrypsin (AAT), and naïve mice. Boosts were similarly administered at week 6. A 2 LD_{50} (1×10^5) dose of live *B. mallei* ATCC23344 was administered i.n. at week 10 and death was monitored twice daily. Survival curves were generated for all groups; however, only the curves corresponding to statistically protective groups ($p < 0.05$) and controls are plotted for clarity. Top graph displays results from animals immunized with protective pools from the X library. Bottom graph displays the survival courses of mouse groups administered the protective pools from the Y library.

to the list of ORFs comprising the Y-pools selected for evaluation. Furthermore, each ORF was considered to represent its full length target gene. This was done because a protective antigen often carries multiple protective epitopes (Crowe et al., 2010), and these are likely to rank differently in potency from one species to another as a result of divergent antigen presentation molecules and processes. Therefore, identification of any portion of a gene is likely to indicate a useful target antigen, as opposed to merely a target epitope. Twelve *B. mallei* genes were identified by this overlapping pool matrix analysis. These candidates are enumerated in **Table 2** along with their resident pools within the screen and any predicted protein functions or homologies found in existing databases.

To evaluate how genetic immunization leads might translate into more conventional protein subunit vaccine formulations, the 12 new gene vaccine candidates were subjected to structural analysis in preparation for testing in a new round of challenge–protection assays as individually administered protein inocula. Many of the target proteins carried multiple predicted transmembrane helices that would make recombinant protein production difficult. These were excluded from the expression constructs in favor of regions predicted to be immunogenic (see Materials and Methods). The BMA_0816 gene was cloned and expressed as three sub-fragments because of its large size. Five candidates (BMA_A0712, BMA_A0768, BMA_0816, BMA_2804, BMA_2821) and the previously described immunogen GroEL (BMA_2001; Amemiya et al., 2007) were bacterially produced with N- and/or C-terminal His tags and purified by standard nickel-affinity chromatography. Each of the six proteins was delivered i.m. with ISCOMs and murine class C motif CpG oligos as adjuvant into groups of 12 BALB/c mice. Boosts were administered at week 4 and then the mice were challenged with live *B. mallei* (2 LD_{50}) at week 7. Survival was monitored and recorded twice daily.

Protection was assessed by generating Mantel–Haenszel survival curves and deriving a log-rank statistic as described above. The results plotted in **Figure 3** show that three of the five tested candidates and GroEL were confirmed as conferring partial protection. Immunization with the protein encoded by BMA_A0768 provided 25% (3/12) endpoint survival while GroEL immunization provided 12.5% (3/24) endpoint survival and both displayed significantly extended times to death ($p = 0.025$ and $p < 0.001$, respectively). The proteins encoded by BMA_2821 and BMA_0816 also conferred significantly extended times to death ($p = 0.0023$ and $p < 0.0001$, respectively) relative to adjuvant only immunized controls. The three significantly protective candidates (BMA_A0768, BMA_2821, and BMA_0816) are highlighted in red in **Table 2**.

Table 2 | Individual *B. mallei* vaccine candidate genes identified from matrix analysis of the ELI challenge–protection assays.

ELI-derived vaccine candidate	Predicted function/homology	Resident ELI pools
BMA_A1219	Tetratricopeptide repeat protein	X95; Y24
BMA_A1678	Selenocysteine-specific translation elongation factor	X76; X95; Y24
BMA_A1678	Putative CpaE protein (pilus assembly)	X76; Y24
BMA_A1325	Major facilitator family sugar transporter	X95; Y24
BMA_A0712[1]	Major facilitator superfamily protein	X75; Y24
BMA_A0768[2]	Mannitol dehydrogenase family protein	X57; Y19
BMA_A0950	Major facilitator family transporter; MerR family transcriptional regulator	X89; Y24
BMA_2821[2]	Toxin secretion ABC transporter, ATP-binding protein (colicinV processing peptidase)	X75; Y15
BMA_2804[1]	Molecular chaperone, Hsp70	X75; Y19
BMA_2468	Glyceraldehyde-3-phosphate dehydrogenase, type I	X57; Y24
BMA_0092	Peptide ABC transporter, ATP-binding protein	X59; Y24
BMA_0816[2]	Maltooligosyl trehalose synthase (putative glycosyl hydrolase)	X89; Y24

[1] *Candidates tested individually are shown in boldface.*

[2] *Vaccine candidates found to be protective are indicated in red type.*

ELI VACCINE CANDIDATES ELICIT SERUM CYTOKINE AND CHEMOKINE RESPONSES

Blood was drawn from the animals described above, immunized with the five *B. mallei* protein antigen candidates or the adjuvant control, 1 week prior to immunization (week −1 relative to prime) as a baseline for each animal and then 1 week after the booster (= week 5 post-prime) as a measure of vaccine elicited responses. Measuring levels at these two time points was designed to display a profile of the hosts' responses to vaccination (**Figure 4**). The influence of the adjuvant on host responses was measured by comparing the pre-immunization profiles to that of the control sera, which was not drawn from naïve mice but from mice immunized with adjuvant only. Prior to immunization, GM-CSF (BMA_0768) and MIP-1β (BMA_0768) showed elevated levels relative to the adjuvant-immunized control sera; whereas IL-12p70 (BMA_A0712) was significantly lower in one of the pre-immune

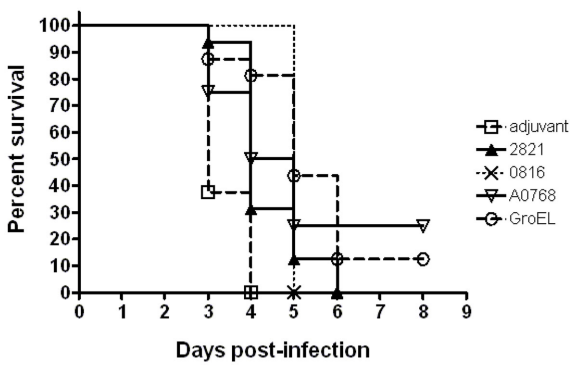

FIGURE 3 | Evaluation of a subset of the vaccine candidates identified by ELI, tested individually. Groups of 12 BALB/c mice were i.p. injected with the five candidates and GroEL (BMA 2001) delivered as recombinant bacterially produced proteins. These were formulated with ISCOMs and CpG's as adjuvants (adjuvant). Boosts were administered at week 4 post-prime and challenged by i.n. route with 2 LD_{50} (1×10^5) *B. mallei* ATCC23344 at week 7. Survival was monitored, recorded and analyzed as described in the Section "Materials and Methods." The Mantel–Haenszel survival curves for the control groups and for the three test groups that displayed statistically significant protection ($p < 0.05$) are plotted. GenBank BMA gene numbers are shown.

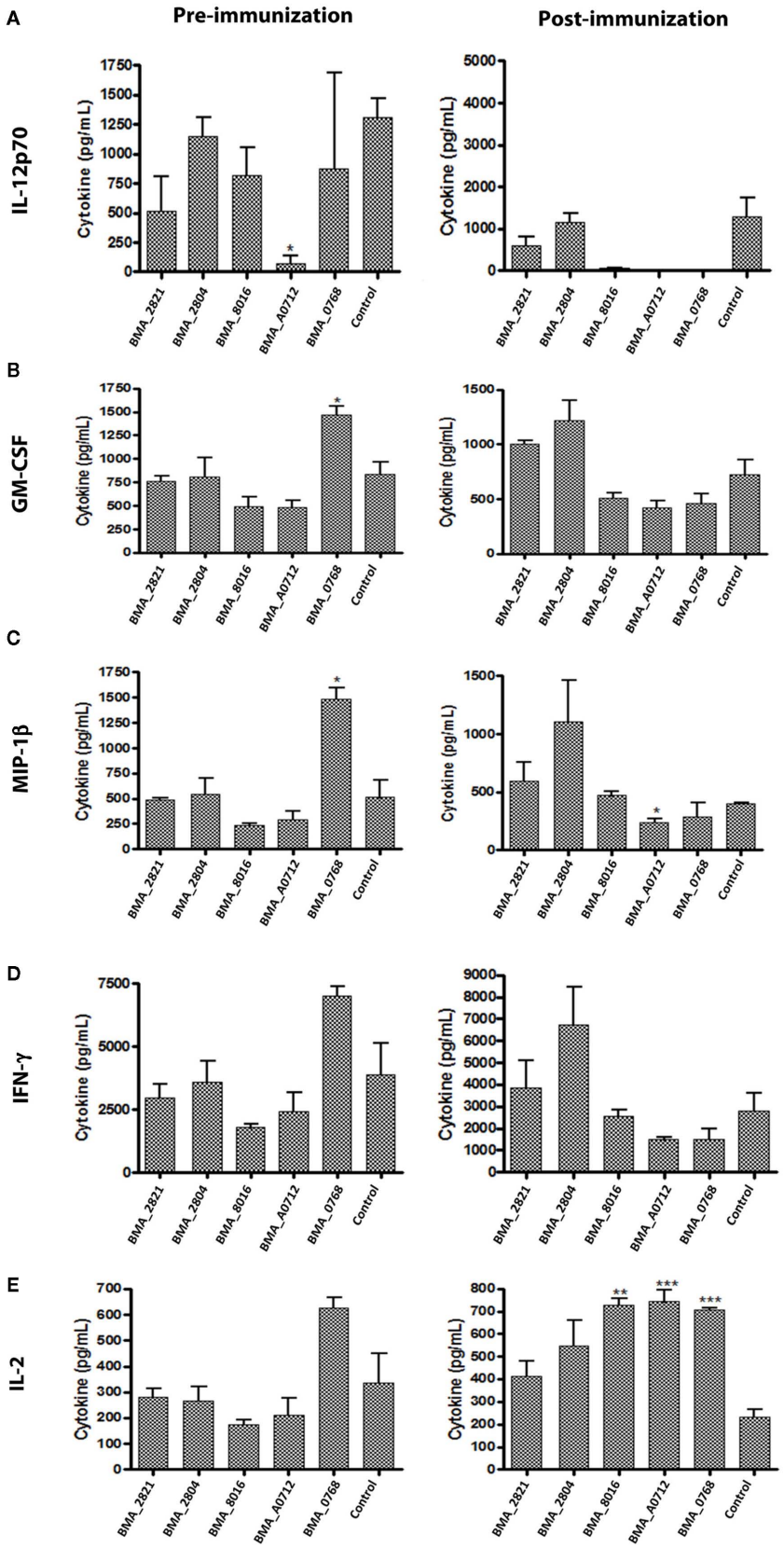

FIGURE 4 | Continued

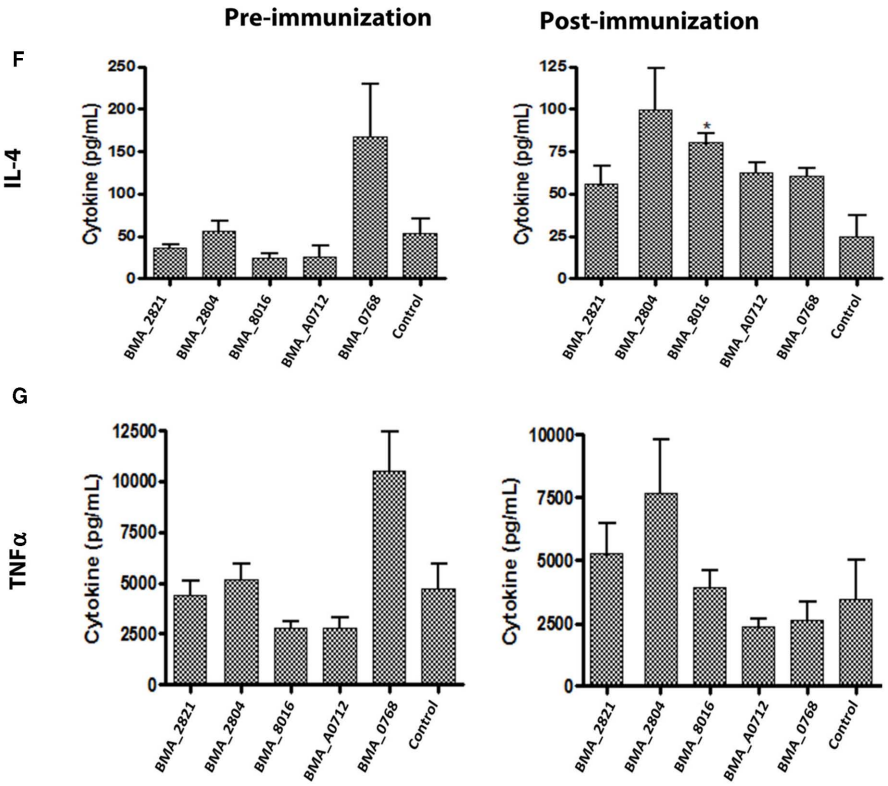

FIGURE 4 | Bioplex analyses of proinflammatory cytokines elicited in peripheral blood of immunized versus unimmunized mice. Blood was drawn (i) 1 week prior to immunization and (ii) 1 week post booster immunization (=5 weeks post-prime) of the mice described in **Figure 3**. Results from these time points are graphed on the left (pre-immunization) and right (post-immunization) panels. Control sera were drawn from adjuvant-immunized mice. Replicates of three animals per group per time point were used to determine the level of cytokine or chemokine indicated above each pair of graphs **(A)** through **(G)**. Sera were collected and analyzed per manufacturer's instructions. Unpaired Student's *t*-test was utilized to determine significance ($p < 0.05$). Error bars are SD with group sera.

sera groups relative to the sera from adjuvant expose mice. This indicates that IL-12p70 may be elicited by the ISCOM and CpG formulation alone. Post-immunization, IL-2 levels were significantly elevated in sera from mice immunized with three of the five antigen candidates (BMA_0816, BMA_A0712, BMA_0768), two of which were protective (**Figure 3**). IL-4 (BMA_0816) and MIP-1β (BMA_A0712) were also significantly different ($p < 0.05$) from the adjuvant-immunized control sera levels, with IL-4 elevated and MIP-1β reduced. These levels represent antigen-specific activity elicited by the vaccine candidates.

DISCUSSION

A functional genomics vaccine candidate screen does not need to assume anything about the properties or characteristics of protective antigens. However the screen presented here does assume that a protective gene can be detected among many simultaneously expressed ones. Support for this assumption lies in its parallel with the antigenic complexity of a live or whole-pathogen vaccine, or a pathogen infection, situations in which the immune system is exposed to a mixture of many antigens. We used ELI to directly test the *B. mallei* ORF-eome for protective components by genetic immunization followed by lethal challenge. A two-dimensional, matrix analysis of a genomic-scale protection assay following vaccination with pools of ORFs indicated 12 gene candidates as being responsible for conferring survival rates as high as ∼90% against i.n. challenges. Five of these 12 vaccine candidates were produced as proteins and tested as individual antigens in the challenge–protection assays; three were found to provide significant, partial protection from a lethal pulmonary infection with *B. mallei*.

The protection level measured following immunization with any of the five tested protein candidates was lower than that achieved by the ORF pools in which the candidates were originally resident. The simplest explanation for this outcome is that the more highly protective candidates were among the seven untested of the 12 matrix-inferred candidates. Even for the five tested candidates, only the portions of the target proteins selected for recombinant expression by bioinformatics were administered; more strongly protective epitopes may have been unintentionally excluded. Alternatively the antigen delivery format, which differed between the two rounds of challenge–protection assays, may be critical. First, the genetic immunization constructs expressed the antigens endogenously within the skin cells of the host, and these constructs carried proteasomal targeting (UB) sequences intended to promote cellular immune responses against the UB-fused antigen. By contrast, the candidates were redesigned in the second

round without UB fusion or their natural secretory leader peptides for *ex vivo* protein production. We had elected to reformulate the candidates from genes into proteins for the secondary round of vaccine testing because of the generally higher level of acceptance of this more traditional subunit vaccine format. Namely, several protein-based vaccines have already been FDA approved (http://www.fda.gov/BiologicsBloodVaccines/Vaccines/ApprovedProducts/UCM093833) while gene vaccines are at this time still in trials. Protein formats have been shown to promote T helper cell 2-like (Th2) responses and antibody production, relative to *in vivo* produced antigen (Chow et al., 1998; Iborra et al., 2007). These responses may not be as protective as Th1 responses against *B. mallei*. As a second difference in delivery format between the two rounds, the mixed versus individual context of the antigen may be relevant. The significance of this format distinction is consistent with several previous ELI screens in which all candidates were tested, and all tested as genes in both initial and secondary screens. In these studies, the mixed pool inocula were frequently more protective than the individually evaluated candidates (Stemke-Hale et al., 2005; Li et al., 2006; Borovkov et al., 2009), as found in this work.

We suggest that the complexity of the ORF pools is important. In this project, we intentionally designed a grid with differing complexities (either 60 or 120 in the X and Y-pools respectively) potentially capturing the undetermined effects of antigen dose, complexity, and competition on immunity. If there were neither negative nor positive interactions among the constituents of the mixed inocula, then we anticipated that maximizing dose would be most important in maximizing any response elicited. Since we delivered constant total genetic doses, this would mean that the lower pool complexity (higher individual ORF doses) of the X-pools would be advantaged over the Y-pools. However the average levels of protection conferred by the X versus the Y-pools, relative to HK *B mallei* and irrelevant antigens were similar. This indicates that dose was not a strong factor in the survival readout. Alternatively, if immunological interactions do occur among the pool constituents, then an ORF's individual performance level may be evaluated relative to that within a pool; however, the performance of an ORF in two different pools of two different complexities cannot be quantitatively interpreted. Antigenic competition has been well described among co-delivered protein antigens (Adorini et al., 1989); however, a range of results have been reported for immune interactions among co-delivered genetic antigens (Braun et al., 1998; Sedegah et al., 2004; Hirao et al., 2011). A combination of competitive and cooperative activities among the antigen pool components would have opposing effects that would blur minor differences in antigen dose. This is consistent with our observations. Nonetheless, the performance of both the X and Y antigen pools were reproducibly superior relative to that of the individually administered antigens. These results suggest that the overarching effect of gene vaccine complexity is cooperative. The three confirmed individual candidates may play a critical role as a specific antigen, while one or more of the remaining constituents of their highly protective resident pools may provide non-specific, or even additional specific, immunological help and modulation. This may be addressed in vaccine development in a number of ways. For example, a small set of cooperatively acting components may be identified in future studies that are highly effective. Protection levels may also be enhanced by immunomodulators that direct responses to those determined to be most effective. Mixed modality immunization regimens such as DNA-prime/protein- or live vectored-boosts may serve to widen the breadth of responses to facilitate greater protection levels. Notably, the ELI screen was done by genetic immunization and a long immunization regimen (18 weeks), whereas the individual components were delivered as proteins in an abbreviated regimen (7 weeks). Perhaps their combination in a mixed modality prime-boost regimen, and an extended immunization period, would be productive.

Bioplex determinations of a set of 23 cytokine and chemokines identified IL-2 as the principal cytokine elicited by the vaccine candidates. IL-2 was significantly elevated relative to controls in the sera from three of the five groups of mice immunized with individual protein antigens; two of these groups displayed significant protection from challenge. IL-4 was also significantly elevated in sera from mice immunized with one of the tested candidates that conferred protection. Notably, the cytokine profile elicited by these subunit vaccines is divergent from those stimulated following exposure to HK *B. mallei*, or the BopA subunit, which includes IFNγ and TNFα τ cell secretion (Whitlock et al., 2008, 2010). This suggests that improved protection might be achieved by either formulating these antigens with a different adjuvant or preparing the antigens in another format (such as genes or gene pools, or live vector) that would modulate the cytokine profile closer to that elicited by other vaccines. However, the strong CD4 T cell and antibody response indicated by expression of IL-2 and IL-4 is consistent with the importance found for B cells in the protective response to HK *B. mallei* (Whitlock et al., 2008). Notably, class C motif CpG oligos were selected as the adjuvant in this study because of the role demonstrated for antibodies in addition to cell-mediated responses in clearing *B. mallei* infections (Bondi and Goldberg, 2008). A more divergent explanation is that these three new antigens direct the host immune system to generate a unique protective response not engendered by previously tested subunits or by the pathogen itself.

In the microbial world, the genomes of *Burkholderia* species rank as some of the most complex, carrying nearly as many base pairs as a eukaryotic yeast genome (Holden et al., 2004; Nierman et al., 2004). *Through the empirical discovery approach described here, we have identified 12 new vaccine candidates for further evaluation* (**Table 2**). A number of these pathogen components were unlikely to have been selected informatically from the genome since the pSORT B-predictions indicated cytoplasmic localizations (**Table 3**). The preliminary testing of a subset of only five of these candidates established that *three conferred significant protection against a pulmonary challenge with virulent B. mallei bacilli.* Of these three protective candidates, two are predicted to encode cytoplasmic enzymes. First, BMA_A0768 displays homology to a mannitol dehydrogenase (MTD) gene, encoding a member of an oxidoreductase family. Mannitol and MTD are known to play roles in host defense and pathogen counter-defense (Jennings et al., 1998). Second, BMA_0816 is homologous to a maltooligosyl trehalose synthase gene, encoding an enzyme that catalyzes transglycosylations (Nakada et al., 1995). In contrast to these genes, the third vaccine candidate, BMA_2821, encodes a membrane protein. It shows homology to a member of the ATP-binding cassette (ABC) transporter family that secretes the peptide

Table 3 | Characteristics of individually protective subunit vaccine candidates.

B. mallei vaccine candidate	Cellular location	Percentage identity to Bpm 96243	Survival curve significance, *p*-value
BMA_A0768	Cytoplasmic[a,b]	99.8	0.025
BMA_2821	Inner membrane[a,b]	99.7	0.002
BMA_0816	Cytoplasmic[a,b]/outer membrane[b]	99.5	<0.0001

[a] *Determined by PSORTb v.3.0.2.*

[b] *Determined by CELLO v.2.5.*

antibiotic colicinV (Zhong et al., 1996). Colicin is encoded on a virulence plasmid and the ABC efflux transporter secretes it (Waters and Crosa, 1991). By conventional criteria, this surface-located virulence-factor secreting protein might have been classified as a putative protective antigen. Notably, another ABC transporter was within the set of 12 ELI-derived candidates, in addition to a sugar transporter; however, neither of these ORFs (BMA_0092 and BMA_A1325, respectively) was individually tested in the vaccine assay.

Sequence alignments of the protective *B. mallei* ORFs to the *B. pseudomallei* K96243 (Bpm 96243) strain homologs show a very high percentage of identity (**Table 3**), suggesting that these antigens may be able to cross-protect against *B. pseudomallei* infection. Further characterization and optimizations of the protective immune responses induced by these new candidates, and exploration of the remaining candidates, may reveal novel pathways to immunity against *B. mallei*, and possibly *B. pseudomallei*. In summary our results provide a basis for the development of a safe and effective *Burkholderia* vaccine, comprised of a set of genome-encoded pathogen components, against pulmonary glanders disease.

AUTHOR CONTRIBUTIONS

Kathryn F. Sykes, Alfredo G. Torres, and D. Mark Estes designed the research project; Gregory C. Whitlock, Mark D. Robida, Barbara M. Judy, Arpaporn Deeraksa, Katherine Taylor, C. Shane Massey, Andrey Loskutov, Alex Y. Borovkov, Jose A. Cano, and Kevin Brown executed the experiments and contributed to the analyses of results; Omar Qazi and Katherine A. Brown designed and produced critical reagents; Kathryn F. Sykes drafted the manuscript, and all authors contributed to the manuscript review and final preparation.

ACKNOWLEDGMENTS

These studies were supported by NIAID/NIH grant U54 AI 057156 from the Western Regional Center of Excellence for Biodefense. The contents are solely the responsibility of the authors and do not necessarily represent the official views of the RCE Programs Office, NIAID, or NIH. The authors would like to sincerely thank many members of the Center for Innovations of Medicine at ASU and the Departments of Microbiology and Immunology and Pathology at the University of Texas Medical Branch for collectively a very significant contribution to this research effort.

REFERENCES

Adorini, L., Appella, E., Doria, G., Cardinaux, F., and Nagy, Z. A. (1989). Competition for antigen presentation in living cells involves exchange of peptides bound by class II MHC molecules. *Nature* 342, 800–803.

Amemiya, K., Bush, G. V., Deshazer, D., and Waag, D. M. (2002). Nonviable *Burkholderia mallei* induces a mixed Th1- and Th2-like cytokine response in BALB/c mice. *Infect. Immun.* 70, 2319–2325.

Amemiya, K., Meyers, J. L., Deshazer, D., Riggins, R. N., Halasohoris, S., England, M., Ribot, W., Norris, S. L., and Waag, D. M. (2007). Detection of the host immune response to *Burkholderia mallei* heat-shock proteins GroEL and DnaK in a glanders patient and infected mice. *Diagn. Microbiol. Infect. Dis.* 59, 137–147.

Barry, M. A., Lai, W. C., and Johnston, S. A. (1995). Protection against mycoplasma infection using expression-library immunization. *Nature* 377, 632–635.

Bendtsen, J. D., Nielsen, H., Von Heijne, G., Brunak, S., Bendtsen, J. D., Nielsen, H., Von Heijne, G., and Brunak, S. (2004). Improved prediction of signal peptides: signalP 3.0. *J. Mol. Biol.* 340, 783–795.

Bondi, S. K., and Goldberg, J. B. (2008). Strategies toward vaccines against *Burkholderia mallei* and *Burkholderia pseudomallei*. *Expert Rev. Vaccines* 7, 1357–1365.

Borovkov, A., Magee, D. M., Loskutov, A., Cano, J. A., Selinsky, C., Zsemlye, J., Lyons, C. R., and Sykes, K. (2009). New classes of orthopoxvirus vaccine candidates by functionally screening a synthetic library for protective antigens. *Virology* 395, 97–113.

Braun, R., Babiuk, L. A., and Van Drunen Littel-Van Den, H. (1998). Compatibility of plasmids expressing different antigens in a single DNA vaccine formulation. *J. Gen. Virol.* 79(Pt 12), 2965–2970.

Chow, Y. H., Chiang, B. L., Lee, Y. L., Chi, W. K., Lin, W. C., Chen, Y. T., and Tao, M. H. (1998). Development of Th1 and Th2 populations and the nature of immune responses to hepatitis B virus DNA vaccines can be modulated by codelivery of various cytokine genes. *J. Immunol.* 160, 1320–1329.

Crowe, S. R., Ash, L. L., Engler, R. J., Ballard, J. D., Harley, J. B., Farris, A. D., and James, J. A. (2010). Select human anthrax protective antigen epitope-specific antibodies provide protection from lethal toxin challenge. *J. Infect. Dis.* 202, 251–260.

Cui, J., Han, L. Y., Cai, C. Z., Zheng, C. J., Ji, Z. L., and Chen, Y. Z. (2005). Prediction of functional class of novel bacterial proteins without the use of sequence similarity by a statistical learning method. *J. Mol. Microbiol. Biotechnol.* 9, 86–100.

Elschner, M. C., Scholz, H. C., Melzer, F., Saqib, M., Marten, P., Rassbach, A., Dietzsch, M., Schmoock, G., De Assis Santana, V. L., De Souza, M. M., Wernery, R., Wernery, U., and Neubauer, H. (2011). Use of a Western blot technique for the serodiagnosis of glanders. *BMC Vet. Res.* 7, 4. doi:10.1186/1746-6148-7-4

Hirao, L. A., Draghia-Akli, R., Prigge, J. T., Yang, M., Satishchandran, A., Wu, L., Hammarlund, E., Khan, A. S., Babas, T., Rhodes, L., Silvera, P., Slifka, M., Sardesai, N. Y., and Weiner, D. B. (2011). Multivalent smallpox DNA vaccine delivered by intradermal electroporation drives protective immunity in nonhuman primates against lethal monkeypox challenge. *J. Infect. Dis.* 203, 95–102.

Holden, M. T., Titball, R. W., Peacock, S. J., Cerdeno-Tarraga, A. M., Atkins, T., Crossman, L. C., Pitt, T., Churcher, C., Mungall, K., Bentley, S. D., Sebaihia, M., Thomson, N. R., Bason, N., Beacham, I. R., Brooks, K., Brown, K. A., Brown, N. F., Challis, G. L., Cherevach, I., Chillingworth, T., Cronin, A., Crossett, B., Davis, P., Deshazer, D., Feltwell, T., Fraser, A., Hance, Z., Hauser, H., Holroyd, S., Jagels, K., Keith, K. E., Maddison, M., Moule, S., Price, C., Quail, M. A., Rabbinowitsch, E., Rutherford, K., Sanders, M., Simmonds, M., Songsivilai, S., Stevens, K., Tumapa, S., Vesaratchavest, M., Whitehead, S., Yeats, C., Barrell, B. G., Oyston, P. C., Parkhill, J., Holden, M. T. G., Titball, R. W., Peacock, S. J., Cerdeno-Tarraga, A. M., Atkins, T., Crossman, L. C., Pitt, T., Churcher, C., Mungall, K., Bentley, S. D., Sebaihia, M., Thomson, N. R., Bason, N., Beacham, I. R., Brooks, K., Brown, K. A., Brown, N. F., Challis, G. L., Cherevach, I., Chillingworth, T., Cronin, A., Crossett, B., Davis, P.,

Deshazer, D., Feltwell, T., Fraser, A., Hance, Z., Hauser, H., Holroyd, S., Jagels, K., Keith, K. E., Maddison, M., Moule, S., Price, C., Quail, M. A., Rabbinowitsch, E., Rutherford, K., Sanders, M., Simmonds, M., Songsivilai, S., Stevens, K., Tumapa, S., Vesaratchavest, M., Whitehead, S., Yeats, C., Barrell, B. G., Oyston, P. C. F., and Parkhill, J. (2004). Genomic plasticity of the causative agent of melioidosis, *Burkholderia pseudomallei*. *Proc. Natl. Acad. Sci. U.S.A.* 101, 14240–14245.

Huppert, M., Sun, S. H., Gleason-Jordon, I., and Vukovich, K. R. (1976). Lung weight parallels disease severity in experimental coccidioidomycosis. *Infect. Immun.* 14, 1356–1368.

Iborra, S., Abanades, D. R., Parody, N., Carrion, J., Risueno, R. M., Pineda, M. A., Bonay, P., Alonso, C., and Soto, M. (2007). The immunodominant T helper 2 (Th2) response elicited in BALB/c mice by the *Leishmania* LiP2a and LiP2b acidic ribosomal proteins cannot be reverted by strong Th1 inducers. *Clin. Exp. Immunol.* 150, 375–385.

Jennings, D. B., Ehrenshaft, M., Pharr, D. M., and Williamson, J. D. (1998). Roles for mannitol and mannitol dehydrogenase in active oxygen-mediated plant defense. *Proc. Natl. Acad. Sci. U.S.A.* 95, 15129–15133.

Kelley, L. A., Sternberg, M. J., Kelley, L. A., and Sternberg, M. J. E. (2009). Protein structure prediction on the web: a case study using the Phyre server. *Nat. Protoc.* 4, 363–371.

Kenny, D. J., Russell, P., Rogers, D., Eley, S. M., and Titball, R. W. (1999). In vitro susceptability of *Burkholderia mallei* in comparison to those of other pathogenic *Burkholderia* spp. *Antimicrob. Agents Chemother.* 43, 2773–2775.

Krogh, A., Larsson, B., Von Heijne, G., and Sonnhammer, E. L. (2001). Predicting transmembrane protein topology with a hidden Markov model: application to complete genomes. *J. Mol. Biol.* 305, 567–580.

Leelarasamee, A. (2004). Recent development in melioidosis. *Curr. Opin. Infect. Dis.* 17, 131–136.

Li, D., Borovkov, A., Vaglenov, A., Wang, C., Kim, T., Gao, D., Sykes, K. F., Kaltenboeck, B., Li, D., Borovkov, A., Vaglenov, A., Wang, C., Kim, T., Gao, D., Sykes, K. F., and Kaltenboeck, B. (2006). Mouse model of respiratory *Chlamydia pneumoniae* infection for a genomic screen of subunit vaccine candidates. *Vaccine* 24, 2917–2927.

Nakada, T., Maruta, K., Tsusaki, K., Kubota, M., Chaen, H., Sugimoto, T., Kurimoto, M., and Tsujisaka, Y. (1995). Purification and properties of a novel enzyme, maltooligosyl trehalose synthase, from *Arthrobacter* sp. Q36. *Biosci. Biotechnol. Biochem.* 59, 2210–2214.

Nierman, W. C., Deshazer, D., Kim, H. S., Tettelin, H., Nelson, K. E., Feldblyum, T., Ulrich, R. L., Ronning, C. M., Brinkac, L. M., Daugherty, S. C., Davidsen, T. D., Deboy, R. T., Dimitrov, G., Dodson, R. J., Durkin, A. S., Gwinn, M. L., Haft, D. H., Khouri, H., Kolonay, J. F., Madupu, R., Mohammoud, Y., Nelson, W. C., Radune, D., Romero, C. M., Sarria, S., Selengut, J., Shamblin, C., Sullivan, S. A., White, O., Yu, Y., Zafar, N., Zhou, L., Fraser, C. M., Nierman, W. C., Deshazer, D., Kim, H. S., Tettelin, H., Nelson, K. E., Feldblyum, T., Ulrich, R. L., Ronning, C. M., Brinkac, L. M., Daugherty, S. C., Davidsen, T. D., Deboy, R. T., Dimitrov, G., Dodson, R. J., Durkin, A. S., Gwinn, M. L., Haft, D. H., Khouri, H., Kolonay, J. F., Madupu, R., Mohammoud, Y., Nelson, W. C., Radune, D., Romero, C. M., Sarria, S., Selengut, J., Shamblin, C., Sullivan, S. A., White, O., Yu, Y., Zafar, N., Zhou, L., and Fraser, C. M. (2004). Structural flexibility in the *Burkholderia mallei* genome. *Proc. Natl. Acad. Sci. U.S.A.* 101, 14246–14251.

Peppoloni, S., Ruggiero, P., Contorni, M., Morandi, M., Pizza, M., Rappuoli, R., Podda, A., and Del Giudice, G. (2003). Mutants of the *Escherichia coli* heat-labile enterotoxin as safe and strong adjuvants for intranasal delivery of vaccines. *Expert Rev. Vaccines* 2, 285–293.

Relman, D. A. (2011). Microbial genomics and infectious diseases. *N. Engl. J. Med.* 365, 347–357.

Sedegah, M., Charoenvit, Y., Minh, L., Belmonte, M., Majam, V. F., Abot, S., Ganeshan, H., Kumar, S., Bacon, D. J., Stowers, A., Narum, D. L., Carucci, D. J., and Rogers, W. O. (2004). Reduced immunogenicity of DNA vaccine plasmids in mixtures. *Gene Ther.* 11, 448–456.

Stemke-Hale, K., Kaltenboeck, B., Degraves, F. J., Sykes, K. F., Huang, J., Bu, C. H., Johnston, S. A., Stemke-Hale, K., Kaltenboeck, B., Degraves, F. J., Sykes, K. F., Huang, J., Bu, C.-H., and Johnston, S. A. (2005). Screening the whole genome of a pathogen in vivo for individual protective antigens. *Vaccine* 23, 3016–3025.

Svarovsky, S., Borovkov, A., and Sykes, K. (2008). Cationic gold microparticles for biolistic delivery of nucleic acids. *Biotechniques* 45, 535–540.

Svarovsky, S. A., Gonzalez-Moa, M. J., Robida, M. D., Borovkov, A. Y., and Sykes, K. (2009). Self-assembled micronanoplexes for improved biolistic delivery of nucleic acids. *Mol. Pharm.* 6, 1927–1933.

Sykes, K. F., and Johnston, S. A. (1999a). Genetic live vaccines mimic the antigenicity but not pathogenicity of live viruses. *DNA Cell Biol.* 18, 521–531.

Sykes, K. F., and Johnston, S. A. (1999b). Linear expression elements: a rapid, in vivo, method to screen for gene functions. *Nat. Biotechnol.* 17, 355–359.

Tang, D. C., Devit, M., and Johnston, S. A. (1992). Genetic immunization is a simple method for eliciting an immune response. *Nature* 356, 152–154.

Ulrich, R. L., Amemiya, K., Waag, D. M., Roy, C. J., and Deshazer, D. (2005). Aerogenic vaccination with a *Burkholderia mallei* auxotroph protects against aerosol-initiated glanders in mice. *Vaccine* 23, 1986–1992.

U'Ren, J. M., Schupp, J. M., Pearson, T., Hornstra, H., Friedman, C. L., Smith, K. L., Daugherty, R. R., Rhoton, S. D., Leadem, B., Georgia, S., Cardon, M., Huynh, L. Y., Deshazer, D., Harvey, S. P., Robison, R., Gal, D., Mayo, M. J., Wagner, D., Currie, B. J., Keim, P., U'ren, J. M., Schupp, J. M., Pearson, T., Hornstra, H., Friedman, C. L. C., Smith, K. L., Daugherty, R. R. L., Rhoton, S. D., Leadem, B., Georgia, S., Cardon, M., Huynh, L. Y., Deshazer, D., Harvey, S. P., Robison, R., Gal, D., Mayo, M. J., Wagner, D., Currie, B. J., and Keim, P. (2007). Tandem repeat regions within the *Burkholderia pseudomallei* genome and their application for high resolution genotyping. *BMC Microbiol.* 7, 23. doi:10.1186/1471-2180-7-23

Waag, D. M., Deshazer, D., Lindler, L. E., Lebeda, F. J., Korch, G. W., and Meselson, M. (eds). (2005). *Glanders, New Insights into an Old Disease*. Totowa, NJ: Humana Press.

Waters, V. L., and Crosa, J. H. (1991). Colicin V virulence plasmids. *Microbiol. Rev.* 55, 437–450.

Whitlock, C., Deeraksa, A., Qazi, O., Judy, B. M., Taylor, K., Propst, K. L., Duffy, A. J., Johnson, K., Kitto, G. B., Brown, K. A., Dow, S. W., Torres, A. G., and Estes, D. M. (2010). Protective response to subunit vaccination against intranasal *Burkholderia mallei* and *B. pseudomallei* challenge. *Procedia Vaccinol.* 2, 71–75.

Whitlock, G. C., Estes, D. M., and Torres, A. G. (2007). Glanders: off to the races with *Burkholderia mallei*. *FEMS Microbiol. Lett.* 277, 115–122.

Whitlock, G. C., Lukaszewski, R. A., Judy, B. M., Paessler, S., Torres, A. G., and Estes, D. M. (2008). Host immunity in the protective response to vaccination with heat-killed *Burkholderia mallei*. *BMC Immunol.* 9, 55. doi:10.1186/1471-2172-9-55

Yu, C.-S., Lin, C.-J., and Hwang, J.-K. (2004). Predicting subcellular localization of proteins for Gram-negative bacteria by support vector machines based on n-peptide compositions. *Protein Sci.* 13, 1402–1406.

Yu, N. Y., Wagner, J. R., Laird, M. R., Melli, G., Rey, S., Lo, R., Dao, P., Sahinalp, S. C., Ester, M., Foster, L. J., and Brinkman, F. S. L. (2010). PSORTb 3.0: improved protein subcellular localization prediction with refined localization subcategories and predictive capabilities for all prokaryotes. *Bioinformatics* 26, 1608–1615.

Zhong, X., Kolter, R., and Tai, P. C. (1996). Processing of colicin V-1, a secretable marker protein of a bacterial ATP binding cassette export system, requires membrane integrity, energy, and cytosolic factors. *J. Biol. Chem.* 271, 28057–28063.

Conflict of Interest Statement: The authors declare that the research was conducted in the absence of any commercial or financial relationships that could be construed as a potential conflict of interest.

Received: 20 August 2011; paper pending published: 15 September 2011; accepted: 26 October 2011; published online: 21 November 2011.

Citation: Whitlock GC, Robida MD, Judy BM, Qazi O, Brown KA, Deeraksa A, Taylor K, Massey S, Loskutov A, Borovkov AY, Brown K, Cano JA, Magee DM, Torres AG, Estes DM and Sykes KF (2011) Protective antigens against glanders identified by expression library immunization. Front. Microbio. ***2****:227. doi: 10.3389/fmicb.2011.00227*

This article was submitted to Frontiers in Cellular and Infection Microbiology, a specialty of Frontiers in Microbiology.

APPENDIX

Table A1 | Challenge protection results from ELI screen.

Group	Protection score (*p*-value)	Rank	Group	Protection score (*p*-value)	Rank
Y1	129 (0.63)	31	X41	222 (0.85)	53
Y2	131 (0.66)	26	X42	128 (0.09)	52
Y3	81 (0.15)	46	X43	126 (0.09)	55
Y4	177 (0.62)	14	X44	83 (0.02)	56
Y5	107 (0.35)	37	X45	129 (0.10)	51
Y6	179 (0.60)	9	X46	174 (0.35)	46
Y7	197 (0.38)	4	X47	228 (0.92)	28
Y8	177 (0.62)	12	X48	186 (0.45)	39
Y9	131 (0.66)	26	X49	177 (0.37)	45
Y10	134 (0.70)	24	X50	231 (0.96)	23
Y11	149 (0.93)	19	X51	269 (0.59)	21
Y12	110 (0.38)	36	X52	273 (0.54)	13
Y13	81 (0.15)	46	X53	276 (0.51)	10
Y14	131 (0.66)	26	X54	230 (0.94)	26
Y15	269 (0.02)	2	X55	273 (0.54)	13
Y16	81 (0.15)	46	X56	273 (0.54)	13
Y17	131 (0.66)	26	X57	372 (0.03)	2
Y18	92 (0.22)	41	X58	270 (0.57)	18
Y19	270 (0.02)	1	X59	365 (0.04)	3
Y20	177 (0.62)	14	X60	183 (0.42)	40
Y21	146 (0.89)	18	X61	227 (0.91)	30
Y22	95 (0.24)	39	X62	210 (0.71)	37
Y23	180 (0.58)	7	X63	231 (0.96)	24
Y24	233 (0.11)	3	X64	291 (0.37)	7
Y25	138 (0.77)	32	X65	183 (0.42)	54
Y26	135 (0.72)	22	X66	180 (0.40)	41
Y27	86 (0.17)	43	X67	159 (0.24)	49
Y28	93 (0.23)	41	X68	222 (0.85)	35
Y29	134 (0.70)	21	X69	180 (0.40)	41
Y30	125 (0.57)	33	X70	180 (0.40)	41
Y31	174 (0.67)	17	X71	134 (0.11)	50
Y32	84 (0.19)	44	X72	221 (0.83)	36
Y33	96 (0.25)	38	X73	237 (0.96)	22
Y34	176 (0.65)	16	X74	273 (0.54)	13
Y35	84 (0.16)	44	X75	321 (0.17)	4
Y36	179 (0.60)	9	X76	317 (0.20)	6
Y37	131 (0.66)	26	X77	180 (0.40)	41
Y38	191 (0.45)	5	X78	224 (0.87)	33
Y39	179 (0.60)	9	X79	270 (0.57)	17
Y40	138 (0.77)	20	X80	270 (0.57)	18
Y41	135 (0.72)	22	X81	189 (0.48)	38
Y42	182 (0.56)	6	X82	173 (0.33)	47
Y43	134 (0.70)	24	X83	176 (0.36)	48
Y44	180 (0.58)	8	X84	270 (0.57)	18
Y45	119 (0.49)	35	X85	230 (0.94)	25
Y46	177 (0.62)	12	X86	276 (0.51)	10
Y47	93 (0.23)	40	X87	276 (0.51)	8
Y48	126 (0.59)	34	X88	227 (0.91)	30
Naïve 1	146 (0.89)		X89	423 (0.003)	1
Irrelevant	126 (0.59)		X90	224 (0.87)	33
Vaccine 1	336 (0.0003)		X91	227 (0.91)	30
Vaccine 2	456 (<0.0001)		X92	276 (0.51)	8

X93	276 (0.51)	10
X94	228 (0.92)	29
X95	318 (0.19)	5
X96	230 (0.94)	26
Naïve 1	224 (0.87)	
Naïve 2	183 (0.42)	
Irrelevant	192 (0.51)	
Vaccine	456 (0.0005)	

Group	**Average spleen weight (g)**	**Rank**
X1	1.43	28
X2	1.25	18
X3	1.67	38
X4	1.53	33
X5	1.04	8
X6	1.13	11
X7	1.19	15
X8	1.46	29
X9	1.13	11
X10	1.02	6
X11	1.51	32
X12	1.29	20
X13	1.32	22
X14	1.61	34
X15	1.30	21
X16	1.62	35
X17	1.62	35
X18	1.50	31
X19	1.62	35
X20	1.35	25
X21	1.49	30
X22	1.71	39
X23	1.20	17
X24	1.90	40
X25	1.07	9
X26	1.18	14
X27	1.19	15
X28	1.33	24
X29	1.02	7
X30	1.01	5
X31	1.32	22
X32	0.91	1
X33	1.27	19
X34	1.15	13
X35	0.97	4
X36	0.95	3
X37	0.91	1
X38	1.36	26
X39	1.11	10
X40	1.36	26
Naïve uninfected	1.00	
Naïve infected	1.25	

frontiers in
MICROBIOLOGY

ORIGINAL RESEARCH ARTICLE
published: 10 January 2012
doi: 10.3389/fmicb.2011.00277

Defense mechanisms of hepatocytes against *Burkholderia pseudomallei*

Antje Bast, Imke H. E. Schmidt, Paul Brauner, Bettina Brix, Katrin Breitbach and Ivo Steinmetz*

Friedrich Loeffler Institute of Medical Microbiology, University of Greifswald, Greifswald, Germany

Edited by:
Alfredo G. Torres, University of Texas Medical Branch, USA

Reviewed by:
Jose A. Bengoechea, Fundacion Caubet – CIMERA Illes Balears, Spain
Yufeng Yao, Shanghai Jiao Tong University School of Medicine, China

****Correspondence:***
Ivo Steinmetz, Friedrich Loeffler Institut für Medizinische Mikrobiologie, Universitätsmedizin Greifswald KdöR, Martin-Luther-Str. 6, 17475 Greifswald, Germany.
e-mail: steinmetz.ivo@uni-greifswald.de

The Gram-negative facultative intracellular rod *Burkholderia pseudomallei* causes melioidosis, an infectious disease with a wide range of clinical presentations. Among the observed visceral abscesses, the liver is commonly affected. However, neither this organotropism of *B. pseudomallei* nor local hepatic defense mechanisms have been thoroughly investigated so far. Own previous studies using electron microscopy of the murine liver after systemic infection of mice indicated that hepatocytes might be capable of killing *B. pseudomallei*. Therefore, the aim of this study was to further elucidate the interaction of *B. pseudomallei* with these cells and to analyze the role of hepatocytes in anti-*B. pseudomallei* host defense. *In vitro* studies using the human hepatocyte cell line HepG2 revealed that *B. pseudomallei* can invade these cells. Subsequently, *B. pseudomallei* is able to escape from the vacuole, to replicate within the cytosol of HepG2 cells involving its type 3 and type 6 secretion systems, and to induce actin tail formation. Furthermore, stimulation of HepG2 cells showed that IFNγ can restrict growth of *B. pseudomallei* in the early and late phase of infection whereas the combination of IFNγ, IL-1β, and TNFα is required for the maximal antibacterial activity. This anti-*B. pseudomallei* defense of HepG2 cells did not seem to be mediated by inducible nitric oxide synthase-derived nitric oxide or NADPH oxidase-derived superoxide. In summary, this is the first study describing *B. pseudomallei* intracellular life cycle characteristics in hepatocytes and showing that IFNγ-mediated, but nitric oxide- and reactive oxygen species-independent, effector mechanisms are important in anti-*B. pseudomallei* host defense of hepatocytes.

Keywords: *Burkholderia*, cytoskeleton, hepatocytes, interferon γ, iNOS, NADPH oxidase, secretion system

INTRODUCTION

The Gram-negative saprophyte *Burkholderia pseudomallei* is the causative agent of melioidosis, an emerging infectious disease of humans and animals in certain areas of the tropics and subtropics. *B. pseudomallei* is an intracellular pathogen that can invade a variety of host cells (Jones et al., 1996). After invasion, *B. pseudomallei* can escape from the endocytotic vesicle of murine macrophage cells into the host cytosol depending on a functional type 3 secretion system-3 (T3SS-3; Stevens et al., 2002; Burtnick et al., 2008; Muangsombut et al., 2008; Gong et al., 2011). Within the cytosol bacteria can multiply and induce the BimA-dependent formation of actin tails, facilitating intracellular motility as well as spreading of *B. pseudomallei* into neighboring cells (Kespichayawattana et al., 2000; Breitbach et al., 2003; Stevens et al., 2005). A recent paper proposed that *B. pseudomallei*-induced cell fusion and the formation of multinucleated giant cells represent the primary path for intercellular spread and plaque formation of this pathogen (French et al., 2011).

Several reports have shown that interferon γ (IFNγ) is essential for the early control of *B. pseudomallei* infection in mice (Santanirand et al., 1999; Breitbach et al., 2006). *In vitro* experiments also demonstrated a pivotal role for IFNγ to eliminate intracellular *B. pseudomallei* in macrophages (Miyagi et al., 1997; Utaisincharoen et al., 2001). We recently demonstrated that the downstream effector molecule of IFNγ, nitric oxide (NO), has a dual role among resistant and susceptible mouse strains after *B. pseudomallei* infection. NO had rather detrimental effects in innate resistant C57BL/6 mice in a murine model of melioidosis and was not involved in killing activity of C57BL/6 macrophages (Breitbach et al., 2006, 2011). In contrast, NO contributed to complete resistance in innate susceptible BALB/c mice and to growth restriction of *B. pseudomallei* in macrophages from those mice (Breitbach et al., 2011). In a previous study we revealed that NADPH oxidase-mediated mechanisms contribute to early resistance in bone marrow-derived macrophages and C57BL/6 mice (Breitbach et al., 2006).

The liver plays an essential role in the innate immune response, providing the first line of defense against microbes crossing the intestinal barrier (Crispe, 2009). Kupffer cells are important for the rapid clearance of microorganisms from the systemic circulation,

Abbreviations: AG, aminoguanidine hemisulfate; Apocynin, 4-hydroxy-3-methoxyacetophenone; BMM, bone marrow-derived macrophages; CAT, catalase; CFU, colony forming units; COX, cyclooxygenase; EPS, exopolysaccharide; IFNγ, interferon γ; IL-1β, interleukin-1β; iNOS, inducible nitric oxide synthase; LAMP-1, lysosomal-associated membrane protein-1; LDH, lactate dehydrogenase; LPS, lipopolysaccharide; MOI, multiplicity of infection; NAC, *N*-acetyl-cysteine; NADPH oxidase, nicotinamide adenine dinucleotide phosphate oxidase; NO, nitric oxide; ROS, reactive oxygen species; SOD, superoxide dismutase; T3SS, type three secretion system; T6SS, type six secretion system; TNFα, tumor necrosis factor.

and can facilitate the generation of a local inflammatory response leading to recruitment of inflammatory cells. Furthermore, hepatocytes can also secrete inflammatory cytokines and chemokines in response to cytokine activation and/or bacterial invasion (Rowell et al., 1997; Santos et al., 2005). However, to date little is known about the antimicrobial responses of hepatocytes. Only few studies indicate that IFNγ can restrict growth of *Listeria monocytogenes* and *Salmonella typhimurium* in murine hepatocytes (Gregory and Wing, 1993; Lajarin et al., 1996).

In previous studies we and others revealed that the organotropism of *B. pseudomallei* for the spleen and liver in melioidosis patients can be mimicked by infection of mice (Hoppe et al., 1999; Santanirand et al., 1999; Liu et al., 2002). Electron microscopic investigations of the murine liver demonstrated that *B. pseudomallei*-containing phagosomes in hepatocytes fuse with lysosomes, leading to bacterial degradation (Hoppe et al., 1999). Therefore, the present study aimed to establish an *in vitro* hepatocyte infection model with human polarized HepG2 cells to study host defense mechanisms against *B. pseudomallei*. We investigated whether *B. pseudomallei* is able to invade and survive within hepatocytes and whether bacterial replication is dependent on the *B. pseudomallei* type 3 or type 6 secretion systems. Finally, we addressed the role of cytokines in enhancing anti-*B. pseudomallei* activity in HepG2 cells and a possible contribution of nitric oxide and reactive oxygen species in the bactericidal activity against *B. pseudomallei*.

MATERIALS AND METHODS

MATERIALS

Cytochalasin D (CytoD), latrunculin B (LatB), jasplakinolide (Jasp), and nocodazole (Noco) were obtained from Enzo Life Sciences (Lörrach, Germany). Catalase–polyethylene glycol (CAT–PEG), superoxide dismutase–polyethylene glycol (SOD–PEG), *N*-acetyl-cysteine (NAC), aminoguanidine (AG), and colchicine (Col) were from Sigma Aldrich (Taufkirchen, Germany). hIFNγ was purchased from Miltenyi Biotec GmbH (Bergisch Gladbach, Germany), and both mIL-1β and mTNFα were from Roche (Mannheim, Germany). Apocynin (Apo) was obtained from Calbiochem (Darmstadt, Germany).

BACTERIAL STRAINS

Burkholderia pseudomallei wild-type strain E8 comprises a soil isolate from the surrounding area of Ubon Ratchathani in northeast Thailand (Wuthiekanun et al., 1996) and was used throughout the study. T3SS-3 mutant ΔBPSS1539 (16:48) and T6SS-1 mutant ΔBPSS1509 (5:45) were generated by Tn5-OT182 mutagenesis of *B. pseudomallei* E8 as previously described (Pilatz et al., 2006). Bacteria were grown on Columbia agar at 37°C for 24 h and adjusted to the desired concentration in Dulbecco's phosphate-buffered saline (D-PBS; Invitrogen, Darmstadt, Germany) or the respective cell culture medium.

CELL CULTURE AND INFECTION OF HepG2 CELLS

Human hepatocellular carcinoma HepG2 cells were obtained from the DSMZ (Deutsche Sammlung von Mikroorganismen und Zellkulturen, Braunschweig, Germany). Cells were cultured in RPMI 1640 medium (Biochrom AG, Berlin, Germany) supplemented with 10% fetal calf serum (PAA Laboratories GmbH, Cölbe, Germany) at 37°C in a humidified atmosphere containing 95% air and 5% CO_2.

Twenty-four hours prior to infection, cells were seeded in 48 well plates (1.5×10^5 cells per well), grown to 80% confluence, and infected with *B. pseudomallei* strain E8 at the indicated multiplicity of infection (MOI). For invasion assays well plates were additionally centrifuged for 4 min at 120 × *g*. After infection for 30 min cells were washed twice with D-PBS and incubated in kanamycin (250 μg/ml) containing medium to eliminate remaining extracellular bacteria. To minimize re-infection and extracellular replication the culture medium was replaced by fresh medium containing 125 μg/ml kanamycin 6 h after infection. At indicated time points (time zero was taken 25 min after incubation under antibiotic-containing medium) the number of intracellular colony forming units (CFU) was determined. Consequently, cells were washed twice with D-PBS and subsequently lysed using 150 μl D-PBS containing 0.5% Tergitol TMN (Fluka, Buchs, Switzerland) and 1% bovine serum albumin (BSA) per well. After 15 min of incubation appropriate dilutions of lysates were plated on Mueller–Hinton agar and incubated at 37°C for 48 h.

Activation of HepG2 cells was performed using 500 ng/ml IFNγ, 50–200 U/ml IL-1β, or 10 ng/ml TNFα 24 h prior to infection. For *in vitro* inhibition of inducible nitric oxide synthase (iNOS), NADPH oxidase, or ROS generation, HepG2 cells were treated by adding 2 mM aminoguanidine (24 h), 500 μM apocynin, or 20 U/ml superoxide dismutase, 200 U/ml catalase, and 200 μM *N*-acetyl-cysteine or corresponding vehicle into the culture medium 1 h (unless otherwise indicated) prior to infection and during the incubation with kanamycin-containing medium. For *in vitro* inhibition of the actin cytoskeleton or the microtubules, HepG2 were incubated for 1 h with 1 μM cytochalasin D, 0.1 μM latrunculin B, 0.5 μM jasplakinolide, 10 μM nocodazole, 5 μM colchicine, or corresponding vehicle, followed by infection with *B. pseudomallei*. All inhibitors and vehicles were kept in the infection medium throughout the experiment.

IMMUNOFLUORESCENCE STAINING

Twenty-four hours prior to infection, HepG2 cells were seeded on collagen type I coated cover slips in 24 well plates (2×10^5 cells per well) and infected with *B. pseudomallei* strain E8 at a MOI of 400 by centrifugation of the well plates for 4 min at 120 × *g*. After infection for 30 min cells were washed twice with D-PBS and incubated in kanamycin (250 μg/ml) containing medium to eliminate remaining extracellular bacteria. At indicated time points HepG2 cells were washed with PBS, incubated for 10 min in ice-cold methanol, and washed three times with IF buffer [0.2% (w/v) BSA, 0.05% (w/v) saponin, 0.1% (w/v) sodium azide in PBS, pH 7.4]. To block non-specific antibody binding, cells were incubated for up to 1 h in IF buffer followed by an overnight incubation at 4°C in a humidity chamber with monoclonal mouse anti-*B. pseudomallei* 3015 γ2b (1:2000; Pilatz et al., 2006) and polyclonal rabbit anti-β-actin (1:100; Cell Signaling, Frankfurt am Main, Germany) or monoclonal mouse anti-lysosomal-associated membrane protein-1 (anti-LAMP-1) γ1 (1:400; BD Biosciences, Heidelberg, Germany) antibodies. After a wash with IF buffer, the immunoreacted primary antibodies were visualized with green

fluorescent Alexa Fluor 488 anti-mouse IgG2b (1:800; Invitrogen, Darmstadt, Germany) and red fluorescent Cy3-conjugated goat anti-rabbit IgG (1:400; Dianova, Hamburg, Germany) or red fluorescent Alexa Fluor 568 anti-mouse IgG1 (1:800; Invitrogen) by incubation for 1 h at room temperature in the dark. After another wash with IF buffer, slices were covered with Fluorprep (bioMérieux, Nürtingen, Germany) and observed by fluorescent microscopy with a BZ-9000 microscope (Keyence Corporation, Neu-Isenburg, Germany).

LDH ASSAY

To quantify the extent of cell damage after infection, release of lactate dehydrogenase (LDH) in cell culture supernatants was determined. HepG2 cells were seeded in 96 well plates (3.75×10^4 cells per well) and infected at the indicated MOI with *B. pseudomallei* for 30 min. Cells were washed twice with D-PBS, and 100 µl of medium containing 250 µg/ml of kanamycin was added to each well to eliminate extracellular bacteria. At the indicated time points, cell culture supernatant was collected, and LDH activity was detected by using the CytoTox-One homogeneous membrane integrity assay (Promega, Mannheim, Germany) according to the manufacturer's instructions. Briefly, 50 µl of supernatant was added to the kit reagent and incubated for 10 min. After addition of stopping solution, the fluorescence intensity was measured using the microplate reader Infinite M200 PRO (Tecan, Crailsheim, Germany) at excitation wavelength of 560 nm and emission wavelength of 590 nm.

REAL-TIME CELL ANALYSIS

HepG2 cells were seeded in 96 well E-plates (3×10^4 cells per well), grown for 24 h, and then infected at the indicated MOI with *B. pseudomallei* for 30 min followed by incubation in kanamycin (250 µg/ml) containing medium. Cellular events were monitored in real-time using the xCELLigence system according to the manufacturer's instructions (Roche, Mannheim, Germany). The system measures electrical impedance across gold microelectrodes integrated into the bottom of tissue culture E-plates providing real-time, quantitative information about the biological status of the cells, including cell number, viability, morphology, and degree of cell adhesion. In the absence of cells on the electrode surface, the electrical impedance describes only the background. Changes in impedance are dependent on either the number of cells attached to the electrodes or the dimensional change of attached cells on the electrode surface. The xCELLigence system detects changes in impedance and calculates them as dimensionless parameter termed Cell Index: $CI = (Z_i - Z_0)/15$ where Z_i is the impedance at an individual time point of the experiment and Z_0 describes the background measurement at the beginning of the experiment. To evaluate the impact of *B. pseudomallei* on HepG2 cells, the normalized cell index (NCI_{ti}) was used. Consequently, all selected wells were set on impedance value of 1 at a given time point (time of infection), and all further values were calculated as the cell index at a given time point (CI_{ti}) divided by the Cell Index at the normalization time point (CI_{nml_time}).

DATA PRESENTATION AND STATISTICAL ANALYSIS

Figures and statistical analysis were performed using GraphPad Prism, version 4.0. Student's *t*-test was used to detect statistically significant differences in the intracellular bacterial numbers. *p*-Values of <0.05 were considered to be statistically significant.

RESULTS

BURKHOLDERIA PSEUDOMALLEI IS ABLE TO INVADE AND REPLICATE WITHIN HepG2 CELLS

The invasion and intracellular replication of *B. pseudomallei* in hepatocytes or hepatocyte cell lines has not been investigated so far. Therefore, we first investigated the invasion and the course of the intracellular bacterial burden in human hepatocellular carcinoma HepG2 cells after infection with *B. pseudomallei* wild-type strain E8 at a MOI of 29 and 599, respectively. As shown in **Figure 1A**, *B. pseudomallei* was able to enter HepG2 cells. Within the first 3 h after infection, a strong reduction in *Burkholderia* counts could be observed which indicates that effective bactericidal defense mechanisms are activated in HepG2 cells in the early phase of infection. Six hours after infection the intracellular bacterial burden increased, suggesting that *B. pseudomallei* is able to multiply within cells. After 24 h 10-fold more bacteria were found in *Burkholderia*-infected HepG2 cells compared to the beginning.

To provide some information about the mechanism used by *B. pseudomallei* to enter HepG2 cells, we analyzed the role of the host actin cytoskeleton as well as microtubules by using well defined inhibitors. As shown in **Figure 1B**, there was a tendency of actin cytoskeleton inhibitors (1 µM cytochalasin D, 0.1 µM latrunculin B, 0.5 µM jasplakinolide) as well as microtubule inhibitors (10 µM nocodazole, 5 µM colchicine) to reduce invasion of *B. pseudomallei*, as determined by enumeration of intracellular bacteria, although statistical significance was not reached. Therefore, our results indicate that the host actin cytoskeleton may contribute to *B. pseudomallei* uptake in HepG2 cells, but other invasion mechanisms may also play an important role.

As *B. pseudomallei* type 3 and type 6 secretion systems (T3SS, T6SS) are important for invasion of murine macrophages or human epithelial cells as well as for intracellular survival (Stevens et al., 2002, 2003; Burtnick et al., 2011), we analyzed whether they are also involved in the replication of *B. pseudomallei* in hepatocytes. Consequently, HepG2 cells were infected with *B. pseudomallei* wild-type strain E8, as well as a type 3 (ΔBPSS1539) and type 6 (ΔBPSS1509) secretion mutant, which have previously been shown to be attenuated *in vivo* (Pilatz et al., 2006). Surprisingly, mutant ΔBPSS1509, but not ΔBPSS1539 revealed a significantly higher invasion in HepG2 cells compared to the wild-type strain (**Figure 1C**). However, 24 h postinfection intracellular CFU counts were at least one log lower in cells infected with both mutant strains than in those infected with the wild-type strain. These results suggest that *B. pseudomallei* can infect and replicate in human hepatocytes and that the T3SS and T6SS contribute to optimal replication.

BURKHOLDERIA PSEUDOMALLEI CAN ESCAPE FROM THE VACUOLE AND INDUCE FORMATION OF ACTIN TAILS IN HepG2 CELLS

To further characterize the hepatocyte–pathogen-interaction we examined the intracellular localization of *B. pseudomallei* wild-type, T3SS, and T6SS mutant strains in HepG2 cells relative to LAMP-1 containing vacuoles as well as actin tail formation. Immunofluorescence microscopy revealed that 8 h after infection

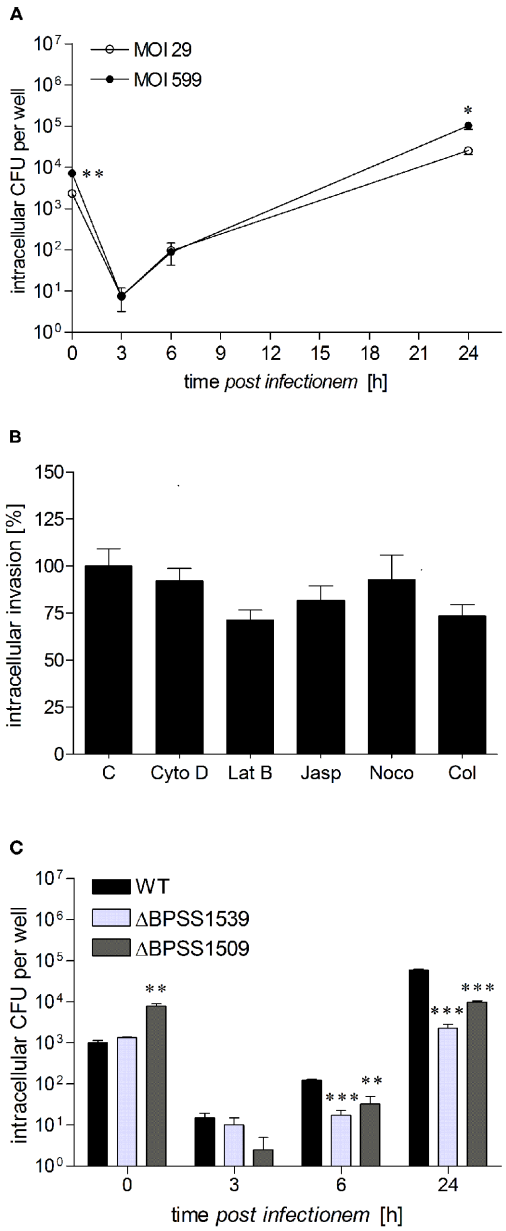

FIGURE 1 | *Burkholderia pseudomallei* can multiply in human hepatocytes. (A) HepG2 cells were infected with *B. pseudomallei* E8 at multiplicities of infection of 29:1 (opened circles) and 599:1 (closed circles), and cells were lysed at different time points after infection to determine the number of viable intracellular bacteria by plating lysates on Mueller–Hinton agar. **(B)** Invasion of *B. pseudomallei* in HepG2 cells at a MOI of ∼400:1 in the presence of inhibitors of actin filaments, including cytochalasin D (CytoD, 1 μM), latrunculin B (LatB, 0.1 μM), and jasplakinolide (Jasp, 0.5 μM) as well as inhibitors of microtubules, including nocodazole (Noco, 10 μM) and colchicine (Col, 5 μM). Invasion of *B. pseudomallei* in the absence of an inhibitor was set to 100%. **(C)** HepG2 cells were infected with either *B. pseudomallei* wild-type (WT), T3SS-3 mutant ΔBPSS1539, or T6SS-1 mutant ΔBPSS1509 using a MOI of ∼40:1, and intracellular replication was monitored as above. Data are presented as mean with SEM of triplicate determinations. One representative experiment out of three independent experiments is shown. Statistical analyses were performed using a Student's *t*-test (*$p < 0.05$, **$p < 0.01$, ***$p < 0.001$).

the wild-type was rarely seen co-localized with regions of LAMP-1 staining (**Figure 2A**), however a part of the *B. pseudomallei* population was able to induce actin tails (data not shown). Sixteen hours after infection the majority of bacteria displayed long actin tails (**Figure 2B**). In contrast, T3SS mutant ΔBPSS1539 was almost exclusively observed in association with LAMP-1, suggesting that the mutant is unable to escape from endocytotic vesicles 8 h after infection (**Figure 2A**). In accordance with our recent study using HeLa cells (Pilatz et al., 2006) this mutant was still able to multiply within the phagosomes of HepG2 cells, leading to large vesicles filled with bacteria. As *B. pseudomallei* was trapped within the phagosomes, no actin tail formation could be observed at this time point (data not shown). However, 16 h after infection some of these huge vacuoles seemed to become leaky and *B. pseudomallei* ΔBPSS1539 could be detected within the cytosol in association with actin tails (**Figure 2B**). As the wild-type the T6SS mutant ΔBPSS1509 was rarely seen associated with LAMP-1 8 h after infection, but actin tails could not be detected at this time point (data not shown). However, 16 h after infection the mutant was able to induce actin tails, but to a lesser degree compared to the wild-type (data not shown).

BURKHOLDERIA PSEUDOMALLEI INFECTION INDUCES CELL DAMAGE OF HepG2 CELLS

To determine whether *B. pseudomallei* affects the viability of hepatocytes, cytosolic LDH activity was measured in cell culture supernatants of infected and control HepG2 cells at 24 h postinfection as an indicator of cytotoxicity. **Figure 3A** demonstrates that infection of HepG2 cells with *B. pseudomallei* wild-type strain E8 induced only a small MOI-dependent release of LDH compared to uninfected cells. However, this slight cytotoxicity was not found

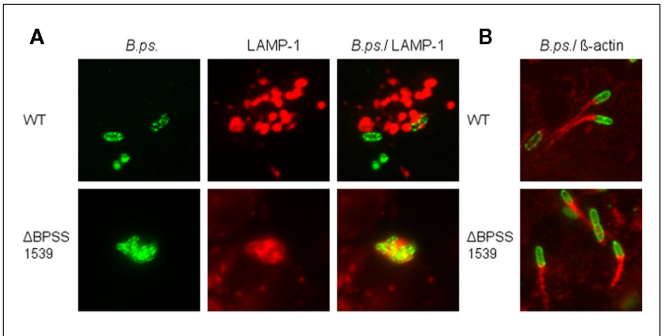

FIGURE 2 | *Burkholderia pseudomallei* is able to escape from the endocytotic vesicle and to form actin tails in hepatocytes. HepG2 cells were infected with either *B. pseudomallei* wild-type (WT) or T3SS-3 mutant ΔBPSS1539 using a MOI of ∼400:1 and analyzed by immunofluorescence microscopy (magnification ×1000). **(A)** Representative micrographs showing the association of intracellular *B. pseudomallei* with LAMP-1-containing vacuoles 8 h after infection. Bacteria were stained green with mouse anti-*B. pseudomallei* EPS (3015 γ2b) and Alexa Fluor 488 anti-mouse IgG2b antibodies. LAMP-1 was stained red with mouse anti-LAMP-1 γ1 and Alexa Fluor 568 anti-mouse IgG1 antibodies. **(B)** Representative micrographs showing the formation of actin tails by *B. pseudomallei* 16 h after infection. Bacteria were stained green with mouse anti-*B. pseudomallei* EPS (3015 γ2b) and Alexa Fluor 488 anti-mouse IgG2b antibodies. Actin tails were stained red with rabbit anti-β-actin and Cy3-conjugated goat anti-rabbit IgG antibodies.

to be mediated by activation of apoptotic caspases 3 and 9 using Western blot analysis (data not shown).

Since *B. pseudomallei* infection led to detachment of hepatocytes after 24 h in a MOI-dependent manner as determined by microscopic analyses (data not shown), we aimed to quantify these cellular damages by performing electrical impedance measurements providing real-time information about the biological status of hepatocytes such as viability, morphology, and degree of cell adhesion. Such an experimental approach has recently been described for meningococcal infection in human brain microvascular endothelial cells (Slanina et al., 2011). HepG2 cells were grown for 24 h leading to an increase of the Normalized Cell Index (**Figure 3B**). Infection with *B. pseudomallei* wild-type strain E8 at MOI of 37 or 350 resulted in a transient decrease of the corresponding Cell Index caused by the cell culture medium exchange. Due to the proliferation and spreading of hepatocytes, non-infected cells led to enhanced electrical impedance within 110 h. In contrast, infection of HepG2 cells with *B. pseudomallei* at a MOI of 37 resulted in a loss of electrical impedance 36 h after infection, whereas infection at a MOI of 350 led to a loss of electrical impedance already 24 h postinfection (**Figure 3B**), correlating with the low LDH release after 24 h (**Figure 3A**). To exclude that the impedance was influenced by bacterial overload of the electrodes, electrical impedance was investigated in response to bacterial growth over the same period. However, no effect on the Cell Index could be observed when bacteria alone were grown in the wells (data not shown).

To determine whether reduced intracellular growth of T3SS and T6SS mutants correlates with an increased viability of hepatocytes, we measured the electrical impedance after infection of HepG2 cells with *B. pseudomallei* wild-type as well as the T3SS (ΔBPSS1539) and T6SS (ΔBPSS1509) mutants at a MOI of ∼400. **Figure 3C** illustrates that the electrical impedance of HepG2 cells after infection with the T6SS mutant ΔBPSS1509 did not differ significantly from the one of uninfected cells whereas infection with the wild-type strain resulted in a strong loss of electrical impedance. The decrease of the Normalized Cell Index observed in HepG2 cells infected with the T3SS mutant ΔBPSS1539 was significantly delayed compared to wild-type infected cells. Our data indicate that *B. pseudomallei* induces cell damage of HepG2 cells depending on a functional T3SS and T6SS.

INTERFERON γ INCREASES ANTIBACTERIAL ACTIVITY OF HepG2 CELLS AGAINST *B. PSEUDOMALLEI*

IFNγ is crucial for *in vivo* resistance against *B. pseudomallei* (Santanirand et al., 1999; Breitbach et al., 2006) and has been shown to restrict replication of *B. pseudomallei* in macrophages (Miyagi et al., 1997; Utaisincharoen et al., 2001). We therefore compared the intracellular growth of *B. pseudomallei* between unstimulated or IFNγ-stimulated (500 ng/ml) HepG2 cells. Although invasion of *B. pseudomallei* into HepG2 cells was comparable, already 3 and 6 h after infection intracellular bacterial load was reduced in IFNγ-activated cells, which was most prominent after 24 h (**Figure 4A**). These data indicate that IFNγ is able to increase the antibacterial capacity of HepG2 cells against intracellular *B. pseudomallei* in the early and late phase of infection.

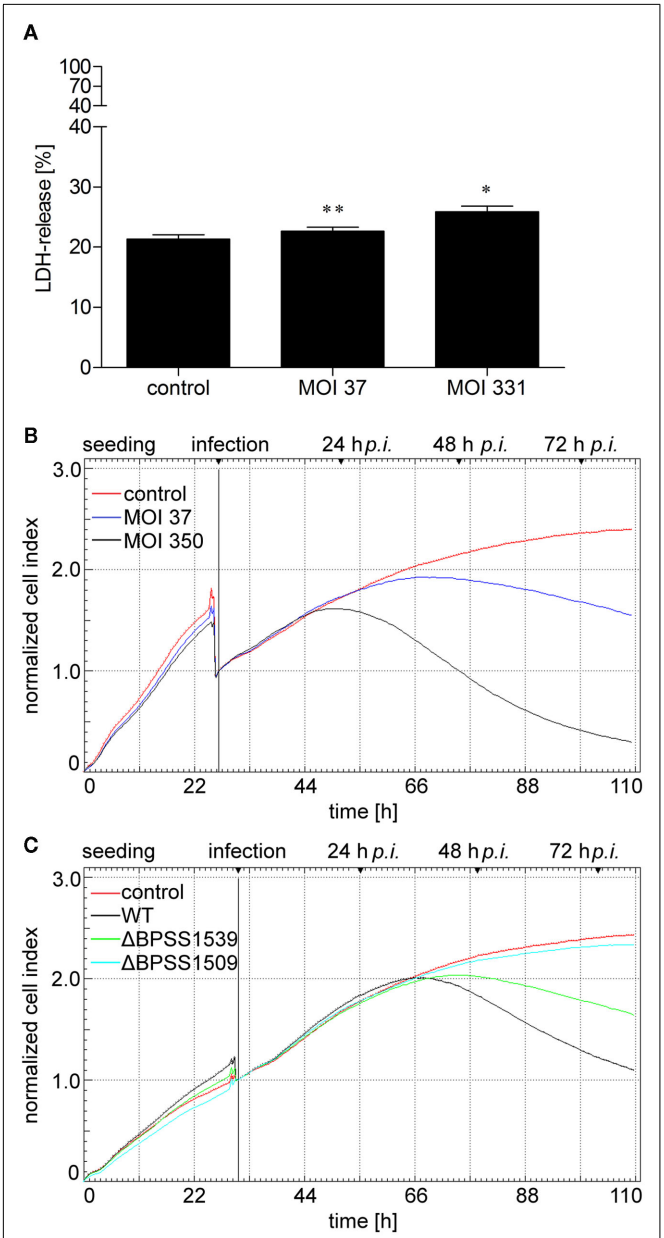

FIGURE 3 | *Burkholderia pseudomallei* infection leads to cell damage of hepatocytes. (A) HepG2 cells were infected with *B. pseudomallei* E8 at multiplicities of infection of 37:1 and 331:1, respectively, and lactate dehydrogenase (LDH) release was determined 24 h after infection. Values are expressed as percentages relative to the LDH activity in supernatants from the 100% lysis control. Data are presented as mean with SEM of triplicate determinations. One representative experiment out of three independent experiments is shown. Statistical analyses were performed using a Student's *t*-test (*$p < 0.05$, **$p < 0.01$). **(B,C)** HepG2 cells were seeded on 96 well E-plates and continuously monitored using the xCELLigence system. At the indicated time point, cells were infected with **(B)** *B. pseudomallei* at MOI of 37:1 and 350:1, respectively, or **(C)** *B. pseudomallei* wild-type (WT), T3SS-3 mutant ΔBPSS1539, or T6SS-1 mutant ΔBPSS1509 at MOI of ∼400:1, and cell response was monitored every 30 min by impedance measurement. One representative experiment out of three independent experiments is shown.

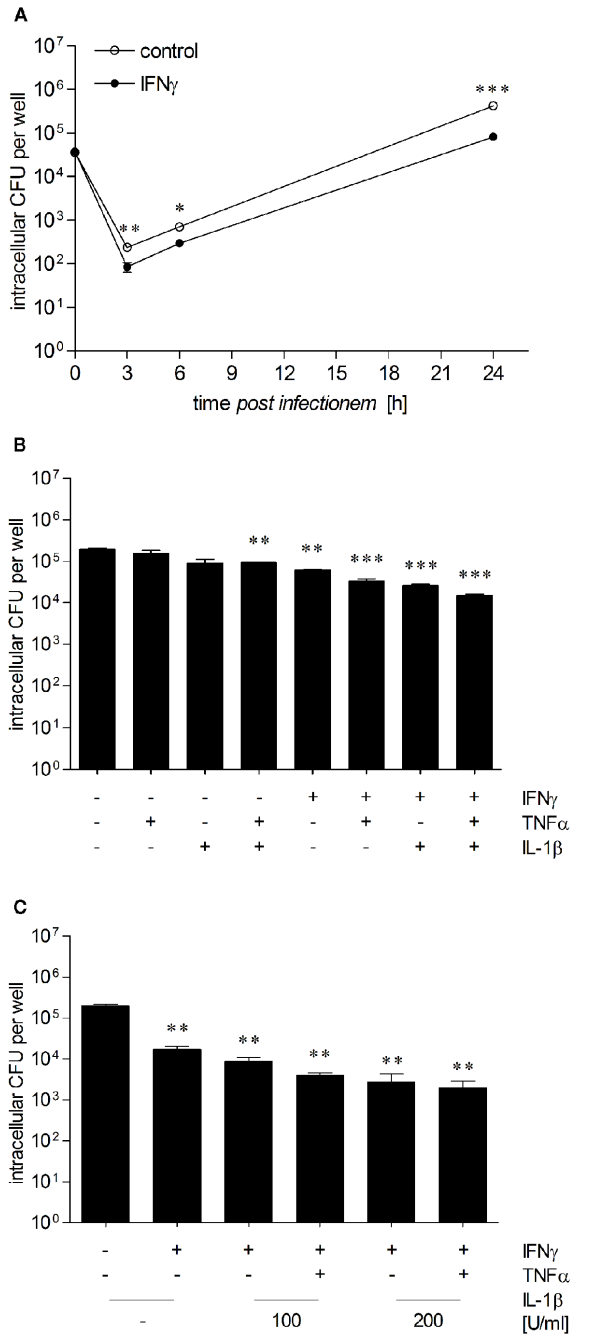

FIGURE 4 | Proinflammatory cytokines increase anti-*B. pseudomallei* activity of hepatocytes. (A) Intracellular survival of *B. pseudomallei* E8 in unstimulated (opened circles) and IFNγ-stimulated (500 ng/ml; closed circles) HepG2 cells infected with an MOI of 36:1. **(B)** Intracellular survival of *B. pseudomallei* E8 24 h after infection (MOI 37:1) of HepG2 cells pretreated with IFNγ (500 ng/ml), IL-1β (50 U/ml), or TNFα (10 ng/ml) alone or in combination. **(C)** Intracellular survival of *B. pseudomallei* E8 24 h after infection (MOI 36:1) of HepG2 cells activated with IFNγ alone (500 ng/ml) or in combination with IL-1β (100–200 U/ml) and TNFα (10 ng/ml). Data are presented as mean with SEM of triplicate determinations. One representative experiment out of three independent experiments is shown. Statistical analyses were performed using a Student's *t*-test (*$p < 0.05$, **$p < 0.01$, ***$p < 0.001$).

PROINFLAMMATORY CYTOKINES ENHANCE ANTIBACTERIAL ACTIVITY OF IFNγ-ACTIVATED HepG2 CELLS

IFNγ, IL-1β, and TNFα have been detected in livers of BALB/c and C57BL/6 mice after *B. pseudomallei* infection (Ulett et al., 2000a,b), and numerous studies have shown that early cytokine responses are important for resistance to intracellular pathogens (Ehlers et al., 1992; Autenrieth et al., 1994; Bohn et al., 1994; Santanirand et al., 1999). To examine the impact of these inflammatory cytokines in controlling intracellular *B. pseudomallei* growth in hepatocytes, we analyzed the intracellular survival kinetics of *B. pseudomallei* in HepG2 cells in the presence of several cytokines. Therefore, HepG2 cells were stimulated with IFNγ (500 ng/ml), IL-1β (50–200 U/ml), TNFα (10 ng/ml), or a combination of these cytokines for 24 h followed by infection with *B. pseudomallei*. As shown in **Figure 4B**, IL-1β or TNFα alone had no or only a marginal effect on intracellular bacterial replication, whereas the combination of both cytokines caused a small, but significant growth inhibition of *B. pseudomallei*. In contrast, IFNγ alone reduced bacterial multiplication. This inhibitory effect was enhanced, when IFNγ was combined with either IL-1β or TNFα. The combination of all three cytokines produced a maintained decrease in intracellular bacterial growth compared to that observed in unstimulated controls (**Figure 4C**), suggesting that IFNγ, IL-1β, and TNFα are essential for the maximal activation of hepatocytes.

INDUCIBLE NITRIC OXIDE SYNTHASE IS NOT ESSENTIAL TO ELIMINATE *B. PSEUDOMALLEI*

Previous studies provided evidence for a crucial role of NO in growth inhibition of *B. pseudomallei* in BALB/c macrophages, whereas NO did not play any role in killing activity of C57BL/6 macrophages (Breitbach et al., 2006, 2011). Thus, we investigated the role of iNOS-generated NO with respect to intracellular elimination of *B. pseudomallei* in HepG2 cells. First, we determined the amount of NO released from untreated and IFNγ-treated HepG2 cells 24 h after infection with *B. pseudomallei*. However, we could neither detect NO in cell culture supernatants nor iNOS protein expression in lysates of infected HepG2 cells (data not shown). To assess the contribution of the NO pathway in the antibacterial effect of activated HepG2 cells, we used the iNOS inhibitor aminoguanidine (2 mM). However, after treatment with the iNOS inhibitor and infection of resting or IFNγ-stimulated HepG2 cells, we could not observe any significant difference in intracellular killing of *B. pseudomallei* (**Figure 5**). This suggests that iNOS-derived NO is not necessary to eliminate *B. pseudomallei* in hepatocytes.

NADPH OXIDASE IS NOT INVOLVED IN THE CONTROL OF *B. PSEUDOMALLEI* INFECTION

In a recent study we demonstrated that NADPH oxidase-mediated mechanisms contribute to early resistance in C57BL/6 mice *in vivo* and in BMM (Breitbach et al., 2006). Consequently, we investigated the role of NADPH oxidase in the intracellular *B. pseudomallei* elimination of hepatocytes. For this reason unstimulated and IFNγ-stimulated HepG2 cells were pretreated with apocynin (500 μM), a potent and selective inhibitor of NADPH oxidase, followed by infection with *B. pseudomallei*. In spite of a significantly higher invasion of apocynin-inhibited cells (data not shown), our

experiments indicated that bacterial growth of *B. pseudomallei* was not impaired by apocynin (**Figure 6**), suggesting that, in contrast to primary murine macrophages, NADPH oxidase does not contribute to antibacterial activity of human hepatocyte cells.

SCAVENGERS/INHIBITORS OF REACTIVE OXYGEN SPECIES DO NOT INHIBIT THE ANTIBACTERIAL ACTIVITY

To further study the involvement of reactive oxygen species as effector molecules of the antibacterial activity of hepatocytes, unstimulated, and IFNγ-stimulated HepG2 cells were incubated with the free radical scavengers catalase (CAT, 200 U/ml), superoxide dismutase (SOD, 20 U/ml), and/or *N*-acetyl-cysteine (NAC, 200 μM) prior to infection with *B. pseudomallei*. **Figure 7** shows that treatment of IFNγ-stimulated HepG2 cells with catalase and SOD slightly, but not significantly reversed the antibacterial activity. The effect of both antioxidant enzymes added at the same time was not further enhanced by addition of NAC. However, treatment of resting HepG2 cells did not increase the number of CFU recovered, indicating that basal, ROS-mediated antibacterial mechanisms do not exist in hepatocytes. Our results imply that reactive oxygen species do not play an important role in the control of *B. pseudomallei* replication.

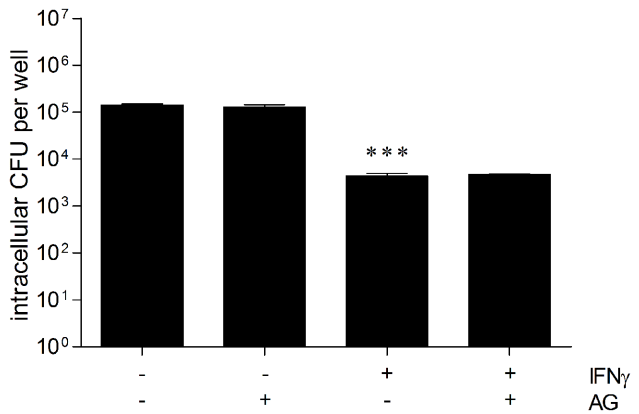

FIGURE 5 | Inducible nitric oxide synthase (iNOS) is not necessary to eliminate *B. pseudomallei* in hepatocytes. Intracellular replication of *B. pseudomallei* E8 24 h after infection (MOI 40:1) of resting and IFNγ-activated (500 ng/ml) HepG2 cells in the presence of iNOS inhibitor aminoguanidine (AG, 2 mM). Data are presented as mean with SEM of triplicate determinations. One representative experiment out of three independent experiments is shown. Statistical analyses were performed using a Student's *t*-test (***$p < 0.001$).

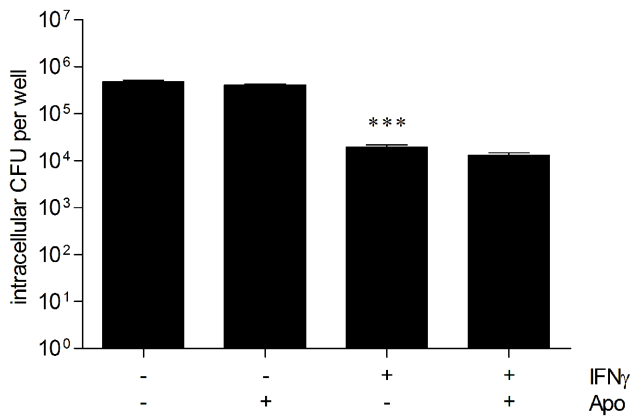

FIGURE 6 | NADPH oxidase is not important for the control of *B. pseudomallei* hepatocyte infection. Intracellular survival of *B. pseudomallei* E8 24 h after infection (MOI 31:1) of resting and IFNγ-activated (500 ng/ml) HepG2 cells in the presence of NADPH oxidase inhibitor apocynin (Apo, 500 μM). Data are presented as mean with SEM of triplicate determinations. One representative experiment out of three independent experiments is shown. Statistical analyses were performed using a Student's *t*-test (***$p < 0.001$).

DISCUSSION

The liver consists of both hepatocytes and different types of non-parenchymal cells including endothelial sinusoidal cells, Kupffer cells, and other immune cells. Although hepatocytes comprise 60% of cells in the liver and 80% of the hepatic volume (Malarkey et al., 2005), their role in antimicrobial defense is poorly understood. As the liver is among the most commonly affected organs in melioidosis, the present study was designed to examine the contribution of hepatocytes in host defense against *B. pseudomallei*.

To our knowledge, this is the first study showing that *B. pseudomallei* can infect and replicate within HepG2 cells (**Figure 1A**). The intracellular multiplication in hepatocytes is in accordance with the well-known ability of *B. pseudomallei* to proliferate inside several cell types, including phagocytic and non-phagocytic cells (Jones et al., 1996; Harley et al., 1998; Kespichayawattana et al., 2000). In addition, our results are consistent with other recently published data describing that intracellular *L. monocytogenes* (Gregory and Wing, 1993; Gregory et al., 1993; Wood et al., 1993; Szalay et al., 1995), *S. typhimurium* (Lajarin et al., 1996), and *Brucella*

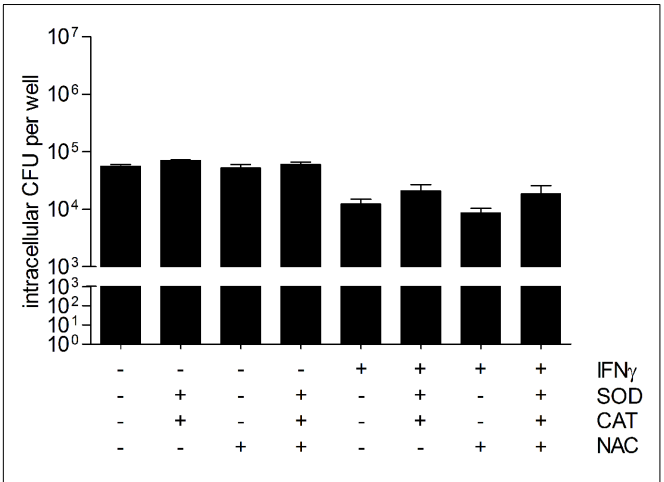

FIGURE 7 | Scavengers/inhibitors of reactive oxygen intermediates do not inhibit the antibacterial activity of hepatocytes. Intracellular survival of *B. pseudomallei* E8 24 h after infection (MOI 42:1) of unstimulated and IFNγ-stimulated (500 ng/ml) HepG2 cells in the presence of antioxidants superoxide dismutase (SOD, 20 U/ml), catalase (CAT, 200 U/ml), and *N*-acetyl-cysteine (NAC, 200 μM). Data are presented as mean with SEM of triplicate determinations. One representative experiment out of three independent experiments is shown. Statistical analyses were performed using a Student's *t*-test.

abortus (Delpino et al., 2010) are able to invade and multiply within primary hepatocytes and hepatoma cells, respectively.

Several *in vitro* studies have demonstrated that *B. pseudomallei* T3SS-3 facilitates bacterial invasion of non-phagocytic cells (Stevens et al., 2003), contributes to escape from endosomes, intracellular survival, and replication (Stevens et al., 2002), and is necessary for the induction of caspase-1-dependent cell death in phagocytic cells (Sun et al., 2005). It has been reported that BsaU seems to be essential for control of needle length in T3SS-3 secretion apparatus (Sun and Gan, 2010) and important for the secretion of the T3SS-3 translocator protein BipD as well as the effector protein BopE (Hii et al., 2008). We report here that the intracellular growth of *B. pseudomallei* in hepatocytes is partially dependent on a functional T3SS, since mutant ΔBPSS1539 (BsaU) exhibited reduced intracellular replication (**Figure 1C**) as well as decreased cell damage (**Figure 3C**) in HepG2 cells. In agreement with our previous study using HeLa cells (Pilatz et al., 2006), we found here that the transposon mutant of BsaU is unable to escape from the endocytotic vesicle after invasion, but is still able to proliferate within the vacuole (**Figure 2A**). We previously described that mutant ΔBPSS1509, encoded within the *B. pseudomallei* T6SS-1 cluster, displays no intracellular growth defect in J774A.1 macrophages and HeLa cells, but is required for virulence in mice (Pilatz et al., 2006). In contrast, the present study indicates that mutant ΔBPSS1509 reveals delayed and reduced induction of actin polymerization (data not shown) as well as decreased intracellular replication (**Figure 1C**) and reduced cell damage (**Figure 3C**) in hepatocytes compared to the wild-type. These results are in line with recent reports showing that different T6SS-1 mutants of *B. pseudomallei* exhibit reduced intracellular growth and cytotoxicity in RAW264.7 macrophages (Burtnick et al., 2011; Chen et al., 2011). Thus, our results suggest that BPSS1539 encoded by T3SS-3 and BPSS1509 encoded by T6SS-1 are potential virulence determinants that enable intracellular growth of *B. pseudomallei* and induce cell damage in hepatocytes. However, these factors are unlikely the main players responsible for intracellular survival in these cells, since HepG2 cells were not able to eliminate the corresponding mutants.

Hepatocytes have been shown to express a variety of cytokines (Rowell et al., 1997; Stonans et al., 1999) and to respond to bacterial or viral infections with enhanced secretion of inflammatory cytokines and chemokines (Rowell et al., 1997; Santos et al., 2005). Since it has been shown that numerous cytokines can modulate resistance to intracellular bacterial infections, primarily by stimulating antimicrobial activities (Ehlers et al., 1992; Autenrieth et al., 1994; Bohn et al., 1994; Santanirand et al., 1999), we investigated the impact of cytokine-activated hepatocytes in intracellular *B. pseudomallei* clearance. IFNγ was previously shown to be a major factor in primary host defense to *B. pseudomallei* (Santanirand et al., 1999; Breitbach et al., 2006). In addition, several reports described that both primary murine hepatocytes and hepatocyte cell lines are efficiently activated by IFNγ to kill intracellular *L. monocytogenes* or *S. typhimurium* (Gregory and Wing, 1993; Lajarin et al., 1996). This study, demonstrating that IFNγ is capable to enhance the anti-*Burkholderia* activity of HepG2 cells (**Figure 4A**) argues for a potential role of activated hepatoma cells in host defense against this pathogen. Although IL-1β and TNFα alone failed to significantly activate antibacterial activity of HepG2 cells, the combination of both cytokines together with IFNγ caused the most prominent growth inhibition in hepatoma cells (**Figures 4B,C**). These results are in line with several reports indicating that murine hepatocytes and hepatoma cell lines stimulated with a combination of IFNγ, TNFα, IL-6, IL-1β, or LPS exhibited the strongest antibacterial activity against *L. monocytogenes* (Szalay et al., 1995; Haponsaph and Czuprynski, 1996) and *S. typhimurium* (Lajarin et al., 1996, 1999). Therefore, our findings suggest that inflammatory cytokines, particularly IFNγ, are important for resistance of hepatocytes against *B. pseudomallei.*

However, the mechanism responsible for the anti-*B. pseudomallei* activity of cytokine-activated hepatoma cells remains unclear. In a previous study we could show that iNOS-generated NO contributes to resistance in innate susceptible BALB/c mice in a murine model of melioidosis as demonstrated by enhanced mortality rates and higher bacterial loads in liver and spleen of aminoguanidine-treated mice compared to untreated control mice (Breitbach et al., 2011). Moreover, inhibition of iNOS in IFNγ-stimulated and *B. pseudomallei*-infected BALB/c-derived macrophage cell lines revealed that reactive nitrogen species are involved in restricting the intracellular growth of *B. pseudomallei* (Miyagi et al., 1997; Utaisincharoen et al., 2001, 2003). Our present data indicate, however, that reactive nitrogen species do not play any role in controlling *B. pseudomallei* growth in hepatocytes since inhibition of NO production by aminoguanidine did not reverse the antibacterial activity of HepG2 cells (**Figure 5**). These results are in good accordance with reports demonstrating that elimination of *L. monocytogenes* (Gregory et al., 1993; Szalay et al., 1995; Haponsaph and Czuprynski, 1996) and *S. typhimurium* (Lajarin et al., 1996) from activated hepatocytes is not mediated by nitric oxide.

Besides the production of NO, the generation of ROS is another potential mechanism in the control of bacterial pathogens (Inoue et al., 1995; Vazquez-Torres et al., 2000; Breitbach et al., 2006). In a previous study we demonstrated that NADPH oxidase is able to restrict intracellular replication of *B. pseudomallei* in primary murine macrophages (Breitbach et al., 2006). But the present findings suggest that neither NADPH oxidase (**Figure 6**) nor other ROS-generating enzymes (**Figure 7**) are involved in the anti-*B. pseudomallei* activity of activated hepatoma cells. In contrast, some reports provided evidence of ROS-dependent mechanisms in both primary murine hepatocytes and hepatocyte cell lines against intracellular *L. monocytogenes* (Gregory and Wing, 1993) or *S. typhimurium* (Lajarin et al., 1996) since antibacterial activity was inhibited by the presence of scavengers or inhibitors of reactive oxygen species. In this context, Lajarin et al. (1999) indicated that cyclooxygenases (COX) are a potential source of ROS in *S. typhimurium* infected murine hepatocyte cell lines, and thus contribute to antibacterial host defense. However, several studies revealed that COX are involved in intracellular replication and survival of different pathogens (Uchiya and Nikai, 2004; Sadikot et al., 2007; Serezani et al., 2007).

In summary, the present study describes the *in vitro* invasion and intracellular replication of *B. pseudomallei* in human hepatocyte HepG2 cells involving type 3 and type 6 secretion systems.

We provide evidence that IFNγ contributes to growth restriction of *B. pseudomallei* whereas the combination with IL-1β and TNFα is necessary for the maximal antibacterial activity of hepatocytes. As the IFNγ-mediated effects are independent of NO and ROS production, we assume that other defense mechanisms are important to inhibit intracellular multiplication of *B. pseudomallei*. Thus, further investigations are required to elucidate the NO- and ROS-independent mechanisms responsible for restricting intracellular growth of *B. pseudomallei* in cytokine-activated hepatocytes.

ACKNOWLEDGMENTS

We are grateful to Claudia Weber and Eylin Topfstedt for excellent technical assistance.

REFERENCES

Autenrieth, I. B., Beer, M., Bohn, E., Kaufmann, S. H., and Heesemann, J. (1994). Immune responses to *Yersinia enterocolitica* in susceptible BALB/c and resistant C57BL/6 mice: an essential role for gamma interferon. *Infect. Immun.* 62, 2590–2599.

Bohn, E., Heesemann, J., Ehlers, S., and Autenrieth, I. B. (1994). Early gamma interferon mRNA expression is associated with resistance of mice against *Yersinia enterocolitica*. *Infect. Immun.* 62, 3027–3032.

Breitbach, K., Klocke, S., Tschernig, T., Van Rooijen, N., Baumann, U., and Steinmetz, I. (2006). Role of inducible nitric oxide synthase and NADPH oxidase in early control of *Burkholderia pseudomallei* infection in mice. *Infect. Immun.* 74, 6300–6309.

Breitbach, K., Rottner, K., Klocke, S., Rohde, M., Jenzora, A., Wehland, J., and Steinmetz, I. (2003). Actin-based motility of *Burkholderia pseudomallei* involves the Arp 2/3 complex, but not N-WASP and Ena/VASP proteins. *Cell. Microbiol.* 5, 385–393.

Breitbach, K., Wongprompitak, P., and Steinmetz, I. (2011). Distinct roles for nitric oxide in resistant C57BL/6 and susceptible BALB/c mice to control *Burkholderia pseudomallei* infection. *BMC Immunol.* 12, 20. doi:10.1186/1471-2172-12-20

Burtnick, M. N., Brett, P. J., Harding, S. V., Ngugi, S. A., Ribot, W. J., Chantratita, N., Scorpio, A., Milne, T. S., Dean, R. E., Fritz, D. L., Peacock, S. J., Prior, J. L., Atkins, T. P., and Deshazer, D. (2011). The cluster 1 type VI secretion system is a major virulence determinant in *Burkholderia pseudomallei*. *Infect. Immun.* 79, 1512–1525.

Burtnick, M. N., Brett, P. J., Nair, V., Warawa, J. M., Woods, D. E., and Gherardini, F. C. (2008). *Burkholderia pseudomallei* type III secretion system mutants exhibit delayed vacuolar escape phenotypes in RAW 264.7 murine macrophages. *Infect. Immun.* 76, 2991–3000.

Chen, Y., Wong, J., Sun, G. W., Liu, Y., Tan, G. Y., and Gan, Y. H. (2011). The regulation of type VI secretion system during *Burkholderia pseudomallei* infection. *Infect. Immun.* 79, 3064–3073.

Crispe, I. N. (2009). The liver as a lymphoid organ. *Annu. Rev. Immunol.* 27, 147–163.

Delpino, M. V., Barrionuevo, P., Scian, R., Fossati, C. A., and Baldi, P. C. (2010). *Brucella*-infected hepatocytes mediate potentially tissue-damaging immune responses. *J. Hepatol.* 53, 145–154.

Ehlers, S., Mielke, M. E., Blankenstein, T., and Hahn, H. (1992). Kinetic analysis of cytokine gene expression in the livers of naive and immune mice infected with *Listeria monocytogenes*. The immediate early phase in innate resistance and acquired immunity. *J. Immunol.* 149, 3016–3022.

French, C. T., Toesca, I. J., Wu, T. H., Teslaa, T., Beaty, S. M., Wong, W., Liu, M., Schroder, I., Chiou, P. Y., Teitell, M. A., and Miller, J. F. (2011). Dissection of the *Burkholderia* intracellular life cycle using a photothermal nanoblade. *Proc. Natl. Acad. Sci. U.S.A.* 108, 12095–12100.

Gong, L., Cullinane, M., Treerat, P., Ramm, G., Prescott, M., Adler, B., Boyce, J. D., and Devenish, R. J. (2011). The *Burkholderia pseudomallei* type III secretion system and BopA are required for evasion of LC3-associated phagocytosis. *PLoS ONE* 6, e17852. doi:10.1371/journal.pone.0017852

Gregory, S. H., and Wing, E. J. (1993). IFN-gamma inhibits the replication of *Listeria monocytogenes* in hepatocytes. *J. Immunol.* 151, 1401–1409.

Gregory, S. H., Wing, E. J., Hoffman, R. A., and Simmons, R. L. (1993). Reactive nitrogen intermediates suppress the primary immunologic response to *Listeria*. *J. Immunol.* 150, 2901–2909.

Haponsaph, R., and Czuprynski, C. J. (1996). Inhibition of the multiplication of *Listeria monocytogenes* in a murine hepatocyte cell line (ATCC TIB73) by IFN-gamma and TNF-alpha. *Microb. Pathog.* 20, 287–295.

Harley, V. S., Dance, D. A., Drasar, B. S., and Tovey, G. (1998). Effects of *Burkholderia pseudomallei* and other *Burkholderia* species on eukaryotic cells in tissue culture. *Microbios* 96, 71–93.

Hii, C. S., Sun, G. W., Goh, J. W., Lu, J., Stevens, M. P., and Gan, Y. H. (2008). Interleukin-8 induction by *Burkholderia pseudomallei* can occur without Toll-like receptor signaling but requires a functional type III secretion system. *J. Infect. Dis.* 197, 1537–1547.

Hoppe, I., Brenneke, B., Rohde, M., Kreft, A., Haussler, S., Reganzerowski, A., and Steinmetz, I. (1999). Characterization of a murine model of melioidosis: comparison of different strains of mice. *Infect. Immun.* 67, 2891–2900.

Inoue, S., Itagaki, S., and Amano, F. (1995). Intracellular killing of *Listeria monocytogenes* in the J774.1 macrophage-like cell line and the lipopolysaccharide (LPS)-resistant mutant LPS1916 cell line defective in the generation of reactive oxygen intermediates after LPS treatment. *Infect. Immun.* 63, 1876–1886.

Jones, A. L., Beveridge, T. J., and Woods, D. E. (1996). Intracellular survival of *Burkholderia pseudomallei*. *Infect. Immun.* 64, 782–790.

Kespichayawattana, W., Rattanachetkul, S., Wanun, T., Utaisincharoen, P., and Sirisinha, S. (2000). *Burkholderia pseudomallei* induces cell fusion and actin-associated membrane protrusion: a possible mechanism for cell-to-cell spreading. *Infect. Immun.* 68, 5377–5384.

Lajarin, F., Rubio, G., Galvez, J., and Garcia-Penarrubia, P. (1996). Adhesion, invasion and intracellular replication of *Salmonella typhimurium* in a murine hepatocyte cell line. Effect of cytokines and LPS on antibacterial activity of hepatocytes. *Microb. Pathog.* 21, 319–329.

Lajarin, F., Rubio, G., Lorenzo, N., Gamiz, P., Hernandez-Caselles, T., and Garcia-Penarrubia, P. (1999). Implication of reactive oxygen species in the antibacterial activity against *Salmonella typhimurium* of hepatocyte cell lines. *Free Radic. Biol. Med.* 27, 1008–1018.

Liu, B., Koo, G. C., Yap, E. H., Chua, K. L., and Gan, Y. H. (2002). Model of differential susceptibility to mucosal *Burkholderia pseudomallei* infection. *Infect. Immun.* 70, 504–511.

Malarkey, D. E., Johnson, K., Ryan, L., Boorman, G., and Maronpot, R. R. (2005). New insights into functional aspects of liver morphology. *Toxicol. Pathol.* 33, 27–34.

Miyagi, K., Kawakami, K., and Saito, A. (1997). Role of reactive nitrogen and oxygen intermediates in gamma interferon-stimulated murine macrophage bactericidal activity against *Burkholderia pseudomallei*. *Infect. Immun.* 65, 4108–4113.

Muangsombut, V., Suparak, S., Pumirat, P., Damnin, S., Vattanaviboon, P., Thongboonkerd, V., and Korbsrisate, S. (2008). Inactivation of *Burkholderia pseudomallei* bsaQ results in decreased invasion efficiency and delayed escape of bacteria from endocytic vesicles. *Arch. Microbiol.* 190, 623–631.

Pilatz, S., Breitbach, K., Hein, N., Fehlhaber, B., Schulze, J., Brenneke, B., Eberl, L., and Steinmetz, I. (2006). Identification of *Burkholderia pseudomallei* genes required for the intracellular life cycle and in vivo virulence. *Infect. Immun.* 74, 3576–3586.

Rowell, D. L., Eckmann, L., Dwinell, M. B., Carpenter, S. P., Raucy, J. L., Yang, S. K., and Kagnoff, M. F. (1997). Human hepatocytes express an array of proinflammatory cytokines after agonist stimulation or bacterial invasion. *Am. J. Physiol.* 273, G322–G332.

Sadikot, R. T., Zeng, H., Azim, A. C., Joo, M., Dey, S. K., Breyer, R. M., Peebles, R. S., Blackwell, T. S., and Christman, J. W. (2007). Bacterial clearance of *Pseudomonas aeruginosa* is enhanced by the inhibition of COX-2. *Eur. J. Immunol.* 37, 1001–1009.

Santanirand, P., Harley, V. S., Dance, D. A., Drasar, B. S., and Bancroft, G. J. (1999). Obligatory role of gamma interferon for host survival in a murine model of infection with *Burkholderia pseudomallei*. *Infect. Immun.* 67, 3593–3600.

Santos, S. A., Andrade, D. R., and Andrade Junior, D. R. (2005). Rat hepatocyte invasion by *Listeria monocytogenes* and analysis of TNF-alpha role in apoptosis. *Rev. Inst. Med. Trop. Sao Paulo* 47, 73–80.

Serezani, C. H., Chung, J., Ballinger, M. N., Moore, B. B., Aronoff, D. M., and Peters-Golden, M. (2007). Prostaglandin E2 suppresses bacterial killing in alveolar macrophages by inhibiting NADPH oxidase. *Am. J. Respir. Cell Mol. Biol.* 37, 562–570.

Slanina, H., Konig, A., Claus, H., Frosch, M., and Schubert-Unkmeir, A. (2011). Real-time impedance analysis of host cell response to meningococcal infection. *J. Microbiol. Methods* 84, 101–108.

Stevens, M. P., Friebel, A., Taylor, L. A., Wood, M. W., Brown, P. J., Hardt, W. D., and Galyov, E. E. (2003). A *Burkholderia pseudomallei* type III secreted protein, BopE, facilitates bacterial invasion of epithelial cells and exhibits guanine nucleotide exchange factor activity. *J. Bacteriol.* 185, 4992–4996.

Stevens, M. P., Stevens, J. M., Jeng, R. L., Taylor, L. A., Wood, M. W., Hawes, P., Monaghan, P., Welch, M. D., and Galyov, E. E. (2005). Identification of a bacterial factor required for actin-based motility of *Burkholderia pseudomallei*. *Mol. Microbiol.* 56, 40–53.

Stevens, M. P., Wood, M. W., Taylor, L. A., Monaghan, P., Hawes, P., Jones, P. W., Wallis, T. S., and Galyov, E. E. (2002). An Inv/Mxi-Spa-like type III protein secretion system in *Burkholderia pseudomallei* modulates intracellular behaviour of the pathogen. *Mol. Microbiol.* 46, 649–659.

Stonans, I., Stonane, E., Russwurm, S., Deigner, H. P., Bohm, K. J., Wiederhold, M., Jager, L., and Reinhart, K. (1999). HepG2 human hepatoma cells express multiple cytokine genes. *Cytokine* 11, 151–156.

Sun, G. W., and Gan, Y. H. (2010). Unraveling type III secretion systems in the highly versatile *Burkholderia pseudomallei*. *Trends Microbiol.* 18, 561–568.

Sun, G. W., Lu, J., Pervaiz, S., Cao, W. P., and Gan, Y. H. (2005). Caspase-1 dependent macrophage death induced by *Burkholderia pseudomallei*. *Cell. Microbiol.* 7, 1447–1458.

Szalay, G., Hess, J., and Kaufmann, S. H. (1995). Restricted replication of *Listeria monocytogenes* in a gamma interferon-activated murine hepatocyte line. *Infect. Immun.* 63, 3187–3195.

Uchiya, K., and Nikai, T. (2004). *Salmonella enterica* serovar *typhimurium* infection induces cyclooxygenase 2 expression in macrophages: involvement of *Salmonella* pathogenicity island 2. *Infect. Immun.* 72, 6860–6869.

Ulett, G. C., Ketheesan, N., and Hirst, R. G. (2000a). Cytokine gene expression in innately susceptible BALB/c mice and relatively resistant C57BL/6 mice during infection with virulent *Burkholderia pseudomallei*. *Infect. Immun.* 68, 2034–2042.

Ulett, G. C., Ketheesan, N., and Hirst, R. G. (2000b). Proinflammatory cytokine mRNA responses in experimental *Burkholderia pseudomallei* infection in mice. *Acta Trop.* 74, 229–234.

Utaisincharoen, P., Anuntagool, N., Limposuwan, K., Chaisuriya, P., and Sirisinha, S. (2003). Involvement of beta interferon in enhancing inducible nitric oxide synthase production and antimicrobial activity of *Burkholderia pseudomallei*-infected macrophages. *Infect. Immun.* 71, 3053–3057.

Utaisincharoen, P., Tangthawornchaikul, N., Kespichayawattana, W., Chaisuriya, P., and Sirisinha, S. (2001). *Burkholderia pseudomallei* interferes with inducible nitric oxide synthase (iNOS) production: a possible mechanism of evading macrophage killing. *Microbiol. Immunol.* 45, 307–313.

Vazquez-Torres, A., Jones-Carson, J., Mastroeni, P., Ischiropoulos, H., and Fang, F. C. (2000). Antimicrobial actions of the NADPH phagocyte oxidase and inducible nitric oxide synthase in experimental salmonellosis. I. Effects on microbial killing by activated peritoneal macrophages in vitro. *J. Exp. Med.* 192, 227–236.

Wood, S., Maroushek, N., and Czuprynski, C. J. (1993). Multiplication of *Listeria monocytogenes* in a murine hepatocyte cell line. *Infect. Immun.* 61, 3068–3072.

Wuthiekanun, V., Smith, M. D., Dance, D. A., Walsh, A. L., Pitt, T. L., and White, N. J. (1996). Biochemical characteristics of clinical and environmental isolates of *Burkholderia pseudomallei*. *J. Med. Microbiol.* 45, 408–412.

Conflict of Interest Statement: The authors declare that the research was conducted in the absence of any commercial or financial relationships that could be construed as a potential conflict of interest.

Received: 26 July 2011; accepted: 24 December 2011; published online: 10 January 2012.

Citation: Bast A, Schmidt IHE, Brauner P, Brix B, Breitbach K and Steinmetz I (2012) Defense mechanisms of hepatocytes against Burkholderia pseudomallei. Front. Microbio. ***2****:277. doi: 10.3389/fmicb.2011.00277*

This article was submitted to Frontiers in Cellular and Infection Microbiology, a specialty of Frontiers in Microbiology.